ACTA POLONIAE PHARMACEUTICA

Drug Research

Acta Poloniae Pharmaceutica – Drug Research

CONTENTS

GENERAL

SHORT COMMUNICATION

REVIEW

GIST OF MEDICINAL PLANTS OF PAKISTAN HAVING ETHNOBOTANICAL EVIDENCES TO CRUSH RENAL CALCULI (KIDNEY STONES)

MUHAMMAD JAWAD NASIM[1], MUHAMMAD HASSHAM HASSAN BIN ASAD[1], DURR-E-SABIH[2],
RAJA MUHAMMAD IKRAM[3], MUHAMMAD SIKANDAR HUSSAIN[3],
MUHAMMAD TAJAMMAL KHAN[4], GHAFOOR AHAMAD[5], SABIHA KARIM[6],
SHUJAAT ALI KHAN[1] and GHULAM MURTAZA[1]*

[1]Department of Pharmacy, COMSATS Institute of Information Technology, Abbottabad 22060 Pakistan
[2]MINAR, Nishtar Hospital, Multan, Pakistan
[3]Government Degree College Dultala, Rawalpindi, Punjab, Pakistan
[4]Department of Botany, Pir Mehr Ali Shah, Arid Agriculture University, Rawalpindi, Pakistan
[5]Department of Zoology, Bahauddin-Zakariya-University, Multan, Pakistan
[6]College of Pharmacy, University of the Punjab, Lahore, Pakistan

Abstract: Human civilization is facing the problem of kidney stones since ancient ages. Although mortality rate is not so high, yet it affects the victim's quality of life. The patient suffers from intense pain and many other symptoms modifying his life style and affecting his socioeconomic status. Many drugs and invasive methods have also been developed for the treatment, but these are highly costly and unaffordable for poor people and the rate of reoccurrence is also high. The use of medicinal plants is both affordable and effective in this respect. In this article, 35 medicinal plants of Pakistan origin and their crucial information have been enumerated in alphabetical order of plant's scientific name, family, place (distribution), part used, local name, habit, major constituents and references. It can also be seen that all parts are used for the treatment of kidney stones. Leaves represent 28% contribution, whole plants and seeds 12%, fruits and roots 11% contribution in this respect. Flowers contribute 8% in the treatment of kidney stone while branches, bark, bushes, buds, milk and shoots contribute only 3% in the removal of kidney stones. Habits of plants were also taken under consideration. It was noticed that herbs are the most useful life form in this regard which contributed 63% for the removal of kidney stone. Shrubs contributed 20%, trees 11% while bushes and weeds contributed 3% for the removal of kidney stones.

Keywords: renal calculi, Pakistan, medicinal plants, crush

One of the major diseases that affect human population since ancient ages are the kidney stones (renal calculi). Kidney stones result in the modification of the victim's behavior with great fear of intense pain and threaten with failure of the kidneys. Urinary stones contain both crystalloid and colloid components. The crystalloid components are mainly calcium oxalate, calcium phosphate, calcium carbonate, magnesium-ammonium phosphate, uric acid and cysteine. Various drugs are available for the treatment of this disease. Moreover, advancements in medical techniques have led to the development of invasive methods of stone disruption like lithotripsy and surgical methods. But these are very expensive methods which are non-affordable by the

poor people and the rate of reoccurrence is also high from 50 to 80% (1). The remedy that is the safest and cheapest includes the use of medicinal plants. Medicinal plants have occupied an important place in the society of developing countries, not only as a source of economy but also for improving quality of life, because 80% of human population prefer using herbal remedies (2).

Modern pharmacopoeia includes at least 25% of the drugs coming from plant origin, 121 of such active substances are being in use currently or synthetic analogs are obtained from natural precursors. Hence, potential of medicinal plants cannot be underestimated (3). Various plants have been reported to be used for the treatment of kidney stones.

* Corresponding author: e-mail: gmdogar356@gamil.coms; phone: +92-992-383591-5; fax: +92-992383441

However, to the best of our knowledge and according to the literature survey, a majority of the medicinal plants of Pakistan have not been scientifically evaluated for their potential in the treatment of kidney stones.

In this article, 35 medicinal plants of Pakistan origin and their crucial information have been enumerated in alphabetical order of plant's scientific name, family, place (distribution), part used, local name, habit, major constituents and references.

METHODOLOGY

Data collection was carried out through internet search on Science Direct, Google and PubMed using biological and chemical abstracts. The key words used for the literature survey for this article were "Medicinal plants of Pakistan, kidney stones, renal calculi, ethnobotanical evidence and natural products". Selection of plants was focused on their use in the treatment of kidney stones in folklore remedies and studied their references in detail. Chemical constituent of medicinal plants were also searched. The outcome of results were rechecked and compared with the literature.

RESULTS AND DISCUSSION

Urolithiasis is a major problem afflicting human civilization for several centuries. It has been observed that its annual incidence is 0.5% in western world. The major phenomenon responsible for stone formation involves calcium oxalate and calcium phosphate accumulation. The phases involved in the accumulation of these two substances include: nucleation, crystal growth, crystal aggregation and crystal retention (55). Nucleation phase involves the formation of a solid crystal. It is the primary step in the formation of renal stone. The underlying cause for nucleation is super-saturation. The homogeneous nucleation involves the nucleation in pure solution, whereas secondary nucleation involves the accumulation of new crystals on pre-existing crystals. Urine is not a pure substance and nucleation in it involves the presence of an existing surface or structure. This phenomenon is called heterogeneous nucleation (58). Heterogeneous nucleation in urine may occur at epithelial cells, RBCs, bacteria, some other crystals, cell debris and urinary casts. Stone formation involves phase change which results in the condensation of dissolved solids transforming these into solid state because of super-saturation. Nucleation is followed by the crystal growth. The crystal growth process begins with the nucleation stage. Super-sat-

uration facilitates the process of cluster formation. In the 3rd phase (crystal aggregation/crystal agglomeration), the crystals stick together and constitute a larger particle. Stabilization is achieved by the bridge formation among the crystalline substance (24). Finally, these crystals are retained in the kidney. The retention is achieved because of adherence of crystals with epithelial cell line (41).

Stone formation inhibitors forbid the agglomeration and growth by developing a layer on the surface of growing calcium crystals or by forming complexes with calcium and oxalate. There are various substances that inhibit the stone formation including both organic and inorganic substances. Inorganic substances include citrates, magnesium and pyrophosphates while organic substances include Tamm-Horsfall proteins, urinary prothrombin fragment 1, protease inhibitor (inter-α-inhibitor), glycosaminoglycans, osteopontin (uropontin), renal lithostathine and other bikunin and calgranulin. High urine flow is also an important inhibitor of kidney stone formation (55).

Phytochemical investigation for use as urolithiatic agent is still an era of thirst. Only a few phytochemicals have been investigated to have a role in urolithiasis. Some terpenoids have been reported to have this activity (56, 57). Some flavonoids like quercetin, kaempferol-3-rhamnoside and kaempferol-3-rhamnogalactoside and tannins have also been reported to have some effect (60).

Plant extracts may contain chemicals and phytochemicals that inhibit the synthesis and growth of crystals. This character of plants may be of significant importance in preventing kidney stone formation. The extracts of plants may also contain constituents that retard crystal agglomeration (58).

The history of use of herbal remedies starts from the very beginning of human civilization. Various plants have been reported to be used in the treatment of disorders, but the knowledge of treatment differ in various areas and it is just like a hidden treasure. The present study is an effort to bring out the hidden treasure of knowledge used in the treatment of kidney stones in Pakistan. In this article, 35 medicinal plants of Pakistan and their crucial information have been enumerated in alphabetical order of plant scientific name, family, place (distribution), part used, local name, habit, major constituents and references (Table 1). These plants are distributed in 21 families of which, Cucurbitaceae represents the maximum contribution with 4 plants. Asteraceae, Fabaceae and Solanaceae are the families contributing 3 plants. Amaranthaceae, Boraginaceae , Chenopodiaceae, Rosaceae and Rutaceae are

Table 1. Medicinal plants of Pakistan used for the treatment in kidney stone.

Scientific Name	Family	Location	Constituent	Constituents active against urolithiasis	Habit	References
Acacia Jacquemontii Benth.	Fabaceae	Sindh*****, Punjab*, Baluchistan**	Diterpenoids	Terpenoids	An erect shrub	4, 56
Achillea millefolium L.	Asteraceae	Himalayan Region and Azad Kashmir *	Saponins, essential oils, flavanoids	Flavonoids	Herb	5, 6, 60, 63
Achyranthus aspera L.	Amaranthaceae	Swat, Bhimber, Azad Jammu and Kashmir*	Saponins, oleanolic acid, flavonoids, dihydroxyketones, alkaloids	Flavonoids	Wild herb	7, 8, 60, 64-66
Aervajavanica (Burm, f.) Schult.	Amaranthaceae	Parachinar, Kurram Agency, Kohat***	Alkaloids, flavonoids, tannins	Flavonoids, tannins	Herb	9-14, 60
Asphodelus tenuifolius Cavan.	Liliaceae	Bhimber****	β-Sitosterol, 1-octacosanol, 1-triacontanol, hexadecanoic acid, tetracosanoic acid, triacontanoic acid, 3-hydroxybenzoic acid and β-sitosterol 3-O-β-D-glucopyranoside	Not yet identified	Herb	15, 16
Bergenia ciliate (Haw.) Sternb.	Saxifragaceae	Azad Kashmir****	Wax, gallic acid, tannin, bergenin, mucilage	Tannin	Herb	17, 60
Bryophyllum pinnatum (Lam.) Oken	Crassulaceae	Bhimber****	Alkaloids, triterpenes, glycosides, flavonoids, steroids, bufadienolides, lipids and organic acids.	Terpenoids, flavonoids	Herb	15, 18, 56, 60
Calendula officinalis L.	Asteraceae	Pooch valley****	Triterpenoids, flavonoids, coumarins, quinones, volatile oil, carotenoids and amino acids	Terpenoids, flavonoids	Herb	19, 20, 56, 60
Chenopodium album L.	Chenopodiacea	Tank***	Oxalic acid, essential oil, vitamin A and C, alkaloid, flavonoid	Flavonoid	Weed	17, 21, 60, 67
Cichorium intybus L.	Asteraceae	Swat****	Inulin, esculin, volatile compounds (monoterpenes and sesquiterpenes), coumarins, flavonoids and vitamins	Flavonoids	Herb	22-24, 60
Citrullus colocynthis (L.) Schrad.	Cucurbitaceae	Dadu*****	Alkaloids, anthraquinones, flavonoids, terpenes, tannins, steroids, cardiac glycosides and saponins	Terpenoids, flavonoids, tannins	Herb	4, 9-11, 25, 26, 56, 60
Citrullus vulgaris Schrad. ex Eckl. and Zeyh.	Cucurbitaceae	Tehsil Pindigheb, District Attock*	Tannin, phytate, oxalate, iron, calcium, zinc	Tannins	Herb	27, 28, 60
Citrus sinensis (L.) Osbeck, Reise Ostind	Rutaceae	Sindh*****	Reducing sugar, saponins, cardiac glycosides, tannins and flavonoids	Flavonoids, tannins	Tree	4, 29, 60

Table 1. cont.

Scientific Name	Family	Location	Constituent	Constituents active against urolithiasis	Habit	References
Citrus aurantifolia (L.) (Christman) Swingle	Rutaceae	Sindh*****	Polymethoxyflavones (PMFs), polymethoxylated flavones, O-glycosylated flavones	Flavonoids	Tree	4, 60
Cucumis melo L.	Cucurbitaceae	Nara Desert, Sindh*****	Alkaloids, triterpenoids, carbohydrates, proteins, flavonoids, phytosterols	Terpenoids, flavonoids	Shrub	30-32, 56, 60
Cucumis sativus L.	Cucurbitaceae	Kohat***	Alkaloids, glycosides, steroids, saponin tannins	Tannins	Herb	30, 33-35
Dolichos biflorus L.	Fabaceae	Sindh*****	Falconoid phenolic	Not yet identified	Herb	30, 36, 37
Ficus carica L.	Moraceae	Chagharzai Valley***	Flavonoid, alkaloid, tannin, saponin	Flavonoids, tannins	Tree	38-40, 60
Haloxylon stocksii (Boiss.)	Chenopodiaceae	Coastal of Karachi*****	Dillenic acid	Not yet identified	Srubs	9-11, 41-43
Heliotropium strigosum Willd.	Boraginaceae	Bhimber****	Flavonoids, essential oil	Flavonoids	Wild herb	15, 35, 60
Micromeria biflora (Buch.-Ham. ex D. Don) Benth.	Labiatae	Pooch valley****	Essential oils	Not yet identified	Herb	17, 19, 44
Nigella sativa L.	Ranunculaceae	Bahawalpur, Bhakkar, Faisalabad, Hasilpur, Lahore, Multan*	Alkaloids, tannins, flavonoids, sterols	Flavonoids, tannins	Herb	38, 45, 46, 60
Rubus ellipticus Smith.	Rosaceae	Swat****	Flavonoids, carbohydrates, steroids, tannins and phenolic compounds, terpenoids, alkaloids	Flavonoids, tannins, terpenoids	Shrub	17, 22, 56, 60, 62
Rosa indica L.	Rosaceae	Sindh*****, Punjab*, Baluchistan**	Linoleic acid, α-linolenic acid, oleic acid, palmitic acid, stearic acid, octadecenoic acid, eicosanoic acid, eicosadienoic acid, erucic acid and minor fatty acids, alkaloids, flavonoids, saponins, tannins and phenols	Flavonoids, tannins	Shrub	4, 60, 65
Rumex hastatus D. Don.	Polygalaceae	Poonch vally****	Phenols, tannins	Tannins	Herb	5, 47, 60
Senna italica/ *Cassia italica* Mill	Fabaceae	Sindh*****	β-Sitosterol, stigmasterol, α-amyrin, 1,5-dihydroxy-3-methylanthraquinone, anthraquinone, alkaloids, steroids and flavonoids (I)	Flavonoids	Shrubs	4, 60, 66
Solanum nigrum L.	Solanaceae	Upper Dir****	Alkaloids, pregnane saponins, solanigroside A, tannins, flavonoids, proteins	Flavonoids, tannins	Herb	4, 48, 60, 68

Table 1. cont.

Scientific Name	Family	Location	Constituent	Constituents active against urolithiasis	Habit	References
Solanum surattense Shord and Wendl	Solanaceae	Poonch valley****	Oil, alkaloids, potassium nitrate, carbohydrates, tannins phenols, gums and mucilages	Tannins	Herb	5, 17, 60, 69
Tamarix aphylla (L.) Karst.	Tamaricaceae	Sindh*****	Glycosylated isoferulic acid, tamarixetin 3,3'-disodium sulfate, dehydrodigallic acid dimethyl ester and isoferulic acid, ferulic acid, kaempferol 7,4'-dimethyl-ether-3-sulfate, quercetin 3-O-isoferulyl-β-glucuronide, alkaloids, flavonoids, tannins	Flavonoids, tannins	Trees shrub	4, 60, 70
Trianthema portulacastrum L.	Aizoaceae	Bhimber***	Tetraterpenoid 1 (trianthenol), flavonoid, (C-methylflavone) , alkaloid (trianthemine)	Terpenoids	Herb	15, 49, 56
Tribulus teretris L.	Zygophyllaceae.	Bhimber****	Saponins , diosgenins, alkaloids, amides, tannins, flavonoids	Flavonoids, tannins	Herb	15, 50, 60, 71
Trichodesma indicum (L.) R. Br.	Boraginaceae	Poonch valley****	Fatty acids and non-steroidal compounds.	Not yet identified	Herb	5, 17, 51
Vitex agnus-castus L.	Verbenaceae	Khuzdar, Wadh**	Iridoids, flavonoids, diterpenoids, essential oils, ketosteroids	Terpenoids, flavonoids	Shrub	52, 53, 56
Withania somnifera (L.) Dunal	Solanaceae	Khushab, Cholistan desert*	Withanolides, cytotoxic lactones, piperidine, anaferine, anahygrine, alkaloids (withanine, somniferine, somnine, tropine, triterpenes	Terpenoids	Herb	43, 44, 54, 56, 72
Zea mays L.	Poaceae	Sindh*****	Flavonoids, alkaloids, phenols, steroids, glycosides, carbohydrates, amino acids, terpenoids, tannins	Flavonoids, tannins terpenoids	Bushes	4, 56, 60, 61

*East of Pakistan, **West of Pakistan, ***North of Pakistan, ****North-west of Pakistan, *****South of Pakistan
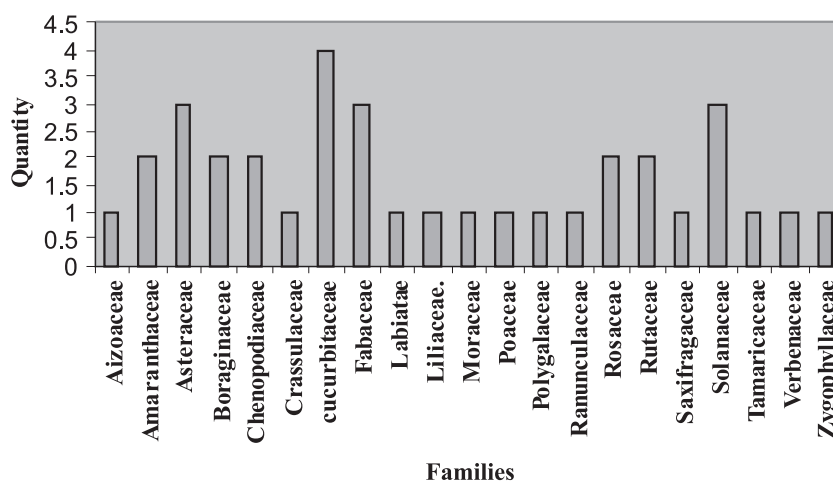
Figure 1. Various families and their number of plants
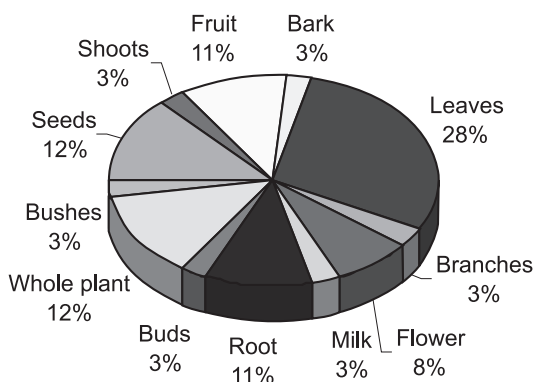
Figure 2. Percentages of various parts used for treatment of kidney stones
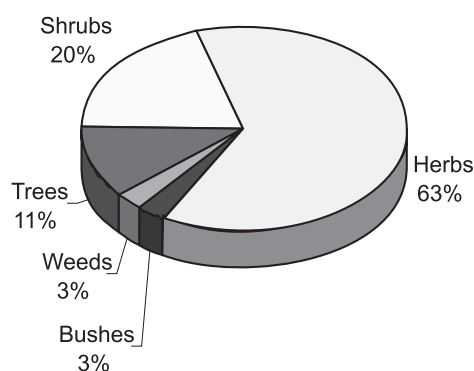
Figure 3. Percentage of different life forms

the families contributing 2 species, while, Aizo-aceae, Crassulaceae, Labiatae, Liliaceae, Moraceae, Poaceae, Polygalaceae, Ranunculaceae, Saxifraga-ceae, Tamaricaceae, Verbenaceae and Zygophyll-aceae, were found with single medicinal plant of such potential (Fig. 1). These plants are distributed throughout Pakistan in all the provinces. It can also be seen that all parts are used for the treatment of kidney stones. Leaves represent 28% contribution, whole plants and seeds 12%, fruit and roots 11% contribution in this respect. Flowers contribute 8% in the treatment of kidney stone while branches, bark, bushes, buds, milk and shoots contribute only 3% in the removal of kidney stones (Fig. 2). Habits of plants were also taken under consideration. It was noticed that herbs are the most useful life form in this regard which contributed 63% for the removal of kidney stones. Shrubs contributed 20%, trees

11% while bushes and weeds contributed 3% for the removal of kidney stones (Fig. 3).

During ethnobotanical search of Pakistan 35 medicinal plants belonging to 21 families were recorded as effective remedies used by the local people for the removal of renal calculi (kidney stones). These crude drugs cause dissolution or breakage of the renal calculi with subsequent expulsion from the body. The phenomenon of dissolution or destruction may be caused by the phytochemicals present in the crude drugs so plants were also searched for chemicals.

CONCLUSION

The present article enlists 35 medicinal plants used by the local people for the treatment and removal of renal calculi in various areas of

Pakistan. The medicinal plants used for the treatment of renal calculi contain such constituents which are active against urolithiasis. These active constituents include flavonoids, terpenoids, and tannins. Chemical investigation of medicinal plants is another important thirsting era that may lead to the understanding of physiology, pathology and pharmacology and use of these plants for various other diseases.

REFERENCES

1. Ziadi S.M.A., Jamil S.S., Singh K., Asif M.: Clinical evaluation of herbo-mineral Unani formulation in urilithiosis. p. 42, Amala Ayurveda Hospital and Research Centre, Thrissur, Kerala, India 2006.

2. Shah G.M., Khan M.A., Ahmad M., Zafar M., Khan A.A.: Afr. J. Biotchnol. 8, 1959, (2009).

3. Shinwari Z. K.: J. Med. Plants Res. 4, 161 (2010).

4. Rahman A.U., Choudhary M.I., Bullo S.: Medicinal plants of Sindh. Indigenous knowledge and scientific facts: Study sponsored by department of planning and development Government of Sindh, pp. 16, 2009.

5. Khan M.A., Khan M.A., Hussain M.: J. Basic Appl. Sci. 8, 35 (2012).

6. Fazal H., Ahmad N., Khan M.A.: Pak. J. Bot. 43, 63 (2011).

7. Murtaza G., Latif U, Haq M.N.U., Sajjad A., Karim S. et al.: J. Food Drug Anal. 21, 1 (2013).

8. Sher A., Mahmood M.F.U, Shah S.N.H., Bukhsh S., Murtaza G.: Adv. Clin. Exp. Med. 21, 705 (2012).

9. Srivastav S., Singh P., Mishra G., Jha K.K., Khosa R.L.: J. Nat. Prod. Plant Resour. 1, 1 (2011).

10. Khan T.I., Dular A.K., Solomon D.M.: Environment 23, 137 (2003).

11. Dagar J.C.: Bull. Nat. Inst. Ecol. 15, 81 (2005).

12. Sharif A., Ahmed E., Malik A., Hassan M.U., Munawar M.A.: J. Chem. Soc. Pak. 33, 439 (2011).

13. Hussain J, Khan F.U., Ullah R., Muhammad Z., Rehman N.U: Pak. J. Bot. 43, 427 (2011).

14. Asad M.H.H.B., Razi M.T., Khan T, Saqib Q.N.U., Murtaza G. et al.: Acta Pol. Pharm. Drug Res. 69, 1031 (2012).

15. Ahmed E.M., Nour B.Y.M., Mohammed Y.G., Khalid H.S.: Env. Health Insight 4, 1 (2010).

16. Mahmood A., Mahmood A., Shaheen H., Qureshi R.A., Sangi Y.: J. Med. Plants Res. 5, 2348 (2011).

17. Safdar M., Riaz N., Imran M., Nawaz H., Malik A., Jabbar A.: J. Chem. Soc. Pak. 31, 122 (2009).

18. Shinwari M. I., Shinwari M.I., Shah M.: Medicinal plants of Margalla hills National park Islamabad. 1st edn., published by D. G. administration, Higher Education Commission, Islamabad, Pakistan 2007.

19. Kamboj A., Saluja A.K.: Kurz. Rev. 3, 364 (2009).

20. Khan M.A., Khan M.A., Hussain M., Mujtaba G.: Ethnobot. Res. Appl. 8, 107 (2010).

21. Shabbir A., Shahzad M., Arfat Y., Ali L, Aziz R.S., Murtaza G. et al.: Afr. J. Pharm. Pharmacol. 6, 2346 (2012).

22. Badshah L., Hussain F.: J. Med. Plants Res. 5, 22 (2011).

23. Ahmad I., Ibrar M., Barkatullah N., Ali N.: J. Bot. 20, 1 (2011).

24. Nandagopal S., Kumari B.D.R.: Adv. Biol. Res. 1, 17 (2007).

25. Jan G., M. Khan A., Ahmad M., Iqbal Z., Afzal A.: J. Med. Plants Res. 5, 2452 (2011).

26. Singh S.: J. Herbal Med. Toxicol. 4, 159 (2010).

27. Mahmood S., Bashir S., Farzana K., Akram M.R., Abrar M.A., Murtaza G.: Philipp. Agric. Sci. 95, 169 (2012).

28. Hayat M.Q., Khan M.A., Ahmad M., Shaheen N., Yasmin G., Akhter S.: Ethnobot. Res. Appl. 6, 35 (2008).

29. Lakshmi A.J., Kaul P.: LWT – Food Sci. Technol. 44, 1821 (2011).

30. Osarumwense P.O., Okunrobo L.O., Imafidon K.E.: Contin. J. Pharm. Sci., 5, 15 (2011).

31. Asad M.H.H.B., Razi M.T., Murtaza G., Azhar S., Khan S.A., Saqib Q.N.U., Hussain I.: J. Med. Plants Res. 6, 3455 (2012).

32. Arora R., Kaur M., Gill N.S.: Res. J. Phytochem. 5, 146 (2011).

33. Razi M.T., Saadullah M., Murtaza G., Hassan W.: Latin Am. J. Pharm. 30, 378 (2011).

34. Das J., Chowdhury A., Biwas S.K., Karmakar U.K., Sharif S.R. et al: Res. J. Phytochem. 6, 25 (2012).

35. Marwat S.K., Khan M.A., Khan M.A., Ahmad M., Zafar M, Fazal-ur-Rehman, Shazia Sultana S.: Am. Eurasian J. Agric. Environ. Sci. 5, 284 (2009).

36. Hussain S., Jamil M., Ullah F., Khan A., Ullah F. et al.: Afr. J. Biotechnol. 9, 7738 (2010).

37. Hazra B., Sarkar R., Mandal S., Biswas S., Mandal N.: Afr. J. Biotechnol. 8, 3927 (2009).

38. Asad M.H.H.B., Murtaza G., Siraj S., Khan S.A., Azhar S. et al.: Afr. J. Pharm. Pharmacol. 5, 2292 (2011).

39. Ahmad M., Khan M.A., Marwat S.K., Zafar M., Khan M.A., Hassan T.U., Sultana S.: Am. Eurasian J. Agric. Environ. Sci. 5, 126 (2009).
40. Shafaghat A.: J. Med. Plants 9, 61 (2010).
41. Sher Z., Khan Z., Hussain F.: Pak. J. Bot. 43, 1445 (2011).
42. Akash M.S.H., Rehman K., Rasool F., Sethi A., Abrar A., Irshad A., Abid A., Murtaza G.: J. Med. Plants Res. 5, 6885 (2011).
43. Waqas M.K., Akhtar N., Ahmad M., G. Murtaza, Khan H.M.S., Iqbal M., Rasul A., Bhatti N.S.: Acta Pol. Pharm. Drug Res. 67, 173 (2010).
44. Hameed, M., Ashraf M., Al-Quriany F., Nawaz T., Ahmad M.S.A., Younis A., Naz N.: Pak. J. Bot. 43, 39 (2011).
45. Jabeen A., Khan M.A., Ahmad M., Zafar M., Ahmad F.: Afr. J. Biotechnol. 8, 763 (2009).
46. Rabbani M.A., Ghafoor A., Masood M.S.: Pak. J. Bot. 43, 191 (2011).
47. Javed S., Shahid A.A., Haider M.S., Umeera A., Ahmad R., Mushtaq S.: J. Med. Plants Res. 6, 768 (2012).
48. Akhtar N., Waqas M.K., Ahmad M., Murtaza G., Saeed T. et al.: Trop. J. Pharm. Res. 9, 329 (2010).
49. Khan B., Hussain S.K.: Community based forest conservation in Upper Dir district, NWFP. pp. 1-20, Final Progress Report, Nov 2005-to-Oct 2006, 2006.
50. Geethalakshmi R., Sarada D.V.L., Ramasamy K.: Int. J. Engin. Sci. Technol. 2, 976 (2010).
51. Kianbakht S., Jahaniani F.: Iran. J. Pharmacol. Ther. 2, 22 (2003).
52. Nasim M.J., Asad M.H.H.B., Sajjad A., Khan S.A., Mumtaz A. et al.: Acta Pol. Pharm. Drug Res. 70, 387 (2013).
53. Tareen R.B., Bibi T., Khan M.A., Ahmad M., Zafar M.: Pak. J. Bot. 42, 1465 (2010).
54. Kuruüzüm-Uz A., Ströch K., Demirezer L.Ö., Axel Z.: Phytochem. 63, 959 (2003).
55. Qureshi R., Maqsood M., Arshad M., Chaudhry A.K.: Pak. J. Botany, 43, 121 (2011).
56. Basavaraj D.R., Biyani C.S., Browning A.J., Cartledge J.J.: J. Eur. Assoc. Urol. Eur. Board Urol. 34, 126 (2007).
57. Sharifa A.A., Jamaludin J., Kiong L.S., Chia L.A,. Osman K.: Sains Malaysiana 41, 33 (2012).
58. Bhattacharjee A., Shashidhara S.C., Aswathanarayana J.: Asian Pacific J. Trop. Biomed. 45, S1162 (2012).
59. Patel M.A., Patel P.K., Seth A.K.: J. Pharmacol. 2, 1169 (2011).
60. Anand R., Patnaik G.K., Kulshreshtha D.K., Dhawan B.N.: Phytother. Res. 8, 417 (1994).
61. Soundararjan P., Mahesh R., Ramesh T., Begum V.H.: Indian J. Exp. Biol. 44, 981 (2006).
62. Bhaigyabati T., Kirithika T., Ramya J., Usha K.: Res. J. Pharm. Biol. Chem. Sci. 2, 986 (2011).
63. Sharma U.S., Kumar A.: J. Diabetol. 2, 4 (2011).
64. Kumar K.L.S., Mustapha M.H., Rajbhandari A., Ramakrishnan R.: Res. J. Pharm. Biol. Chem. Sci. 2, 2 (2011).
65. Abhijit D.: Achyranthes L: Int. J. Pharm. Sci. Rev. Res. 9, 72 (2011).
66. Manjari S.A., Kanti C.C., Sarojini N., Sriti K.: Int. J. Res. Ayurveda & Pharm. 2, 1595 (2011).
67. Dabai Y.U., Kawo A.H., Aliyu R.M.: Afr. J. Pharm. Pharmacol. 6, 914 (2012).
68. Pande M., Pathak A.: Asian J. Exp. Biol. Sci. 1, 91 (2010).
69. Gogoi P., Islam M.: IOSR J. Pharm. 2, 455 (2012).
70. Shahiladevi H., Jayanthi G., Jegadessan M.: Ancient Sci. Life 26, 59 (2006).
71. Shafaghat A.: J. Med. Plants 9. 61 (2010).
72. Gomathi S., Shanmugapriya A., Bharathi V., Gayathri G., Karpagam T.: IJPI'S J. Pharmacog. Herb. Formul. 2, 48 (2012).
73. Rani A., Baranwal N.R., Nema R.K.: Asian J. Biochem. Pharm. Res. 4, 195 (2012).

PARACETAMOL: MECHANISM OF ACTION, APPLICATIONS AND SAFETY CONCERN

MARTA JÓŹWIAK-BĘBENISTA* and JERZY Z. NOWAK

Department of Pharmacology, Chair of Pharmacology and Clinical Pharmacology
at the Medical University of Łódź, Żeligowskiego 7/9, 90-752 Łódź, Poland

Abstract: Paracetamol / acetaminophen is one of the most popular and most commonly used analgesic and antipyretic drugs around the world, available without a prescription, both in mono- and multi-component preparations. It is the drug of choice in patients that cannot be treated with non-steroidal anti-inflammatory drugs (NSAID), such as people with bronchial asthma, peptic ulcer disease, hemophilia, salicylate-sensitized people, children under 12 years of age, pregnant or breastfeeding women. It is recommended as a first-line treatment of pain associated with osteoarthritis. The mechanism of action is complex and includes the effects of both the peripheral (COX inhibition), and central (COX, serotonergic descending neuronal pathway, L-arginine/NO pathway, cannabinoid system) antinociception processes and "redox" mechanism. Paracetamol is well tolerated drug and produces few side effects from the gastrointestinal tract, however, despite that, every year, has seen a steadily increasing number of registered cases of paracetamol-induced liver intoxication all over the world. Given the growing problem of the safety of acetaminophen is questioned the validity of the sale of the drug without a prescription. This work, in conjunction with the latest reports on the mechanism of action of paracetamol, trying to point out that it is not a panacea devoid of side effects, and indeed, especially when is taken regularly and in large doses (> 4 g/day), there is a risk of serious side effects.

Keywords: paracetamol, acetaminophen, toxic effects, mechanism of action, cyclooxygenase, cannabinoid, serotonergic, prostaglandin-endoperoxide synthases

Paracetamol (an international name used in Europe) and **acetaminophen** (an international name used in the USA) are two official names of the same chemical compound derived from its chemical name: N-a**cet**yl-**para**-**am**inophen**ol** (the segment ''cet'' inserted between ''para'' and ''amino'') and N-**acet**yl-para-**aminophen**ol. This drug has a long history and, as it often happens with important discoveries, it was found by chance. In the 80s of the 19th century, two young doctors at the University of Strasburg, in order to eradicate worms by mistake dispensed acetanilide to a patient instead of naphthalene (Fig. 1). They noticed that the drug had a small impact on intestinal parasites, however, it significantly decreased high temperature. Young doctors - Arnold Chan and Paul Heppa - quickly published their discovery and acetanilide was introduced into medical practice in 1886 under the name of antifebrin (1). Soon it appeared that although the production of this drug was very cheap, acetanilide
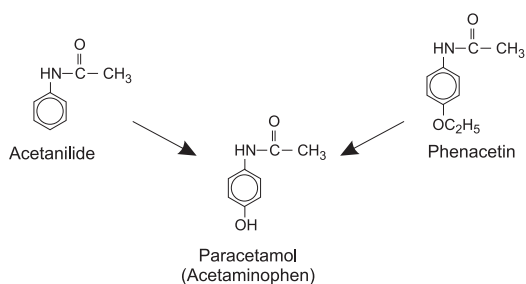
Figure 1. Chemical structure of analgesics - aniline derivatives. Phenacetin until the 80s of the 20th century was included in the composition of numerous mixtures. Saridon (Roche firm) and the so-called in Polish "tablets with cross" produced by Polpharma SA in Starogard Gdański (previously Starogardzkie Zakłady Farmaceutyczne Polfa) and Marcmed from Lublin are the most well-known preparations. Due to its carcinogenic action damaging the kidneys and the liver as well as the patients' tendency towards an overuse, the drug was withdrawn from the American market in 1983 (in Saridon, phenacetin was replaced by paracetamol). In Poland, it happened as late as in 2004

* Corresponding author: e-mail: marta.jozwiak-bebenista@umed.lodz.pl; phone/fax: +48 42 639-32-90
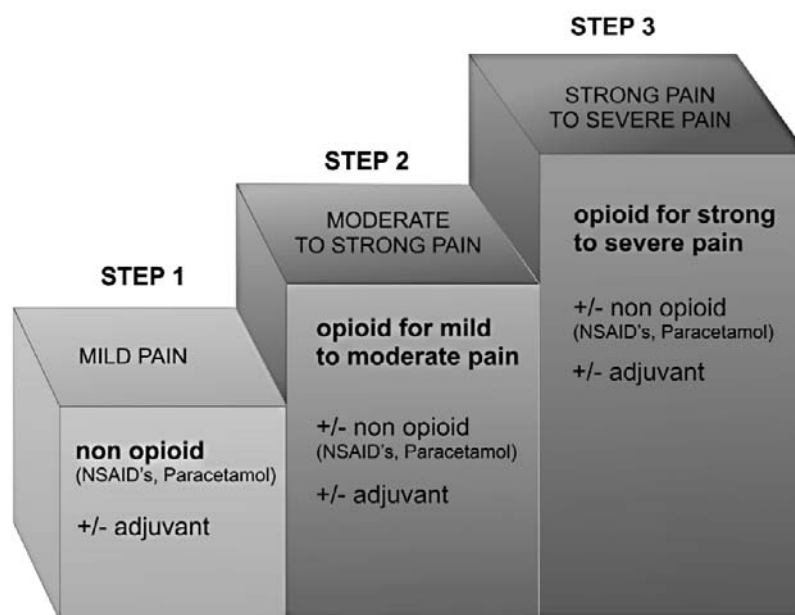
Figure 2. Paracetamol on the WHO analgesic ladder (the rules for using analgesics, which consider individual intensity of pain).

could not be used as an antipyretic medicament due to its high toxicity, the most alarming of which was methemoglobinemia. This resulted in a great deal of research on less toxic derivatives of acetanilide. Phenacetin and N-acetyl-p-aminophenol appeared to be the most satisfying compounds, which had been earlier synthesized by Harmon Northrop Morse in 1878 (Fig. 1) (2). The first clinical trials with those two acetanilide derivatives were performed by a German pharmacologist Joseph von Mering. On the basis of the obtained results, a faulty conclusion was drawn that paracetamol was characterized by high toxicity similar to acetanilide, therefore phenacetin was the first derivative to be introduced into medical practice in 1887. Phenacetin was widely used in analgesic mixtures until the time when it was associated with the development of analgesic nephropathy after a prolonged usage (3). In Poland, phenacetin was used as a component of very popular and available everywhere analgesic ''tablets with the cross''. In fact, acetaminophen/paracetamol became popular half a year later in 1948 when Bernard Brodie and Julius Axelrod demonstrated that paracetamol was the main active metabolite of acetanilide and phenacetin responsible for their analgesic and antipyretic action and that methemoglobinemia was induced by another metabolite, phenylhydroxylamine (4). That discovery revolutionized the pharmaceutical market of analgesic drugs and since then paracetamol has started its staggering career.

The use of paracetamol

Paracetamol was introduced into the pharmacological market in 1955 by McNeil Laboratories as a prescribed analgesic and antipyretic drug for children under its trade name *Tylenol Children's Elixir* (the name *tylenol* derives from its chemical name – N-ace**tyl**-p-aminoph**enol**). One year later, 500-mg tablets of paracetamol were available over the counter in Great Britain under the trade name of *Panadol,* which were produced by Frederick Stearns & Co, the branch of Sterling Drug Inc. In Poland, paracetamol became available in 1961 and since then it has belonged to the one of the most frequently sold analgesic medications. There are about a 100 preparations in the trade offer, which contain paracetamol alone or in combination with other active substances.

The paracetamol place on the WHO analgesic ladder, which precisely defines the rules for application of analgesic drugs, is impressive. This drug has been placed on all three steps of pain treatment intensity. In different pains of moderate intensity, paracetamol as a weak analgesic together with nonsteroidal analgesic drugs or coanalgesics (e.g., caffeine) is a basic non-opioid analgesic (the first step of the analgesic ladder). When pain maintains or increases, paracetamol is used as an additional analgesic with weak (e.g., caffeine, tramadol) or strong (e.g., morphine, phentanyl) opioids from the second and third step of the analgesic ladder, respectively,

Fig. 2). Paracetamol, if efficient, is a recommended oral analgesic of a first choice to be used for a long time, e.g., in symptomatic treatment of slight and moderate pain occurring in osteoarthritis as well as in muscle or tendon pains. Moreover, it is a drug of choice in patients in whom application of non-steroidal anti-inflammatory drugs (NSAIDs) are contraindicated, e.g., in the case of gastric ulcers, hypersensitivity to aspirin, impairments in blood coagulation, in pregnant women, nursing mothers and children with fever accompanying a disease (5). The use of paracetamol in children requires special care and maintain in an adequate dosage (based on age), which significantly differs from standard adult. The recommended dosage for children consider the metabolism of paracetamol, which determines the toxicity of the drug, especially hepatotoxicity (see below). In children, paracetamol metabolism changes with age: in younger children the sulfation pathway is dominated route of paracetamol elimination (which is mature at birth); the glucuronidation pathway takes about two years to mature. The oxidation of paracetamol, which takes place mainly with the participation of the enzyme CYP2E1 in neonates is negligible, because the activity of CYP2E1 increases with age, reaching the adult value at age 1-10 years. For comparison, in adults, paracetamol is metabolized mainly in the liver *via* glucuronidation (50-60%), sulfation (25-30%) and oxidation (< 10%) (see below in the section on adverse effects). Therefore, according to Ji et al. (6), the proposed dosage of paracetamol in children up to 12 years is as follows:

- under 2 years – no recommended dose; treatment under the supervision of a physician;
- 2-3 years – 160 mg (daily dose divided into two dose units, i.e., 2×80 mg); total dose corresponds to 1/2 of a single dose for an adult, i.e., 325 mg;
- 4-6 years – 240 mg (daily dose divided into three dose units, i.e., 3×80 mg); total dose corresponds to 3/4 of a single dose for an adult;
- 6-9 years – 320 mg (daily dose divided into four dose units, i.e., 4×80 mg); total dose is the same as a single dose for an adult;
- 9-11 years – 320-400 mg (daily dose divided into four-five dose units, i.e., 4-5 $\times$ 80 mg; total dose corresponds to 1-1 1/4 of a single dose for an adult;
- 11-12 years – 320-480 mg (daily dose divided in the four-six dose units, i.e 4-6 $\times$ 80 mg; total dose corresponds to 1 – 1 1/2 of a single dose for an adult.

According to the 20th edition of Drugs of Contemporary Therapy (Polish), the acetaminophen dosage schedules in pediatric patients should be as follows: 10-15 mg/kg oral dose and 15-20 mg/kg rectal dose every 4-6 h, maximum of 5 doses/day; in newborns orally or rectally 10 mg/kg of body weight every 4 h or 15 mg/kg every 6 h (maximum daily dose in newborns is 60 mg/kg).

Mechanism of action

Although paracetamol was discovered over 100 years ago and has been widely used in medical practice for more than half the century, its mechanism of action has not been elucidated until now (7). It has analgesic and antipyretic properties similarly to NSAIDs, but contrary to them, it does not possess any anti-inflammatory activity. When applied in recommended doses, it does not induce typical for NSAIDs gastrointestinal side effects. However, it suppresses prostaglandin production likewise NSAIDs.

Due to lack of an anti-inflammatory component, paracetamol has not been regarded as a member of the NSAIDs family in pharmacological textbooks, although what is interesting, it has been always discussed together with these drugs. Therefore, the discussion on the mechanism of action of paracetamol should begin from the analysis of NSAIDs action.

All conventional NSAIDs inhibit the conversion of arachidonic acid (AA) into prostaglandin H - PGH_2. The stage is catalyzed by prostaglandin H synthase (PGHS), at present referred to as cyclooxygenase (COX) within which isoenzymes COX-1 (PGHS-1) and COX-2 (PGHS-2) occur (8). The prevalence and the role of the third isoenzyme COX-3 is the subject of ongoing to date discussions (read further). PGHS is a bifunctional enzyme and possesses two different enzymatic activities: cyclooxygenase and peroxidase (POX). The conversion of AA→PGH_2 involves two reactions: cyclization of AA to unstable 15-hydroxyperoxide (PGG_2) with the involvement of a cyclooxygenase component and double oxidation in position 9 and 11; whereas the reduction of PGG_2 molecule to its 15-hydroxy analogue, unstable structure of PGH_2, takes place due to peroxidase activity of PGHS (POX).

Prostaglandin H_2 (PGH2) is a substrate for specific synthases, tissue-dependent isomerases catalysing its further conversions into different endogenous regulators, namely: prostaglandins of the D (PGD_2), E (PGE_2), F (PGF_2) series and prostacyclin (PGI_2; prostacyclin is not a prostaglandin and a commonly used abbreviation is historically conditioned) and thromboxanes (TXA_2 and TXB_2). They all are characterized by different biological activity and

many of them have anti-inflammatory properties. Thus, the action of NSAIDs, which inhibits the stage of conversion AA→PGH$_2$, and also the formation of the aforementioned regulators, have some favorable (anti-inflammatory, analgesic and antipyretic) and side effects (associated with the inhibition of synthesis of particular regulators in different tissues). A precise mechanism of NSAID action together with therapeutic and side effects has been presented in the recently published large study by Nowak and Dzielska-Olczak (9) and Nowak (10, 11).

While traditional NSAIDs and selective COX2 inhibitors inhibit cyclooxygenase (PGHS) through competing with arachidonic acid for the active site of the enzyme (12), paracetamol is likely to act as a factor reducing a ferryl protoporphyrin IX radical cation (Fe^{4+}=OPP^{*+}) within the peroxidase site of the PGHS enzyme. In turn, the Fe^{4+}=OPP^{*+} generates tyrosine radicals in the place of PGHS cyclooxygenase, which are essential for catalyzation of AA oxidation reaction (12-16) (Fig. 3). Due to a fact that hydroperoxides of fatty acids, like PGG$_2$ (reduced by POX), oxidize porphyrin within the peroxidase site of the enzyme, cyclooxygenase inhibition by paracetamol is difficult in the presence of high peroxide levels. Graham and Scott suggested that paracetamol should be classified to the group of the so-called atypical NSAIDs, determined as peroxide sensitive analgesic and antipyretic drugs (PSAAD) (17).

For the last decades, it was thought that paracetamol reveals analgesic and antipyretic properties by acting centrally and its inhibitory effect on COX-1 and COX-2 activity, i.e., prostaglandin synthesis was low. This concept was based on the original research carried out by Vane and colleagues, which was published at the beginning of the 70s of the previous century. Those authors observed that paracetamol decreased prostaglandin synthesis ten times stronger in the brain than in the spleen (18).[1]

At that time COX isoforms were not known because isoenzyme, COX-2, was identified only at the beginning of the 90s of the previous century (25, 26). Ten years later, the experiments performed on the dog's brain tissue revealed the presence of the third COX isoform, COX-3, which demonstrated special sensitivity to paracetamol (27). However, it soon appeared that so sensitive to paracetamol COX-3 does not function in the human organism. The human analogue of dog's COX-3, which occurs in some tissues especially of the central nervous system, is an alternative splice variant of COX-1 without a preferential sensitivity to paracetamol, encoding proteins of amino acid sequence different from COX and not exhibiting COX activity (28-30). Thus, COX-3 involvement in the mechanism of action of paracetamol in humans has not been justified, which has been confirmed by Kis et al. as well as by Hinz and Brune (15, 29). However, the discussions regarding a potential role of identified three COX isoenzymes in the mechanism of paracetamol action are still being continued (31-34).

The concept regarding COX-dependent central mechanism of paracetamol action has not stood the test of time (29). Firstly, the studies by Graham and Scott have shown that paracetamol really inhibited prostaglandin synthesis in well-functioning cells, however, it did not exert the same effect in the tissue/cell homogenate, where the concentration of arachidonic acid is low (35). Secondly, paracetamol has been found to have an inhibitory impact on COX-1 and COX-2 activity in peripheral tissues, although not to the same extent, since a stronger effect was always observed in relation to COX-2, especially in the cells of the vascular endothelium.

---

[1] In numerous academic textbooks including those published during the last decade, the central mechanism of paracetamol action has been discussed emphasizing its weaker inhibitory effect on the cyclooxygenase activity and prostaglandin production as compared to NSAIDs. The early study by Flower and Vane from 1972 in the prestige magazine *Nature* announced the mechanism of paracetamol activity even in its title: "*Inhibition of prostaglandin synthetase in brain explains the antipyretic activity of paracetamol (4-acetamidophenol)*" (18). Scientific prestige of the future Nobel prize winner, John R. Vane, was so high that despite later published articles, which did not completely confirm the original results of the British researchers (19-21) that study was still citied and its results were considered the substantial basis of the mechanism of paracetamol action for many pharmacologists and doctors.

Flower and Vane indicated that prostaglandin production in the brain was 10-fold more sensitive to paracetamol action than in the spleen (18). At that time, John R. Vane, the future Noble Prize winner in physiology and medicine (John R. Vane, Sune K. Bergstrom and Bengt I. Samuelsson – "Nobel Prize" in 1982 for discoveries on prostaglandin and related biologically active substances) was the author of many other essential for medicine innovative observations that were published in prestige magazines, e.g. "*Inhibition of prostaglandin synthesis as a mechanism of action for aspirin-like drugs*" (22). John Vane, using a guinea pig lung homogenate in his study, concluded that analgesic, antipyretic and anti-inflammatory action of aspirin, indomethacin and salicylate is associated with a lower prostaglandin production resulting from cyclooxygenase inhibition (COX). Other articles published in the same magazine *Nature* by Vane et al.: "*Indomethacin and aspirin abolish prostaglandin release from spleen*" and by Smith and Willis: "*Aspirin selectively inhibits prostaglandin production in human platelets*" contained the results confirming those observations (23, 24). It is worth remembering that COX isoenzymes were not discovered at that time.

prostaglandin H synthase (PGHS)
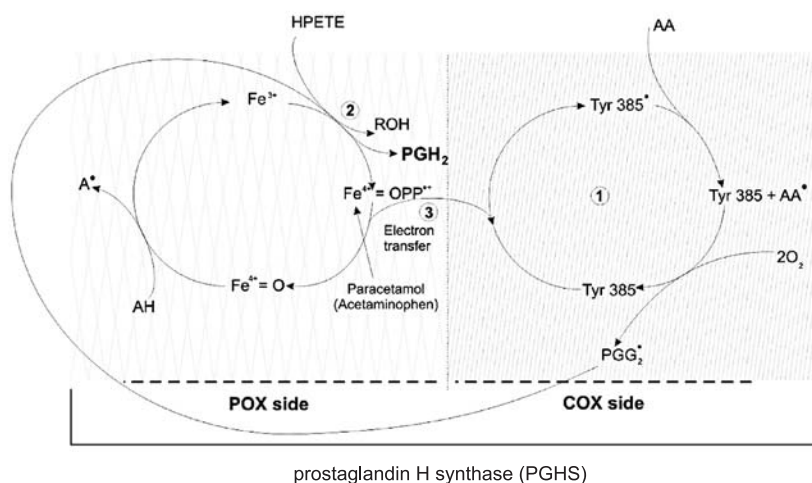
Figure 3. The complex of prostaglandin H synthase (PGHS) including two components: cyclooxygenase (COX) and hydroperoxidase (POX) is a bifunctional enzyme, responsible for the metabolism of arachidonic acid (AA) to prostaglandin PGH_2. The reaction occurs *via* two stages: **1.** AA oxidation to PGG_2 depends on tyrosine radical (Tyr385°) in the COX site. **2.** PGG_2 undergoes reduction to PGH_2 in the POX site, which results in the oxidation of the peroxidase heme radical. **3.** A formed ferryl protoporphyrin IX radical cation ($Fe^{4+}=OPP^{•+}$) generates Tyr385° radicals. Thus, the POX part is "self-sufficient", whereas COX depends on POX. Paracetamol reduces an iron cation in protoporphyrin IX radical ($Fe^{4+}=OPP^{•+}$) in the POX part, which contributes to a lower amount of Tyr385° radical formation. Abbreviations: AA – arachidonic acid; AA° – arachidonic acid radical; A° - oxidized cosubstrate; AH – reduced cosubstrate; Fe^{3+} - enzyme at rest; $Fe^{4+}=O$ – protoporphyrin IX (heme); $Fe^{4+}=OPP^{•+}$ - protoporphyrin radical IX; HPETE – hydroperoxides of fatty acids; $PGG_2^{•}$ - prostaglandin G_2 containing peroxide radical; PGH_2 – prostaglandin H; ROH – alcohol; Tyr385°⁻ tyrosine radical (12, 16, 38).

Hinz et al. indicated that orally administered paracetamol at a dose of 1 g inhibited 80% of the COX-2 activity in human blood monocytes (36). The results of extensive studies by Hinz and Brune published in the years 2006-2012 reveal that paracetamol is a preferential inhibitor of COX-2 isoenzyme, however, its effect depends to a great extent on the state of environmental oxidation/reduction (redox) (15, 37).

Among other possibilities of the central action of paracetamol, its stimulating effect on descending serotoninergic pathways, which are involved in inhibition of pain sensations has been discussed. This theory has been confirmed by *in vivo* studies on animals as well as on humans. Alloui et al. carried out the study on analgesic and anti-inflammatory action of paracetamol in rats which were given caragenin. No anti-inflammatory effect of paracetamol was observed, however, central antinociceptive effect of this drug with the involvement of the 5-HT_3 subtype of serotonin receptors was detected (38). The study on healthy volunteers in whom the pain was induced through electrical stimulation of the median nerve showed that analgesic action of paracetamol was completely blocked in the group of subjects treated with paracetamol combined with tropisetron or granisetron (5-HT_3 receptor antagonists) (39, 40).

Data concerning central action of paracetamol through its effect on descending serotoninergic pathways do not exclude a hypothesis assuming the presence (or coexistence) of the inhibition of prostaglandin synthesis (35). Prostaglandin PGE_2 modulates numerous physiological processes and can also modulate nociceptive and autonomic processes *via* its influence on descending serotoninergic antinociceptive system (41).

Novel studies on the mechanism of action of paracetamol regard it as a pro-drug, which due to its active metabolites demonstrates an association with the endocannabinoid system. It has been observed that in mouse brain and spinal cord, paracetamol is subject to deacetylation to p-aminophenol that in turn reacts with arachidonic acid affected by fatty acid amide hydrolase (FAAH), resulting in the formation of an active metabolite of the drug, the fatty acid amide N-arachidonoylphenolamine (AM404) (42, 43). AM404 does not act directly on cannabinoid receptors, however, it increases activity of endocannabinoid system in an indirect way (44). On one hand, this compound is a strong activator of the vanilloid receptor subtype 1 (TRPV1), being a ligand of receptors for cannabinoids CB_1, and on the other hand, it leads to an increase in the endogenous pool of these compounds as an inhibitor of the

endogenous cannabinoid (anandamide) reuptake (45). Endogenous cannabinoids, e.g., anandamide, act antinociceptively both at the level of the spinal cord as well as the brain. The study on rats performed by Bertolini et al. presented that an earlier administration of the CB_1 receptor inhibited AM404 activity and completely blocked analgesic action of paracetamol in the animals (46). Moreover, cannabinoids considerably lower body temperature through the activation of CB_1 receptors in the pre-optic area (47). It has been known that analgesic derivatives of aniline have a similar action as cannabinoids, such as mood improvement, psychic relaxation and sedation. Such properties have not been observed so far in the case of paracetamol, although some authors ascribe poor sedative properties to it (29, 48). Furthermore, different concentrations of AM404 have been found to inhibit COX-1 and COX-2 enzymes. This mechanism may be important especially in such areas of the brain in which a high concentration of FAAH enzyme can be observed, e.g., in the mesencephalic trigeminal nucleus, primary sensory neurons. In these areas of the brain an increased production of the active metabolite AM404 can be found, and this in turn may to a certain degree explain the inhibitory action of paracetamol towards cyclooxygenases in the CNS (46).

Inhibition of nitrogen oxide (NO) formation might be also an alternative mechanism of analgesic action of paracetamol. The L-arginine/NO pathway activated by substance P and NMDA receptors leads to NO synthesis, which is an important neurotransmitter in the nociceptive processes of the spinal cord (49, 50).

Summing up, paracetamol acts at all levels of pain stimulus conduction from the tissue receptors through the spinal cord to the thalamus and the cerebral cortex in which pain sensations are evoked. The mechanism of analgesic action of paracetamol is complex. The following possibilities are still taken

Table 1. Advantages and disadvantages of paracetamol therapy.

Advantages (when the drug is administered in the recommended therapeutic doses max. 4 g/24 h)
wide therapeutic application
checked and examined
well tolerated
good bioavailability after oral administration ($t_{1/2}$ 2h)
fast elimination
cheep
a small number of interactions with other drugs
low toxicity at low doses (≤ 2 g / d) to the digestive tract and kidneys
low toxicity in children
rare side effects (main allergic skin reactions)
available in different pharmaceutical forms
Disadvantages
metabolized to a toxic metabolite (N-acetyl-p-benzoquinone imine)
therapeutic index (often not efficient at a low dose)
long-term application may cause: • renal functioning disorder • higher blood pressure • increased prevalence of heart infarction
low therapeutic efficiency • analgesic action at a dose of 1 g administered 2, 3, and 4 times a day • low anti-inflammatory action
hepatotoxicity • increased aminotransferase activity at therapeutic doses • hepatic failure in the case of overuse (two-fold overuse of a therapeutic dose) • enhanced previous liver damage caused by alcohol consumption • combinations with traditional NSAIDs can result in a higher prevalence of digestive tract ulceration

into consideration: affecting both peripheral (inhibition of COX activity) and central (COX, descending serotoninergic pathways, L-arginine/NO pathway, cannabinoid system) antinociceptive processes as well as the redox mechanism (51). The studies on the mechanism of paracetamol action require further verification - they should concern not only the therapeutic action of this drug but also more frequently reported poisoning, especially strong hepatotoxicity resulting from the drug overdose since numerous preparations containing paracetamol are available without a prescription.

Paracetamol on the pharmaceutical market

Paracetamol is available on the market under different trade names in simple (sold over the counter) or more complex preparations combined with an additional active substance obtainable only by prescription (with tramadol) or without it (in combination with codeine phosphate, ascorbic acid or diphenhydramine hydrochloride as well as NSAIDs such as ibuprofen or propyphenazone. Paracetamol occurs in the form of tablets, effervescent tablets, suspension, powder to prepare oral liquid medicine (sachets) and rectal suppositories. When administered orally, clinical effect of paracetamol appears after 30 min. Paracetamol content in oral medicaments differs; most frequently it equals 500 mg, however, there are preparations (most often complex) which contain 325 mg of paracetamol or 750 mg (e.g., Febrisan, Coldrex) or even 1000 mg (e.g., Efferalgan Forte, Codrex MaxGrip, Flucontrol Hot). The fastest action of paracetamol, already after 15 min, occurs in the case of using fast-release tablets, enriched with sodium bicarbonate which enhances stomach emptying. Due to this process, paracetamol quicker passes to the small intestine where it undergoes absorption (e.g., Panadol Rapid®). When administered rectally (suppositories), bioavailability of paracetamol is lower, about two thirds of availability as compared to oral administration. The time necessary to achieve the therapeutic concentration for suppositories is 120-180 min, which means that analgesic action occurs after 2-3 h since the drug intake. Bioavailability and speed of absorption of paracetamol in the form of suppositories depend on numerous factors: the drug dose (in adults usually 650 mg; in children 80-325 mg), the size of the suppository (the smaller and the lower dose the better bioavailability is), the type of vehicle (the higher vehicle lipophilicity, the greater bioavailability and the faster effect but the shorter time of drug action) and the degree of rectal vascularization. Slower absorption of paracetamol applied *via* rectum (sup-

positories) differs from other analgesic medicaments: e.g., sodium diclophenac in the form of suppositories in the preparations Dicloberl (50 mg of the active substance) or Dicloratio (25, 50 and 100 mg) achieves the maximal blood concentration after 30 min since the application, in the preparations: Diclac and Diclofenac GSK (50 or 100 mg) or Voltaren (25, 50, 100 mg) – after 60 min, and in Olfen (50 and 100 mg) – after 2 h (data according to Pharmindex 2012). These data show that the speed of absorption of an active substance from the drug administered *per rectum* (affecting the occurrence of the therapeutic effect) is influenced by the form and composition of the adjuvant substances contained in suppositories; the same factors affect the suppositories containing paracetamol. Slower absorption of the drug is usually associated with its longer presence in the organism, i.e., with a longer time of action, which in the case pain complaints is of considerable importance.

Paracetamol can be also used intravenously (*i.v.*) and therefore is widely used in the hospital health service, e.g., in the postoperative pain therapy (it has been evidenced that administration of paracetamol especially during the first hour of treatment is more efficient in reducing pain intensity than given orally), in order to quickly decrease high fever or in the case when another route of administration is not possible (52, 53). At the beginning, propacetamol – precursor of paracetamol (Pro-Dafalgan®, Bristol-Myers Squibb; Pro-Efferalgan, UPSA) was used which after the *i.v.* administration underwent hydrolysis to paracetamol and diethylglycine under the influence of plasma esterases. In 2005, an intravenous form of new generation paracetamol was registered as a solution ready to be infused at the concentration of 500 mg/50 mL or 1 g/100 mL (Perfalgan®, Bristol-Myers Squibb) which completely removed proparacetamol from medical practice (53, 54).

Side effects

When appropriate dosage of medicaments containing paracetamol is used, i.e., maximum dose of 4 g/24 h, (as one can read in the leaflet) no serious side effects have been observed, besides possible allergic skin reactions, although after higher doses or prolonged duration of taking the drug, some side effects may occur, especially in the liver (Table 1) (55). Interesting is that at the beginning of 2013, the United States Food and Drug Administration (US FDA) introduced paracetamol on the list of the preparations, which will undergo specific monitoring on the basis of information from the system on

adverse reactions (FEARS, the FDA Adverse Event Reporting System) collected during the period from October to December 2012. The preparations containing paracetamol will be evaluated in terms of inducing adverse skin reactions.

After ingestion of paracetamol, about 90% of the compound undergoes metabolism in the liver in conjugation with glucuronic acid (50-60%), sulfuric acid (25-35%) and cystine (approximately 3%) to form pharmacologically inactive metabolites, which are eliminated with urine. A small amount of the drug (about 5%) is eliminated in an unchanged form by kidneys. Subsequent 5% of paracetamol is subjected to N-hydroxylation in the liver with the involvement of cytochrome P450 enzymes (particularly CYP2E1) to form a toxic metabolite N-acetyl-p-benzoquinone imine (NAPQI), which is very quickly inactivated by glutathione sulfhydryl groups and excreted with urine as mercapturic acid (46).

Severe liver impairment after paracetamol overdose was documented for the first time in Great Britain in 1966 (56). Since then, a steady increase in the number of accidental or intended poisonings has been noted all over the world including Poland. The main cause of this situation is a huge amount of preparations containing paracetamol, which are available on the pharmaceutical market without any prescription (according to the 20th edition of Dugs of Contemporary Therapy, the number of such preparations reaches 92 items, including 39 single and 53 complex products). Depletion of hepatic glutathione stores occurs as a result of the intensive metabolism following intentional and unintentional overdose of paracetamol (ingestion of more than 4 g/24 h, i.e., over 8 tablets, 500 mg each!). In such a situation, paracetamol becomes a dangerous and life-threatening drug because a highly reactive NAPQI metabolite covalently binds to hepatocyte macromolecules leading to impoverishment of enzymatic systems and structural and metabolic damage to the liver (potential lethal hepatic necrosis). In the later stage of poisoning, renal tubular necrosis and hypoglycemic coma may appear (57). It is worth mentioning that the weakened hepatic function (caused by slimming, malnutrition, hepatitis C virus (HCV), human immunodeficiency virus

(HIV)), alcohol overuse or application of paracetamol combined with drugs inducing cytochrome P450 (rifampicin, barbiturates, carbamazepine) can lead to hepatic impairment much easier, even when the compound is used in therapeutic doses. Development of acute hepatic failure as a result of paracetamol overuse (i.e., 7.5-15 g /24 h) as well as the methods of its treatment have been precisely discussed in many studies for the last ten years (46, 58-60). The authors of the present study concentrate on other (likely to be potential) adverse reactions of paracetamol, which result from its mechanism of action.

Results of recent reports on paracetamol as a peripheral selective COX-2 inhibitor encourage researchers to analyze this drug more critically. The question arises as to whether paracetamol revealing a similar pharmacological profile to coxibs may induce the same side effects, especially when the drug is used for a long time.[2] A permanent blockade of prostaglandin synthesis through selective COX-2 inhibitors is currently regarded as a cause of adverse cardiovascular reactions in patients after a prolonged use of these drugs (15, 36, 37, 61). Long-lasting COX-2 inhibition decreases the production of vasoprotective prostacyclin (PGI_2) by vascular endothelial cells, which inhibits platelet aggregation and has vasodilational capacity. This impairs the balance between tromboxane and prostacyclin and causes thrombus formation. Contrary to the inflammatory tissue, the endothelial cells possess a low level of peroxides, so they are not likely to inhibit paracetamol activity against COX-2 (14).

It has been shown that oral administration of paracetamol at the dose of 500 mg decreases the amount of excreted with urine 2,3-dinor-6-keto $PGF_{1\alpha}$, the main stable inactive metabolite of prostacyclin, whose synthesis is mediated by endothelial COX-2 (62). Likewise, 50% reduction in this metabolite excretion in the urine of pregnant women was noted after ingestion of 1 g of paracetamol (63). Taking into consideration aforementioned results obtained by Hinz et al. (36), regarding over 80% inhibition of COX-2 in the vascular endothelium caused by paracetamol, it can be speculated that such a mechanism of action would be responsible

---

[2] Coxibs, NSAIDs selectively inhibiting COX-2 activity, do not affect (in therapeutic doses) COX-1 at the same time. Due to such a mechanism of coxibs, their side effect on the digestive system, which happens in the case of traditional NSAIDs, was eliminated. However, later clinical observations indicated that patients using coxibs for a long time developed adverse cardiovascular reactions. Thus, because of a higher risk of such perturbations in those patients, coxibs (etoricoxib, lumiracoxib, rofecoxib and valdecoxib) have been withdrawn from sale. Rofecoxib known under the trade name of Vioxx (Merck & Co.) was withdrawn as the first one in 2004 after the 5-year existence on the pharmaceutical market; valdecoxib (Bextra, Pfizer) was the next drug withdrawn in 2005. At present, only one drug of this type, celecoxib (Celebrex; Pfizer Europe), is used in Poland.

for adverse cardiovascular reactions in patients who take this drug regularly. It should be emphasized that paracetamol due to its short half-life (approximately 2 h) induces a short-lasting inhibition of COX-2 activity. Thus, in order to eliminate pain it is necessary to administer repeated 1 g doses of paracetamol for maintaining constant (80%) inhibition of COX-2. This fact has to be considered by a doctor prior to making the decision about long-term treatment with paracetamol in order to avoid the drug overdose.

Epidemiological data reveal that long-lasting administration of paracetamol affects blood pressure. *Nurses' Health Studies* present two cohort investigations performed among younger and older women. One of them demonstrated that in patients who regularly took paracetamol (over 500 mg/24 h), a relative risk (RR) for development of hypertension was considerably higher as compared to women who did not use this drug (RR 1.93 for older women; RR 1.99 for younger) (64). Moreover, it worth emphasizing that the risk associated with paracetamol was similar to traditional NSAIDs (RR 1.78 for older women; RR 1.60 for younger). The second cohort investigation carried out in the same study group indicated that in women who frequently used paracetamol (= 22 days a month), the risk of serious cardiovascular events (such as heart infarction or cerebral stroke) was nearly the same as after traditional NSAIDs (RR 1.35 for paracetamol; RR 1.44 for traditional NSAIDs). Similarly, application of paracetamol in the amount of 15 tablets or more per week is associated with the risk of cardiovascular events comparable to traditional NSAIDs (RR 1.68 for paracetamol; 1.86 for traditional NSAIDs) (65). According to the guidelines of the American Heart Association acetaminophen (paracetamol) is nowadays a drug of choice in patients with concomitant cardiovascular disorders (66). The prospective double-blind trial was performed in patients with stable coronary disease who used paracetamol at the dose of 1 g three times a day for two weeks and the drug increased their blood pressure. Its effect was similar to that exerted by diclofenac and ibuprofen.

Paracetamol due to its selective action towards COX-2 and similarly to coxibs but contrary to typical NSAIDs does not possess antiaggregatory properties. The drug does not inhibit blood platelet action when taken at a single oral dose of 1000 mg. However, clinical studies indicate antiaggregatory action of paracetamol in the case of parenteral administration in high doses (67, 68). Paracetamol can be safely used in the digestive tract; on one hand due to its non-acidic chemical structure

(unlike acidic NSAIDs gathering in the gastric epithelial cells) and on the other hand, due to a weak impact on COX-1. However, the results of epidemiological studies suggest that paracetamol at daily doses higher than 2-2.6 g increases the risk of serious side effects in the upper segment of the digestive tract such as bleeding or perforations (69). Therefore, it is postulated that a long-term effect of paracetamol on the digestive tract should be examined in randomized studies, especially in patients with osteoarthrisis who require high doses of this drug for a long time. Paracetamol like coxibs does not induce bronchial spasm in patients with aspirin asthma. In the strategy for treatment of pain in asthmatics, it is recommended to ingest this drug at doses lower than 1000 mg in order to avoid potential bronchial spasm (15).

Bearing in mind a preferential action of paracetamol on COX-2, the differences between the drug discussed and coxibs, selective inhibitors of this isoenzyme, should be emphasized. Paracetamol in opposition to selective inhibitors of COX-2, despite a similar mechanism of action, reveals weak anti-inflammatory activity. It is likely to result from the extracellular accumulation of arachidonic acid and peroxides in the inflammatory tissues, which reduce an inhibitory effect of paracetamol on the prostaglandin production (Fig. 3) (14, 35). Indeed, paracetamol did not decrease prostanoid concentrations in the joint fluid of patients suffering from osteoarthrisis (70). On the other hand, paracetamol reduced tissue swelling with similar to ibuprofen efficiency after the oral cavity surgery in humans (71). There have been also some studies which demonstrated anti-inflammatory action of paracetamol, e.g., nociceptive inhibition and carrageenan-induced rat paw edema (72). Therefore, the notion that paracetamol exhibits weak anti-inflammatory properties seems to be more legitimate than the assumption that this drug is devoid of such an action.

As regards safety of paracetamol application in pregnancy, prospective cohort studies in humans have not shown an increase in the prevalence of developmental fetal anomalies in pregnant women who took paracetamol in therapeutic doses, although in some experimental studies on animals paracetamol administered at doses twice as high as the maximum single dose demonstrated embriotoxic action (73). Considering the fact that paracetamol is the drug of choice in pregnant women, it should be emphasized that epidemiological studies report the possibility of the association between application of this drug in pregnancy and development of asthma

in early childhood. The metabolism of paracetamol has been suggested to be responsible for this effect because a large amount of glutathione is used to deactivate the toxic metabolite. Lungs of the developing fetus might deplete glutathione, the main antioxidant of this organ, which can lead to oxidative stress and inflammation of the respiratory airways. In some investigations, the occurrence of wheezing breath in very small children was observed, which however, is a very weak indicator of asthma (74). Epidemiological studies from different research centres provide controversial results on the association between paracetamol ingestion by pregnant women and the development of bronchial asthma later in childhood (74, 75). This happens because a number of other factors such as fever, cold, inflammation of fetal membranes or other infections of pregnant women can induce development of asthma in small children, leading thus to falsification of study results. Thus, a randomized study with placebo as a control could solve this problem. However, such a study would be unethical from the point of view of good clinical practice (GCP) which requires application of a standard drug as a comparator, and as NSAIDs are contraindicated in pregnancy, one group of women with pain and fever would not be treated at all. At present, there is no convincing evidence allowing to unequivocally determine that application of paracetamol in pregnant women may lead to asthma development in small children. Therefore, paracetamol still remains an analgesic and antipyretic drug of choice in pregnant patients. However, it should be stressed that the aforementioned data do not concern complex preparations containing paracetamol or those for *i.v.* infusion (safety for this route of administration has not been determined due to lack of sufficient clinical data).

Precautions and attempts to counteract toxicity of paracetamol

Due to an easy overdose of paracetamol, the US FDA has proposed to implement new solutions, which to a certain degree would limit this growing problem. A decrease in the maximum permissible single dose of paracetamol from 1000 mg to 650 mg seems to be one of the crucial problems. Thus, a question arises what will happen to numerous OTC preparations containing paracetamol in the dose exceeding 650 mg. It has been suggested that higher doses of this drug, i.e., above 325 mg should be available only by prescription (according to the information of the US FDA; www.fda.gov). Another suggested solution postulated by FDA is

the withdrawal of packages containing high amounts of paracetamol from the market, e.g., containers comprising even 100 single doses (e.g., Apap - 100 tablets, Codipar - 50 tablets), and the introduction of blisters that should enable the patient to control the amount of ingested drug. Furthermore, the packaging should be labelled with the information about the risk of liver damage caused by the overuse of the drug. It also seems justifiable to use only one international name, either paracetamol or acetaminophen, and not two different names of the same drug because it can be misleading for the patient (if not properly informed the unaware patient can ingest the same active substance under different names). The most drastic proposal suggested by FDA is the withdrawal of all complex drugs, both available over the counter (OTC) and by prescription, because, as the various study results indicate, they are responsible, to a great degree, for acute paracetamol poisoning. The data obtained by the Toxic Exposure Surveillance System (TESS) in 2005 showed that among all acute paracetamol poisonings, 6.3% (i.e., 3,845 of the 61,289 reported) was caused by OTC preparations and 1.5% (41 of the 2,698 reported) involved severe hepatic damage, while 54% of overdoses (i.e., 1,470 of the 2,698 reported) were recorded in the case of using complex drugs available by prescription. As regards the latter drugs, it has not been completely elucidated to which extent a narcotic ingredient present in the preparation contributed to the poisoning (76). At present, in all complex preparations available by prescription in the USA, a single dose of contained paracetamol cannot exceed 325 mg, whereas the way of the drug dosage, despite a decrease in a single dose, remains the same. Although paracetamol is not so toxic for children as for adults (children do not have a well-developed cytochrome P450 system so the toxic metabolite is not formed), FDA also recommends that liquid paracetamol should be available only in a single established dose, e.g., 160 mg/5 mL (according to FDA information; www.fda.gov).

Another solution aimed at prevention of paracetamol hepatotoxicity in Great Britain was the introduction of tablets containing paracetamol and methionine, which after the conversion into cysteine and then glutathione in hepatocytes would inactivate the active metabolite, NAPQI. Moreover, due to such a combination, there is no time wasted from the moment of intentional or unintentional ingestion of a toxic dose of paracetamotol to the application of antidote, e.g., N-acetylcysteine (hepatic damage occurs 24 h after the overdose). Nowadays, the only such preparation registered in Great Britain is

Paradote (Penn Pharmaceuticals) containing 500 mg of paracetamol and 100 mg of methionine. Other preparations of this type, e.g., Pameton (SmithKline Beecham), have been withdrawn. In other European countries and the USA such combinations of paracetamol do not exist on the pharmaceutical market because so far no efficient and safe dosage of methionine has been established for patients; also safety of the long-term application of these preparations has not been investigated yet (some carcinogenic effect of methionine has been suggested). Besides, the price of such a drug is higher than for a preparation containing paracetamol alone (77).

In the light of novel studies, the application of traditional NSAIDs in combination with paracetamol has not been recommended, particularly when active substances occur in higher doses (8, 69). Rahme et al. (69) published the retrospective cohort study performed in 644,183 patients aged over 65 years who had been receiving paracetamol (at daily doses: < 3 g and > 3 g) and/or traditional NSAIDs (with or without a proton pump inhibitor) for 6 years. The risk of hospitalization due to gastrointestinal events (ulceration, perforation, bleeding from the upper or lower segment of the digestive tract) appeared to be two-fold higher in the case of taking paracetamol in combination with traditional NSAIDs as compared to NSAIDs used in monotherapy. The authors of that study (69), as well as other researchers analyzing the problem of interaction between paracetamol and NSAIDs (8), explain the results in relation to the additional COX-1 inhibition caused by paracetamol. This hypothesis seems to be reliable in the light of new data showing that paracetamol synergistically enhances inhibitory effect of diclofenac on platelet activity (68, 78). Thus, safety and usefulness of complex preparations containing paracetamol combined with NSAIDs appearing on the pharmaceutic market are still the matter of discussion. It is worth paying attention to preparations containing paracetamol and NSAIDs (ibuprofen and propyphenazone) available on the Polish market without a prescription (Cefalgin and Saridon - paracetamol + propyphenazone and Metafen and Nurofen ultima - paracetamol + ibuprofen). The aforementioned drugs contain paracetamol at doses of 250-500 mg and NSAIDs: ibuprofen - 200 mg or propyphenazone - 150 mg. According to the manufacturers information, a single dose of these drugs is 1-2 tablets with the possibility of three-fold application per day. Considering the maximum dosage (2 tablets 3 times a day), a total dose of paracetamol would range from 1.5 g to 3 g, which is in compliance with the contemporary knowledge (8, 69) if

used sporadically. It should be remembered that a single dose of paracetamol should not exceed 1 g and daily dose 4 g; the US FDA suggests these values should be decreased to 0.65 g and 3.25 g, respectively. In the case of combined application of paracetamol with NSAIDs, paracetamol dosage should be considerably lower than the aforementioned values.

CONCLUSIONS

Summing up, paracetamol monotherapy is efficient, well tolerated by the majority of patients and safe, on condition that the drug is administered at therapeutic doses. Table 1 sums up the advantages and disadvantages of paracetamol. We should, however, bear in mind that the paracetamol overuse or application even at therapeutic doses in some situations like improper slimming, smoking, alcohol abuse or ingestion of other medicines may cause severe hepatic damage or death. Therefore, the question arises as to whether the patient knows that a safe dose of paracetamol (assuming that the above-mentioned situations are not present) comprises only eight tablets of 500 mg or four sachets, each one containing 1000 mg, per day and that paracetamol is ''hidden'' in other preparations under different names (here are about 100 simple and complex preparations in Poland). Thus, it is very important to the patient to be warned by doctors or pharmacists about the risk connected with the ingestion and particularly with the overuse of this drug. It appears in the light of new data that despite frequent application of paracetamol as an efficient analgesic and antipyretic drug, the action of this medicament has not been completely understood and this little unknown part may cause irreversible damage to the organism when the drug is overused. A long-term application of high doses of paracetamol carries the risk of adverse reactions typical for COX-2 inhibitors (coxibs) such as hypertension, heart infarction or renal failure. It results from a peripheral selective inhibition of COX-2 by paracetamol. Moreover, it appears that the use of paracetamol combined with NSAIDs is not beneficial because an increase in the occurrence of gastrointestinal events can be observed. On the other hand, *i.v.* administered paracetamol at high doses inhibits platelet aggregation, which is very important in the treatment of patients with disorders of hemostasis.

It should be remembered that despite the fact that paracetamol has a wide clinical application it is not a drug devoid of side effects. Therefore, before taking a decision about the treatment of the patient

with paracetamol, each time a balance of benefits and losses should be made so as to perform the adequate and efficient therapy. The aim of the present study was not to deny the rationality of paracetamol use but only to draw the attention of doctors prescribing this drug and pharmacists selling the drug as well patients taking it to the fact that this drug should be used only in situations which are indispensable. In the light of the contemporary research it is not possible to answer the question included in the title of the present study "Do we know all about paracetamol" but the nearest years will obviously provide the answer whether the decision taken in 1956 to introduce paracetamol as an OCT drug was correct.

Acknowledgment

REFERENCES

1. Chan A., Hepp P.: Centralbl. Klein. Med. 7, 561 (1886).
2. Morse H.N.: Ber. Deutscher Chem. Ges. 11, 232 (1878).
3. Von Mering J.: Ther. Monatsch. 7: 577 (1893).
4. Brodie B.B., Axelrod J.: J. Pharmacol. Exp. Ther. 94, 29 (1948).
5. Leung L.: J. Prim. Health Care 4, 254 (2012).
6. Ji P., Wang Y., Li Z., Doddapaneni S. et al.: J. Pharm. Sci. 101, 4383 (2012).
7. Howard S.S.: Pain Physician 12, 269 (2009).
8. Hinz B., Brune K.: J. Pharmacol. Exp. Ther. 300, 367 (2002).
9. Nowak J.Z., Dzielska-Olczak M.: Pulse of Medicine (Polish), educational issue, (2012).
10. Nowak J.Z.: Mil. Pharm. Med. 5, 33 (2012a).
11. Nowak J.Z.: Mag. Lek. Okul. 6, 57 (2012b).
12. Anderson B.J.: Pediatric Anesthesia 18, 915 (2008).
13. Aronoff D.M., Oates J.A., Boutaud O.: Clin. Pharmacol. Ther.79, 9 (2006).
14. Boutaud O., Aronoff D.M., Richardson J.H. et al.: Proc. Natl. Acad. Sci. USA 99, 7130 (2002).
15. Hinz B., Brune K.: Ann. Rheum. Dis. 71, 20, (2012).
16. Ouellet M., Percival M.D.: Arch. Biochem. Biophys. 387, 273 (2001).
17. Graham G.G., Scott K.F.: Inflammopharmacology 11, 401 (2003).
18. Flower R.J., Vane J.R.: Nature 240, 410 (1972).
19. Lanz R., Polster P., Brune K.: Eur. J. Pharmacol. 130, 105 (1986).
20. Swierkosz T.A., Jordan L., McBride M. et al.: Med. Sci. Monit. 8, 496 (2002).
21. Warner T.D., Vojnovic I., Giuliano F. et al.: J. Pharmacol. Exp. Ther. 310, 642 (2004).
22. Vane J.R.: Nat. New Biol. 231, 232 (1971).
23. Ferreira S.H., Moncada S., Vane J.R.: Nat. New Biol. 231, 237 (1971).
24. Smith J.B., Willis A.L.: Nat. New Biol. 231, 235 (1971).
25. Fu J.Y., Masferrer J.L., Seibert K. et al.: J. Biol. Chem. 265, 16737 (1990).
26. Xie W.L., Chipman J.G., Robertson D.L. et al.: Proc. Natl. Acad. Sci. USA 88, 2692 (1991).
27. Chandrasekharan N.V., Dai H., Roos K.L. et al.: Proc. Natl. Acad. Sci. USA 99, 13926 (2002).
28. Dinchuk J.E., Liu R.Q., Trzaskos J.M.: Immunol. Lett. 86, 121 (2003).
29. Kis B., Snipes J.A., Busija D.W.: J. Pharmacol. Exp. Ther. 315, 1 (2005).
30. Simmons D.L., Chandrasekharan N.V., Hu D. et al.: J. Pharmacol. Exp. Ther. 315,1412 (2005).
31. Ayoub S.S., Colville-Nash P.R., Willoughby D.A. et al.: Eur. J. Pharmacol. 538, 57 (2006).
32. Botting R.M.: J. Physiol. Pharmacol. 57, 113 (2006).
33. Botting R.M.: Pharmacol. Rep. 62, 518 (2010).
34. Schwab J.M., Beiter T., Linder J.U. et al.: FASEB J. 17, 2174 (2003).
35. Graham G.G., Scott K.F.: Am. J. Ther. 12, 46 (2005).
36. Hinz B., Cheremina O., Brune K.: FASEB J. 22, 383 (2008).
37. Hinz B., Dormann H., Brune K.: Arthritis Rheum. 54, 282 (2006).
38. Alloui A., Chassaing C., Schmidt J. et al.: Eur. J. Pharmacol. 443, 71 (2002).
39. Pickering G., Estčve V., Loriot M.A. et al.: Clin. Pharmacol. Ther. 84, 47 (2008).
40. Pickering G., Loriot M.A., Libert F. et al.: Clin. Pharmacol Ther. 79, 371 (2006).
41. Nakamura K., Li Y.Q., Kaneko T. et al.: Neuroscience 103, 763 (2001).
42. Högestätt E.D., Jönsson B.A.G., Ermund A.: J. Biol. Chem. 280, 31405 (2005).
43. Ottani A., Leone S., Sandrini M. et al.: Eur. J. Pharmacol. 531, 280 (2006).
44. Kelley B.G., Thayer S.A.: Eur. J. Pharmacol. 496, 33 (2004).
45. Zygmunt P.M., Chuang H., Movahed P. et al.: Eur. J. Pharmacol. 396, 39 (2000).
46. Bertolini A., Ferrari A., Ottani A. et al.: CNS Drug Rev. 12, 250 (2006).

47. Ovadia H., Wohlman A., Mechoulam R. et al.: Neuropharmacology 34, 175 (1995).
48. Autret E., Reboul-Marty J., Henry-Launois B. et al: Eur. J. Clin. Pharmacol. 51, 367 (1997).
49. Bjorkman R.: Acta Anaesthesiol. Scand. Suppl. 103, 1 (1995).
50. Bujalska M.: Pol. J. Pharmacol. 56, 605 (2004).
51. Smith H.S.: Pain Physician 12, 269 (2009).
52. Moller P.L., Sindet-Pedersen S., Petersen C.T. et al.: Br. J. Anaesth. 94, 642 (2005).
53. Pasero C., Stannard D.: Pain Management Nursing 13, 107 (2012).
54. Walson P.D., Jones J., Chesney R. et al.: Clin. Ther. 28, 762 (2006).
55. Graham G.G., Scott K.F., Day R.O.: Drug Safety 28, 227 (2005).
56. Davidson D.G., Eastham W.N.: Br. Med. J. 2, 497 (1966).
57. Mour G., Feinfeld D.A., Caraccio T. et al.: Ren. Fail. 27, 381 (2005).
58. Mahadevan S.B., McKiernan P.J., Davies P. et al.: Arch. Dis. Child. 91, 598 (2006).
59. Stirnimann G., Kessebohm K., Lauterburg B.: Swiss Med. Wkly. 140, w13080 (2010).
60. Waring W.S.: Expert Rev. Clin. Pharmacol. 5, 311 (2012).
61. Cannon C.P., Curtis S.P., FitzGerald G.A. et al.: Lancet 368, 1771 (2006).
62. Grèen K., Drvota V., Vesterqvist O.: Prostaglandins 37, 311 (1989).
63. O'Brien W.F., Krammer J., O'Leary T.D. et al.: Am. J. Obstet. Gynecol. 168, 1164 (1993).
64. Forman J.P., Stampfer, M.J., Curhan, G.C.: Hypertension 46, 500 (2005).
65. Chan A.T., Manson J.E., Albert C.M. et al.: Circulation 113, 1578 (2006).
66. Sudano I., Flammer A.J., Roas S. et al.: Curr. Hypertens. Rep. 14, 304 (2012).
67. Hinz B., Brune K.: Trends Pharmacol. Sci. 29, 391 (2008).
68. Munsterhjelm E., Munsterhjelm N.M., Niemi T.T. et al.: Anesthesiology 103, 712 (2005).
69. Rahme E., Barkun A., Nedjar H. et al.: Am. J. Gastroenterol. 103, 872 (2008).
70. Seppälä E., Nissilä M., Isomäki H. et al.: Clin. Rheumatol. 4, 315 (1985).
71. Bjørnsson G.A., Haanaes H.R., Skoglund L.A.: Br. J. Clin. Pharmacol. 55, 405 (2003).
72. Honoré P., Buritova J., Besson J.M.: Pain 63, 365 (1995).
73. Scialli A.R., Ang R., Breitmeyer J. et al.: Reprod. Toxicol., 30, 495 (2010a).
74. Scialli A.R., Ang R., Breitmeyer J. et al.: Reprod. Toxicol. 30, 508 (2010b).
75. Kang E.M., Lundsberg L.S., Illuzzi J.L. et al.: Obstet. Gynecol. 114, 1295 (2009).
76. Larson A.M., Polson J., Fontana R.J. et al.: Hepatology 42, 1364 (2005).
77. Heptonstall J.P.: B.M.J. 332, 795 (2006).
78. Brune K., Hinz B.: Ann. Rheum. Dis. 70, 1521 (2011).

ANALYSIS

AMPHETAMINES IN WASTEWATER OF THE CITY POZNAŃ (POLAND) - ESTIMATION OF DRUG ABUSE

PIOTR NOWICKI, JOLANTA KLOS and ZENON J. KOKOT*

Poznań University of Medical Sciences, Faculty of Pharmacy, Department of Inorganic and Analytical Chemistry, 6 Grunwaldzka St., 60-780 Poznań, Poland

Abstract: The aim of the study was to determine the profile of amphetamines consumed by a community in Poland. Amphetamine, methamphetamine and MDMA (ecstasy) were detected in wastewater samples collected from the main Wastewater Treatment Plant in the city of Poznań (about 687 000 people) using liquid chromatography/tandem mass spectrometry (LC-MS-MS). Back-calculations used in the sewage epidemiology approach were applied to estimate the level of consumption of the drugs being analyzed. These types of studies were carried out for the first time in Poland for a considerable period – from June 2009 to December 2010. The analysis of variance (ANOVA) confirmed significant monthly differences in amphetamine consumption. The concentration of amphetamine, methamphetamine and MDMA in wastewater samples and the levels of their consumption were lower than reported in other European countries, but unexpectedly, the ratio of consumed methamphetamine to MDMA and the consumption level of methamphetamine were relatively high. This study shows that sewage epidemiology is a promising tool, especially when combined with classical methods, to estimate illicit drugs use in a particular population. Therefore, efforts should be made to monitor the profiles and consumption levels of drugs and to extend the scope of the research to other illicit substances, especially cannabinoids and cocaine.

Keywords: illicit drugs, amphetamines, wastewater, HPLC-MS/MS

Consumption of illicit drugs is increasing each year, with some changes in the profile of the drugs used. The available data concerning drug consumption are published in the national and European reports. Official figures of the prevalence of drug abuse are currently derived from population surveys integrated with crime statistics, medical records, drug production, and seizure rates. However, such an estimation of illicit drugs consumption only gives the general picture and is very subjective as it is based on information from the consumers themselves. Moreover, surveys are expensive to conduct and only a few European countries collect information every year, although there are some differences in their methodology, so results should be interpreted with caution.

According to the European Monitoring Centre for Drugs and Drug Addiction Annual Report 2010 (1), cannabis remains the most popular illicit drug in Europe, although levels of consumption differ considerably between countries. In the eastern countries, the prevalence level of cannabis consumption is increasing and often exceeds the level found in Western Europe. Cocaine is the second most commonly used illicit drug in Europe at a high and still rising level. The problem of amphetamine use is mainly reported by countries in northern Europe, although methamphetamine use remains largely restricted to the Czech Republic and Slovakia, as well as their neighboring countries. In many eastern countries amphetamine (or methamphetamine) remains the most commonly used stimulant drug. Based on surveys conducted in Poland in 2008, cannabis and amphetamine are the most commonly used illicit drugs (1, 2).

Within the last few years a new approach, termed 'sewage epidemiology', has been applied in order to estimate the consumption levels of illicit drugs recommended by EMCDDA. This method proposed by Daughton and Thernes (1999) was first implemented by the Zucatto research group (3-5) to estimate the level of consumption of cocaine in some Italian cities, and was based on an analysis of surface and wastewater samples. Such investiga-

tions have been conducted in the last few years in other European countries, such as Belgium (6-8), United Kingdom (9), Italy - Florence (10), Spain (11-13), Croatia (14), and Switzerland (15), as well as in Canada (16) and the United States of America (17). Combined with a classical population survey approach, this will provide an integrated and powerful tool not only for studying drug use trends in the population, but also for assessing the effectiveness of various treatments applied for drug abuse prevention.

The new methodology provides the possibility of monitoring the consumption levels of illicit drugs in a specific area over a long period of time and for making comparisons with national reports based on the population surveys. The sewage approach was first applied in this area of Poland and is especially valuable because of the length of time required for such investigations.

EXPERIMENTAL

Wastewater samples

The study was performed in Poznań, Poland's fifth largest city. The samples were collected from the central wastewater treatment plant, which, at the time served almost the whole city including its suburbs, in total about 687 000 people. Two wastewater samples (10 L each) were collected twice a week, on Monday and on Wednesday, from June 2009 to December 2010. All samples were collected at the same point before any chemical and physical treatment, with the exception of sedimentation, and the mean flow rate was 130 000 m^3/day. Analysis of the samples was performed the same day immediately after collection.

Reagents

All pure standards: amphetamine, methamphetamine, 3,4-methylenedioxyamphetamine (MDA), 3,4-methylenedioxymethamphetamine (MDMA or ecstasy), 3,4-methylenedioxyethylamphetamine (MDEA) and their deuterated molecules used as internal standards: amphetamine-d_6, methamphetamine-d_9, MDA-d_5, MDEA-d_5 and MDMA-d_5 were purchased from Certilliant, a Sigma-Aldrich Company. The standards (solutions in methanol (1 mg/mL)) were diluted to 10 ng/μL with methanol and stored in the dark at -20°C. All other reagents were acquired from J.T. Baker (USA).

Sample treatment and analysis

Samples were filtered on a glass microfiber filter GF/A 1.6 μm (Whatman, Kent, U.K.), prior to extraction were spiked with 15 ng of each internal standard and the pH was adjusted to 7.0 ± 0.4 with phosphate buffer (pH = 7.0). Solid-phase extraction of the substances being analyzed was performed using Bakerbond Narc-2 mixed mode cartridges, which were conditioned with methanol (2 mL) followed by deionized water (2 mL) and then by phosphate buffer (2 mL, 0.1 M, pH 7.0). Next, the sample was passed through the cartridges under a vacuum at a flow rate of 10 mL/min. When the sample was eluted under gravity, the column was washed with deionized water (2 mL) followed by hydrochloric acid (0.1 M, 0.5 mL) and then by methanol (0.5 mL). A vacuum was applied and the cartridges were dried for 20-30 min. The analytes were eluted into a vial with a mixture of chloroform : isopropanol : ammonium hydroxide (80 : 30 : 3.2 mL). The eluates of two samples (each 10 L) were pooled and dried under a nitrogen stream.

Liquid chromatography – tandem mass spectrometry

The pooled and dried samples were redissolved in 200 μL of mobile phase, centrifuged and transferred into glass vials for instrumental analysis. Twenty microliters of the solution were injected in the LC-MS spectrometer (Agilent HPLC 1200 series, 6410B Triple Quad LC/MS System). Chromatographic separation was performed using a capillary column (Agilent Zorbax XDBC18, 4.6 × 50 mm × 1.8 μm) at a flow rate of 0.45 mL/min. The mobile phase were solutions: water with formic buffer (pH~3.2) and acetonitrile with a gradient from 10 to 70% of acetonitrile (6.5 min.). The capillary voltage was 4000 V, the temperature was 300°C, the auxiliary and collision gas was N_2. The collision energy and tube lens were optimized separately for each analyte and standards. All selected analytes were analyzed in positive ionization mode (ESI+). Identification and quantification were performed using two characteristic transitions in multiple-reaction monitoring (MRM) mode for the fragmentation products of the protonated or deprotonated pseudomolecular ions of each substance and each deutered analogue (Tab. 1).

A 8-point calibration curve was constructed at 4, 8, 12, 16, 20, 24, 28 and 32 ng for amphetamine, methamphetamine, MDA and MDMA and the solutions were spiked with 30 ng of all internal standards. Validation was carried out according to the Funk methodology (18), including testing homogeneity, linearity, homogeneity of variances (precision), outliers and securing the lower range limit. The matrix effect was determined by analyzing 50

Table 1. Conditions for MRM determination of illicit drugs.

Substance	Retention time (min)	Fragmentor voltage	Precursor ion m/z	Product ion I m/z and collision energy (eV)	Product ion II m/z and collision energy (eV)
Amphetamine-d$_6$	3.4	60	142.1	125.1 (8)	93.1 (17)
Amphetamine	3.4	70	136	119.1 (5)	91.1 (17)
MDA-d$_5$	3.6	70	185.1	168.1 (5)	110.1 (21)
MDA	3.6	60	180.1	163 (5)	105.1 (21)
Methamphetamine-d$_9$	3.8	80	159.2	125.1 (5)	93.05 (17)
Methamphetamine	3.8	80	150.1	119.1 (8)	91 (17)
MDMA-D5	3.9	80	199.1	165 (9)	107.1 (25)
MDMA	3.9	80	194.1	163.1 (5)	105.1 (25)

Table. 2. Validation according to Funk (DIN 32645).

Substance	a	b	Residual standard deviation	Process standard deviation	Process variation coefficient (%)	Decision limit DL (ng/L)	Detection limit LOD (ng/L)	Quantification limit (LOQ) (ng/L)
	y = bx + a					(DIN 32645)		
Amphetamine	531	1270	2.57	0.20	1.12	0.36	0.71	1.07
						range 1 - 2.4		
Methamphetamine	15555	126.7	6.96	0.55	3.06	0.81	1.65	2.32
						range 3.5 – 7		
MDMA	40.28	1143	6.09	1.11	6.09	0.89	1.77	2.66
						range 3 - 4.8		

mL of wastewater samples spiked with internal standards. The recoveries for the whole process of sample preparation, filtration and extraction were set within the range 0.80-0.93. The detection limits (LOD) and quantification limits (LOQ) for the whole method were calculated by spiking wastewater samples with different amounts of the substances analogously, just as on the calibration curve. The results of all validation activities are shown in Table 2.

Back-calculation of community drug use

Estimation of community drug use was done according to the method described by Zuccato et al. [3] (Fig. 1). Because surveys conducted in Poland show that amphetamine is a commonly used illicit drug, a group of amphetamine-like stimulants was chosen for analysis (amphetamine, methamphetamine, MDA, MDMA, MDEA). In the case of amphetamines, the substances which are used as drug target residues (DTR) are the parent drugs, because all are excreted mainly as unchanged compounds. The concentrations of these substances were very low, and therefore the dried residues of two untreated wastewater samples (each 10 L) after filtration and SPE extraction were pooled and combined by redissolving them in a mobile phase to perform HPLC-MS-MS analysis. The mean concentrations of DTR in ng/L of all samples collected in one month were multiplied by the mean flow monthly rate in the Wastewater Treatment Plant (WWTP) to give the amount of DTR (grams) discharged per month. This value was then divided by the number of people served by the WWTP to estimate the grams of DTR excreted in wastewater per person per month and finally normalized to a value of grams per month per 1000 people. Cocaine consumption was originally estimated by Zuccato from the data for its major metabolite, benzoylecgonine (BE), so a molar ratio of 1.05 was applied to compensate for the higher molecular weight of BE compared with cocaine. In the case of amphetamines the parent drug is determined and therefore the molar ratio is 1, so the correction factor for the estimation takes into consideration only the percentage of the drug dose excreted as DTR (for amphetamine it is 30, for
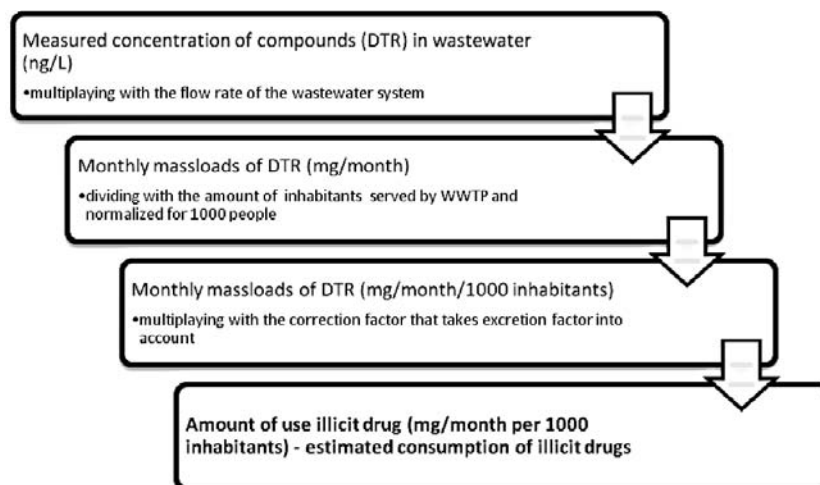
Figure 1. Scheme of the overview of applied back-calculations in the sewage epidemiology approach
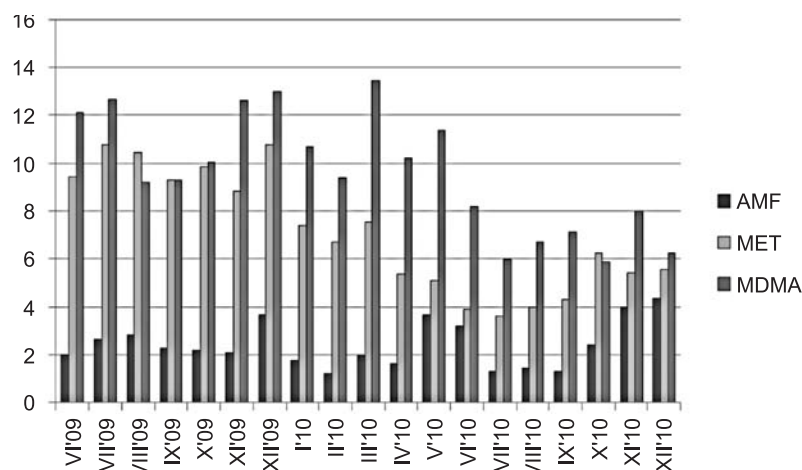
Figure 2. Mean loads DTR/mg/month/1000 people from June 2009 to December 2010 for amphetamine (AMF), methamphetamine (MET) and MDMA (ecstasy)

methamphetamine 43 and for MDMA 65). Correction factors (the fraction of the consumed parent drug extracted as DTR in urine and the parent drug-to-DTR molar mass ratio) were 3.3 for amphetamine, 2.3 for methamphetamine and 1.5 for ecstasy. Finally, the amount of illicit drugs consumed monthly by 1000 people was estimated.

Because of the procedure and the low concentrations of compounds analyzed (DTR), only monthly levels of consumption could be compared and the significance of monthly differences was checked by ANOVA analysis of variance. There was no possibility to observe the daily profile of illicit drugs consumed.

It is also possible to estimate the number of doses consumed by the local community (1000 people) per day or month by dividing the consumption value by a single typical dose for each illicit drug. The typical oral dose for amphetamine and methamphetamine is 30 mg, but for MDMA (ecstasy) it is 100 mg. However, it is recommended to focus on the amount of illicit drugs estimated for 1000 people per day or the amount of DTR excreted per day per 1000 people and these results should be monitored for a period of time to give an objective insight into the level and profile of illicit drugs consumed by the local community.

Table 3. Results of determination of amphetamine (AMF), methamphetamine (MET) and MDMA (ecstasy) and estimated consumption.

Month	Concentration (ng/L)			DTR mass loads mg/month/1000 ppl			Drug consumption mg/month/1000 ppl			Number of doses dose/month/1000 ppl		
	AMF (± 0.03)	MET (± 0.07)	MDMA (± 0.07)	AMF	MET	MDMA	AMF	MET	MDMA	AMF	MET	MDMA
Jun'09	0.25	1.22	1.56	1.99	9.42	12.12	6.573	21.66	18.18	0.22	0.72	0.14
Jul'09	0.32	1.35	1.54	2.64	10.78	12.64	8.70	24.78	18.96	0.29	0.82	0.14
Aug'09	0.40	1.46	1.29	2.84	10.42	9.21	9.37	23.98	13.82	0.31	0.80	0.10
Sep'09	0.34	1.38	1.38	2.27	9.30	9.27	7.49	21.40	13.91	0.25	0.71	0.10
Oct'09	0.30	1.37	1.39	2.18	9.83	10.04	7.22	22.61	15.06	0.24	0.75	0.11
Nov'09	0.30	1.26	1.82	2.18	8.84	12.61	7.22	20.34	18.92	0.24	0.68	0.14
Dec'09	0.48	1.41	1.71	3.64	10.76	13.00	12.02	24.76	19.50	0.40	0.82	0.15
Jan'10	0.34	1.41	2.03	1.78	7.42	10.69	5.89	17.06	16.04	0.19	0.57	0.12
Feb'10	0.25	1.37	1.92	1.24	6.70	9.39	4.09	15.40	14.08	0.14	0.51	0.11
Mar'10	0.27	1.03	1.83	1.97	7.56	13.44	6.52	17.38	20.16	0.22	0.58	0.15
Apr'10	0.29	0.96	1.83	1.63	5.38	10.21	5.40	12.38	15.31	0.19	0.41	0.12
May'10	0.59	0.81	1.82	3.68	5.08	11.39	12.13	11.68	17.01	0.40	0.39	0.13
Jun'10	0.69	0.83	1.75	3.22	3.90	8.20	10.63	8.97	12.31	0.35	0.30	0.09
Jul'10	0.25	0.69	1.14	1.32	3.60	5.97	4.38	8.28	8.96	0.15	0.27	0.07
Aug'10	0.24	0.66	1.12	1.43	3.99	6.72	4.73	9.19	10.08	0.16	0.31	0.08
Sept'10	0.23	0.76	1.27	1.32	4.30	7.14	4.36	9.89	10.71	0.14	0.33	0.08
Oct'10	0.48	1.24	1.17	2.43	6.24	5.90	8.02	14.36	8.85	0.27	0.48	0.06
Nov'10	0.64	0.87	1.29	3.97	5.41	8.02	13.11	12.44	12.02	0.44	0.41	0.09
Dec'10	0.71	0.91	1.02	4.34	5.58	6.27	14.32	12.83	9.41	0.47	0.43	0.07

RESULTS

The results of a nineteen-month study of wastewater concerning amphetamine, methamphetamine and MDMA (ecstasy) are reported in Table 3 and Figure 2. The bar graph presents population-standardized DTR mean monthly loads collected from June 2009 to December 2010. As far as analysis of very low concentration is concerned, in this case it was necessary to perform validation of the analytical process. Table 2 contains basis figures related to the quality assurance of quantification. Table 3 presents figures calculated according to the method given in the calculation chapter, i.e., monthly DTR loads, drug consumption of amphetamines (also referred to as collective drug consumption rates) and estimated doses consumed per 1000 people. For the correct interpretation of increasing or decreasing tendencies, data grouped by month were analyzed by a one-way ANOVA and Multiple Comparison Test. The results of this analysis are presented in Table 4 and in Figure 3. ANOVA shows significant differences between the means of monthly DTR loads (mg/month/1000 people) except for February-July-September 2010 and June 2009-March 2010 in the case of amphetamine, and April-September 2010 and August-December 2009 in the case of methamphetamine.

As far as amphetamine is concerned, an increase was noted in December 2009, May and June 2010 and another increase in the monthly load of amphetamine was noticeable in November and December 2010. A decrease in amphetamine use was observed in February 2010 and from June to September 2010.

As far as methamphetamine is concerned, there is a visible decreasing tendency in monthly loads from June 2009 to July 2010 with the exception of December 2009 when a single increase was observed. There was an increase in DTR mass loads from August 2010 to the end of research but this was significantly smaller than in the initial period of monitoring.

MDMA DTR mass loads showed the highest values in June and July 2009 compared to November to December 2009. Two increases were recorded in 2010, namely in March and May. From June 2010 to the end of the research, a downward trend was observed.

DISCUSSION

Monitoring of any figures connected with DTR extraction loads or estimated local community consumption of the drugs analyzed showed that this method can detect any fluctuations and trends in consumption that occur during the course of a week, month or year (depending on the methods of sampling). The analysis of profiles of drugs consumed which are summarized in Table 3 or in a bar graph (Fig. 2) showed an increase in amphetamine and methamphetamine consumption during the traditional periods of examinations at high schools and universities and institutions at higher education level i.e., November-December and May-June. As for ecstasy, the increase in consumption is visible in November, December, May, June as well as in the

Table 4. Results of analysis of variance ANOVA.

	Sums of squares (SS)	Degree of freedom (dF)	Mean squares (SS/df) (MS)	F-statistics	Prob > F (p)
	Amphetamine				
Columns	65.9156	18	3.66198	13902.48	5.24361e-097
Error	0.015	57	0.00026		
Total	65.9307	75			
	Methamphetamine				
Columns	449.216	18	24.9564	106918.78	2.97059e-122
Error	0.013	57	0.0002		
Total	449.229	75			
	MDMA				
Columns	452.88	18	25.16	187006.79	3.57393e-129
Error	0.008	57	0.0001		
Total	452.887	75			
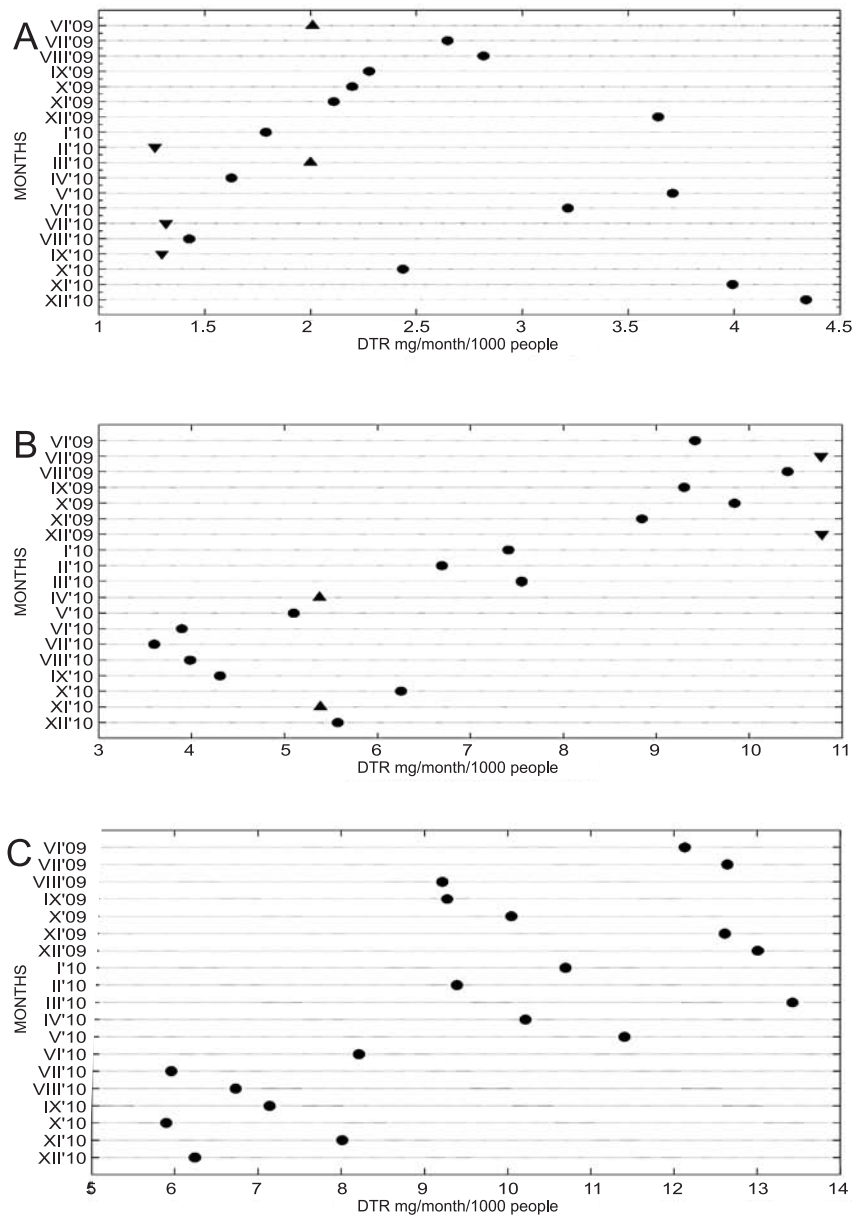
Figure 3. **A**. Amphetamine. **B.** Methamphetamine. **C.** MDMA (ecstasy). Multiple comparisons. Visualization of the difference between group means (DTR loads/mg/month/1000 people). Triangle in the vertical line - no significant difference, circle – significant difference

June-July holiday period. In the case of all three amphetamines, there is a noticeably rapid decrease (April 2010 to July) followed by increasing consumption to December 2009-end of research. It is hard to explain this phenomena but the authors connect this information with the closing down of all designer drug shops in Poland in October 2010. Following this, the small increase can be related to the lack of availability of designer drugs on the market.

Our data prove that amphetamines are commonly present in wastewater and they can be used as a valuable and exact parameter to estimate profile, tendency and consumption figures. These parameters are good tools for evaluating the efficiency of anti-drug activities and the validity of expenditures on individual projects. Comparisons of the estimated values of doses consumed per 1000 people with the results from other European countries reveal that there is a low level of daily consumption of amphet-

amine and MDMA in our city. It should be indicated that the ratio of methamphetamine to MDMA consumed is much higher than in other countries and there is unexpected and relatively high level of consumption of methamphetamine compared with other amphetamines. Such a discrepancy in the level of consumption is hard to explain, because the general consensus is that amphetamine is the far more widely consumed drug. It is important to remember that this research was carried out during a period when the designer drug trade flourished in Poland. Furthermore, according to the National Bureau for Drug Prevention, there has recently been a significant increase in the production and consumption of methamphetamine in Czech Republic due to the liberal laws there. Moreover, the latest police reports of the discovery of an alleged methamphetamine manufacturing laboratory in Poznań seem to confirm the results of this study.

There is also an agreement between surveys conducted by the National Bureau in 2009 (2) and our research, namely that amphetamines are among the most commonly used illicit drugs in Poland. However, the profile of amphetamines consumed was investigated here for the first time. It will be interesting to determine the level of illicit drugs in wastewater samples over a long period of time to monitor the changes in profiles and the levels of drug consumption and to extend the scope of the research to other substances, especially to cannabinoids and cocaine.

CONCLUSIONS

"Sewage epidemiology" is a powerful tool to monitor the levels and profile of illicit drugs consumed by the local community and it has been already applied successfully by research groups in many countries. Compared with surveys, this methodology gives an objective picture of the drug abuse and constitutes a real-time approach to estimate the consumption of illicit drugs in a given area. For the first time in Poland, such an investigation was carried out over a relatively long period of time, from June 2009 to December 2010 and the results are published. The concentrations of three amphetamines were determined in a wastewater samples from a large Polish city, Poznań. The levels of consumption of amphetamine, methamphetamine and MDMA were lower than in other European countries, but the levels of methamphetamine and MDMA were relatively higher compared with the level of amphetamine consumption. Our study proved that the profile and the levels of

consumption of illicit drugs in our country might be quite different from those in the Western Europe.

Acknowledgments

REFERENCES

1. EMCDDA (European Monitoring Centre for Drugs and Drug Addiction). Annual Report 2010. The state of the drug problem in Europe. Lisbon: EMCDDA, 2010. http://www. emcdda.europa.eu/publications/annual-report/2010

2. Malczewski A., Kidawa M., Struzik M., Strzelecka A., 2010. EMCDDA. National Report (2009 data) to the EMCDDA by the Retinox National Focal Point. Poland. New Development, Trends and in-depth information on selected issues. http://www.emcdda.europa. eu/html.cfm/index142525EN.html

3. Zuccato E., Chiabrando C., Castiglioni S., Calamari D., Bagnati R., Schiarea S., Fanelli R.: Environ. Health Glob. 4, 1 (2005)

4. Zuccato E., Chiabrando C., Castiglioni S., Calamari D., Bagnati R., Schiarea S., Fanelli R.: Environ. Health Perspect. 116, 1027 (2008).

5. Zuccato E., Castiglioni S., Bagnati R., Chiabrando C., Grassi P., Fanelli R: Water Res. 42, 961 (2008).

6. van Nuijs A.L.N., Pecceu B., Theunis L., Dubois N., Charlier C., Jorens P.G., Bervoets L., Blust R., Neels H., Covaci A.: Environ. Pollut. 157, 123 (2009).

7. van Nuijs A.L.N., Mougel J.F., Tarcomnicu I., Bervoets L., Blust R., Jorens P.G., Neels H., Covaci A.: Environ. Int. 37, 612 (2011).

8. Tarcomnicu I., van Nuijs A.L.N., Simons W., Bervoets L., Blust R., Jorens P.G., Neels H., Covaci A.: Talanta 83, 795 (2011).

9. Kasprzyk-Hordern B., Dinsdale R.M., Guwy A.J.: Environ. Pollut. 157, 1773 (2009).

10. Mari F., Politi L., Biggeri A., Accetta G., Trignano C., Di Padua M., Bertol E.: Forensic Sci. Int. 189, 88 (2009).

11. Boleda R.M., Galceran M.T., Ventura F.: Water Res. 43, 1126 (2009).

12. Bijlsma L., Sancho J.V., Pitarch E., Ibáñez M., Hernández F.: J. Chromatogr. A 1216, 3078 (2009).

13. Bueno M.M.J., Ucles S., Hernando M.D., Fernandez-Alba A.R.: Talanta 85, 157 (2011).

14. Terzic S., Senta I., Ahel M.: Environ. Pollut. 158, 2686 (2010).

15. Berset J.D., Brenneisen R., Mathieu C.: Chemosphere 81, 859 (2010).

16. Metcalfe C., Tindale K., Li H., Rodayan A., Yargeau V.: Environ. Pollut. 158, 3179 (2010).

17. Burlet-Hunt S.L., Snow D.D., Damon T., Shockley J., Hoagland K.: Environment. Pollut. 157, 786 (2009).

18. Funk W., Dammann V., Donnevert G.: Quality Assurance in Analytical Chemistry, Wiley-VCH Verlag GmbH, Weinheim 2007.

DRUG BIOCHEMISTRY

3,5-DIMETHOXY-(4-METHOXYPHENYL)BENZAMIDE SUPPRESSES ADIPOGENESIS IN 3T3-L1 CELLS

JIN TAEK HWANG[1], SANGHEE KIM[2], INWOOK CHOI[1] and SANG YOON CHOI[1]*

[1]Korea Food Research Institute, Seongnam 463-746, Republic of Korea
[2]College of Pharmacy, Seoul National University, Seoul 152-742, Republic of Korea

Abstract: In this study, the adipogenesis-suppressing effect of 3,5-dimethoxy(4-methoxyphenyl)benzamide (DMPB), a derivative of the anti-obesity substance resveratrol, was measured in 3T3-L1 cells. The results show that DMPB effectively suppressed the hormone-induced differentiation of 3T3-L1 cells, compared to resveratrol at the same concentration, and reduced the protein expression of fatty acid synthase and acetyl-CoA carboxylase. In addition, DMPB was observed to decrease the PPAR-γ transcription activity, which was increased by rosiglitazone, in a concentration-dependent manner. From the above results, it is considered that DMPB shows strong potential as an anti-obesity substance.

Keywords: adipogenensis, antiobesity, resveratrol derivative, PPAR-γ, FAS, ACC

Obesity is characterized by increasing the number and size of adipocytes due to hormonal changes and imbalances in the energy metabolism caused by excessive fat intake (1, 2). Obesity is a major factor in the development of heart disease, cancer, hypertension, diabetes, and degenerative arthritis (3-5). 3T3-L1 cell, a fibroblast cell has been widely used in obesity research, and can differentiate into an adipocyte under appropriate conditions (6, 7). Peroxisome proliferator-activated receptor γ (PPAR-γ) is an important factor for developing adipocyte and is a target for insulin sensitizing drugs as glitazones. Activation of PPAR-γ by glitazones leads to fatty acids in the adipocytes. Fat accumulation also leads to an increase in the gene expression of fatty acid synthase (FAS) and fatty acid-binding protein 4 (FABP4), which are responsible for fat synthesis, transport and deposit (8). Therefore, it is of interest to modulate adipocyte differentiation through regulating these transcriptional factors.

In fact, the International Obesity Task Force has estimated that one third of the world's population will become obese (BMI >30 kg/m^2) within the next 20 years or so if the present trend of increasing incidence of obesity continues. However, because the currently used anti-obesity drugs - such as orlistat, sibutramine and sertraline - have several reported side effects (9), research and development of anti-obesity substances to replace these drugs are being actively conducted.

With regard to natural anti-obesity substances, resveratrol and genistein, which are contained in grapes and beans, respectively, have been reported as having anti-obesity effects (10-12). Resveratrol, a kind of stilbene present in nature, is a phytoalexin that is naturally synthesized in some plants against the attacks of pathogens such as bacteria and fungi (13). In this study, the adipogenesis-suppressing activity of 3,5-dimethoxy-(4-methoxyphenyl)benzamide (DMPB), a derivative of resveratrol, was measured in 3T3-L1 cells as part of the search for new anti-obesity substances, and its excellent anti-obesity-related activity was confirmed.

EXPERIMENTAL

Materials

DMPB was synthesized by the method previously reported (14). Resveratrol was purchased from Sigma-Aldrich (Fig. 1); 3T3-L1 cells were from the American Type Culture Collection (Manassas, VA); FAS and acetyl-CoA carboxylase (ACC) antibodies were from Cell Signaling Technology and a PPAR-γ transcription factor assay kit was from Cayman Chemical.

* Corresponding author: e-mail: sychoi@kfri.re.kr; phone: +82-31-780-9307; fax: +82-31-709-9876

Cell culture

The 3T3-L1 fibroblast cells were cultured using Dulbecco's modified Eagle's medium (DMEM) culture medium containing 10% FBS, at 37°C, 5% CO_2.

Adipocyte differentiation-suppressing activity

The 3T3-L1 cells were grown and placed in a 48-well plate and treated with a hormone mixture (10 µg/mL insulin, 0.5 µM dexamethasone, and 0.5 mM isobutylmethylxanthine) for 48 h, and then transferred to DMEM medium containing insulin. Each sample was treated for 8 days and observed for adipocyte differentiation. Upon completion of differentiation, the cells were washed with PBS twice and then fixed with 3.7% formaldehyde. After incubating the cells for 1 h using Oil Red O dye, isopropanol was added, and absorbance was
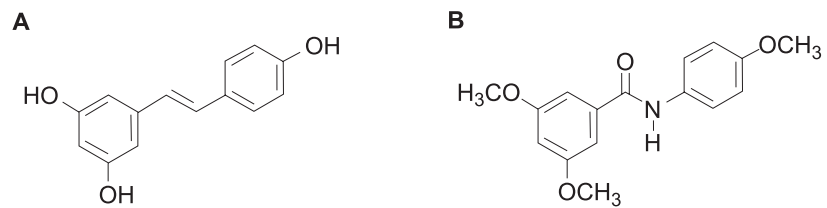
Figure 1. Chemical structure of resveratrol (**A**) and DMPB (**B**).
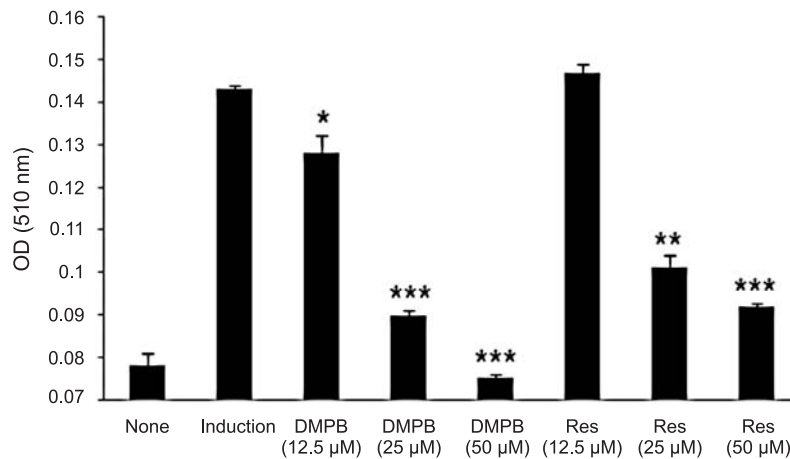
Figure 2. Inhibitory effect of DMPB on 3T3-L1 adipocyte differentiation. Induction: hormone mixture treated group. DMPB: hormone mixture and DMPB treated group. Res: hormone mixture and resveratrol treated group. Data are the mean ± SD values of three experiments. *p < 0.05, **p < 0.01, ***p < 0.001 compared with the Induction group

Figure 3. The morphology of 3T3-L1 cells treated with a hormone mixture and DMPB. Induction: hormone mixture treated group. DMPB: hormone mixture and DMPB treated group

measured at 510 nm to estimate the amount of triglycerides.

FAS and ACC expression

The 3T3-L1 cells were washed twice with ice-cold PBS and then lysed with lysis buffer (50 mM Tris-HCl, 1% Triton X-100, 0.5% sodium deoxycholate, 150 mM NaCl, 1 mM EDTA, 1 mM PMSF, 1 mM sodium orthovanadate, 1 mM NaF, and 0.2% protease inhibitor cocktail, pH 7.2). The collected protein was centrifuged at 14.000 rpm for 5 min, whereupon the supernatant was collected for protein quantification. Next, 30 μg of the protein was loaded in 10% SDS-PAGE for electrophoresis, transferred to a nitrocellulose membrane and reacted with ACC antibodies (1 : 500) or FAS antibodies (1 : 1000), and then detected by enhanced chemiluminescence (ECL).
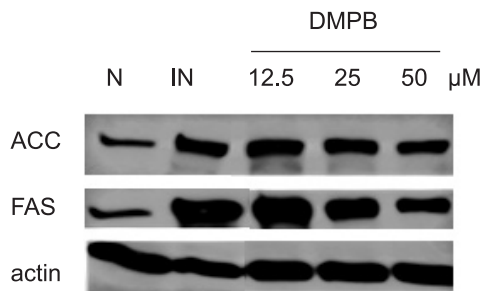
Figure 4. Effects on the intracellular level of ACC and FAS in 3T3-L1 cells. Induction: hormone mixture treated group. DMPB: hormone mixture and DMPB treated group.

PPAR-γ transcription activity

The effect of DMPB on PPAR-γ in 3T3-L1 cells was measured using a PPAR-γ transcription factor assay kit (Cayman Chemical). The 3T3-L1 cells were treated with rosiglitazone 80 μM and each concentration of DMPB, and then the cell extract was added to a dsDNA sequence-coated plate. The PPAR-γ antibodies and the secondary antibodies were reacted in order, and then a detection reagent was added and absorbance was measured at 450 nm.

Statistical analysis

Data are the mean ± SD values from three independent experiments. Statistical significance of the obtained data was determined by Student's *t*-test.

RESULTS AND DISCUSSION

Inhibitory effect on adipocyte differentiation

After confirming the absence of cytotoxicity in DMPB at concentrations less than 50 μM, the effect of DMPB on adipocyte differentiation was measured and compared with that of resveratrol, as shown in Figure 2. DMPB suppressed the hormone mixture-induced differentiation of adipocytes from 3T3-L1 cells in a concentration-dependent manner, and even strongly suppressed the differentiation at a concentration of 50 μM, as with the non-treated group. In particular, DMPB demonstrated higher adipocyte differentiation suppressing activity at all concentrations compared to resveratrol at the same concentrations. The morphology 3T3-L1 cells treat-
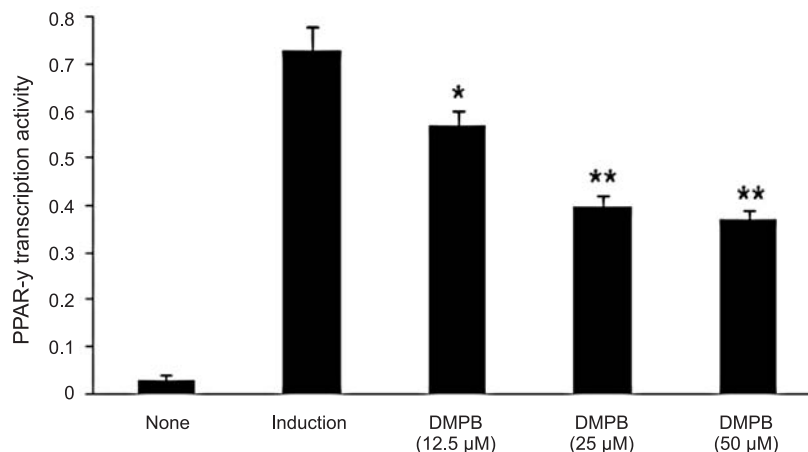
Figure 5. Inhibitory effect of DMPB on PPAR-γ transcriptional activity. Induction: rosiglitazone treated group. DMPB: rosiglitazone and DMPB treated group. Data are the mean ± SD values of three experiments. *p < 0.05, **p < 0.01, compared with the Induction group

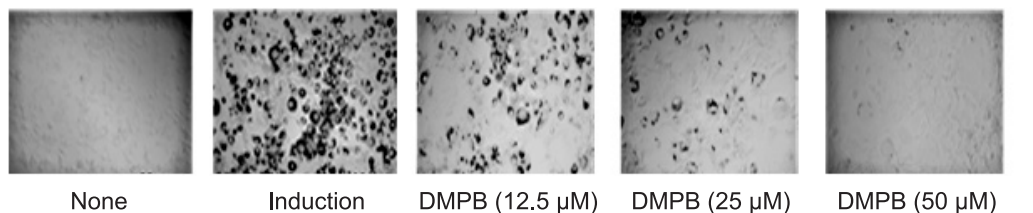ed with a hormone mixture and DMPB are shown in Figure 3.

FAS and ACC expression suppressing effect

Fat is composed of fatty acids and glycerol. During the initial stage of fatty acid synthesis in the cell, acetyl-CoA carboxylase (ACC), which is a critical enzyme in the process, induces carboxylation of acetyl-CoA and promotes the production of malonyl-CoA (15-17). Fatty acid is synthesized by the action of FAS, an enzyme with MW 250 kDa, from malonyl-CoA as a substrate (18, 19). Therefore, it is expected that FAS and ACC inhibitors can effectively reduce lipid production and suppress obesity. The effect of DMPB on the expression of fatty acid metabolism-related proteins such as FAS and ACC, the major factors in the suppression of obesity, was measured as shown in Figure 4. DMPB reduced the increase in the production of FAS and ACC in 3T3-L1 cells induced by a hormone mixture in a concentration-dependent manner. Thus, it can be stated that DMPB reduces lipid production by suppressing fatty acid biosynthesis.

PPAR-γ activity suppressing effect

PPAR-γ is known as a glitazone receptor which controls fatty acid storage and glucose metabolism (20). Because genes activated by PPAR-γ promote the uptake of fatty acid and glucose for its conversion to fatty acids in adipocytes and so deposition of triacylglycerols in these cells to induce obesity, a substance that suppresses PPAR-γ could exhibit an anti-obesity effect (21). The effect of DMPB on PPAR-γ in 3T3-L1 cells was measured, and was observed to suppress the activation of PPAR-γ by rosiglitazone in a concentration-dependent manner (Fig. 5). Thus, it is considered that DMPB reduces fatty acid production by reducing the production of FAS and ACC, while simultaneously suppressing fat absorption by inhibiting PPAR-γ activity.

REFERENCES

1. Field B.C., Chaudhri O.B., Bloom S.R.: Br. J. Clin. Pharmacol. 68, 830 (2009).
2. Roth J., Szulc A.L., Danoff A.: Am. J. Clin. Nutr. 93, 875 (2011).
3. Adams K.F., Schatzkin A., Harris T.B., Kipnis V., Mouw T., Ballard-Barbash R., Hollenbeck A., Leitzmann M.F.: N. Engl. J. Med. 355, 763 (2006).
4. Horwich T.B., Fonarow G.C.: J. Am. Coll. Cardiol. 55, 283 (2010).
5. Strazzullo P., D'Elia L., Cairella G., Garbagnati F., Cappuccio F.P., Scalfi L.: Stroke 41, 418 (2010).
6. Rosen E.D., Spiegelman B.M.: Annu. Rev. Cell Dev. Biol. 16, 145 (2000).
7. Kiess W., Petzold S., Töpfer M., Garten A., Blüher S., Kapellen T., Körner A., Kratzsch J.: Best Pract. Res. Clin. Endocrinol. Metab. 22, 135 (2008).
8. Kim G.S., Park H.J., Woo J.H., Kim M.K., Koh P.O., Min W., Ko Y.G. et al.: BMC Complement. Altern. Med. 12, 1 (2012).
9. Bray G.A.: Clin. Chest Med. 30, 525-538 (2009).
10. Zhang M., Ikeda K., Xu J.W., Yamori Y., Gao X.M., Zhang B.L.: Phytother. Res. 23, 713 (2009).
11. Baile C.A., Yang J.Y., Rayalam S., Hartzell D.L., Lai C.Y., Andersen C., Della-Fera M.A.: Ann. N. Y. Acad. Sci. 1215, 40 (2011).
12. Behloul N., Wu G.: Eur. J. Pharmacol. 698, 31 (2013).
13. Voloshyna I., Hussaini S.M., Reiss A.B.: J. Med. Food 15, 763 (2012).
14. Choi S.Y., Hwang J.S., Kim S., Kim S.Y.: Biochem. Biophys. Res. Commun. 349, 39 (2006).
15. Tong I.: Cell Mol. Life Sci. 62, 1784 (2005).
16. Kreuz S., Schoelch C., Thomas L., Rist W., Rippmann JF., Neubauer H.: Diabetes Metab. Res. Rev. 25, 577 (2009).
17. Wakil S.J., Abu-Elheiga L.A.: J. Lipid Res. 50, 138 (2009).
18. Ronnett G.V., Kim E.K., Landree L.E., Tu Y.: Physiol. Behav. 85, 25 (2005).
19. Wolfgang M.J., Lane M.D.: J. Biol. Chem. 281, 37265 (2006).
20. Anghel S.I., Bedu E., Vivier C.D., Descombes P., Desvergne B., Wahli W.: J. Biol. Chem. 282, 29946 (2007).
21. Grun F., Blumberg B.: Endocrinology 147, 50 (2006).

ANTIMICROBIAL PEPTIDES AS POTENTIAL TOOL TO FIGHT BACTERIAL BIOFILM

MAŁGORZATA DAWGUL*, MAGDALENA MACIEJEWSKA, MACIEJ JASKIEWICZ, ANNA KARAFOVA and WOJCIECH KAMYSZ

Department of Inorganic Chemistry, Faculty of Pharmacy, Medical University of Gdansk, Hallera 107, 80-416 Gdańsk Poland

Abstract: Recently, the topic of biofilm has met a huge interest of researchers owing to a significant role played by this microbial life form in severe infections. These well organised three-dimensional microbial communities are characterized by a strong resistance to antimicrobials. Biofilms significantly contribute to morbidity and mortality as related infections are very difficult to treat due to their tendency to relapse after the withdrawal of antibiotics. According to the literature, antimicrobial peptides (AMPs) have a high potential as future antibiofilm agents. AMPs can influence various stages of biofilm formation and exhibit antimicrobial activity against a broad spectrum of microorganisms including multi-drug resistant strains. The purpose of the present study was to determine the activity of antimicrobial peptides against biofilms formed by a variety of bacterial strains. To do this, the following antimicrobial peptides were synthesized: Citropin 1.1, Lipopeptides Palm-KK-NH$_2$ and Palm-RR-NH$_2$, Omiganan, Pexiganan and Temporin A. Antimicrobial activity of the compounds and conventional antibiotics was determined for planktonic cells and biofilms formed by reference strains of Gram-positive (*Staphylococcus aureus*, *S. epidermidis, Streptococcus pneumoniae*, *Streptococcus pyogenes*) and Gram-negative (*Escherichia coli*, *Pseudomonas aeruginosa*, *Proteus mirabilis*) bacteria. AMPs exhibited a strong antibacterial activity against Gram-positive strains, while Gram-negative bacteria were less susceptible. Antimicrobial activity of the tested peptides against biofilms formed by Gram-positive organisms was significantly stronger as compared to that of conventional antimicrobials.

Keywords: antimicrobial peptides, lipopeptides, bacterial biofilm

Biofilm represents the basic living form of most microorganisms in natural environment and can be defined as a sessile microbial community growing on various surfaces. This highly specialized three dimensional structure is characterized by a strong resistance to antimicrobials. In extreme cases, susceptibility to antibiotic can be decreased by up to 1000 fold (1, 2). Biofilms of various species of bacteria and fungi can be formed on the surfaces of medical devices (central venous catheters, heart valves, urinary catheters, endotracheal tubes and intrauterine devices), this resulting in implant-related infections (3, 4). As one of the most common biomaterials, contact lenses constitute a suitable surface for microbial adhesion. Bacterial ocular infections are rather rare complications due to the usage of this biomaterial. However, their consequences might be severe. The ability of microbes to form biofilm on contact lenses plays a significant role in pathogenesis of several infections, such as bacterial conjunctivitis, microbial keratitis, contact lens acute red eye (CLARE) and contact lens peripheral ulcer. The etiological factors for bacterial ocular infections are: *Staphylococcus aureus, Streptococcus pneumoniae, Haemophilus influenzae, Staphylococcus epidermidis, Enterococcus spp., Moraxella spp., Escherichia coli, Streptococcus pyogenes, Serratia marcescens, Pseudomonas aeruginosa, Proteus mirabilis* and *Neisseria gonorrhoeae* (5-7). The standard treatment for bacterial eye infections is topical antibiotic therapy. Application of a broad spectrum antibiotics causes that the effectiveness of conventional antimicrobials becomes gradually suppressed. Antimicrobial peptides (AMPs) exhibit excellent activity against a number of pathogens responsible for ocular infections. AMPs are essential part of innate human immunity and their activity against broad-spectrum bacteria is well known. Owing to their unique mechanism and fast killing kinetics, the risk of the development of microbial resistance is

* Corresponding author: e-mail: mdawgul@gumed.edu.pl; phone: +48-58-3493225; fax: +48-58-3493224

significantly lower as compared to that of conventional antibiotics. There are several literature reports on successful use of AMPs in prevention of formation of biofilms as well as in elimination of the structures formed.

In vitro tests demonstrated activity of human cathelicidin LL-37 and peptide STAMP G10KHc against biofilms formed by Pseudomonas aeruginosa. LL-37 also disrupted the development of biofilms formed by Staphylococcus epidermidis and Pseudomonas aeruginosa (8, 9). Dendrimeric peptides inhibited the biofilm formation and killed pregrown biofilms of E. coli. Short cationic lipopeptides demonstrated strong antibiofilm activity against clinical strains of Staphylococcus aureus (10).

Also numerous in vivo models have been developed to confirm the potential of AMPs as future antibiofilm agents. A chimeric peptide – DD13-RIP (composed of a dermaseptin derivative and an RNA III-inhibiting peptide) proved its ability to prevent staphylococcal infection in a rat graft infection model with methicillin-resistant S. aureus (MRSA) or S. epidermidis (MRSE) (11). The efficacy of Tachyplesin III was successfully applied in a rat model of P. aeruginosa urethral stent infection to prevent the biofilm formation (12). The efficacy of the treatment of central venous catheter infection caused by S. aureus and E. faecalis with linezolid was improved when the catheters were pretreated with IB-367 (13). Application of contact lenses with melamine allowed to reduce the CLARE in the P. aeruginosa guinea pig model (14).

AMPs can act at various stages of biofilm formation through different mechanisms of action. Therefore, the compounds have the potential as novel antimicrobials to prevent the formation of biofilm as well as to eradicate the preformed structures from the surface of contact lenses.

The aim of the present study was to evaluate a group of synthesized AMPs as potential antibiofilm agents against structures formed by some strains associated with ocular infections.

MATERIALS AND METHODS

Antimicrobial peptides

All tested peptides (Citropin 1.1, Lipopeptides Palm-KK-NH2 and Pam-RR-NH$_2$, Omiganan, Pexiganan and Temporin A) were synthesized manually by Fmoc chemistry on polystyrene resin modified by Rink Amide linker (15). Deprotection of the Fmoc group was carried out in 20 min using a 20% piperidine in dimethylformamide (DMF). Then, the resin was washed with DMF and DCM (dichloromethane) and a chloranil test was accomplished. All amino acids were coupled using the mixture of DMF/DCM (1 : 1, v/v) in the presence of coupling agents such as 1-hydroxybenzotriazole (HOBt) and diisopropylcarbodiimide (DIC). The degree of acylation was monitored by chloranil test. The peptides were cleaved from the resin with a mixture consisting of trifluoroacetic acid (TFA), water, triisopropylsilane (TIS) and phenol (92.5 : 2.5 : 2.5 : 2.5, v/v/v/v) as scavengers. In the next step, the peptide compounds were precipitated with cold diethyl ether and lyophilized. All crude products were purified by reversed-phase high performance liquid chromatography (RP-HPLC) in a gradient of acetonitrile – water containing 0.1% TFA. Identity of the peptides was confirmed by matrix-assisted laser desorption ionization - time of flight (MALDI-TOF) mass spectrometry (16).

Antimicrobial activity

Minimum inhibitory concentration (MIC) and minimum bactericidal concentration (MBC) were determined for several contact-lens involved bacterial pathogens: Staphylococcus aureus ATCC 25923, Staphylococcus epidermidis PCM 2118, Streptococcus pneumoniae ATCC 49619, Streptococcus pyogenes PCM 465, Escherichia coli ATCC 25922, Pseudomonas aeruginosa ATCC 9027, Proteus mirabilis PCM 543. MIC assays for the peptides and antibiotics (bacitracin, ciprofloxacin, gentamicin, erythromycin, neomycin and polymyxin B) were performed by the broth dilution method with Mueller Hinton II broth according to the procedures recommended by CLSI (Clinical and Laboratory Standards Institute). Polypropylene 96-well plates with bacteria at initial inoculums of 5×10^5 CFU/mL exposed to tested compounds were incubated for 18 h at 37°C. MIC was taken as the lowest drug concentration at which a visible growth of microbes was inhibited. MBC was taken as the lowest concentration of compound that allowed for 99.9% reduction of the initial inoculums. Biofilms cultured on polystyrene plates for 1, 2 and 3 days were exposed to graded concentrations of peptides and antibiotics. After a 24 h incubation, resazurin was added as a cell-viability reagent and the minimum biofilm eradication concentration (MBEC) was read. The experiments were performed in triplicate.

RESULTS

Activity against planktonic cells

The tested compounds have shown a diverse activity in the MIC/MBC assay performed for refer-

Figure 1. Activity of selected antimicrobial peptides and conventional antibiotics against biofilms formed by *Escherichia coli* ATCC 25922 on polystyrene surface for 1, 2 and 3 days

Figure 2. Activity of selected antimicrobial peptides and conventional antibiotics against biofilms formed by *Pseudomonas aeruginosa* ATCC 9027 on polystyrene surface for 1, 2 and 3 days
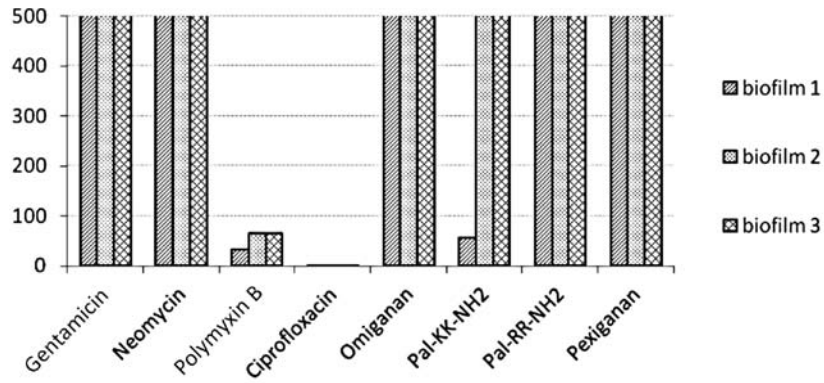

Figure 3. Activity of selected antimicrobial peptides and conventional antibiotics against biofilms formed by *Proteus m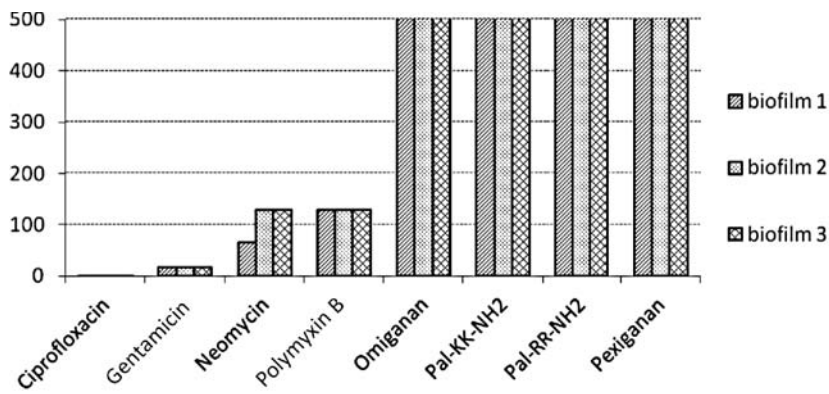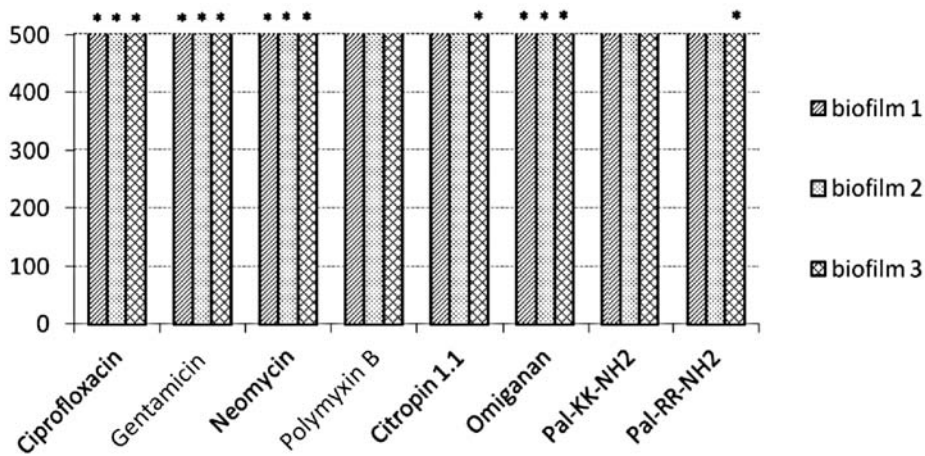irabilis* PCM 543 on polystyrene surface for 1, 2 and 3 days (* - antimicrobial activity not observed at tested concentrations 1-512 mg/L)

Table 1. Activity of peptides and conventional antimicrobials against planktonic cells of tested bacterial strains (bacteriostatic).

MIC/ MBC	Escherichia coli	Proteus mirabilis	Pseudomonas aeruginosa	Staphylococcus aureus	Staphylococcus epidermidis	Streptococcus pneumoniae	Streptococcus pyogenes
Bacitracin	512 / >512	>512 / >512	>512/>512	128 / 128	32 / 64	128 / 512	128 / 256
Ciprofloxacin	0.25 / 0.25	0.25 / 0.25	0.25 / 0.25	0.5 / 0.5	0.25 / 0.5	0.25 / 0.5	0.5 / 1
Erythromycin	64/ bs.	256 / bs.	128 / bs.	0.25 / bs.	2 / 4	0.5 / 1	4 / 16
Gentamicin	2/2	1 / 2	2 / 2	1 / 2	0.25 / 0.25	2 / 4	0.5 / 0.5
Neomycin	4/4	2 / 8	4 / 8	2 / 4	0.25 / 0.5	8 / 16	1 / 2
Polymyxin B	0.25 / 0.25	0.25 / 0.25	0.25 / 0.25	0.5 / 0.5	0.25 / 0.5	0.25 / 0.5	0.5 / 1
Citropin 1.1	32 / 64	256 / 512	128 / 256	16 / 16	8 / 8	16 / 16	16 / 32
Omiganan	16 / 64	256 / 512	32 / 128	4 / 8	1 / 2	8 / 16	8 / 16
Pal-KK-NH$_2$	8 / 16	256 / 512	64 / 64	8 / 16	1 / 1	8 / 16	8 / 16
Pal-RR-NH$_2$	16 / 32	256 / 512	64 / 256	8 / 16	1 / 1	8 / 8	4 / 8
Pexiganan	8 / 8	256 / 512	4 / 4	4 / 8	0.5 / 0.5	8 / 8	8 / 16
Temporin A	256 / >512	>512 / >512	512 / >512	8 / 8	4 / 8	4 / 8	4 / 8

ence strains of bacteria (Tab. 1). Apart from bacitracin which turned out to be the least active, conventional antimicrobials demonstrated a relatively stronger activity as compared to that of AMPs. The growth of *Escherichia coli* was inhibited by ciprofloxacin and polymyxin B at the a concentration of 0.25 mg/L whereas the most active peptides were effective at 8 mg/L. Even still larger discrepancies were observed for the remaining Gram-negative strains. These bacteria were susceptible to ciprofloxacin, gentamicin, neomycin and polymyxin B, while AMPs, bacitracin and erythromycin displayed rather a weak antibacterial activity. The tested peptides have shown a markedly stronger activity against Gram-positive bacteria. The most susceptible strain was *Staphylococcus epidermidis* (MIC value of lipopeptides, pexiganan and omiganan were 0.5-1 mg/L). Erythromycin and bacitracin displayed a stronger activity towards Gram-positive strains as well. The remaining conventional antibiotics showed approximately equal antimicrobial activity against all tested bacteria. In general, the tested compounds presented bactericidal mode of action as their MBCs were equal or twice higher in comparison with their MICs. Only erythromycin showed bacteriostatic action against *S. aureus, P. aeruginosa* and *P. mirabilis*.

Activity against biofilm

The tested antimicrobials exhibited a very diverse activity against biofilms depending on the tested strain and the maturity of structure. For instance, *E. coli* formed biofilm susceptible to ciprofloxacin applied at a concentration of 1 mg/L and to polymyxin B at concentrations of 32-64 mg/L. Gentamicin, neomycin and antimicrobial peptides eliminated preformed biofilms at the highest concentration applied (Fig. 1). Biofilms formed by *P. aeruginosa* were susceptible to ciprofloxacin, and gentamicin (MBEC obtained for 3 days old structures = 4 and 16 mg/L respectively). A lower activity was exhibited by neomycin and polymyxin B, while AMPs turned out to be the weakest antibiofilm agents (MBEC = 512 mg/L) (Fig. 2). *P. mirabilis* formed biofilms resistant to almost all the tested compounds. Only polymyxin B and lipopeptide Palm-KK-NH$_2$ were active at the concentration of 512 mg/L. Citropin 1.1 was effective at the same concentration against biofilm grown for 1 and 2 days, while a 3-day structure was unsusceptible. The remaining compounds did not show antibiofilm activity up to a concentration of 512 mg/L (Fig. 3).

Antimicrobial peptides were very effective against biofilm formed by Gram-positive bacteria. *Staphylococcus aureus* formed biofilms resistant to the conventional antibiotics, while AMPs acted on all the formed structures at concentrations of 32-64 mg/L (Fig. 4). Also *S. epidermidis* biofilms were much more senstitive to AMPs in comparison to conventional compounds. A remarkable dependence of the maturity of the structure on the activity of the antibiotics was observed. Namely, biofilms grown for 1 day were sensitive to all compounds, while after 3 days bacteria were resistant to gentamicin, neomycin and ciprofloxacin (Fig. 5). All the living forms of *Streptococcus pyogenes* were very susceptible to ciprofloxacin, while neomycin and antimicrobial peptides were active at higher concentrations. Again, erythromycin and gentamicin turned out to be ineffective at the tested concentrations (Fig. 6). Similar results were obtained for *S. pneumoniae*. However, the activity of ciprofloxacin against biofilm after 3 days was significantly lower (Fig. 7).

DISCUSSION AND CONCLUSION

Extended wear of contact lenses significantly contributes to the development of corneal infections (17). Several side effects related to wearing of con-

Figure 4. Activity of selected antimicrobial peptides and conventional antibiotics against biofilms formed by *Staphylococcus aureus* ATCC 25923 on polystyrene surface for 1, 2 and 3 days (* - antimicrobial activity not observed at tested concentrations 1-512 mg/L)
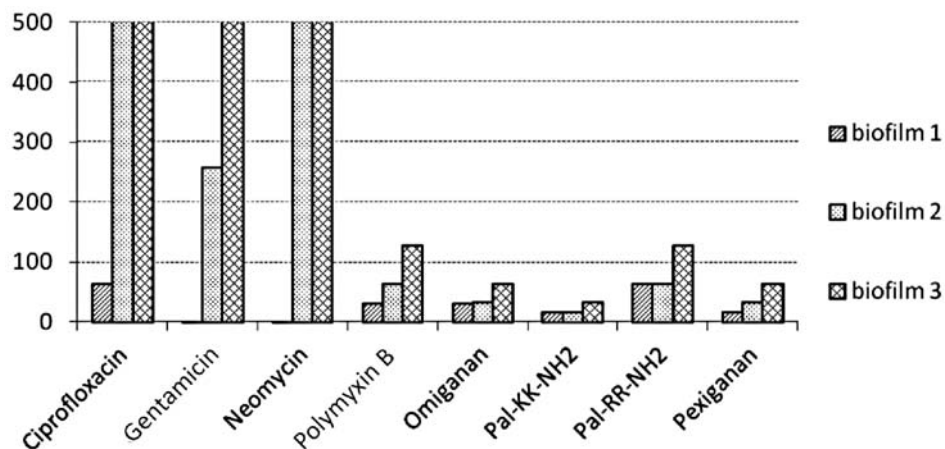
Figure 5. Activity of selected antimicrobial peptides and conventional antibiotics against biofilms formed by *Staphylococcus epidermidis* PCM 2118 on polystyrene surface for 1, 2 and 3 days

tact lenses occur due to the bacterial adhesion to their surface. In order to reduce the bacterially driven adverse responses, novel materials and contact lens liquids that contain safe antimicrobials should be considered.

The eye possesses an array of native defense components protecting the ocular structures against microbial infections. The tear film is one of the crucial elements of this protection. It contains antimicrobials and is responsible for the purification, nutrition and moisturizing of the eye (18). The tear film contains a plenty of proteins and peptides which include lysozyme, mucins and endogenous antimicrobial peptides. These molecules together with complement compounds constitute the main elements of the antimicrobial defense of human tears (19). Defensins seem to be interesting candidates as therapeutic agents for ocular infections. These compounds belong to AMPs found in human eye and display antimicrobial activity against a broad spectrum of microorganisms (20). Owing to the mechanism based on altering of the permeability properties of the microbial cell plasma membrane (21), the risk to develop bacterial resistance to AMPs is relatively low. This hypothesis was confirmed by several *in vitro* studies. The resistance of *Pseudomonas aeruginosa* to peptides was increased only by two to fourfold after 30 passages below their MIC (22), while

Figure 6. Activity of selected antimicrobial peptides and conventional antibiotics against biofilms formed by *Streptococcus pyogenes* PCM 465 on polystyrene surface for 1, 2 and 3 days (* - antimicrobial activity not observed at tested concentrations 1-512 mg/L)
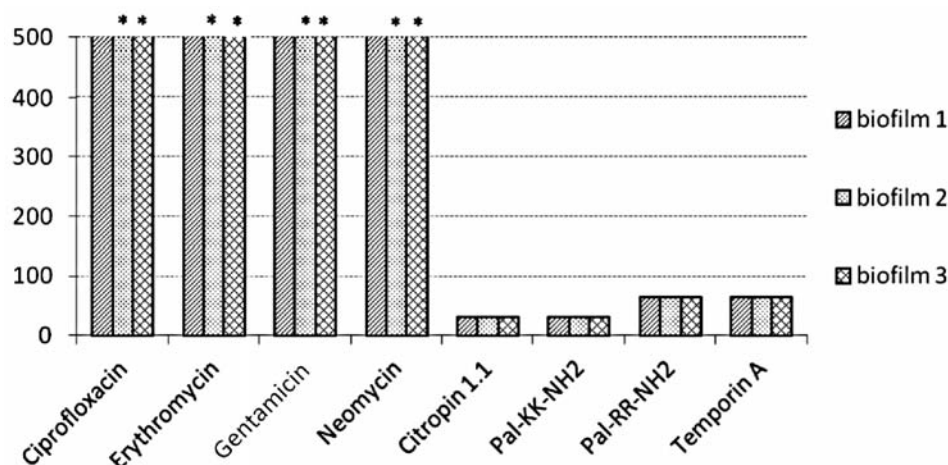

Figure 7. Activity of selected antimicrobial peptides and conventional antibiotics against biofilms formed by *Streptococcus pneumoniae* ATCC 49619 on polystyrene surface for 1, 2 and 3 days (* - antimicrobial activity not observed at tested concentrations 1-512 mg/L)
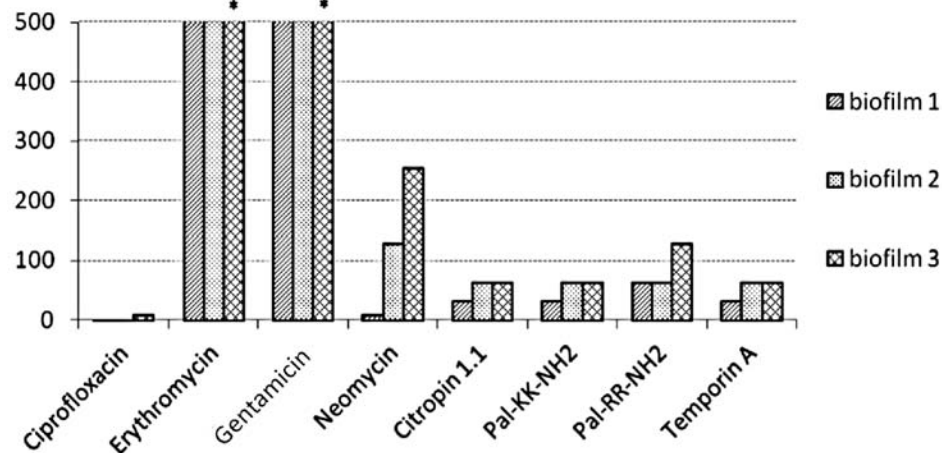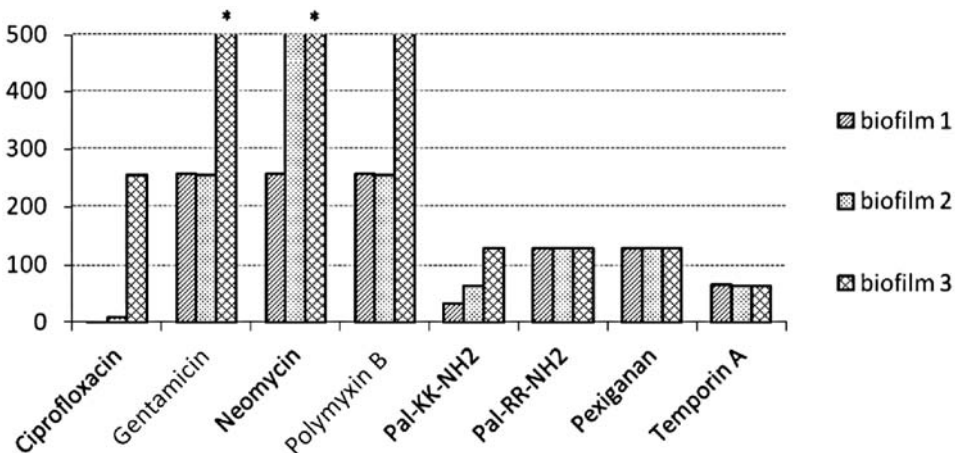
the application of lipopeptide Laur-KK-NH$_2$ proved to reduce the ability of strains of *Enterococcus faecalis* to daptomycin (23).

The above mentioned phenomena together with the activity of AMPs against multi-drug resistant microorganisms and their fast killing kinetics (24, 25) in comparison to the majority of the conventional antibiotics represent suitable features for novel antimicrobials. It is worth noting that antimicrobial peptides also demonstrate strong antimicrobial activity against biofilm structure. Microbial cells in such communities are very difficult to eliminate with conventional antibiotics, while the same cells are sensitive in their planktonic state (1). Bacteria and fungi colonizing the surface of contact lenses are very likely to grow in this living form.

Although antimicrobial peptides clearly represent a great potential for the management of ocular infections, their practical usage remains at a very early stage of development (26). Ophthalmic pharmaceutical companies have not focused on AMPs as yet, but several *in vitro* and *in vivo* studies have been performed worldwide by scientific groups.

In vitro activity of AMPs against numerous pathogens that could be linked with ocular infections, has been confirmed. Human β-defensins HB43, HB55 and HBPM4 demonstrated activity towards meticillin-resistant *S. aureus* (MRSA), while strains *P. aeruginosa* strain was susceptible to HBD-1, HBD-2 HBD-3, HBCM2, HBCM3 and HB14 (27). Human β-defensin 3 was also an effective agent against *S. aureus* in the biofilm form (28). Defensins isolated from rabbits (NP-1, NP-5) showed an *in vitro* activity against pathogens isolated from human and horses suffering ocular infections (29).

LL-37, a human cathelicidin was also found to be expressed in human corneal and conjunctival epithelia (30). The compound disrupted the formation of biofilm as well as eradicated the pre-grown biofilms of *Pseudomonas aeruginosa*. LL-37 also inhibited the attachment and development of biofilms of *Staphylococcus epidermidis* (31).

Lactoferrin (LF), a human antimicrobial protein present in saliva, milk and tears prevented the formation of biofilm by *Streptococcus gordonii* and *S. mutans* in oral cavity (32, 33). LF also showed a synergic action with lysozyme and vancomycin against *S. epidermidis* biofilms (34). Another promising candidate to fight biofilm is lactoferricin B – a product of enzymatic digestion of LF. Application of the compound in combination with conventional antifungals allowed to reduce their dosage significantly. The combinations were active towards common keratitis-associated fungal pathogens (*Aspergillus fumigatus*, *Fusarium solani*, *Candida albicans*) in both living forms: planktonic cells and biofilms (35).

A number of sequences isolated from other organisms and their analogues have also been tested. Mannis et al. have tested peptides CCI A, B, C and COL-1 on human ocular isolates and in a rabbit model of *Pseudomonas keratitis*. The compounds were effective *in vitro* but not *in vivo* (26). Derivatives of cecropin demonstrated activity against strains isolated from patients suffering ocular infections (36). Cecropin-mellitin hybrid peptides were effective in the management of *P. aeruginosa* ocular infection developed in rabbits (37), while contact lenses with another hybrid peptide – melamine (mellitin-protamine), reduced the CLARE in the *P. aeruginosa* guinea pig model (14). In contrast to mellitin, the hybrids proved non toxic to the eukaryotic cells. We have synthesized an analogue of indolicidin-peptide primarily isolated from borvine neutrofils – omiganan. The compound eradicated staphylococcal biofilm at a considerably low concentration and exhibited some activity against structures formed by *Escherichia coli*.

An amphibian peptide citropin 1.1 demonstrated synergic action with rifampin and minocycline against a *S. aureus* biofilm (38). In our study, the compound alone was very effective against biofim formed by *S. aureus* and *S. pyogenes*. The determined MBEC were significantly lower in comparison to those obtained for conventional antimicrobials. Moreover, its activity did not depend on the time of biofilm cultivation. Another amphibian peptide temporin A was also active against biofilm formed by Gram-positive strains. The tested amphibian peptides demonstrated a minor antibacterial activity against Gram-negative strains. Similar results were obtained for pexiganan - an analogue of another amphibian peptide – magainin II. A peptide obtained from hemocytes of the horseshoe crab, tachyplesin III prevented the formation of *Pseudomonas aeruginosa* biofilm in a rat model of ureteral stent infection (12). Another study reported iseganan as a potential adjunctive agent to linezolid in the treatment of central venous catheter infection (13).

In our study, Palm-KK-NH$_2$ and Palm-RR-NH$_2$ proved to be potent agents towards Gram-positive biofilm displaying some activity towards both living forms of Gram-negative strains, while in the previous work both compounds were the most active lipopeptides tested against staphylococcal biofilms produced by dermatological isolates of *S. aureus* (10).

Based on the literature data and the obtained results we can expect that AMPs could be applied for the management as well as prevention of ocular infections. However, before the application of the peptides in ophthalmology several issues need to be considered, such as their toxicity, immunogenicity, stability and route of administration.

In general, AMPs have shown a considerably stronger antimicrobial activity against biofilm formed by Gram-positive bacteria than conventional antibiotics. A significantly lower activity of AMPs was observed in the case of Gram-negative strains. As the Gram-positive organisms are the most common isolates among ocular infections (39), we can assume that antimicrobial peptides possess a potential for development as therapeutic antimicrobials for the ocular infections. Moreover, immobilization of AMP onto the surface of biomaterials such as contact lenses might result in reduction of biofilm formation.

Acknowledgments

REFERENCES

1. Nikolaev Yu.A., Plakunov V.K.: Microbiology 76, 125 (2007).
2. Potera C.: Environ. Health Persp. 118, 288 (2010).
3. Vergidis P., Patel R.: Inf. Dis. Clin. North Am. 26, 173 (2012).
4. Aslam S., Darouiche R.O.: Int. J. Artif Organs 34, 752 (2011).
5. Willcox M.D., Holden B.A.: Biosci. Rep. 21, 445, (2001).
6. Szczotka-Flynn L.B., Pearlman E., Ghannoum M.: Eye Contact Lens. 36, 116 (2010).
7. Wu P., Stapleton F., Willcox M.D.: Eye Contact Lens. 29, 63 (2003) .
8. Overhage J., Campisano A., Bains M., Torfs EC., Rehm B.H., Hancock R.E.: Infect. Immun. 76, 4176 (2008).
9. Hell E., Giske C.G., Nelson A., Römling U., Marchini G.: Lett. Appl. Microbiol. 50, 211 (2010).
10. Dawgul M., Barańska-Rybak W., Kamysz E., Karafova A., Nowicki R., Kamysz W.: Future Med. Chem. 4, 1541 (2012).
11. Balaban N., Gov Y., Giacometti A., Cirioni O., Ghiselli R., Mocchegiani F., Orlando F. et al.: Antimicrob. Agents Chemother. 48, 2544 (2004).
12. Minardi D., Ghiselli R.., Cirioni O., Giacometti A., Kamysz W., Orlando F., Silvestri C. et al.: Peptides 28, 2293 (2007).
13. Ghiselli R., Giacometti A., Cirioni O., Mocchegiani F., Silvestri C., Orlando F., Kamysz W. et al.: J Parenter. Enteral Nutr. 31, 463 (2007).
14. Willcox M.D., Hume E.B., Aliwarga Y., Kumar N., Cole N.: J. Appl. Microbiol. 105, 1817 (2008).
15. Fields G.B., Noble R.L.: Int. J. Pept. Protein Res. 35, 161 (1990).
16. Christensen T.: Acta Chem. Scand. B 33, 763 (1979).
17. Keay L., Stapleton F., Schein O.: Eye Contact Lens. 33, 346 (2007).
18. Rolando M., Zierhut M.: Surv. Ophthalmol. 45, 203 (2001).
19. Johnson M.E., Murphy P.J.: Prog. Retin. Eye Res. 23, 449 (2004).
20. De Smet K., Contreras R.: Biotechnol. Lett. 27, 1337 (2005)
21. Schauber J., Gallo R.L.: J. Allergy Clin. Immunol. 124, 13 (2009).
22. Zhang L., Parente J., Harris S.M., Woods D.E., Hancock R.E.W., Falla T.J.: Antimicrob. Agents Chemother. 49, 2921 (2005).
23. Cirioni O., Kamysz E., Ghiselli R, Kamysz W., Silvestri C., Orlando F., Rimini M. et al.: J. Antimicrob. Chemother. 66, 859 (2011).
24. Baranska-Rybak W., Dawgul M., Bielinska S., Kraska B., Piechowicz L., Kamysz W.: J. Microbiol. Biotechnol. 21, 536 (2011)
25. Giuliani A., Pirri G., Nicoletto S.F.: Cent. Eur. J. Biol. 2, 1 (2007).
26. Mannis M.J.: Trans. Am. Ophthalmol. Soc. 100, 243 (2002).
27. Silva N.C., Sarmento B., Pintado M.: Int. J. Antimicrob. Agents 41, 5 (2013).
28. Huang Q., Yu HJ., Liu GD., Huang XK., Zhang LY., Zhou YG., Chen JY. et al.: Orthopedics 35, 53 (2012).
29. Cullor J.S., Mannis M.J., Murphy C.J., Smith W.L., Selsted M.E., Reid T.W: Arch. Ophthalmol. 108, 861 (1990).
30. Gordon Y.J., Huang L.C., Romanowski E.G., Yates K.A., Proske R.J., McDermott A.M.: Curr. Eye Res. 30, 385 (2005).
31. Hell E., Giske C.G., Nelson A., Römling U., Marchini G.: Lett. Appl. Microbiol. 50, 211 (2010).
32. Arslan S.Y., Leung K.P., Wu C.D.: Oral Microbiol. Immunol. 24, 411 (2009).

33. Flanagan J.L., Willcox M.D.P.: Biochimie 91, 35 (2009).
34. Leitch E.C., Willcox M.D.: Curr. Eye Res. 19, 12 (1999).
35. Sengupta J., Saha S., Khetan A., Sarkar S.K., Mandal S.M.: J. Infect. Chemother. 18, 698 (2012).
36. Gunshefski L., Mannis M.J., Cullor J.S., Schwab I.R., Jaynes J., Smith WL.: Cornea 13, 237 (1994).
37. Nos-Barbera S., Portoles M., Morilla A., Ubach J., Andreu D., Paterson CA.: Cornea 16, 101 (1997).
38. Cirioni O., Giacometti A., Ghiselli R., Kamysz W., Orlando F., Mocchegiani F., Silvestri C. et al.: Peptides 27, 1210 (2006).
39. Khosravi AD., Mehdinejad M., Heidari M.: Singapore Med. J. 48, 741 (2007).

DRUG SYNTHESIS

SYNTHESIS, PRO-APOPTOTIC ACTIVITY AND 2D-QSAR STUDIES OF NEW ANALOGUES OF FLUPHENAZINE

JOANNA ŻYTA[1], AGATA JASZCZYSZYN[2]*, PIOTR ŚWIĄTEK[3], KAZIMIERZ GĄSIOROWSKI[2]
and WIESŁAW MALINKA[3]

[1]Faculty of Chemistry, University of Wrocław, Joliot-Curie 14, 50-383 Wrocław, Poland
[2]Department of Basic Medical Sciences, Wrocław Medical University,
Borowska 211, 50-556 Wrocław, Poland
[3]Department of Drug Chemistry, Wrocław Medical University, Borowska 211, 50-556 Wrocław, Poland

Abstract: A series of 10 novel analogues of fluphenazine (FPh) were synthesized. Influence of the synthesized analogues of FPh on frequency of apoptosis and necrosis in cultures of human lymphocytes genotoxically damaged *in vitro* with benzo[*a*]pyrene (B[*a*]P; 7,5 μM, 48 h) was compared with the effect of FPh. Activity of the tested compounds was expressed by ED_{50} (pro-apoptotic activity) and TD_{50} (pro-necrotic effect, cytotoxicity). It was noticed that compounds **3–9** and **12** exerted a pro-apoptotic effect markedly stronger than that of FPh. Additionally, compounds **3**, **9** and **10** exhibited the weakest influence on frequency of necrotic lymphocyte in cultures. 2D-QSAR analysis was done in order to find quantitative relationship between structures of the tested analogues and their pro-apoptotic activity or pro-necrotic effect in B[*a*]P-damaged cell cultures. Several statistically significant QSAR models were generated. Information obtained from 2D-QSAR study will be used in further design of analogues of FPh more active in cancer chemoprevention.

Keywords: fluphenazine analogues, synthesis, pro-apoptotic activity, 2D-QSAR study

Phenothiazine derivatives (Pht), among them also fluphenazine (FPh), exert an anti-psychotic activity by binding and inhibition of an array of presynaptic dopaminergic receptors and for years various drugs from phenothiazine family have been used in psychopharmacotherapy (1). Aside from their neuroleptic activity Pht also possess cancer chemopreventive activity – they inhibit the calmodulin, the protein kinase C, and decrease the transporter function of P-glycoprotein (2, 3). Importantly, recent papers documented an anti-cancer activity of various Pht in cultures of human cancer cell lines (4, 5). Randomized prospective trials of patients with schizophrenia, treated with phenothiazines found that the occurrence rate of cancer was smaller than in healthy people from the control group (6). The mechanism of cancer prevention by Pht is weakly known. However, some experimental results showed that various phenothiazine compounds are able to induce *in vitro* a programmed cell death (apoptosis) in tumor cells and/or in genotoxically damaged cells (7, 8). It is broadly accepted that

a stimulation of apoptosis in cancer cells could be an important mechanism of action of cancer chemopreventive drugs, and it is reasonable that a pro-apoptotic activity should prevail against a cytotoxic activity in the activity profile requested for those drugs (9, 10).

Pht have been used for years in the treatment of patients with schizophrenia, and recently they are also assayed for anti-mutagenic and anti-cancer activities (11). It was estimated that Pht exhibited strong pro-apoptotic activity *in vitro* (10, 12). However, their usefulness in cancer therapy in humans is limited by the serious adverse effects on the central nervous system, mainly the extrapyramidal symptoms and induction of the iatrogenic parkinsonism (13). The FPh analogues, synthesized by us, possess several structural modification of the side chain, lower value of log of the octanol/water partition coefficient or higher molecular weight than the parent compound. Therefore, we suggest that their penetration through blood-brain barrier into the central nervous system should be markedly weaker

and extrapyramidal side effects will be decreased in comparison with FPh.

In the present study, 10 novel analogues of FPh were synthesized and evaluated for their pro-apoptotic activity and pro-necrotic effect (cytotoxicity) in cultures of human lymphocytes genotoxically damaged *in vitro* by incubation with benzo[*a*]pyrene (B[*a*]P; 7,5 μM, 48 h). 2D-QSAR analysis was done in order to find quantitative relationship between structures of the tested compounds and their pro-apoptotic activity or pro-necrotic effect in B[*a*]P-damaged cell cultures. Information obtained from 2D-QSAR study will be used in further design of FPh analogues more active in cancer chemoprevention.

EXPERIMENTAL

Chemistry

Melting points are uncorrected. ^{1}H NMR spectra were recorded in $CDCl_3$ at 80 MHz using a Tesla spectrometer or at 300 MHz using a Bruker spectrometer. [1]H chemical shifts were reported in δ (ppm). Elemental analyses were within ± 0.4% of the theoretical values and were performed on a Carlo Erba NA-1500 analyzer. All reactions were monitored by thin-layer chromatography on 0.25 mm Merck silica gel (60 F_{254}) and visualized by UV light (λ = 264 or 365 nm). Flash chromatography was performed on a silica gel Kieselgel 60 (70–230 mesh) Merck.

10-(2,3-Epoxypropyl)-2-trifluoromethylphenothiazine (2)

To a stirred solution of 1.335 g (0.005 mol) of 2-trifluoromethylphenothiazine **1** in 5 mL of dimethylformamide 0.4 g (0.01 mol) of sodium hydride (60% dispersion in mineral oil) was added and the stirring was continued at room temperature for 1 h. Then, 0.85 mL (0.01 mol) of 1-bromo-2,3-epoxypropane was added and the stirring was continued for 3 h. Afterwards, the mixture was diluted with ice-cold water. The liberated in form of dark oil crude product was purified through flash chromatography (cyclohexane/toluene 1 : 1, v/v, R_f – 0.34). The epoxide **2** was obtain in 43% yield.

Formula: $C_{16}H_{12}F_3NOS$; m.w.: 323.33, m.p. 66–67°C; ^{1}H NMR (δ, ppm): 2.73–2.99 (m, 2H, CH_2), 3.22–3.39 (m, 1H, CH), 3.71–4.38 (m, 2H, N_{10}-CH_2), 6.92–7.24 (m, 7H, PhtH)

General procedure for preparation of analogues 3–11

A solution of 0.4 g (0.00124 mol) of epoxide **2** and 0.00124 mol of an appropriate amine in 10 mL of

ethanol was refluxed under stirring for 4–18 h. Then, the solvent was evaporated under reduced pressure and the residue was purified through flash chromatography. The obtained products **3–11** were in next step transformed to the corresponding salts by means of ethanol saturated with gas hydrogen chloride.

10-{3-[N,N-bis-(2-hydroxyethyl)amino]-2-hydroxypropyl}-2-trifluoromethylphenothiazine hydrochloride (3)

Formula: $C_{20}H_{24}ClF_3N_2O_3S$; m.w.: 464.93; m.p.: 192–194°C; 55.5% yield; chromatography: (ethyl acetate/methanol 3 : 1, v/v, R_f = 0.45); ^{1}H NMR (δ, ppm): 3.23–3.41 (m, 6H, $N(CH_2)_3$), 3.70–4.51 (m, 7H, N_{10}-CH_2CH and $2CH_2OH$), 5.17 (brs, 2H, $2CH_2OH^{ex}$), 5.84 (brs, 1H, $CHOH^{ex}$), 6.85–7.30 (m, 7H, PhtH), 7.83 (brs, 1H, N^+H^{ex}).

S(+)-10-[3-(1-ethyl-2-hydroxyethylamino)-2-hydroxypropyl]-2-trifluoromethylphenothiazine hydrochloride (4)

Formula: $C_{20}H_{24}ClF_3N_2O_2S$; m.w.: 448.93; m.p.: 187–189°C; 27% yield; chromatography: (ethyl acetate/methanol 5 : 1, v/v, R_f = 0.47); ^{1}H NMR (δ, ppm): 0.81–0.89 (m, 3H, CH_3), 1.54–1.64 (m, 2H, CH_2CH_3), 2.93–3.12 (m, 2H, CH_2N), 3.46–3.63 (m, 1H, CH), 3.73–3.80 (m, 2H, CH_2OH), 4.17–4.25 (m, 3H, N_{10}-CH_2CH), 4.94 (brs, 1H, CH_2OH^{ex}), 5.74 (brs, 1H, $CHOH^{ex}$), 6.95–7.06 (m, 2H, PhtH), 7.14–7.28 (m, 5H, PhtH), 7.45 (brs, 1H, N^+H^{ex}), 8.69 (brs, 1H, NH^{ex}).

10-[3-(2,3-Dihydroxypropylamino)-2-hydroxypropyl]-2-trifluoromethylphenothiazine hydrochloride (5)

Formula: $C_{19}H_{22}ClF_3N_2O_3S$; m.w.: 450.90; m.p.: 56–58°C; 42% yield; chromatography: (ethyl acetate/methanol 1.5 :1, v/v, R_f = 0.42); ^{1}H NMR (δ, ppm): 2.80–3.06 (m, 4H, CH_2NCH_2), 3.40–3.46 (m, 2H, CH_2OH), 3.90–4.02 (m, 2H, N_{10}-CH_2), 4.12–4.14 (m, 1H, CH), 4.40–4.44 (m, 1H, CH), 6.89–7.01 (m, 2H, PhtH), 7.08–7.22 (m, 5H, PhtH), 8.16 (brs, 1H, NH).

10-[3-(Morpholin-4-yl)-2-hydroxypropyl]-2-trifluoromethylphenothiazine hydrochloride (6)

Formula: $C_{20}H_{22}ClF_3N_2O_2S$; m.w.: 446.91; m.p.: 138–140°C; 10.5% yield; chromatography: (ethyl acetate/methanol 4 : 1, v/v, R_f = 0.80); ^{1}H NMR (δ, ppm): 2.97–3.03 (m, 6H, $3NCH_2$), 3.89–3.98 (m, 4H, CH_2OCH_2), 4.21–4.31 (m, 3H, N_{10}-CH_2CH), 5.59 (brs, 1H, $CHOH^{ex}$), 6.99–7.08 (m, 2H, PhtH), 7.16–7.31 (m, 5H, PhtH), 12.23 (brs, 1H, NH^{ex}).

10-{3-[4-(2-Hydroxyethyl)piperazin-1-yl]-2-hydroxypropyl}-2-trifluoromethylphenothiazine dihydrochloride (7)

Formula: $C_{22}H_{28}Cl_2F_3N_3O_2S$; m.w.: 526.42; m.p.: 88–90°C; 48.6% yield; chromatography: (ethyl acetate/methanol 4 : 1, v/v, R_f = 0.26); ^1H NMR (δ, ppm): 2.39–2.62 (m, 12H, $CH_2N(CH_2CH_2)_2NCH_2$), 3.56–3.61 (m, 2H, CH_2-OH), 3.93–4.14 (m, 3H, N_{10}-CH_2CH), 4.76 (brs, 1H, CH_2OH^{ex}), 6.94–7.02 (m, 2H, PhtH), 7.14–7.24 (m, 5H, PhtH).

10-{3-[4-(2-Furoil)piperazin-1-yl]-2-hydroxypropyl}-2-trifluoromethylphenothiazine dihydrochloride (8)

Formula: $C_{25}H_{26}Cl_2F_3N_3O_3S$; m.w.: 576.46; m.p.: 140–142°C; 46.5% yield; chromatography: (ethyl acetate, R_f = 0.62); ^1H NMR (δ, ppm): 2.42–2.64 [m, 6H, $CH_2N(CH_2)_2$], 3.68–3.81 [m, 4H, $N(CH_2)_2$], 4.00-4.11 (m, 3H, N_{10}-CH_2CH), 6.37–6.46 (m, 1H, C_5.-H), 6.86–7.38 (m, 9H, 7PhtH and $C_{3',4'}$-H)

10-{3-[4-(N-isopropylcarbamoylmethyl)piperazin-1-yl]-2-hydroxypropyl}-2-trifluoromethylphenothiazine dihydrochloride (9)

Formula: $C_{25}H_{33}Cl_2F_3N_4O_2S$; m.w.: 581.50; m.p.: 73–75°C; 47% yield; chromatography: (ethyl acetate/methanol 5 : 1, v/v, R_f = 0.61); ^1H NMR (δ, ppm): 1.14 (d, 6H, 2×CH_3, J = 2.5 Hz), 2.51 (s, 10H, $CH_2N(CH_2CH_2)_2N$), 2.94 (s, 2H, NCH_2CO), 3.91–4.21 (m, 4H, N_{10}-CH_2CH and CH_3CHCH_3), 4.55–4.63 (brs, 1H, NH^{ex}), 6.86–7.33 (m, 7H, PhtH).

10-{3-[4-(4-Acetyl-4-phenyl)piperidin-1-yl]-2-hydroxypropyl}-2-trifluoromethyl-phenothiazine hydrochloride (10)

Formula: $C_{29}H_{30}ClF_3N_2O_2S$; m.w.: 563.11; m.p.: 113–115°C; 49% yield; chromatography: (ethyl acetate, R_f = 0.60); ^1H NMR (δ, ppm): 1.88 (s, 3H, CH_3), 2.18–2.66 (m, 10H, $CH_2N(CH_2CH_2)_2$), 3.90–4.16 (m, 3H, N_{10}-CH_2CH), 6.93–7.32 (m, 12H, 7PhtH and 5ArH).

10-[3-(3-N,N-diethylcarbamoyl)piperidin-1-yl)-2-hydroxypropyl]-2-trifluoromethyl-phenothiazine hydrochloride (11)

Formula: $C_{26}H_{33}ClF_3N_3O_2S$; m.w.: 544.07; m.p.:114–116°C; 43% yield; chromatography: (ethyl acetate/methanol 4 : 1, v/v, R_f = 0.46); ^1H NMR (δ, ppm): 1.02 (t, J = 7.2 Hz, 3H, CH_3), 1.19 (t, J = 7.2 Hz, 3H, CH_3), 2.18–2.44 (m, 4H, NCH_2CH_2CH), 2.62–2.76 (m, 2H, NCH_2CH_2), 2.95–3.05 (m, 2H, NCH_2CH_2), 3.22–3.37 (m, 4H, $CH_3CH_2NCH_2CH_3$), 3.46–3.56 (m, 2H, $CHCH_2N$), 3.80–3.88 (m, 2H, N_{10}-CH_2), 4.22–4.30 (m, 1H, CHOH), 4.51–4.64 (m, 1H, CH_2 $CHCH_2$), 6.96–7.04 (m, 2H, PhtH), 7.12–7.32 (m, 5H, PhtH), 11.52 (brs, 1H, N^+H).

10-{4-[4-(2-Pyrimidinyl)piperazin-1-yl]-butyl}-2-trifluoromethylphenothiazine dihydrochloride (12)

A mixture of 1.34 g (0.005 mol) of 2-trifluoromethylphenothiazine **1**, 2.24 g (0.0075 mol) of 8-(2-pyrimidinyl)-8-aza-5-azaspiro[4,5]decane bromide and 1.04 g (0.0075 mol) of anhydrous K_2CO_3 in 30 mL of xylene was stirred and heated under reflux for 20 h. The hot reaction mixture was filtered and the filtrate was concentrated *in vacuo*. The residue was purified through flash chromatography (ethyl acetate/hexane 3 : 1, v/v, R_f = 0.44). The free base was converted to the hydrochloride salt **12**.

Formula: $C_{25}H_{28}Cl_2F_3N_5S$; m.w.: 558.57; m.p.: 78–80°C; 10% yield; ^1H NMR (δ, ppm): 1.72–2.04 (m, 4H, -CH_2CH_2-), 2.30–2.57 (m, 6H, -$CH_2N(CH_2)_2$), 3.74–3.85 (m, 4H, $N(CH_2)_2$) 3.95–4.12 (m, 2H, N_{10}-CH_2), 6.38–6.47 (m, 1H, $H_{5-pyrimidine}$), 6.82–7.18 (m, 7H, PhtH), 8.25 (s, 1H, $H_{pyrimidine}$), 8.28 (s, 1H, $H_{pyrimidine}$).

Biological activity

Lymphocytes were isolated from venous blood obtained from five healthy male donors aged 20–26. Cells were separated by the standard technique of blood centrifugation with Histopaque-1077 (Sigma, MO, USA) (14). Lymphocytes were counted and cultured for 48 h in the presence of lectin PHA-M (2% v/v) and the standard genotoxic agent - B[*a*]P (7.5 µM, 37°C). The tested compounds: FPh or its chemical analogues, were added to the cultures for 2 h. At the end of a culture time cells were centrifuged, diluted with buffered salt solution (PBS) and stained with fluorochrome mixture - the Annexin V-FITC/propidium iodide staining kit (Sigma, MO, USA) (14). Smears of the stained cell suspensions were examined under a fluorescence microscope, and frequency of necrotic (red fluorescence), apoptotic (green fluorescence) and viable cells (non-stained) were scored among 500 cells randomly found under the microscope image. The effect of 10 analogues of FPh on frequency of apoptosis (A) and necrosis (N) in genotoxically damaged cell cultures were expressed in proportion to the appropriate reference culture (A_o or N_o). The reference lymphocyte cultures were genotoxically damaged with B[*a*]P and incubated with the FPh. The biological activity of the tested compounds was

expressed by (pro-apoptotic activity) ED_{50} and (pro-necrotic effect, cytotoxicity) TD_{50} and showed as A/N index.

Computational details

Molecular structures of all 10 new synthesized compounds were optimized using DFT (Density Functional Theory) method with the B3LYP hybrid exchange-correlation energy functional and 6-31g* basis set (Gaussian03 software package) (15). Because the basic tertiary nitrogen atom in the

aliphatic chain could to be highly protonated at physiological pH – both the neutral and monoprotonated forms were analyzed (16). Initial molecules were built in GaussView program based on the crystal structure of trifluoperazine hydrochloride, which was found in literature data (17). In QSAR investigation, a three-dimensional structure of the compounds inevitably is a key parameter (18, 19). This parameter is crucial in interaction between potential drug and its biological target (20, 21). To obtain the low-energy conformations of new FPh analogues we
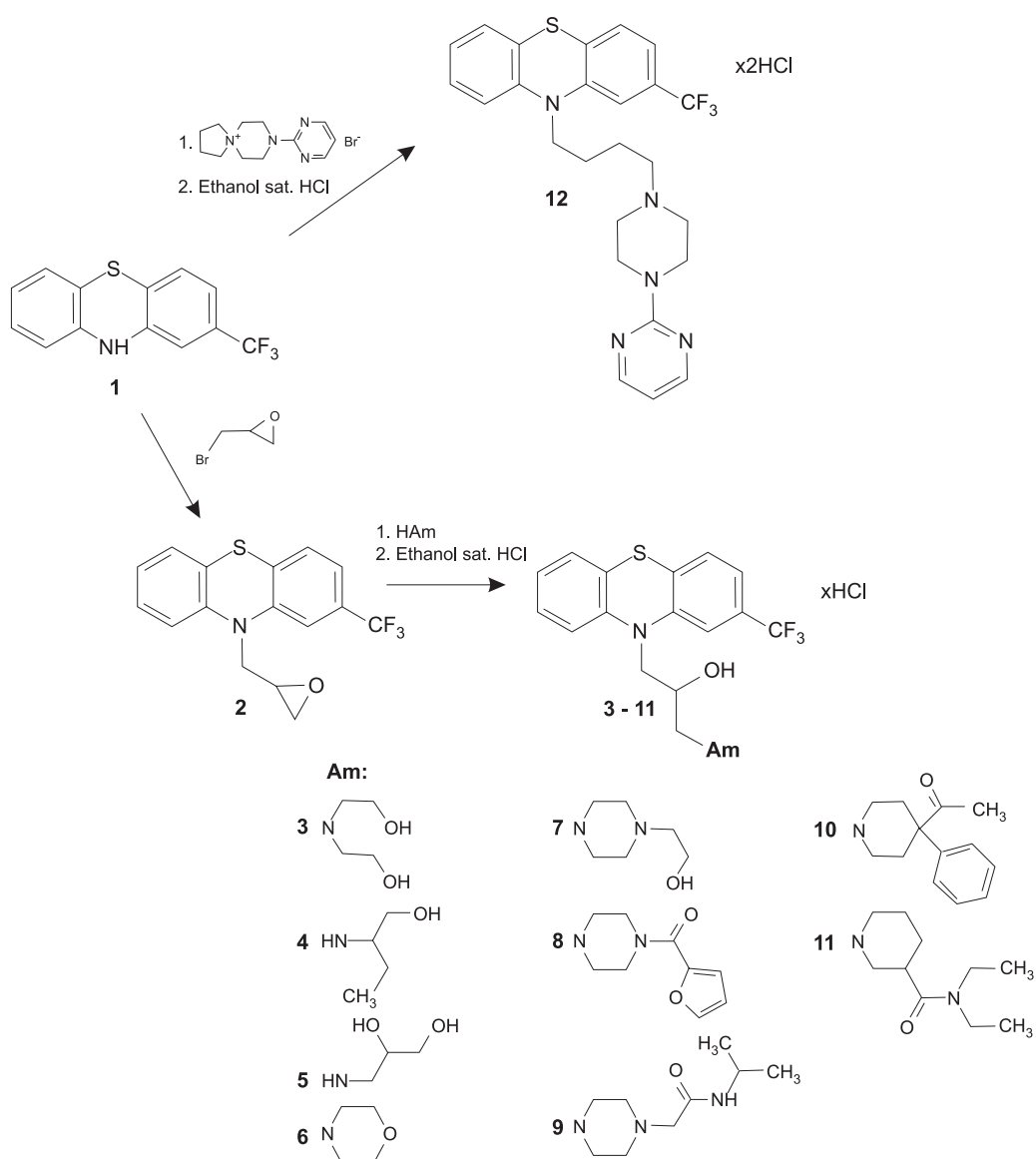
Scheme 1. Synthesis of new analogues of FPh

performed conformational analysis of all compounds using one of the semi-empirical methods – Austin Model 1 (AM1). In succeeded investigation we used only the conformation with the lowest energy. We assumed that this three- dimensional structures were the same that (or similar to) bioactive conformation of the investigated compounds. All molecular modeling calculations (geometry optimization and conformational analysis) were performed using Gaussian03 software. 2D-QSAR study was done using Molecular Operating Environment software (MOE) (22, 23). The molecular structures of new analogues of FPh are presented in Scheme 1.

RESULTS AND DISCUSSION

Synthesis of the compounds

The new compounds **3–11** and **12** were synthesized as illustrated in Scheme 1. In the case of compounds **3–11**, the key intermediate was 10-(2,3-epoxypropyl)-2-trifluoromethyl-phenothiazine **2**. It was prepared *via* the treatment of commercially available 2-trifluoromethylphenotiazine **1** with 1-bromo-2,3-epoxypropane at room temperature in the presence of sodium hydride. The products **3–11** were obtained in the oxirane ring opening reaction of epoxide **2** with the appropriate amines. In contradistinction to remaining compounds, product **12** was prepared in one-step reaction of alkilation of initial phenotiazine **1** by means of 8-(2-pyrimidinyl)-8-aza-5-azaspiro[4,5]decane bromide. From the post reaction mixtures, the expected phenotiazines **3–11** and **12** were separated by column chromatography or crystallization. The yield of reactions was in the range of 10–55%. No effort was made to optimize the reaction conditions to increase the yields. It is known that during the synthesis, as shown in Scheme 1, secondary reactions such as polymerization and condensation diminish the yield (24). For pharmacological purposes the obtaining free bases of compounds **3-11** and **12** were converted to the corresponding water soluble hydrochlorides.

Biological activity

In vitro pro-apoptotic activity and pro-necrotic effect (cytotoxicity) of newly synthesized analogues of FPh were carried out in cultures of human lymphocytes genotoxically damaged by incubation with B[*a*]P (7.5 μM, 48 h). Results revealed that tested analogues of FPh differed markedly in their pro-apoptotic activity and pro-necrotic effect. It was noticed that compounds **3**, **4**, **6–9** and **12** exerted a pro-apoptotic effect markedly stronger than that of fluphenazine, and compounds **3**, **9** and **10** exhibited the weakest influence on frequency of necrotic lymphocyte in cultures (Table 1). The A/N ratios calculated for compounds **5**, **10** and **11** were lower by 10–15 times in comparison to the parent compound (FPh), whereas those calculated for compounds **3**, **9** and **12** were 3–7.5 times higher as that calculated for FPh (Table 1).

2D-QSAR study

In the classical 2D-QSAR investigation the database is divided into a training and a test set.

Table 1. Experimental values of ED_{50} and TD_{50}, and calculated pED_{50}, pTD_{50} and A/N index.

COMPOUND	ED_{50} [μM]	pED_{50}	TD_{50} [μM]	pTD_{50}	A/N index
3	7.33	**5.13**	46.88	**4.33**	**3.24**
4	6.00	**5.22**	29.41	**4.53**	**2.47**
5	14.3	**4.84**	14.89	**4.83**	**0.53**
6	6.70	**5.17**	25.87	**4.59**	**1.95**
7	7.46	**5.13**	46.37	**4.33**	**3.15**
8	8.17	**5.09**	32.02	**4.49**	**1.98**
9	7.40	**5.13**	44.66	**4.35**	**3.05**
10	19.5	**4.71**	11.02	**4.96**	**0.28**
11	10.33	**4.99**	13.91	**4.86**	**0.68**
12	6.98	**5.16**	102.85	**3.99**	**7.44**
FPh	8.58	**5.07**	16.97	**4.77**	**1.0**

pED_{50} = log [1/(ED_{50} × 10^{-6})]; pTD_{50} = log [1/(TD_{50} × 10^{-6})]; A/N index: the results (ED_{50}/TD_{50}) obtained in cultures with the tested compound compared to reference cultures (FPh = 1.0)

Table 2. Symbols for the QSAR descriptors and their definition.

Code of descriptor	Description
chil_C	Carbon connectivity index (order 1). This is calculated as the sum of $1/\mathrm{sqrt}(d_id_j)$ over all bonds between carbon atoms i and j where $i < j$.
E_sol	Solvation energy. In the Potential Setup panel, the term enable flag is ignored, but the term weight is applied.
GCUT_PEOE_1	The GCUT descriptors are calculated from the eigenvalues of a modified graph distance adjacency matrix. Each ij entry of the adjacency matrix takes the value $1/\mathrm{sqr}(d_{ij})$ where d_{ij} is the (modified) graph distance between atoms i and j. The diagonal takes the value of the PEOE partial charges. The resulting eigenvalues are sorted and the smallest, 1/3-ile, 2/3-ile and largest eigenvalues are reported.
dipoleX	The x component of the dipole moment (external coordinates).
E_stb	Bond stretch-bend cross-term potential energy. In the Potential Setup panel, the term enable flag is ignored, but the term weight is applied.
a_hyd	Number of hydrophobic atoms.
DASA	Absolute value of the difference between ASA+ and ASA- where ASA+ -water accessible surface area of all atoms with positive partial charge (strictly greater than 0) and ASA- water accessible surface area of all atoms with negative partial charge (strictly less than 0).
PEOE_VSA_4	Sum of v_i where q_i is in the range (-0.25,-0.20). (PARTIAL CHARGE DESCRIPTOR)
SlogP	Log of the octanol/water partition coefficient (including implicit hydrogens). This property is an atomic contribution model that calculates logP from the given structure; i.e., the correct protonation state (washed structures). Results may vary from the logP(o/w) descriptor. The training set for SlogP was ~7000 structures.
PEOE_VSA_POL	Total polar van der Waals surface area. This is the sum of the v_i such that $|q_i|$ is greater than 0.2. The v_i are calculated Rusing a connection table approximation.
E_oop	Out-of-plane potential energy. In the Potential Setup panel, the term enable flag is ignored, but the term weight is applied.
E_vdw	van der Waals component of the potential energy. In the Potential Setup panel, the term enable flag is ignored, but the term weight is applied.

Because we had only 10 compounds we resign from this division. To perform quantitative structure-activity relationship study we calculated molecular descriptors for all compounds in database. Molecular descriptors are transformed into numbers - different chemical information (physicochemical properties) contained in the molecule. MOE program can calculate over 600 molecular descriptors including topological indices, structural keys, E-state indices, physical properties (such as log of the octanol/water partition coefficient, molecular weight and molar refractivity), topological polar surface area (TPSA) and CCG's VSA descriptors with applicability to both biological activity and ADME property prediction (ADME - **a**bsorption, **d**istribution, **m**etabolism, and **e**xcretion). Table 2 defines the QSAR descriptors used in our work.

The consecutive steps were: calculation, selection and evaluation of chemical structure descriptors for each compound in the database. Molecular descriptors were obtained with the QuaSAR-descriptor panel implemented in MOE molecular modeling software. Descriptors with constant and near-constant values (the same or almost the same value for each compound in the training set) were eliminated. Also descriptors that are highly degenerate (strong interrelationship between descriptors) and those that showed very low correlation with biological activity ($r^2 < 0.2$) were reduced. To find correlation between molecular structure of the new synthesized analogues of FPh and its physicochemical properties (which were expressed by molecular descriptors) we used PLS (Partial Least Squares) statistical method. The final result of this investigation was to generate a few 2D-QSAR models. Next steps, like: validation, cross-validation (LOO: leave-one-out procedure) of the models, detection of outliers and modification of the QSAR models were used to improve the statistical power of the obtained QSAR equations. Compounds that "do not fit" into the equation (the greatest standard deviation), so-called outliers, were eliminated and not included in the formed models. If it was necessary and/or possible, also a number of descriptors was reduced in individual equations. It is

a very popular and effective method to improve the statistical quality of QSAR models. To build QSAR models, therefore, were not used every time all structures. A lack of the values of expected biological activity: pED_{50} pTD_{50} in Tables 3 and 4 for certain compounds indicates that these structures weren't used to the building of the respective models (there were so-called outliers).

Interpretation of the 2D-QSAR models was the last step, which is presented in the next chapter. In order to select suitable (proper) descriptors that could affect the biological activity of the investigated compounds, correlation analysis was performed. PLS statistical method was used to establish the 2D-QSAR models. Below, we provide a few QSAR equations which were generated from both neutral and protonated forms of FPh analogues, and a pro-apoptotic activity and a pro-necrotic effect, were used as a measure of biological activity of tested compounds.

In the case of pro-apoptotic activity of compounds as dependent and descriptors as independent value we obtained following 2D-QSAR equations:
Model 1 and Model 2 for neutral forms of investigated compounds:
Model 1: pED_{50}= 5.89554 – 0.10098 × chil_C – 0.00220 × E_sol; R^2 = 0.91; XR^2 = 0.86; RMSE = 0.04; XRMSE = 0.05.

Model 2: pED_{50}= 6.94063 – 0.05506 × a_hyd + 1.43680 × GCUT_PEOE_1; R^2 = 0.97; XR^2 = 0.90; RMSE = 0.03; XRMSE = 0.05.

Model 3, 4 and 5 for monoprotonated forms:
Model 3: pED_{50}= 5.29996 – 0.11336 × dipoleX – 0.14243 × E_stb R^2 = 0.91; XR^2 = 0.75; RMSE = 0.08; XRMSE = 0.05.

Model 4: pED_{50}= 4.88967 + 0.00117 × DASA – 0.11526 × dipoleX; R^2 = 0.91; XR^2 = 0.78; RMSE = 0.07; XRMSE = 0.04.

Model 5: pED_{50}= 4.95715 – 0.11096 × dipoleX +0.01803 × PEOE_VSA_4; R^2 = 0.94; XR^2 = 0.74; RMSE = 0.08; XRMSE = 0.04.

In the above models adequacy was measured as the square of correlation coefficient (R^2), root mean square error (RMSE), cross-validated R^2 (XR^2) and cross-validated RMSE (XRMSE). The predictive power of the obtained models was expressed by statistical parameters: R^2 and XR^2 values, which should be close to one and resemble each other. The best models were obtained for neutral form. Equation 2 with the highest correlation coefficient (0.97) and cross-validated correlation coefficient XR^2 (0.90) seems to be the best model. This
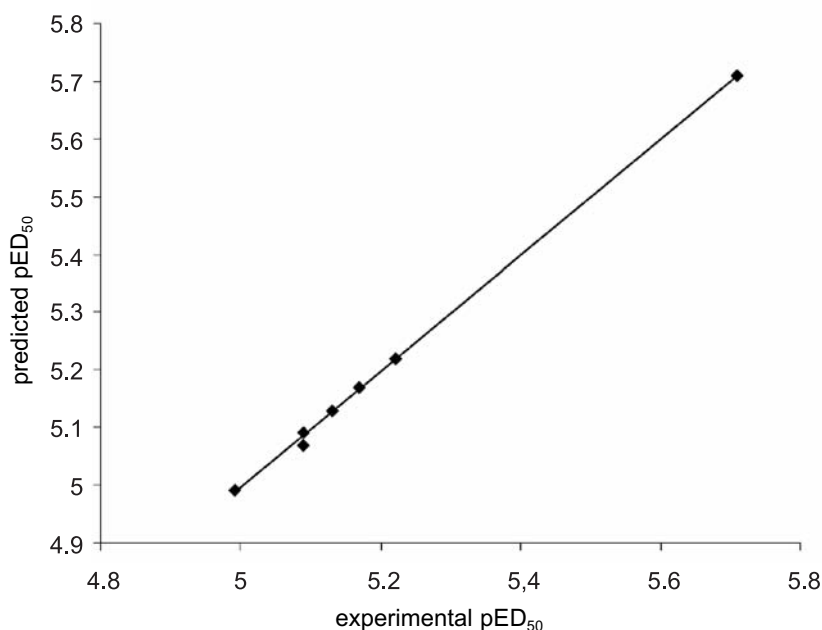

Figure 1. Plot of predicted pED_{50} against observed values for QSAR model by Equation 2

Table 3. Experimental pED$_{50}$ and predicted pED$_{50}$ values for investigated compounds.

Compound	Experimental pED$_{50}$	Predicted pED$_{50}$				
		Model 1	Model 2	Model 3	Model 4	Model 5
3	5.13	5.17	5.13	5.08	5.11	5.10
4	5.22	5.12	5.22	5.23	5.19	5.17
5	4.84	—	—	4.85	4.87	4.82
6	5.17	5.18	5.17	5.15	5.10	5.12
7	5.13	5.14	5.13	5.07	5.15	5.12
8	5.09	5.11	5.09	5.19	5.10	5.15
9	5.13	5.10	—	—	—	—
10	4.71	4.71	4.71	4.73	4.70	4.72
11	4.99	5.01	4.99	—	—	—
12	5.16	5.15	—	5.11	5.12	5.16
FPh	5.09	5.11	5.07	5.11	5.17	5.14

Table 4. Experimental pTD$_{50}$ and predicted pTD$_{50}$ values for investigated compounds.

Compound	Experimental pTD$_{50}$	Predicted pTD$_{50}$		
		Model 1	Model 2	Model 3
3	4.33	4.33	4.26	4.49
4	4.53	4.55	4.55	4.47
5	4.83	—	—	4.63
6	4.59	4.54	4.62	a.52
7	4.33	4.40	4.41	4.63
8	4.49	4.61	4.51	4.50
9	4.35	—	—	—
10	4.96	5.00	4.98	4.98
11	4.86	4.84	4.84	—
12	3.99	—	—	3.99
FPh	4.77	4.60	4.69	4.62

model correlate pED$_{50}$ value with two molecular descriptors: a_hyd and GCUT_PEOE_1. Only first parameter has clear structural interpretation, physico-chemical meaning - it reflects a number of hydrophobic atoms in a tested compound. This descriptor is negatively correlated with pED$_{50}$ value so increasing their value will lead to a decrease of pED$_{50}$ (reduced pro-apoptotic activity of the investigated compounds). Models 3, 4 and 5 show correlation coefficients about 0.9 (very high) but their cross-validated correlation coefficients is smaller than in models 1 and 2. In this three models the same descriptor appears - dipoleX. This is an x component of the dipole moment. It can be suggested that

reducing this parameter may increase biological activity. The predictive power of obtained models experimental and predicted pro-apoptotic activity were listed in Table 3 and showed in Figure 1.

In the case of a pro-necrotic effect of compounds as dependent- and descriptors as independent value we obtained the following 2D-QSAR equations:

Model 1 and Model 2 for neutral forms of investigated compounds:
Model 1: pTD$_{50}$ = 3.72121 + 0.2042 × SlogP; R^2 = 0.86; XR^2 = 0.81; RMSE = 0.10; XRMSE = 0.08.
Model 2: pTD$_{50}$ = 4.04217 + 0.17981 × SlogP −

0.00515 × **PEOE_VSA_POL; R² = 0.95; XR² = 0.87; RMSE = 0.05; XRMSE = 0.08**

Monoprotonated forms of the investigated compounds:

Model 3: pTD$_{50}$ = 3.54723 − 0.06107 × E_oop + 0.01836 × **E_vdw; R² = 0.95; XR² = 0.87 RMSE = 0.14; XRMSE = 0.17.**

In models 1 and 2 we applied a descriptor – SlogP - that was log of the octanol/water partition coefficient. This parameter is very important especially for bioactive compounds – drugs which should overpass biological lipid membranes (for example blood-brain barrier). The above QSAR equations suggest that increasing this value may increase the biological activity. Also other two descriptors: PEOE_VSA_POL and E_oop play an important role in pro-necrotic effect (cytotoxicity) of new synthesized analogues of FPh – but are negatively correlated with pTD$_{50}$.

Experimental pTD$_{50}$ and predicted pTD$_{50}$ values for tested compounds are presented in Table 4.

CONCLUSION

2D-QSAR equations, described in this publication, indicate the relationship between biological activity and the corresponding descriptors. Table 2 presents abbreviations, full names and description of all the descriptors used in the final 2D-QSAR models. Some of them have quite clear physical meaning, but unfortunately, most of them is often "a combination of" a few physical and chemical properties. Rarely happens that the biological activity of the drug is dependent on one or a few obvious and clear properties. Many factors have an influence on the biological activity of the compound and getting to know them isn't easy. Time-consuming and costly researches of specialists in the drug design confirm this facts. Obtained 2D-QSAR models allow to predict the activity of a new compound on the basis of its structure without the need of its synthesis. Estimate of the expected (predicted) biological activity for the next analog can be made by optimizing the geometry of the compound in a suitable computer program and using appropriate computational quantum chemistry methods and then compute the so-called molecular descriptors. Then, the obtained values of descriptors are substituted for the found earlier, reliable 2D-QSAR models and used to calculate a predicted value for the biological activity of a new derivative of the analyzed group of compounds. In order to propose structural modifications that can be taken into account in the further synthesis of next analogues, we plan to carry out a three-dimensional QSAR analysis (COMFA and CoMSIA). It involves the generation, for a series of compounds, so-called molecular field, which allows to visual identification of areas with positive or negative impact on the biological activity (spatial maps of steric and electrostatic interactions). This will be the next step in the study of the relationship between the pro-apoptotic activity and the structure of new analogues of FPh.

We found the obtained QSAR models suitable for predicting the activity of new synthesized FPh analogues. On the basis of QSAR equations we shall be able to propose new structures of Pht, which should exert a strong pro-apoptotic activity and a weak pro-necrotic effect on genotoxically-damaged cells and cancer cells.

REFERENCES

1. Claxton K.L., Chen J.J., Swope D.M.: J. Pharm. Pract. 20, 415 (2007).
2. Jaszczyszyn A. Gąsiorowski K., Świątek P., Malinka W., Cieślik-Boczula K., Petrus J., Czarnik-Matusewicz B.: Pharmacol. Rep. 64, 16 (2012).
3. Jaszczyszyn A. Gąsiorowski K., Świątek P., Malinka W., Cieślik-Boczula K., Petrus J., Czarnik-Matusewicz B.: Współcz. Onkol. 16, 332 (2012).
4. Bisi A., Meli M., Gobbi S., Tolomeo M., Dusonchet L.: Bioorg. Med. Chem. 16, 6474 (2008).
5. Morak-Młodawska B., Jeleń M., Pluta K.: Pol. Merkuriusz Lek. 26, 671 (2009).
6. Catts V.S., Catts S.V., O'Toole B.I., Frost A.D.: Acta Psychiatr. Scand. 117, 323 (2008).
7. Gil-Ad I., Shtaif B., Levkovitz Y., Nordenberg J., Taler M., Korov I., Weizman A.: Oncol. Rep. 15, 107 (2006).
8. Choi J.H., Yang Y.R., Lee S.K., Kim S.H., Kim Y.H., Cha J.Y., Oh S.W., Ha J.R., Ryu S.H., Suh P.G.: Ann. N. Y. Acad. Sci. 1138, 393 (2008).
9. Sun S.Y., Hail N., Lotan R.: J. Natl. Cancer Inst. 96, 662 (2004).
10. Jaszczyszyn A., Gąsiorowski K., Świątek P., Malinka W.: Onkol. Pol. 12, 143 (2009).
11. Gąsiorowski K., Jaszczyszyn A.: Onkol. Pol. 11, 147 (2008).
12. Jaszczyszyn A., Gąsiorowski K., Świątek P., Malinka W.: Onkol. Pol. 14, 43 (2011).

13. Levinson D.F., Simpson G.M., Lo E.S., Cooper T.B., Singh H., Yadalam K., Stephanos M.J.: Am. J. Psychiatry 152, 765 (1995).

14. Jaszczyszyn A., Gąsiorowski K.: Chemopreventive mechanisms of action of newly synthesized analogs of fluphenazine (Polish) Borgis® Wydawnictwo Medyczne, Warszawa 2006.

15. Frisch M.J., Trucks G.W., Schlegel H.B., Scuseria G.E., Robb M.A., Cheeseman J.R., Montgomery Jr J.A., Vreven T., Kudin K.N., Burant J.C., Millam J.M., Iyengar S.S., Tomasi J., Barone V., Mennucci B., Cossi M., Scalmani G., Rega N., Petersson G.A., Nakatsuji H., Hada M., Ehara M., Toyota K., Fukuda R., Hasegawa J., Ishida M., Nakajima T., Honda Y., Kitao O., Nakai H., Klene M., Li X., Knox J.E., Hratchian H.P., Cross J.B., Adamo C., Jaramillo J., Gomperts R., Stratmann R.E., Yazyev O., Austin A.J., Cammi R., Pomelli C., Ochterski J.W., Ayala P.Y., Morokuma K., Voth G.A., Salvador P., Dannenberg J.J., Zakrzewski V.G., Dapprich S., Daniels A.D., Strain M.C., Farkas O., Malick D.K., Rabuck A.D., Raghavachari K., Foresman J.B., Ortiz J.V., Cui Q., Baboul A.G., Clifford S., Cioslowski J., Stefanov B.B., Liu G., Liashenko A., Piskorz P., Komaromi I., Martin R.L., Fox D.J., Keith T., Al-Laham M.A., Peng C.Y., Nanayakkara A., Challacombe M., Gill P.M.W., Johnson B., Chen W., Wong W., Gonzalez C., Pople J.A.: Gaussian 03, Revision C.02, Gaussian, Inc., Wallingford CT 2004.

16. Tsakovska I.M.: Bioorg. Med. Chem. 11, 2889 (2003).

17. McDowell J.J.H.: Acta. Cryst. B 36, 2178 (1980).

18. Pajeva I.K., Wiese M.: J. Med. Chem, 45, 5671 (2002).

19. Pajeva I.K., Globisch C., Wiese M.: J. Med. Chem. 47, 2523 (2004).

20. Pajeva I.K., Wiese M.: J. Med. Chem. 41, 1815 (1998).

21. Tsakovska I., Pajeva I.: Curr. Drug Targets 7, 1123 (2006).

22. MOE, Molecular Operating Environment, 2005.06; Chemical Computing Group Inc.: Montreal 2005.

23. Systat 11, 12 software (Systat Software, Inc.).

24. Leuschner J., Schafer H., Leuschner F.: Eur. J. Med. Chem. 29, 241 (1994).

NEW RENIN INHIBITORS CONTAINING PHENYLALANYLHISTIDYL-γ-AMINO ACID DERIVATIVES IN P₃ - P₁' POSITION

IWONA WINIECKA*, DOROTA MARSZAŁEK, ANNA GOLDNIK,
PAWEŁ JAWORSKI and ALEKSANDER P. MAZUREK

Department of Drug Chemistry, Medical University of Warsaw, Banacha 1, 02-097 Warszawa, Poland

Abstract: Five potential inhibitors of renin have been designed and obtained. In the molecule position $P_3 – P_1'$, crucial for indicating inhibitory activity, all contain phenylalanylhistidylaminoalcanoyl group, ready for interaction with the hydrophobic pocket $S_3 – S_1$ of renin molecule. The aminoalcanoyl fragment consists of pseudodipeptidic units derivative of γ-amino acids: of 4-amino-3-hydroxybutanoic acid (AHBA) [26], 4-amino-5-(4-ethoxyphenyl)-3-hydroxypentanoic acid (AEPHPA) [13], 4-amino-5-cyclohexyl-3-hydroxypentanoic acid (ACHPA) (1) and 4-amino-3-hydroxynonanoic acid (AHNA) [21]. At the $P_3 – P_2$ position of obtained compounds an unnatural fragment, derivative of Phe-His dipeptide, was placed ande isoamyl amid of 6-aminohexanoic acid was attached at the end of the molecule (εAhx-Iaa). The preliminary *in vitro* tests indicated that all compounds were inactive. However, they provided valuable information on P_3-P_2 fragment possible structure modification able to produce a resonable renin activity inhibition. All synthesized inhibitors were chymotrypsin-resistant.

Keywords: renin inhibitors, hydrophobic pocket, position P_3 - P_1', inhibitory activity, pseudodipeptide unit, γ-amino acid.

The rennin-angiotensin system (RAS) is an enzymatic hormonal mechanism regulating blood pressure and water-electrolyte management of the organism. Excessive activity of RAS constitutes the pathogenesis of cardiovascular diseases, such as arterial hypertension, congestive heart failure or ischemic heart disease. The crucial link of this system is renin, an enzyme belonging to the class of acidic aspartyl proteases. The key role of renin in the body comprises the conversion of the specific substrate – angiotensinogen – into the decapeptide angiotensin I, by breaking the bond between two amino acids Leu[10] – Val[11]. Angiotensin I is then transformed into octapeptide angiotensin II under the influence of angiotensin-converting enzyme (ACE). Angiotensin II exerts negative pressor activity on the cardiovascular system by specific receptors AT_1. Recent years have seen a dynamic development of drugs inhibiting this system, such as convertase inhibitors and antagonists of AT_1 receptor. The introduction of the first renin inhibitor aliskiren (2) into treatment in 2007 opened new perspectives for the treatment of cardiovascular system diseases. The results of contemporary tests conducted in various research facilities on the dependence of action on the structure of renin inhibitors indicate that apart from hydrogen bonds, the hydrophobic ligand – enzyme interaction has the essential impact on the activity (1).

To examine the influence of the interaction of the inhibitor molecule part at its $P_3 – P_1'$ position with hydrophobic sites of renin active centre on the biological activity of the enzyme, we have designed and synthesized five new compounds (see Table 1):

Boc – Phe (4-OMe) – His (NⁱᵐBzl) – ACHPA – εAhx – Iaa   [12]
Boc – Phe (4-OMe) – His (NⁱᵐTrt) – AEPHPA – εAhx – Iaa   [20]
Boc – Phe (4-OMe) – His (NⁱᵐTrt) – AHNA – εAhx – Iaa   [25]
Boc – Phe (4-OMe) – His (NⁱᵐBzl) – AHBA – εAhx – Iaa   [32]
Boc – Phe (4-OMe) – His (NⁱᵐBzl) – AHNA – εAhx – Iaa   [37]

The compounds were designed on the basis of the amino acid sequence of angiotensinogen fragment 8 – 13,

8	9	10	11	12	13
Phe –	His –	Leu –	Val –	Ile –	His –
P_3	P_2	P_1	P_1'	P_2'	P_3'
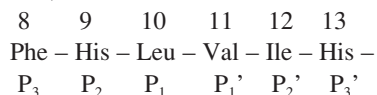
that in physiological conditions combines with renin as shown in Figure 11.

* Corresponding author: e-mail: iwona.winiecka@wum.edu.pl

Table 1. Physicochemical and analytical properties of the synthesized compounds.

Compd. No.	Structure	Formula m.w.	Yield (%)	M.p. (°C)	$[\alpha]_D^{20}$ (c, MeOH)	TLC, R_f*	HPLC (% purity)	Log P
4	Boc-His(N^{im}Bzl)-ACHPA-OEt	$C_{31}H_{46}O_7N_4$ 586.71	67.00	144-145	-34.8 (1.0)	0.41 (A)	-	-
8	Boc-Phe(4-OMe)-His-(N^{im}Bzl)-ACHPA-OEt	$C_{39}H_{57}O_8N_5$ 747.44	48.00	Semi-solid	-36.0 (1.2)	0.38 (A)	-	-
12	Boc-Phe(4-OMe)-His(N^{im}Bzl)-ACHPA-Ahx-Iaa	$C_{50}H_{75}O_8N_7$ 902.20	26.00	Semi-solid	-25.0 (1.0)	0.35 (A)	99.57	6.14
14	Boc-Phe(4-OMe)-His(N^{im}Trt)-OMe	$C_{41}H_{44}O_6N_4$ 688.84	80.00	73-76	+18.2 (1.1)	0.64 (A) 0.21 (E)	-	-
15	Boc-AEPHPA-OEt	$C_{20}H_{31}O_6N$ 381.48	78.00	83-85	-22.0 (1.0)	0.16 (B)	-	-
18	Boc-Phe(4-OMe)-His(N^{im}Trt)-AEPHPA-OEt	$C_{55}H_{63}O_8N_5$ 933.65	39.00	94-96	-20.0 (1.0)	0.62 (A)	-	-
20	Boc-Phe(4-OMe)-His(N^{im}Trt)-AEPHPA-Ahx-Iaa	$C_{64}H_{81}O_9N_7$ 1091.41	28.00	Semi-solid	-15.0 (1.1)	0.71 (A)	99.78	9.50
21	Boc-AHNA-OEt	$C_{16}H_{32}O_5N$ 317.41	85.00	49-50	-4.7 (1.4)	0.38 (B)	-	-
23	Boc-Phe(4-OMe)-His(N^{im}Trt)-AHNA-OEt	$C_{51}H_{63}O_8N_5$ 873.60	47.00	Oil	+28.0 (1.2)	0.64 (A)	-	-
25	Boc-Phe(4-OMe)-His(N^{im}Trt)-AHNA-Ahx-Iaa	$C_{60}H_{81}O_8N_7$ 1028.36	23.00	Oil	+23.0 (1.0)	0.68 (A)	99.04	9.28
26	Boc-AHBA-OEt	$C_{11}H_{21}O_5N$ 247.30	60.00	Semi-solid	-14.7 (1.0)	0.10 (B)	-	-
28	Boc-His(N^{im}Bzl)-AHBA-OEt	$C_{22}H_{34}O_6N_4$ 450.56	8.00	117-123	-21.5 (1.1)	0.63 (D)	-	-
30	Boc-Phe(4-OMe)-His(N^{im}Bz)-AHBA-OEt	$C_{32}H_{45}O_8N_5$ 627.77	34.00	Semi-solid	-29.4 (1.0)	0.67 (C)	-	-

Table 1. cont.

Compd. No.	Structure	Formula m.w.	Yield (%)	M.p. (°C)	$[\alpha]_D^{20}$ (c, MeOH)	TLC, R_f^*	HPLC (% purity)	Log P
32	Boc-Phe(4-OMe)-His(N^{im}Bzl)-AHBA-Ahx-Iaa	$C_{43}H_{63}O_8N_7$ 806.04	21.00	Semi-solid	-22.0 (1.2)	0.75 (A)	95.96	7.21
33	Boc-His(N^{im}Bzl)-AHNA-OEt	$C_{29}H_{44}O_6N_4$ 662.82	61.00	97 – 98	-16.0 (1.0)	0.42 (E)	-	-
35	Boc-Phe(4-OMe)-His(N^{im}Bzl)-AHNA-OEt	$C_{36}H_{53}O_8N_5$ 707.36	32.00	Oil	-31.3 (1.0)	0.57 (C)	-	-
37	Boc-Phe(4-OMe)-His(N^{im}Bzl)-AHNA-Ahx-Iaa	$C_{48}H_{71}O_8N_7$ 874.12	19.00	Semi-solid	-26.4 (1.2)	0.71 (D)	96.97	5.92

The elemental analysis results were within ±0.4% of theoretical values. Hydrophobicity of the compounds expressed as log P value was calculated by a computational method (24). Mobile phase systems (v/v) were: CH_3Cl-MeOH 95 : 5 (A), hexane-AcOEt 80 : 20 (B), CH_3Cl-MeOH 50 : 50 (C), CH_3Cl-MeOH 90 : 10 (D), CH_3Cl-MeOH 98 : 2 (E)

In the molecule position $P_3 – P_1$', crucial for the inhibitory activity, all planned compounds contain non-peptide derivatives of phenylalanylhistidyl-γ-amino acids. In order to increase stability, Leu-Val dipeptide in position P_1 - P_1' sensitive to proteolytic activity of renin, was replaced with hydrophobic pseudodipeptide derivatives of unnatural γ-amino acids AHBA, AHNA, AEPHPA, ACHPA. Previously obtained renin inhibitors containing 4-amino-5-cyclohexyl-3-hydroxypentanoic acid (ACHPA) exhibited medium or high inhibitory activity (1, 3). Inhibitors containing 4-amino-3-hydroxybutanoic acid (AHBA), 4-amino-3-hydroxynonanoic acid (AHNA), 4-amino-5-(4-ethoxyphenyl)-3-hydroxypentanoic acid (AEPHPA) have not been obtained and tested so far. We have assumed that the structural differences between hydrophobic groups in the applied pseudopeptides would allow us to determine the most optimal interaction of these molecule's fragments with the hydrophobic pocket S_1. In position P_1 the compounds [25, 37] contain unbranched aliphatic side chain (fragment C_5 - C_9 in AHNA molecule). Probably, the long flexible chain, having adopted sufficiently beneficial conformation, will adjust well to the hydrophobic pocket, similarly to cyclohexyl substituent in position 5 of ACHPA molecule, which is confirmed by high inhibitory activity of obtained inhibitors containing this pseudopeptide (4, 5). This beneficial biological effect arises from the capacity of C - C bonds to change position around carbon atom C_5 and the cyclohexane ring capacity to adopt the "chair" conformation, which results in the most beneficial adjustment of the hydrophobic pocket to hydrocarbon radical. It seems interesting to compare the biological activity of the inhibitor with the cycloaliphatic ring [12] with compound [20] containing an aromatic 4-ethoxyphenyl substituent in position 5 of AEPHPA molecule. Theoretically, lower affinity of the flat, rigid aromatic ring to the hydrophobic pocket, as compared to the cycloaliphatic ring, may be balanced by a small aliphatic ethoxy substituent present in position 4 of the phenyl ring, due to the possible presence of specific subpockets in site S_1, similarly to the case of site S_3. The presence of a moderately polar ethoxy group of the side chain, in fragments P_1 of the inhibitor molecules, due to its probable participation in the hydrogen bonding in sub pockets, may impact not only the activity, but also pharmacokinetic properties such as solubility at physiological pH and bioavailability. Designing compound [32] (of minimum hydrophobicity) without a side chain and with a 4-carbon frame of 4-amino-3-hydroxybutanoic acid is to answer the question of whether and in

Table 2. ¹H NMR spectra of the synthesized compounds.

Compd. no.	Solvent	Chemical shifts δ, ppm
4	CDCl₃	0.72-1.84 (m, 13H, C₆H₁₁, 2HC₅); 1.24 (t, 3H, CH₃); 1.42 (s, 9H, C₄H₉); 2.28-2.56 (m, 2H, 2HC₂); 2.92-3.12 (m, 2H, 2HCβ); 4.05-4.20 (m, 2H, OCH₂); 4.26-4.36 (m, 1H, 1HC₃); 5.03 (d, J = 2Hz, 2H, CH₂ᵦ𝓏ₗ); 6.26 (d, J = 4 Hz, 1H, NH); 6.75 (d, J = 10Hz, 1H, HCⁱᵐ); 7.26 (s, 5H C₆H₅); 7.5 (s, 1H, HCⁱᵐ).
8	CDCl₃	0.72-1.86 (m, 15H, C₆H₁₁, 2HC₂, 2HC₅); 1.25 (t, 3H, CH₃); 1.36 (s, 9H, C₄H₉); 2.73-3.24 (m, 4H, 2HCβHis, HCαPhe, HC₄); 3.78 (s, 3H, OCH₃); 4.14 (q, 2H, OCH₂); 4.20-4.73 (m, 4H, 2HCᵦPhe, HCαHis, HC₃); 5.01 (s, 2H, CH₂Bzl); 6.64-6.91 (m, 3H, CHⁱᵐ, 2×NH); 6.92-7.20 (m, 4H, C₆H₄); 7.27 (s, 5H, C₆H₅); 7.33 (s, 1H, CHⁱᵐ); 8.25 (d, J = 12Hz, 1H, NH).
12	CDCl₃	0.72-1.85 (m, 28H, C₆H₁₁, 2HC₅, 2×CH₃Iaa, 2HCᵦIaa, HC γ Iaa, 3×CH₂Ahx), 1.36 (s, 9H, C₄H₉); 1.86-2.00 (d, J = 12Hz, 2H, 2HC₂); 3.47 (s, br, 2H, 2HCᵦHis); 4.08 (s, 3H, OCH₃); 4.24-4.51 (m, 10H, CH₂Phe, HC α His, 2HCαIaa, 2CH₂αAhx); 4.76 (s, 2H, CH₂ Bzl); 6.64 (d, J = 8Hz, 4H, C₆H₄); 6.82 (d, J = 8Hz, 1H, NH); 7.78-7.94 (m, 4H, 2×HCⁱᵐ, 2×NH); 8.08 (d, J = 8Hz, 1H, NH).
14	CDCl₃	1.34 (s, 9H, C₄H₉); 2.86-3.12 (m, 4H, 2×CH₂); 3.59 (s, 3H, OCH₃ester); 3.72 (s, 3H, OCH₃ether); 4.11 (q, 1H, HC₂); 4.39 (d, J = 5Hz, 1H, NH); 4.77 (q, 1H, CH); 5.23 (d, J = 6Hz, 1H, NH); 6.53 (s, 1H, CHⁱᵐ); 7.02-7.38 (m, 20H, C₆H₄, 3×C₆H₅, CHⁱᵐ).
15	CDCl₃	1.24 (t, 3H, CH₃ester); 1.39 (t, 3H, CH₃ether); 1.41 (s, 9H, C₄H₉); 2.32-2.35 (m, 1H, CH); 2.53-2.62 (m, 1H, CH); 2.84 (d, J = 9Hz, 2H, 2HC₅); 3.62-3.96 (m, 2H, CH₂); 4.00 (q, 2H, OCH₂ester); 4.13 (q, 2H, OCH₂ester); 4.92 (d, J = 10Hz, 1H, NH); 6.81; 7.14 (dd, J = 8Hz, 8 = Hz, 4H, C₆H₄).
18	CDCl₃	1.99 (t, 3H, CH₃); 1.33 (s, 9H, C₄H₉); 2.39-2.57 (m, 2H, CH₂); 2.75-3.02 (m, 2H, CH₂); 3.41 (d, J = 3,41Hz, 1H, CH); 3.76 (s, 3H, OCH₃); 3.94-4.12 (m, 6H, 2×OCH₂, CH₂); 4.30 (q, 1H, CH); 4.66-4.78 (m, 1H, CH); 5.41 (s, br, 1H, NH); 6.78-7.45 (m, 21H, 3×C₆H₅, C₆H₄, 2×CHⁱᵐ); 7.72 (s br, 1H, NH); 7.87 (s br, 1H, NH).
20	CDCl₃	0.87 (d, J = 6Hz, 6H, 2×CH₃Iaa); 1.12-1.46 (m, 8H, 2HCαIaa, HCγIaa, HC, 2×CH₂Ahx); 1.24 (s, 9H, C₄H₉); 1.47-1.83 (m, 12H, 2HC₂, 2HC₅, 2HCᵦIaa, 3×CH₂Ahx); 2.16 (t, 3H, CH₃); 2.62-3.00 (m, 2H, 2×HC); 3.79 (s, 3H, OCH₃); 3.89 (s, 2H, OCH₂); 3.99 (q, 2H, OCH₂); 4.18 (q, 1H,HC₄); 4.51 (d, J = 5Hz, 2H, CH₂); 5.08 (s, 1H, NH); 5.93(s, 1H, NH); 6.65 (s, 1H, NH); 6.75-6.94 (m, 5H, C₆H₄, NH); 6.95-7.50 (m, 21H, 3×C₆H₅, C₆H₄, 2×CHⁱᵐ); 9.39 (s, br, 1H, NH).
21	CDCl₃	0.88 (t, 3H, CH₃); 1.24-1.40 (m, 7H, CH₃ester, 2×CH₂); 1.44 (s, 9H, C₄H₉); 2.43-2.60 (m, 2H, CH₂); 3.50 (s, 1H, NH); 4.06 (s, 1H, CH); 4.16 (q, 2H, OCH₂); 4.77 (d, J = 9.6Hz, 1H, NH).
23	CDCl₃	0.87 (t, 3H, CH₃ester); 1.10-1.38 (m, 7H, CH₃, 2×CH₂) 1.41 (s, 9H, C₄H₉); 2.96-3.01 (m, 2H, CH₂His); 3.58-3.65 (m, 2H, CH₂ Phe(4-OMe)); 3.77 (s, 3H, OCH₃); 4.13 (q, 2H, OCH₂); 4.80-4.87 (m, 1H, CH); 6.03 (d, J = 9.6Hz, 1H, NH); 6.19 (d, J = 8.4Hz, 1H, NH); 6.81 (d, J = 9.6Hz, 1H, NH); 7.10-7.50 (m, 21H, C₆H₄, 3×C₆H₅, 2×CHⁱᵐ).
25	CDCl₃	0.82-1.56 (m, 26H, C₄H₉, 2HC₅, 2×CH₃ Iaa, 2HCᵦ Iaa, HCγIaa, 3×CH₂Ahx); 1.92 (d, J = 10.2Hz, 2H CH₂); 3.4-3.6 (m, 2H, CH₂His); 3.8 (q, 2H, CH₂His); 4.02-4.40 (m, 5H, CH₂Phe(4-OMe), OCH₃); 6.20-6.22 (dd, J = 9.6Hz, J = 9.6Hz, 1H, NH); 6.66 (d, J = 8.4Hz, 2H, 2HCⁱᵐ); 7.24-8.20 (m, 21H, C₆H₄, 3×C₆H₅, 2×HCⁱᵐ); 7.10-7.16 (m, 1H, NH).
26	CDCl₃	1.20-1.31 (m, 3H, CH₃ester); 1.45 (s, 9H, C₄H₉); 2.41-2.58 (m, 2H, CH₂); 3.03-3.39 (m, 2H, CH₂); 4.06-4.28 (m, 3H, OCH₂, CH); 5.04 (s, br,1H, NH).
28	CDCl₃	1.25 (s, 3H, CH₃ester); 1.41 (s, 9H, C₄H₉); 1.90-1.94 (m, 2H, CH₂); 3.11 (d, 2H, CH₂); 4.07-4.20 (m, 3H, HCβ, OCH₂); 4.45 (s,br, 1H, CHα His); 5.09 (s, 2H, CH₂Bzl); 5.85 (s, br, 1H, NH); 5.88 (s, br, 1H, NH); 6.74 (s, 1H, HCⁱᵐ); 7.15-7.37 (m, 5H, C₆H₅); 7.74 (s, 1H, HCⁱᵐ).
30	CDCl₃	1.25-1.42 (m, 12H, C₄H₉, CH₃ester); 1.9 (d, J = 9Hz, 2H, 2HC₂); 3.05 (d, J = 5.4Hz, 2H, 2HCᵦHis); 3.4-3.8 (m, 9H, CH₂Phe, CH₂Bzl, HCₐHis, HC₃, OCH₃); 4.95-4.38 (m, 2H, OCH₃); 4.55 (d, J = 7.2Hz, 1H, HC); 4.95 (d, J = 7.2Hz, 1H, HC); 6.78-7.13 (m, 7H, C₆H₅, 2HCⁱᵐ).

Table 2. cont.

Compd. no.	Solvent	Chemical shifts δ, ppm
32	CDCl$_3$	0.91-1.92 (m, 26H, C$_4$H$_9$, 2HC$_5$, 2×CH$_3$Iaa, HC$_2$Iaa, 2HC$_\beta$Iaa, 3×CH$_2$Ahx); 1.93-2.15 (m, 4H, 2HC$_2$ Ahx, 2HC$_3$ (Phe-4OMe); 3.01 (s, br, 2H, 2HC$_\beta$His); 3.41-3.59 (m, 1H, HC); 3.67-3.83 (m, 5H, OCH$_3$, CH$_2$Phe); 4.12-4.19 (m, 4H, CH$_2$Bzl, 2HCPhe); 4.5 (d, J = 6.3 Hz, 1H, HC), 4.9 (d, J = 7.2Hz, 1H, HC); 5.12-5.38 (m, 7H, C$_6$H$_5$, 2HC^{im}).
33	CDCl$_3$	0.85 (t, 3H, CH$_3$), 1.18-1.38 (m, 16H, C$_4$H$_9$, CH$_3$ ester, 2×CH$_2$); 2.32-2.52 (m, 2H, 2HC$_2$); 2.88-3.22 (m, 2H, 2HC$_\beta$); 4.5 (s, 1H, HC$_3$); 5.11 (d, J = 5.2Hz, 2H, CH$_2$Bzl); 5.4-5.73 (m, 4H, HC$_\alpha$His, CH$_3$); 5.92 (s, 1H, NH); 6.16 (s, 1H, NH); 6.83 (d, J = 8.7Hz, 1H, CH^{im}); 7.03-7.90 (m, 8H, C$_6$H$_5$, CH, 2CH); 7.68 (d, J = 10.2Hz, 1H, HC^{im}).
35	CDCl$_3$	0.85 (t, 3H, CH$_3$ ester); 1.2-1.34 (m, 16H, C$_4$H$_9$, 2HC$_2$, 2HC$_5$, CH$_3$); 1.5-1.6 (m, 2H, 2HC$_\beta$); 2.26-2.44 (m, 2H, 2HC$_\beta$); 2.78-3.18 (m, 5H, HC$_\alpha$His, HC$_3$, CH$_2$Bzl, HC$_\alpha$Phe); 3.74 (s, 3H, OCH$_3$); 4.12 (q, 2H, OCH$_3$); 4.30 (d, J = 6Hz, 1H, NH); 4.76 (q, 1H, HC$_3$); 5.06 (d, J = 12Hz, 2H CH$_2$Bzl); 5.36 (d, J = 6.4Hz, 1H, NH); 5.6-5.9 (s, br, 4H HC$_\alpha$His, CH$_3$); 7.06 (d, J = 8.6Hz, 1H, HC^{im}); 7.14-7.40 (m, 12H, C$_6$H$_4$, C$_6$H$_5$, CH, 2HC); 7.75 (d, J = 4Hz, 1H, HC^{im},); 8.04 (d, J = 6.6Hz, 1H, NH).
37	CDCl$_3$	0.76-0.96 (m, 6H, 2×CH$_3$Iaa); 1.02-1.76 (m, 26H, 2HC$_\alpha$Iaa, HC$_\beta$Iaa, 2HC$_3$, C$_4$H$_9$, 2HC$_2$, 2HC$_5$, 2HC$_\beta$Iaa, 3×CH$_2$Ahx); 2.43 (s, 2H, 2HC$_\beta$); 2.9-3.1 (m, 2H, CH$_2$His); 3.3-3.5 (s, br, 1H, CH); 3.72 (s, 3H, OCH$_3$); 3.6-3.75 (m, 5H, CH$_2$Phe, CHPhe, CH$_2$Bzl); 3.9 (d, J = 9Hz, 1H, CH); 4.48 (s, 1H, NH); 4.95 (s, 1H, NH); 6.72 (d, J = 7.8Hz, 1H, HC^{im}); 7.2-7.32 (m, 11H, C$_6$H$_4$, C$_6$H$_5$, 2HC); 7.33 (d, J = 4.8 Hz, 1H, HC^{im}).

what way the hydrophobic activity of only a fragment C_1-C_4 of molecule with probable domination of the hydrogen bond OH bounding the designed rennin inhibitors to S_1 area of rennin fragment. In all obtained compounds, there is an unnatural fragment Phe (4-OMe)- His (N ^{im}Bzl) [12, 32, 37] and Phe (4-OMe)- His (N^{im}Trt) [20, 25] at position P_3 - P_2. In the digestive tract the natural dipeptide is subject to proteolysis catalyzed by chymotrypsin. To achieve stability of renin inhibitors in the digestive tract the site P_3 - P_2 should be modified in such a way so as to prevent or significantly hamper formation of the hydrogen and hydrophobic bonds of this fragment with the active centre of chymotrypsin. The substitution of the phenyl ring in position 4 with methoxy group (Phe (4-OMe)) decreases the affinity to chymotrypsin without hampering its capacity to bind with the active centre of renin (6). Position P_3 absolutely requires the presence of the aromatic ring, which is evidenced by previous synthesis of active inhibitors containing in this position 4-metoxyphenyl ring (7), as well as obtaining inactive inhibitors devoid of this ring (8). This arises from the fact that the crucial element of the active site S_3 is the subpocket S_{3sp} (Figure 11), which is specific to the phenyl ring (9, 10).

It is now a well-known fact that the structural modification of position P_2 plays a significant role for the activity and selectivity of analogs. A large, bifurcated hydrophobic pocket S_2 of renin may adjust both hydrophobic and polar pharmacophores, thus enabling significant modification of the enzyme – ligand interaction. The fact that the conformation of the side chain in P_2 is not strictly dependent on the location of the bond shows that exact prediction of the enzyme – ligand interaction is relatively difficult (1, 11-13). Our team previously obtained active inhibitors of renin containing aliphatic amino acids with a small hydrophobic side chain instead of histidine (His) in position P_2 (7, 14, 15). This fact suggests that apart from the formation of a hydrogen bonding with the nitrogen atom of the imidazole ring, there is a possibility of simultaneous presence of significant hydrophobic reaction with a hydrophobic subpocket in site S_2. To verify these hypotheses, in designed inhibitors, we introduced into their position P_2 a histidine molecule substituted at the nitrogen atom in the imidazole ring with large substituents with hydrophobic properties. It seems interesting to compare the location of the benzyl substituent (Bzl) with one rigid aromatic ring [12, 32, 37] in the subpocket S_2, with the analogue containing a bifurcated 3-ring triphenylmethyl substituent (Trt) characterized by increased hydrophobicity [20, 25].
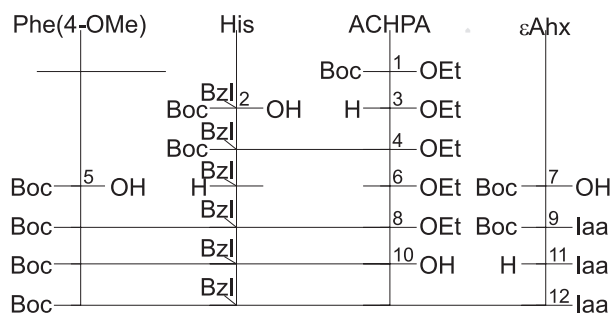
Figure 1. Synthesis of Boc–Phe (4-OMe)–His (N^{im}Bzl)–ACHPA–εAhx–Iaa [12]
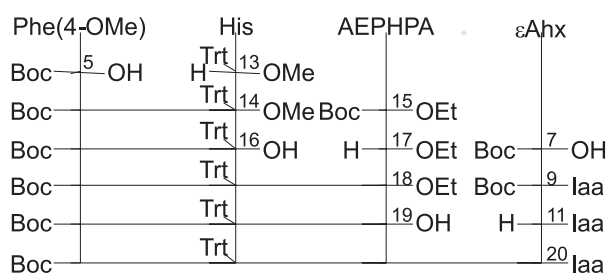
Figure 2. Synthesis of Boc–Phe (4-OMe)–His (N^{im}Trt)–AEPHPA–εAhx–Iaa [20]
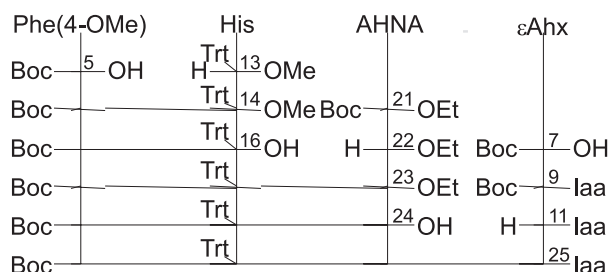
Figure 3. Synthesis of Boc–Phe (4-OMe)–His (N^{im}Trt)–AHNA–εAhx–Iaa [25]

Moreover, the presence of spatially large side chains in P_2 may protect the peptide bond in position P_3 - P_2 against the activity of chymotrypsin. In all five renin inhibitors obtained by us, the tert-butoxycarbonyl (t-Boc) substituent was placed at the N-end, and isoamylamide of 6-aminohexanoic acid (εAhx-Iaa)

was introduced into position P_2' - P_3'. It is assumed that hydrophobic grouping with branched alkyl structure (t-Boc) may improve the absorption from the digestive tract due to the increase in lipophilicity (16). Branched alkylamide of the unnatural amino acid of linear and flexible structure (εAhx-Iaa)

placed in position P_2' - P_3' protects the C-end of the molecule from enzymatic degradation and may have inhibitory effect due to good affinity to the hydrophobic site S_2' - S_3' of the active centre of renin, which is confirmed by the numerous active and stable inhibitors containing εAhx-Iaa at C-end that we have obtained in recent years (3, 17-19).

EXPERIMENTAL

Chemistry

The structures of inhibitors considered in the present work are shown in Figures 6 to 10. The inhibitors [12, 20, 25, 32, 37] as well as their intermediates were synthesized according to the schemes presented in Figures 1 to 5. The applied methods are
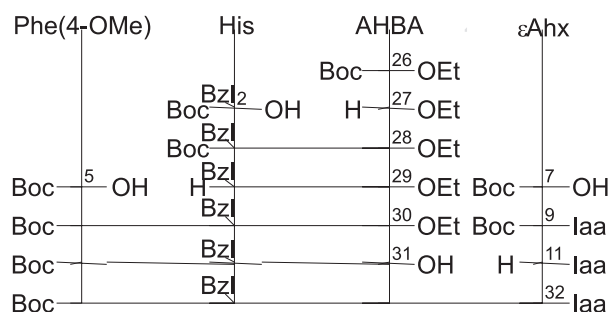
Figure 4. Synthesis of Boc–Phe (4-OMe)–His (N^{im}Bzl)–AHBA–εAhx–Iaa [32]
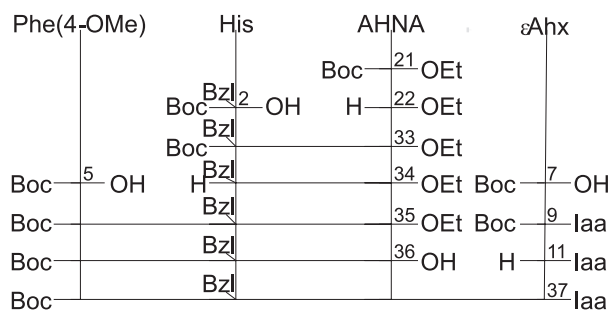
Figure 5. Synthesis of Boc–Phe (4-OMe)–His (N^{im}Bzl)–AHNA–εAhx–Iaa [37]
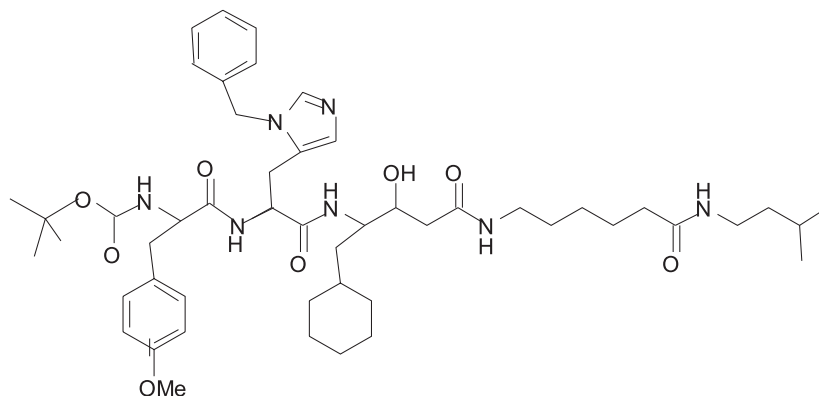
Figure 6. [N-(tert-butoxycarbonyl)-4-methoxyphenylalanyl]-N^{im}benzylhistidyl-(3S, 4S)-4-amino-5-cyclohexyl-3-hydroxypentanoyl-ε-aminohexanoic acid isoamylamide Boc–Phe (4-OMe)–His (N^{im}Bzl)–ACHPA–εAhx–Iaa [12]
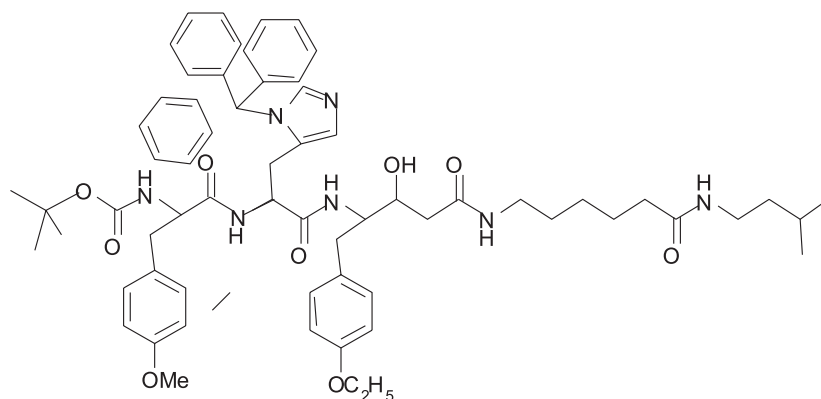
Figure 7. [N-(tert-butoxycarbonyl)-4-methoxyphenylalanyl]-N^{im}tritylhistidyl-(3S, 4S)-4-amino-5-(4-ethoxyphenyl)-3-hydroxypentanoyl-ε-aminohexanoic acid isoamylamide Boc – Phe (4-OMe) – His (N^{im}Trt) – AEPHPA – εAhx – Iaa [20]
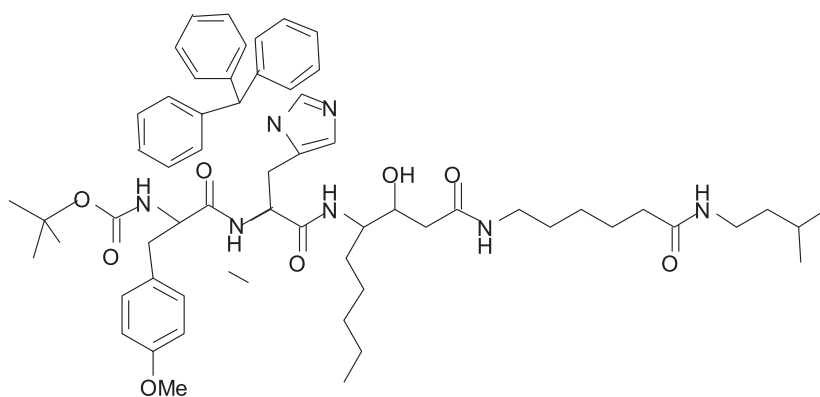
Figure 8. [N-(tert-butoxycarbonyl)-4-methoxyphenylalanyl]-N^{im}tritylhistidyl-(3S, 4S)-4-amino-3-hydroxynonanoyl-ε-aminohexanoic acid isoamylamide Boc – Phe (4-OMe) – His (N^{im}Trt) – AHNA – εAhx – Iaa [25]
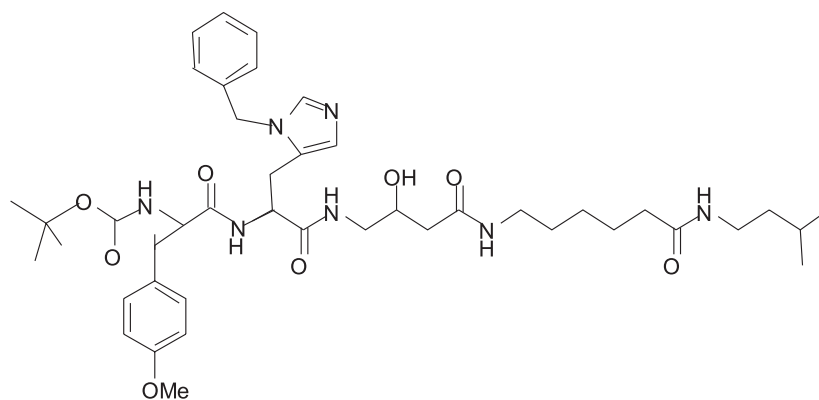
Figure 9. [N-(tert-butoxycarbonyl)-4-methoxyphenylalanyl]-N^{im}benzylhistidyl-(3S, 4S)-4-amino-3-hydroxybutanoyl-ε-aminohexanoic acid isoamylamide Boc – Phe (4-OMe) – His (N^{im}Bzl) – AHBA – εAhx – Iaa [32]
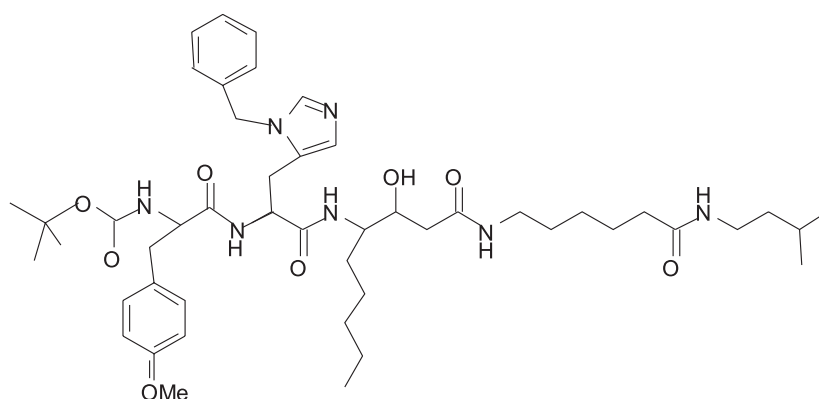
Figure 10. [N-(tert-butoxycarbonyl)-4-methoxyphenylalanyl]-N^{im}benzylhistidyl-(3S, 4S)-4-amino-3-hydroxynonanoyl-ε-aminohexanoic acid isoamylamide Boc – Phe (4-OMe) – His (N^{im}Bzl) – AHNA – εAhx – Iaa [37]
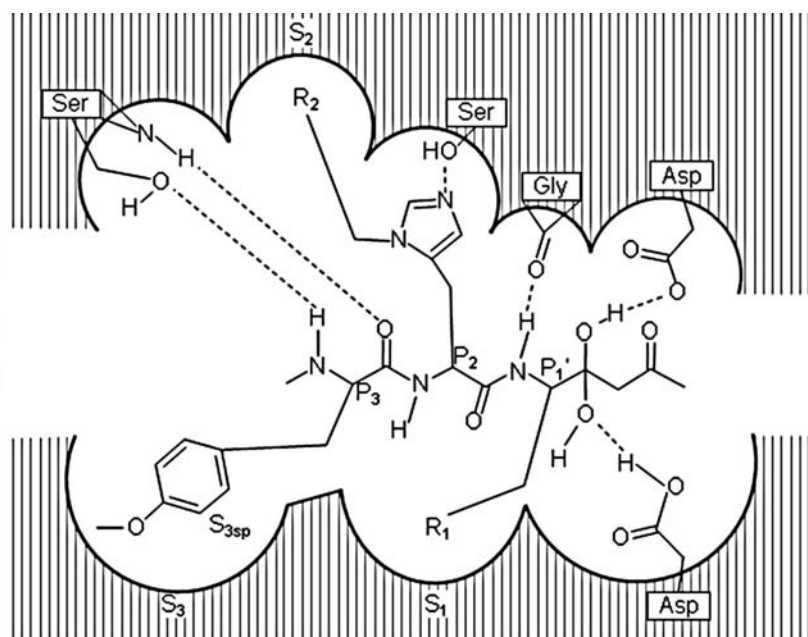
Figure 11. Schematic interaction mode of P$_3$-P$_1$ fragment with hydrophobic pocket of renin active center; R$_1$ = cyclohexyl, butyl or 4-ethoxyphenyl, R$_2$ = benzyl or trityl

specified below in the syntheses section. Physicochemical properties of the inhibitors, as well as their newly synthesized intermediates [**4**, **8**, **14**, **15**, **18**, **21**, **23**, **26**, **28**, **30**, **33**, **35**] are presented in Tables 1 and 2.

Reagents Boc - Phe (4-OMe) - OH, His (N^{im}Bzl) - OEt, His (N^{im}Trt) - OEt, porcine kidney renin and N-acetylrenin substrate tetradecapeptide were acquired from recognized vendor. ACHPA was synthesized according to the Maibaum protocol

(20). Solvents were of analytical purity. Tetrahydrofuran (THF) was distilled from Na/benzophenone under N$_2$. Dichloromethane and dimethylformamide (DMF) were dried over 4 Å molecular sieves. The peptides were synthesized by the N,N-dicyclohexylcarbodiimide/1-hydroxybenzotriazole (DCC/HOBt) method of fragment condensation in solution (21). Column chromatography (CC) on silica gel (Merck, grade 230 to 400 mesh) was used to separate and purify all synthesized com-

pounds. TLC was carried out on 0.25 mm thickness silica gel plates (Merck, silica gel 60 F254). The solvent systems used in TLC and CC were CHCl$_3$/MeOH in various ratios. The spots were visualized with 0.3% ninhydrin in EtOH/AcOH (97 : 3, v/v). Perkin-Elmer Microanalyser was used to carry out elemental analyses. Böetius apparatus was used to determine melting points. Bruker DM 300 MHz Avance 300 WB spectrometer was applied to record ^{1}H NMR spectra. Chemical shifts were measured relative to tetramethylsilane (TMS) as δ units (ppm). Optical rotations were measured at the Na-D line with the use of AP-300 (Atago) polarimeter in a 5 cm polarimeter cell. HPLC analyses of purity and activity of synthesized inhibitors were performed on a Shimadzu apparatus equipped with a pump LC-10AT, detector UV SPD-10A and recorder Chromax 2001. The peaks were recorded at 213 nm. The separation was carried out in the reverse phase system (Ultrasphere C8, Wild Pore C8, Symmetry C18) with various mobile phases.

Syntheses

Introduction of the N-tert-Boc group

This group was introduced in a commonly used manner (22).

Removal of the N-tert-Boc group

Boc-amino acid or Boc-peptide (1 mmol) in a solution of 4 M HCl in dioxane was stirred at room temperature for 30 min. The solution was concentrated *in vacuo*, then the residue was evaporated twice with diethyl ether and dried *in vacuo* (23).

Esterification and hydrolysis

Boc-amino acids were esterified with CH$_3$I or C$_2$H$_5$I as described earlier (16). Boc – ACHPA – OEt, Boc – AHNA – OEt, Boc – AEPHPA – OEt and Boc – AHBA – OEt were formed from monoethyl malonate used to prepare these compounds (18). Alkaline hydrolysis of ester group was carried out as described earlier (20).

Coupling reaction with DCC/HOBt

The coupling was performed in a commonly used manner by fragment condensation as shown in schemes in Figures 1-5.

Biochemical assay

Determination of the inhibition of renin activity

Renin inhibiting activity of the synthesized potential inhibitors was determined *in vitro*. HPLC method was used to determine the concentration of renin substrate The activity of the compounds was tested in the following concentrations: 10^{-5}, 10^{-6}, 10^{-7}, 10^{-8}, 10^{-9}, 10^{-10}, 10^{-11} M. All synthesized compounds showed no inhibiting activity, even in the highest tested concentration 10^{-5} M.

RESULTS AND DISCUSSION

Preliminary *in vitro* tests of the synthesized compounds showed a lack of renin-inhibiting effect of all five new potential inhibitors and their resistance to chymotrypsin. However, the lack of inhibitory activity of compounds: [**12**, **20**, **25**, **32**, **37**] containing histidine with hydrophobic benzyl and trityl (Trt) substituents in position P$_2$ is likely to result from the difficulty for big rigid and ring-type substituents to fit to subpocket S$_2$. Therefore, it should be assumed that straight or branched flexible alkyl chains capable of adopting a proper conformation in subpocket S$_2$ may be the most optimal substituent of imidazole nitrogen atom of histidine. Quite contrary, a big hydrophobic trityl or benzyl substituent constitutes an effective spatial obstacle which in combination with Phe (4-OMe) in position P$_3$ results in stabilization of P$_3$ - P$_2$. Low solubility of these compounds at certain concentration causing difficulties during *in vitro* activity tests may be yet another reason for absence of biological activity of designed and obtained inhibitors. This low solubility is caused by high lipophilicity of a molecule resulting from the presence of hydrophobic side chains and hydrophobic branched structures of N- and C-end, however, the objective of our tests was to verify the determinants of maximum interaction of the molecule with all hydrophobic sites of the active centre of renin and the influence of this interaction on inhibitory activity and stability of inhibitors.

REFERENCES

1. Welob R.L., Schiering N., Sedrani R., Maibaum J.: J. Med. Chem. 53, 7490 (2010).
2. Weintraub H.S., Tran H., Schwartzbard A.: Cardiol. Rev. 19, 90 (2011).
3. Paruszewski R., Jaworski P., Bodnar M., Dudkiewicz-Wilczyńska J., Roman I.: Chem. Pharm. Bull. 53, 1305 (2005).
4. Boger J., Payne L.S., Perlow D.S., Lohr N.S., Poe M., Blaine E.H., Ulm E.H. et al.: J. Med. Chem. 28, 1779 (1985).
5. Dellaria J.F., Maki R.G., Bopp B.A., Cohen J., Kleinert H.D., Luly J.R., Merits I., Plattner J.J., Stein H.H. : J. Med. Chem. 30, 2137 (1987).
6. Plattner J.J., Marcotte P.A., Kleinert H.D., Stein H., Greer J. et al.: J. Med. Chem. 31, 2277 (1988).

7. Paruszewski R., Jaworski P., Winiecka I., Tautt J., Dudkiewicz J.: Chem. Pharm. Bull. 50, 850 (2002).

8. Winiecka I., Dudkiewicz-Wilczyńska J., Roman I., Paruszewski R.,: Acta Pol. Pharm. Drug Res. 67, 367 (2010).

9. Chen A., Campeau L.C., Cauchon E., Chefson A., Ducharme Y., Dubé D., Falgueyret J.P. et al.: Bioorg. Med. Chem. Lett. 20, 5074 (2010).

10. Sund C., Belda O., Wiktelius D., Sahlberg C., Vrang L., Sedig S., Hamelink E. et al.: Bioorg. Med. Chem. Lett. 21, 358(2011).

11. Greenby W.J.: Med. Res. Rev. 2, 173 (1990).

12. Maibaum J., Feldman D.L.: Annu. Rev. Med. Chem. 44, 105 (2009).

13. Kempf D.I., de Lara E., Stein H.H., Cohen J., Egan D.A., Plattner J.J.: J. Med. Chem. 33, 371 (1990).

14. Paruszewski R., Jaworski P., Winiecka I., Tautt J., Dudkiewicz J.: Pharmazie 54, 102 (1999).

15. Paruszewski R., Jaworski P., Tautt J., Dudkiewicz J.: Boll. Chim. Farm. 134, 551 (1995).

16. Paruszewski R., Strzałkowska M.: Pol. J. Chem. 64, 149 (1990).

17. Paruszewski R., Jaworski P., Tautt J., Dudkiewicz J.: Boll. Chim. Farm. 133, 301 (1994).

18. Paruszewski R., Jaworski P., Tautt J., Dudkiewicz J.: Pharmazie 52, 206 (1997).

19. Paruszewski R., Tautt J., Dudkiewicz J.: Pol. J. Pharmacol. 45, 75 (1993).

20. Maibaum J., Rich D.H.: J. Org. Chem. 53, 869 (1988).

21. König W., Geiger R., Chem. Ber. 103, 788 (1970).

22. Schwyzer R., Sieber P., Kappeler H., Helv. Chim. Acta 42, 2622 (1959

23. Anderson G.W., McGregor A.C.: J. Am. Chem. Soc. 79, 6180 (1957).

24. Ghose A.K., Prichett A., Crippen G.M.: J. Comput. Chem. 9, 80 (1988).

NEW LEAD STRUCTURES IN THE ISOXAZOLE SYSTEM: RELATIONSHIP BETWEEN QUANTUM CHEMICAL PARAMETERS AND IMMUNOLOGICAL ACTIVITY

MARCIN MĄCZYŃSKI[1]*, STANISŁAW RYNG[1], JOLANTA ARTYM[2], MAJA KOCIĘBA[2], MICHAŁ ZIMECKI[2], KATARZYNA BRUDNIK[3] and JERZY T. JODKOWSKI[3]

[1]Department of Oorganic Chemistry, Faculty of Pharmacy,
Wroclaw Medical University, Borowska 211a, 50-556 Wrocław, Poland
[2]Laboratory of Immunobiology, Institute of Immunology and Experimental Therapy,
Polish Academy of Sciences, Weigla 12, 53-114 Wrocław, Poland
[3]Department of Physical Chemistry, Faculty of Pharmacy, Wroclaw Medical University,
Borowska 211a, 50-556 Wrocław, Poland

Abstract: Potential immunological activities of three compounds: RM54 and its two derivatives RM55 and RM56, were evaluated in several, selected *in vitro* and *in vivo* tests such as: mitogen-induced lymphocyte proliferation, cytokine production, the humoral immune response *in vitro* and carrageenan test. Leflunomide served as a reference drug. The studied compounds showed differential, generally immunosuppressive properties. RM56 exhibited stronger suppressive activities as compared to RM54 and RM55. In particular, RM56 displayed the strongest activity in suppression of the carrageenan inflammation that was correlated with strong suppression of the humoral immune response *in vitro* and lymphocyte proliferation. Density Functional Theory (DFT) was employed to shed a light on molecular properties of the investigated compounds. The geometrical parameters of the studied molecular structures were fully optimized at the B3LYP/6-311G(d,p) level. The atomic charges distribution derived on the base of the Mulliken population analysis was correlated with immunological activity of RM54, RM55 and RM56. The obtained relationships show that the isoxazole ring plays an important role in the observed immunological activities. We also suggest that due to strong anti-inflammatory and anti-proliferative properties of RM-56, potential therapeutic applications of this derivative can be broad.

Keywords: isoxazole, DFT, immune response, TNF-α, carrageenan inflammation, mice

Among drugs targeting the immune system a few categories, both of natural origin and synthetic ones can be mentioned, such as calcineurin inhibitors (cyclosporine, tacrolimus) or isoxazole derivatives (acivicin, leflunomide) of well documented biological activity. Although these therapeutics are commonly used, their side-effects encourage to search new compounds characterized by more beneficial therapeutic properties.

Our efforts to obtain new immunomodulatory compounds resulted in synthesis of new amide derivatives of 5-amino-3-methyl-4-isoxazolecarboxylic acid (1). The compounds demonstrated strong and differential immunological activities. In the first series, we initially found high antitumor activity of the compounds *in vivo* (2), and subsequently lack of cytotoxicity associated with an immunostimulatory action (3). These findings opened new possibilities in search for new antitumor drugs that act by a different mechanism than cytotoxicity. Therefore, syntheses of three series of amide derivatives (aromatic, heterocyclic and aliphatic) were designed. The syntheses resulted in obtaining a series of amide derivatives of 5-amino-3-methyl-4-isoxazolecarboxylic acid **I-III** (2-4) (Fig. 1).

After establishing interdependences between types of the amide substituent, the most intriguing question regarding structure-activity relationship was whether the immunostimulatory effect was dependent on the amide structure. The previously conducted studies on quantitative activity relationship indicated special correlations between charge of the carbonyl groups atoms and the biological
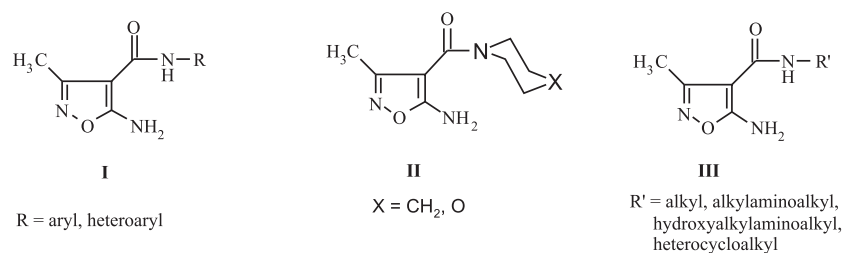
Figure 1. The structures of amide derivatives of 5-amino-3-methyl-4-isoxazolecarboxylic acid
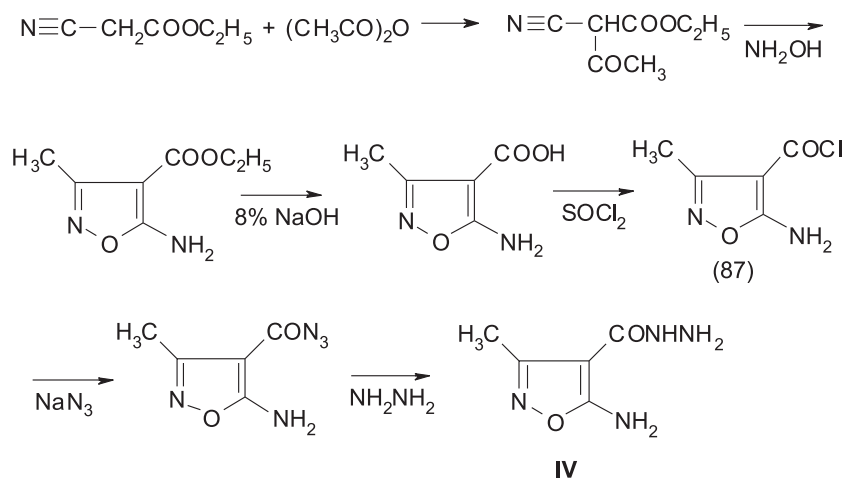

Figure 2. The synthesis and structure of hydrazide of 5-amino-3-methyl-4-isoxazolecarboxylic acid **IV**
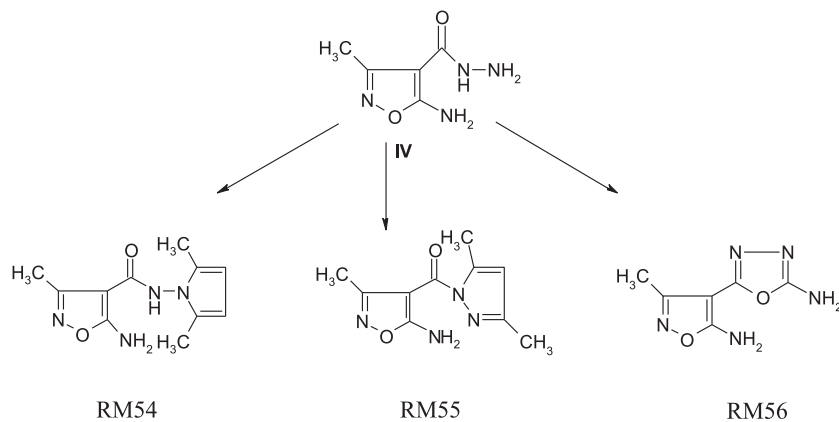

Figure 3. The synthesis and structures: 5-amino-3-methyl-4-(2,5-dimethylpyrrole-aminocarbonyl)-isoxazole RM54, 5-amino-3-methyl-4-(3,5-dimethylpyrazolecarbonyl)-isoxazole RM55 and 5-amino-3-methyl-4-[2-(5-amino-1,3,4-oxadiazole)]-isoxazole RM56

Table 1. The structural and spectroscopic (IR, ^{1}H NMR) data for the obtained compounds.

Compound	Chemical structure	Spectroscopic data
RM54		IR (cm^{-1}): C=O 1712; ^{1}H NMR (DMSO-d$_6$, δ, ppm): 2.1 (s, 6H, 2CH$_3$-pyrrole); 2.4 (s, 3H, CH$_3$-isoxazole); 5.7 (s, 2H, -NH$_2$); 7.6 (s, 2H, 2CH-pyrrole); 9.7 (s, 1H, NH)
RM55		IR (cm^{-1}): C=O 1708, ^{1}H NMR (DMSO-d$_6$, δ, ppm): 2.16 (s, 3H, CH$_3$-pyrazole); 2.21 (s, 3H, CH$_3$-pyrazole); 2.4 (s, 3H, CH$_3$-isoxazole); 6.2 (s, 2H, -NH$_2$); 8.2 (s, 1H, pyrazole)
RM56		IR (cm^{-1}): =C-O-C= 1688, ^{1}H NMR (DMSO-d$_6$, δ, ppm): 2.3 (s, 3H, CH$_3$); 8.6 (s, 4H, 2NH$_2$-isoxazole and oxadiazole)

effect exerted by the amide groups of the derivatives. In the course of the earlier conducted investigations encompassing synthesis and immunological activity we found interdependences between structure and activities of the synthesized compounds. Most active series of compounds were studied in a more detailed manner using quantum-chemical methods and most relevant interdependencies were found by comparing immune activity with distribution of atom charges. These correlations occurred most frequently between activity and atom charges located predominantly on isoxazole heteroatoms and atoms of amide and carbonyl groups (5).

Therefore, it seemed particularly interesting to obtain new derivatives possessing significant differences within these groups and to assess their biologic activities. To address the problem, a new half-product, substrates and appropriate methods were elaborated to enable obtaining such differentiated derivatives.

In the reactions of hydrazide of 5-amino-3-methyl-4-isoxazolecarboxylic acid **IV** (Fig. 2) with acetonylacetone (hexanedione-2,5), acetylacetone (pentanedione-2,4) and bromocyanide we obtained new lead structures: 5-amino-3-methyl-4-(2,5-dimethylpyrrole-aminocarbonyl)-isoxazole RM54, 5-amino-3-methyl-4-(3,5-dimethylpyrazolecarbonyl)-isoxazole RM55 and 5-amino-3-methyl-4-[2-(5-amino-1,3,4-oxadiazole)]-isoxazole RM56,

respectively (see Fig. 3) (6-8). As a results of these syntheses we obtained a compound with the amide group where the nitrogen atom was bound to the pyrrole nitrogen atom RM54, in compound RM55 the amide nitrogen atom was integrated within the heterocyclic structure of pyrazole, and in compound RM56 atoms: C, N and O of the amide group could be found in the heterocyclic structure of oxadiazole. These combinations enabled evaluation of effects of the amide group on the biologic activity of the new structures. In each of the products, at location 4 of the isoxazole ring, five-element heteroaromatic substituent exists, which significantly improved the bioaccessibility.

These findings prompted us to synthesize isoxazole derivatives where most essential differences occur within amide structures. As a result, compound RM54 possessing a complete amide group, and compound RM55, where the nitrogen atom in the amide group belongs to the pyrazole structure were obtained. In compound RM56 the whole amide group participates in the oxadiazole structure.

The aim of this study was to evaluate the immunosuppressive activities of the derivatives in relation to quantum chemistry analysis. The calculated atomic charge distributions in RM54, RM55 and RM56 were used to obtain relationships between structure and immunological activity of the studied compounds.

Table 2. The structural parameters of the most stable conformers of RM54, RM55 and RM56 calculated at the B3LYP/6-311G(d,p) in the presence of DMSO.

Atom RM54	Atomic charge (e) RM54	Atom RM55	Atomic charge (e) RM55	Atom RM56	Atomic charge (e) RM56
1 O	**-0.2755**	**1 O**	**-0.2753**	**1 O**	**-0.2750**
2 N	**-0.2130**	**2 N**	**-0.2099**	**2 N**	**-0.2208**
3 C	**0.5743**	**3 C**	**0.5585**	**3 C**	**0.5850**
4 C	-0.4443	4 C	-0.4041	4 C	-0.4349
5 C	0.4886	5 C	0.4620	5 C	0.4000
6 N	-0.3308	6 N	-0.3397	6 N	-0.3430
7 N	-0.3079	7 N	-0.3212	7 N	-0.3087
8 C	**0.2042**	**8 C**	**0.1790**	**8 C**	**0.2087**
9 O	-0.4512	9 O	-0.3825	9 O	-0.2925
10 N	-0.4694	10 N	-0.4546	10 N	-0.4748
11 C	0.1380	11 C	0.1731	11 C	0.4443
12 C	-0.2123	12 C	-0.3261	12 N	-0.4881
13 C	-0.3036	13 C	-0.2256	13 C	-0.2390
14 H	0.1522	14 H	0.1353	14 H	0.1402
15 H	0.1529	15 H	0.1326	15 H	0.1399
16 H	0.1399	16 H	0.1184	16 H	0.1270
17 H	0.2637	17 H	0.2540	17 H	0.2639
18 H	0.2647	18 H	0.2664	18 H	0.2563
19 C	0.1381	19 C	0.2280	19 H	0.2551
20 C	-0.2544	20 C	-0.2138	20 H	0.2566
21 C	-0.2542	21 C	-0.2607		
22 H	0.1252	22 H	0.1315		
23 H	0.1244	23 H	0.1352		
24 H	0.1245	24 H	0.1350		
25 H	0.1251	25 H	0.1264		
26 H	0.1257	26 H	0.1218		
27 H	0.1256	27 H	0.1368		
28 C	-0.2124	28 H	0.1196		
29 H	0.2758				
30 H	0.0931				
31 H	0.0931				
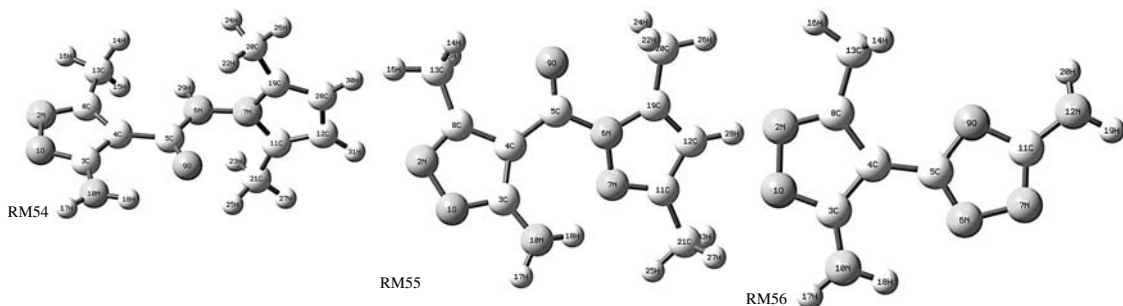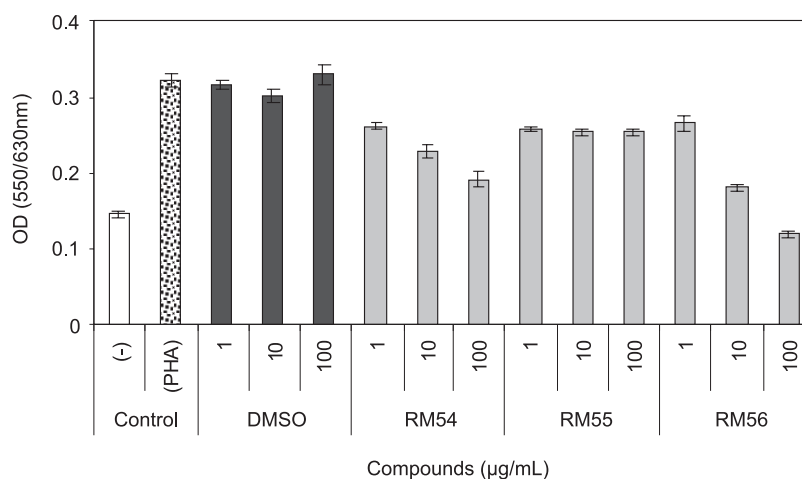
RM54   RM55   RM56

Figure 4. Effects of the compounds on PHA-induced proliferation of human PBMC. RM54, RM55 and RM56 were added to the human PBMC cultures at concentrations: 1, 10 and 100 μg/mL. PHA was added at a concentration of 5 μg/mL. After a four-day incubation, the proliferative response of the cells was determined. Appropriate DMSO dilutions served as control cultures. (-) – no additions. The data are presented as a mean OD value from quadruplicate wells ± SE. Statistics: DMSO *vs.* RM54: 1 μg/mL: p = 0.0133; 10 μg/mL: p = 0.0045; 100 μg/mL: p = 0.0001; DMSO *vs.* RM55: 1 μg/mL: p = 0.0051; 10 μg/mL: NS (p = 0.0901); 100 μg/mL: p = 0.0039; DMSO *vs.* RM56: 1 μg/mL: p = 0.0219; 10 μg/mL: p = 0.0001; 100 μg/mL: p = 0.0001 (ANOVA)
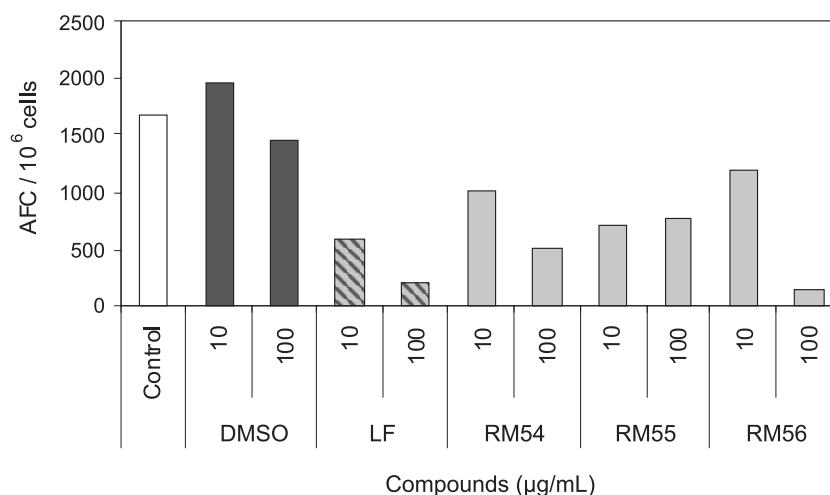
Figure 5. Effect of the compounds on the secondary humoral immune response of mouse splenocytes to sheep erythrocytes. Splenocytes from mice sensitized with SRBC were restimulated with SRBC *in vitro*. The compounds were added to the cell cultures in the beginning of the 4-day incubation at concentration 10 and 100 μg/mL. The results are shown as the mean values of AFC numbers from 4 wells ± SE, calculated per 10^6 viable cells. Statistics: DMSO *vs.* leflunomide (LF): 10 μg/mL: p = 0.0002; 100 μg/mL: p = 0.0003; DMSO *vs.* RM54: 10 μg/mL: p = 0.0067; 100 μg/mL: p = 0.0086; DMSO *vs.* RM55: 10 μg/mL: p = 0.0003; 100 μg/mL: NS (p = 0.1217); DMSO *vs.* RM56: 10 μg/mL: NS (p = 0.0580); 100 μg/mL: p = 0.0002 (ANOVA)

EXPERIMENTAL

Chemistry

Melting points were determined on a Büchi apparatus (Laboratoriums-Technik AG, Flawil, Switzerland), heated table Kofler system (Wagner & Munz) and were uncorrected. Thin layer chromatog-raphy (TLC) was carried out on Polygram SIL G/UV 254 nm glass silica gel plates (Macherey-Nagel), using the developing system $CHCl_3$ – CH_3OH 9 : 1 v/v, and detected with UV Fisher Bioblock Scientific 254 nm lamps. IR spectra were recorded with a Specord M-80 spectrophotometer (Carl Zeiss, Jena, Germany) in Nujol mull support-
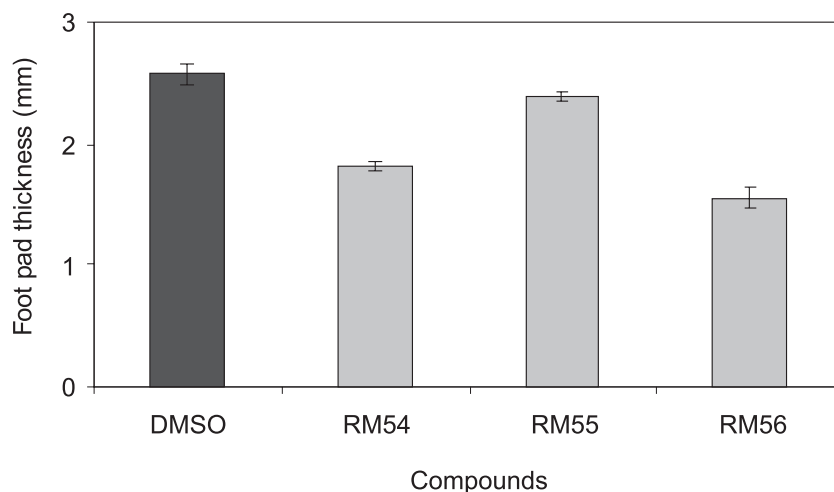
Figure 6. Effect of the compounds on carrageenan reaction in mice. Mice were given 2% carrageenan solution *s.c.* into hind foot pads and after 3 h the foot pad thickness was measured. The compounds (100 μg/mouse) were administered *i.p.* at 48 h and 24 h before carrageenan injection. Control – mice treated with appropriate dilutions of DMSO. The background foot pad thickness (1.5 mm) of naive mice was subtracted from the response of sensitized mice. The results are presented as the mean foot pad thickness from 5 mice/group (10 determinations) and expressed in mm. Statistics: DMSO *vs.* RM54 p = 0.0025; DMSO *vs.* RM55 NS (p = 1.0000); DMSO *vs.* RM56 p = 0.0001 (ANOVA).
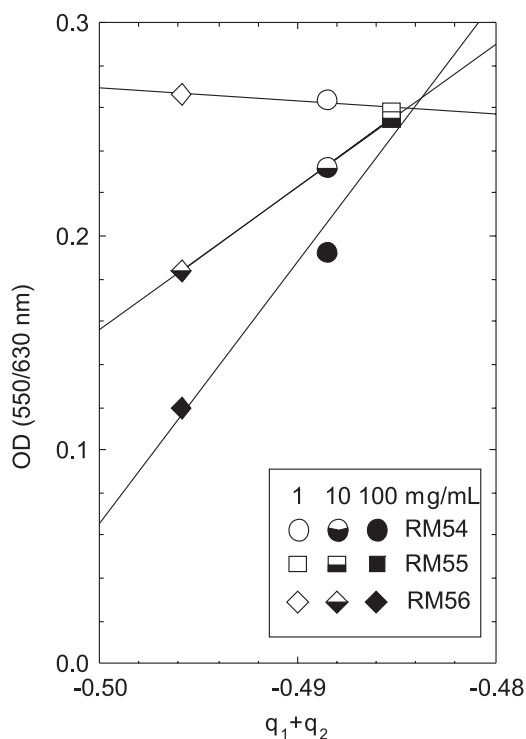
Figure 7. The effects of the studied compounds on PHA-induced proliferation of human PBMC as a function of the sum of the charges on atoms O(1) and N(2) denoted by $q_1 + q_2$

ed on a KBr disk, and ^{1}H NMR spectra were obtained in DMSO-d_6 using a Bruker ARX 300 MHz spectrometer (using TMS as the internal standard). Mass spectrometry was performed on micrOTOF-Q spectrometer (manufactured by Bruker Daltonic) using electrospray ionization (ESI) method, in cation mode with two quadrupole analizators and time of flight (TOF). The spectroscopic data are presented in Table 1. Elemental analyses were performed within ± 0.3% of the theoretical values (Carlo Erba NA, 1500 analyzer).

Compounds preparation

New derivatives of isoxazole were synthesized by using 5-amino-3-methyl-4-isoxazolecarboxylic acid hydrazide and three different compounds in the presence of isopropanol.

Synthesis of 5-amino-3-methyl-4-(2,5-dimethyl-pyrrole-aminocarbonyl)-isoxazole RM54

The mixture of isopropanol (50 mL) and hexane-2,5-dione (3.3 mmol) was added to the 5-amino-3-methyl-4-isoxazolecarboxylic acid hydrazide (3 mmol). The solution was heated for 10 min to the boiling temperature with stirring and refluxed for 7 h. Then, the suspension was cooled and filtered. The crude product was recrystallized from ethanol. White crystal product was obtained with 49.3% of the theoretical yield and the melting temperature was 224-225°C.

Synthesis of 5-amino-3-methyl-4-(3,5-dimethyl-pyrazolecarbonyl)-isoxazole RM55

The mixture of isopropanol (50 mL) and pentane-2,4-dione (3.3 mmol) was added to the 5-amino-3-methyl-4-isoxazolecarboxylic acid hydrazide (3 mmol). The solution was stirred and heated

for 10 min to the boiling temperature and refluxed for 2 h. The solvent was evaporated under pressure to obtain a dry sediment. Then, 50 mL of THF was added. The mixture was heated to the boiling, cooled and finally filtered. The crude product was recrystallized from ethanol. A white crystal product was received with 56% of theoretical yield. The melting temperature was 159-161°C.

Synthesis of 5-amino-3-methyl-4[2-(5-amino-1,3,4-oxadiazole)]-isoxazole RM56

The mixture of isopropanol (50 mL), cyanogen bromide (12 mmol) and anhydrous K_2CO_3 (109 mmol) was added to 5-amino-3-methyl-4-isoxazole-carboxylic acid hydrazide (12 mmol). The solution was stirred and heated for 10 min to the boiling point and refluxed for 2 h. Potassium bromide was separated by filtration, then the solution was evaporated under pressure to obtain a dry sediment. Then, the THF (50 mL) was added and the mixture was heated to the boiling point. Then, the solution was cooled, filtered and recrystallized from ethanol. A white crystal product was obtained with 72% of the theoretical yield. The melting point was 225°C.

Biology
Animals

CBA mice of both sexes, 8-12 week old, delivered by the Institute of Laboratory Medicine, Łódź, Poland, were used in this study. Mice had free access to laboratory chow and filtered tap water. The local ethics committee approved the study.

Reagents

RPMI-1640 medium was purchased from Sigma-Aldrich, fetal calf serum (FCS) from Gibco, lipopolysaccharide (LPS) from *Escherichia coli* serotype O111:B4, phytohemagglutinin A (PHA), MTT (3-[4,5-dimethylthiazol-2-yl]-2,5-diphenylte-trazolium bromide) and leflunomide (LF) were from Sigma-Aldrich. Sheep erythrocytes (SRBC) were delivered by Wroclaw University of Life and Environmental Sciences, Wrocław, Poland. SRBC were stored in Alsever's solution at 4°C until use. The studied peptides were initially dissolved in DMSO and subsequently in a culture medium at concentration of 1 mg/mL (stock solution).

Isolation of the peripheral blood mononuclear cells (PBMC)

Venous blood was withdrawn into heparinized syringes and diluted twice with PBS. PBMC were isolated by centrifugation on Ficoll-uropoline gradient (density 1.077 g/mL) and centrifuged at $800 \times g$ for 20 min at 4°C. The interphase cells, consisting of lymphocytes (20%) and monocytes (80%) were then washed three times with Hanks' medium and resuspended in a culture medium, referred to below as the culture medium, consisting of RPMI-1640, supplemented with 10% FCS, L-glutamine, sodium pyru-
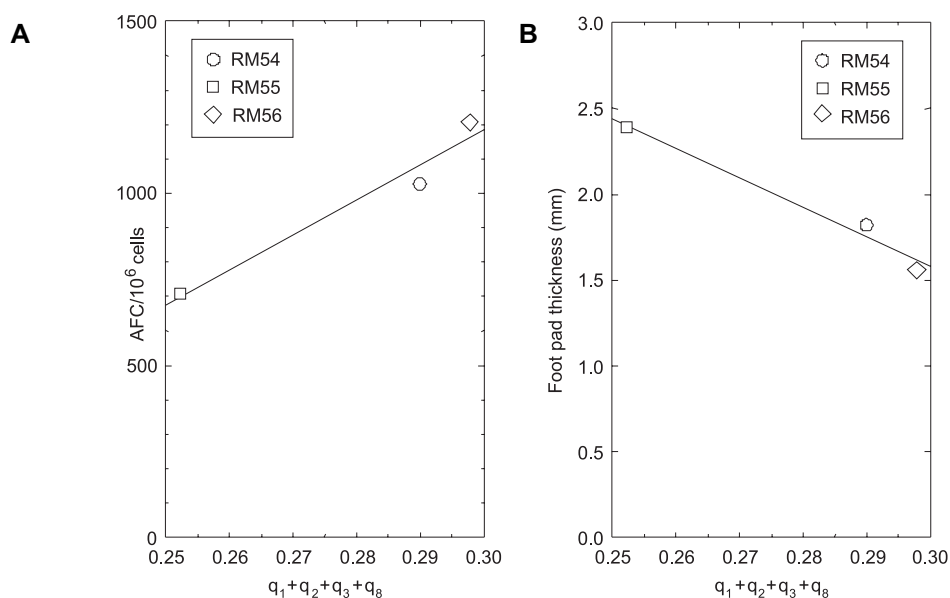

Figure 8. The relationships between the atomic charges on the atoms of isoxazole ring (N, O, C_3 and C_8) denoted by $q_1 + q_2 + q_3 + q_8$ and: (**A**) AFC production at the compounds concentrations of 10 µg/mL, (**B**) carrageenan-induced foot pad thickness *in vivo* at 100 µg dose

Table 3. The structural parameters of the studied compounds calculated at the B3LYP/6-311G(d,p) level in the presence of DMSO as a solvent.

RM54

Molecular mass: 234.11168 amu, total energy at 0 K (ZPE included): -796.982775 a.u., rotational constants: 0.90884, 0.26950, 0.26208 GHz, ionization potential: 5.64 eV, dipole moment: 1.3808 D.

Atom	Orthogonal coordinates (Å) charge (e)			Atomic (cm^{-1})	Harmonic frequencies		
1 O	3.981831	-0.368706	-0.016442	-0.2755	18	30	59
2 N	3.759306	1.052151	0.030687	-0.2130	70	90	123
3 C	2.799897	-0.985774	-0.030625	0.5743	133	150	160
4 C	1.766247	-0.049524	0.004003	-0.4443	173	208	231
5 C	0.368556	-0.458515	-0.013156	0.4886	237	283	283
6 N	-0.583019	0.539861	0.024551	-0.3308	292	305	350
7 N	-1.924977	0.243634	0.009498	-0.3079	360	371	426
8 C	2.460766	1.203609	0.041797	0.2042	512	533	569
9 O	0.041647	-1.646574	-0.059493	-0.4512	589	608	626
10 N	2.766620	-2.316306	-0.060574	-0.4694	631	639	713
11 C	-2.695039	0.019413	1.145843	0.1380	729	761	776
12 C	-3.966762	-0.248993	0.701250	-0.2123	784	788	832
13 C	1.916697	2.597597	0.089391	-0.3036	863	909	981
14 H	1.296997	2.808506	-0.786413	0.1522	986	1024	1034
15 H	1.314898	2.754949	0.988649	0.1529	1041	1055	1057
16 H	2.739652	3.311767	0.102640	0.1399	1062	1064	1106
17 H	3.611751	-2.855924	-0.152389	0.2637	1120	1226	1241
18 H	1.853943	-2.747353	-0.117744	0.2647	1330	1343	1373
19 C	-2.690042	0.110090	-1.144433	0.1381	1377	1410	1413
20 C	-2.107326	0.285834	-2.506495	-0.2544	1415	1440	1468
21 C	-2.118772	0.087974	2.520193	-0.2542	1468	1473	1482
22 H	-1.327472	-0.454016	-2.714334	0.1252	1483	1485	1495
23 H	-1.676331	1.066490	2.733054	0.1244	1520	1539	1562
24 H	-1.661064	1.276711	-2.638822	0.1245	1587	1624	1644
25 H	-1.337427	-0.663741	2.672256	0.1251	1688	3018	3020
26 H	-2.891651	0.167255	-3.255125	0.1257	3036	3062	3062
27 H	-2.906054	-0.091988	3.253329	0.1256	3093	3114	3114
28 C	-3.963695	-0.192125	-0.728042	-0.2124	3129	3220	3234
29 H	-0.333357	1.516571	0.060423	0.2758	3552	3619	3702
30 H	-4.807179	-0.356269	-1.382112	0.0931			
31 H	-4.813219	-0.463618	1.336589	0.0931			

vate, 2-mercaptoethanol and antibiotics, at density of 2×10^6 cells/mL.

Proliferation of PBMC

The isolated PBMC were distributed into 96-well flat-bottom plates in 100 μL aliquots (2×10^5 cells/well). PHA was added at a concentration of 5 μg/mL. The compounds were tested at doses 1, 10 and 100 μg/mL. DMSO at appropriate dilutions served as control. After a four-day incubation in a cell culture incubator, the proliferative response of the cells was determined by the colorimetric MTT method (9). The data are presented as a mean OD value from quadruplicate wells ± SE.

Table 3. cont.
RM55
Molecular mass: 220.09603 amu, total energy at 0 K (ZPE included): -757.702611 a.u., rotational constants: 0.88871, 0.40029, 0.28722 GHz, ionization potential: 6.43 eV, dipole moment: 6.82 D.

Atom	Orthogonal coordinates (Å) charge (e)			Atomic (cm^{-1})	Harmonic frequencies		
1 O	2.845387	-1.703010	-0.267236	-0.2753	30	42	98
2 N	3.609139	-0.549855	0.107309	-0.2099	120	127	158
3 C	1.550209	-1.378849	-0.331433	0.5585	178	191	207
4 C	1.387176	-0.022599	-0.012675	-0.4041	219	248	261
5 C	0.270773	0.911572	-0.029803	0.4620	309	338	354
6 N	-1.074556	0.439062	-0.034944	-0.3397	362	401	437
7 N	-1.394116	-0.858541	0.281460	-0.3212	457	502	585
8 C	2.740466	0.412131	0.238645	0.1790	593	618	620
9 O	0.446643	2.120760	-0.032098	-0.3825	648	659	680
10 N	0.715297	-2.344151	-0.720811	-0.4546	723	768	788
11 C	-2.714284	-0.913661	0.304456	0.1731	794	830	879
12 C	-3.273295	0.356713	0.004356	-0.3261	904	988	1005
13 C	3.239529	1.765111	0.634506	-0.2256	1029	1053	1060
14 H	3.046909	2.491372	-0.155586	0.1353	1064	1064	1067
15 H	2.724235	2.119030	1.529202	0.1326	1101	1159	1184
16 H	4.311020	1.712281	0.830396	0.1184	1248	1313	1335
17 H	1.077534	-3.284399	-0.777091	0.2540	1367	1404	1416
18 H	-0.258813	-2.189481	-0.464052	0.2664	1418	1442	1456
19 C	-2.218289	1.208613	-0.203578	0.2280	1464	1464	1465
20 C	-2.255684	2.658909	-0.555471	-0.2138	1472	1473	1487
21 C	-3.431995	-2.189895	0.607587	-0.2607	1516	1542	1598
22 H	-1.667980	2.871634	-1.450205	0.1315	1613	1647	1695
23 H	-4.133018	-2.052936	1.434950	0.1352	3036	3049	3053
24 H	-1.848439	3.275820	0.246807	0.1350	3088	3109	3118
25 H	-2.723944	-2.974008	0.877874	0.1264	3122	3124	3133
26 H	-3.292096	2.947490	-0.736038	0.1218	3249	3405	3646
27 H	-4.010511	-2.525920	-0.257629	0.1368			
28 H	-4.319133	0.613240	-0.054588	0.1196			

The secondary humoral immune response to SRBC

Mice were sensitized intraperitoneally (*i.p.*) with 0.2 mL of 5% SRBC suspension in 0.9% NaCl. After 4 days, spleens from these mice were isolated, splenocyte single cell suspension was prepared and resuspended in the culture medium at a density of 5 × 10^6/mL. The cells were distributed to 24-well culture plates in 1 mL aliquots and 0.05 mL of 0.005% SRBC suspension was added as antigen. The compounds were added to the cultures at the beginning of the 4-day incubation period at concentration of 10 and 100 µg/mL. The numbers of antibody-forming cells (AFC) in the cultures were determined using a method of local hemolysis in agar gel (10) and presented as the mean values of cell number/10^6 cells ± SE from quadruplicate determinations.

Carrageenan test

Mice were given 2% carrageenan solution, subcutaneously (*s.c.*), into hind foot pads and after 3 h the foot pad thickness was measured by means of

Table 3. cont.
RM56
Molecular mass: 181.05997 amu, total energy at 0 K (ZPE included): -657.045234 a.u., rotational constants: 1.57484, 0.57551, 0.42276 GHz, ionization potential: 5.81 eV, dipole moment: 4.15 D.

Atom	Orthogonal coordinates (Å) charge (e)			Atomic (cm^{-1})	Harmonic frequencies		
1 O	-3.014411	-0.369925	-0.017540	-0.2750	52	99	103
2 N	-2.824848	1.056285	-0.013534	-0.2208	141	159	196
3 C	-1.817519	-0.961016	-0.001509	0.5850	248	261	271
4 C	-0.815050	-0.000141	0.011123	-0.4349	313	360	386
5 C	0.581021	-0.312113	0.013676	0.4000	414	443	512
6 N	1.127191	-1.488103	0.014991	-0.3430	546	558	610
7 N	2.521357	-1.294541	-0.006937	-0.3087	625	695	729
8 C	-1.527439	1.236208	0.004287	0.2087	750	761	783
9 O	1.522133	0.687976	0.005007	-0.2925	858	970	976
10 N	-1.741004	-2.295523	0.026876	-0.4748	1023	1027	1048
11 C	2.694004	-0.010106	-0.005613	0.4443	1063	1097	1119
12 N	3.845707	0.707713	0.058380	-0.4881	1144	1340	1376
13 C	-0.977018	2.626167	0.012604	-0.2390	1414	1435	1463
14 H	-0.363100	2.791374	0.900795	0.1402	1468	1470	1553
15 H	-0.343967	2.794519	-0.861432	0.1399	1589	1604	1635
16 H	-1.792765	3.348875	0.004946	0.1270	1658	1688	3047
17 H	-2.561747	-2.858185	-0.130138	0.2639	3105	3133	3544
18 H	-0.821553	-2.708941	-0.057363	0.2563	3570	3671	3691
19 H	4.678833	0.183717	-0.167939	0.2551			
20 H	3.815719	1.629423	-0.354429	0.2566			

a spring caliper. The compounds were administered *i.p.* at a dose of 100 µg per mouse at 48 h and 24 h before carrageenan injection (11).

Statistics

The results are presented as the mean values ± standard error (SE). Brown-Forsyth's test was used to determine the homogeneity of variance between groups. When the variance was homogenous, analysis of variance (ANOVA) was applied, followed by *post hoc* comparisons with the Tukey's test to estimate the significance of the difference between groups. Significance was determined at $p < 0.05$. Statistical analysis was performed using STATISTICA 7.0 for Windows.

Computational details

The Density Functional Theory (DFT) was used in the calculations of the electronic structure of the compounds under investigation. The DFT technique used in the present calculations utilizes the Becke's three parameter functional (12) together with the local correlation part of Vosko et al. (13) and the nonlocal part of Lee et al. (14) denoted as B3LYP. All molecular structures were fully optimized using the analytical gradients method without any symmetry constraints to locate the lowest-energy isomers of the studied isoxazole derivatives. Vibrational frequency calculations were carried out on each optimized structure to make sure that they are true minima on the respective energy surfaces (absence of any imaginary frequency). All quantum mechanical *ab initio* calculations were carried out using the Gaussian 09 program (15) package. The geometrical parameters of the studied molecular structures were calculated with the 6-311G(d,p) basis set. The atomic charges were derived on the base of the Mulliken population scheme. All calculations were performed in the presence of DMSO as a solvent. However, the results of calculations show that the modification of the structural parameters of the studied molecules in the presence of DMSO is only small.

RESULTS AND DISCUSSION

Effect of the compounds on PHA-induced PBMC proliferation

Figure 4 presents effects of the compounds on PHA-induced proliferation of human PBMC. All compounds had the ability to suppress the proliferation in a dose-dependent manner. The inhibitory potency of the compounds was increasing in the following sequence: RM55, RM54 and RM56.

Effect of the compounds on the secondary humoral immune response of mouse splenocytes to sheep erythrocytes

In the model of secondary, humoral immune response to sheep erythrocytes (SRBC), all the studied compounds at concentrations of 10 and 100 μg/mL, displayed to various degrees suppressive activities (Fig. 5). Leflunomide, the reference drug, was significantly inhibitory (70 and 87%, respectively). The degrees of the inhibitory effects for the studied compounds were the following: RM54 – 50 and 65%, RM55 – 64 and 48%, and RM56 – 39 and 89% (for 10 and 100 mg/mL, respectively).

Effect of the compounds on carrageenan reaction in mice

The compounds were tested in the carrageenan model of foot pad inflammation in mice (Fig. 6). The compounds were administered *i.p.* at 100 μg doses, 48 h and 24 h before elicitation of the carrageenan reaction. The reaction was measured at 3 h after administration of carrageenan. It appeared that only two compounds exhibited strong anti-inflammatory property: RM54 inhibited the reaction by 30% and RM56 by 40%. RM55 was not active (8% inhibition).

The studied compounds demonstrated differential, immunosuppressive properties. RM56 exhibited stronger immunosuppressive properties as compared to RM54.

In particular, its deepest anti-inflammatory property in the carrageenan test is worth noticing, and was, in addition, correlated with the strongest suppression of the humoral immune response *in vitro* and the proliferative response of lymphocytes to PHA. Its mechanism of action probably differs from that of leflunomide (16), since RM54 markedly stimulated IL-6 (data not shown) which controls inflammatory processes by stimulation of acute protein production (17). On the other hand, the immunological activity of RM56 differs from that of another strong immune suppressor RM 33 (18, 19) which was devoid of antiproliferative proper-

ties. In conclusion, potential application of RM56 could be broad, such as inhibition of autoimmune diseases progression and other inflammatory processes, tumor growth and prevention of allograft rejection.

Quantum chemistry analysis

The results of the performed *ab initio* calculations including the optimized geometrical parameters, the harmonic vibrational frequencies, the rotational constants, the dipole moments, the vertical ionization potentials, and the total energies at 0 K (ZPE included) of the studied molecular structures are presented in Table 3.

The investigated RM54, RM55 and RM56 compounds are conformationally complicated molecules with many rotational degrees of freedom. At low values of the rotational barriers, the conformers can easy interconvert one to another at room temperature. The molecular arrangements and a key of atom numbering of the most stable rotational isomers of RM54, RM55 and RM56 are given in Table 2. The results of geometry optimization show that the values of bond distances and angles derived for the studied compounds are very close to those observed in the other isoxazole derivatives.

The isoxazole and pyrrole rings are almost perpendicular in the most stable conformer of RM54. The dihedral angle C(5)-N(6)-N(7)-C(11) is 89.5°. The amine group –NH$_2$ is almost co-planar with isoxazole ring. The torsion angles H(18)-N(10)-C(3)-C(4) and H(17)-N(10)-C(3)-O(1) are of 3.7° and 5.3°, respectively. The contact distance O(9)…H(18) of 2.12 Å enables a stabilization of molecule of RM54 by the intramolecular hydrogen bond. The atomic charges of the nitrogen and oxygen atoms, O(1) and N(2) of isoxazole ring are found negative of 0.276e and 0.213e, respectively. The harmonic frequency $\nu_{C=O}$ of 1688 cm^{-1} of RM54 was calculated at the B3LYP/6-311G(d,p) level of theory.

The most stable isomer of RM55 is also not a flat structure. The dihedral angle C(4)-C(5)-N(6)-N(7) between the isoxazole and pyrazole rings of RM55 is found of 19.6°. The amine group is almost co-planar with isoxazole ring, similarly to RM54. The interatomic distances, N(7)…H(18), O(9)…H(14), O(9)…H(15), O(9)…H(22) and O(9)...H(24) are of 1.90 Å, 2.76 Å, 2.62 Å, 2.65 Å and 2.58 Å, respectively. This enables a formation of the intramolecular hydrogen bonds. The oxygen O(1) and nitrogen N(2) atoms of RM55 are negative of 0.2753e and 0.2099e, respectively. The calculated frequency $\nu_{C=O}$ of RM55 is 1695 cm^{-1}.

RM56 is the smallest studied molecule, which consists of 20 atoms. Both isoxazole and oxadiazole rings of RM56 are almost co-planar. In contrast to RM54 and RM55, the most stable conformer of RM56 is a nearly flat molecular structure. The hydrogen bond occurs between the N(6) and H(18) atoms of RM56. The values of the charge on the atoms O(1) and N(2) are similar to those derived for RM54 and RM55.

Theoretical correlations

The differences in the observed immunosuppressive properties of the studied derivatives of isoxazole are a good reason for theoretical investigations. The performed *ab initio* calculations provided useful information on the electron charge distribution in RM54, RM55 and RM56 molecules. The isoxazole ring is common part to any studied compound and can be considered as the reference molecular subunit. The charge distribution of the isoxazole ring should be related with the electronic structure of whole molecule. The O(1) and N(2) atoms are the most characteristic points of the isoxazole ring. The results of calculations show that these atoms are distinctly negative centers of the isoxazole ring capable of forming a stable complex with water or the other polar solvent. One can expect that the atomic charges on the O(1) and N(2) atoms should be correlated with immunological activity of the studied compounds.

Figure 7 shows the relationships between the sum of the charges on atoms O(1) and N(2) denoted by $q_1 + q_2$ and the effects of the studied compounds on PHA-induced proliferation of human PBMC. At any concentration of RM54, RM55 and RM56 the linear correlation retains validity.

The analysis of the atomic charge distribution of RM54, RM55 and RM56 showed that the influence of these compounds on either the secondary humoral immune response of mouse splenocytes to sheep erythrocytes or the carrageenan reaction in mice depends on charges of greater number of atoms of the isoxazole ring. The plots in Figure 8 A,B show that the sum of atomic charges of the O(1), N(2), C(3) and C(8) atoms can be successfully used in description of the influence of RM54, RM55 and RM56 compounds on AFC production and foot pad thickness in the carrageenan test. It seems that a directly proportional correlation exists between the increasing immunological activities of the compounds: RM55 < RM54 < RM56 and the sum of atomic charges on the isoxazole ring (Fig. 8AB). The obtained relationships also show that the isoxazole ring plays an important role in the observed immunological activities and that the flat structure of RM56 determines its highest immunological activity.

REFERENCES

1. Ryng S., Machoń Z., Wieczorek Z., Zimecki M., Mokrosz M.: Eur. J. Med. Chem. 33, 831 (1998).
2. Ryng S., Zimecki M., Fedorowicz A., Koll A.: Pol. J. Pharmacol., 51, 257 (1999).
3. Ryng S., Machon Z., Wieczorek Z., Zimecki M.: Pharmazie 54, 359 (1999).
4. Ryng S., Zimecki M., Sonnenberg Z., Mokrosz M.J.: Arch. Pharm. (Weinheim) 332, 158 (1999).
5. Ryng S., Zimecki M., Fedorowicz A., Koll A.: Quant. Struct.-Act. Relat. 18, 236 (1999).
6. Ryng S., Zimecki M.: PL195740B1 (2007).
7. Ryng S., Zimecki M.: PL195741B1 (2007).
8. Ryng S., Zimecki M.: PL195739B1 (2007).
9. Hansen M.B., Nielsen S.E., Berg K.: J. Immunol. Methods 119, 203 (1989).
10. Mishell R.I., Dutton R.W.: J. Exp. Med. 126, 423 (1967).
11. Levy L.: Life Sci. 8, 601 (1969).
12. Becke A.D.: J. Chem. Phys. 98, 5648 (1993).
13. Vosko S.H., Wilk L., Nusair M.: Can. J. Phys. 58, 1200 (1980).
14. Lee C., Yang W., Parr R.G.: Phys. Rev. B Condens. Matter 37, 785 (1988).
15. Frisch M.J., Trucks G.W., Schlegel H.B., Scuseria G.E., Robb M.A., Cheeseman J.R., Scalmani G., Barone V., Mennucci B., Petersson G.A., Nakatsuji H., Caricato M., Li X., Hratchian H.P., Izmaylov A.F., Bloino J., Zheng G., Sonnenberg J.L., Hada M., Ehara M., Toyota K., Fukuda R., Hasegawa J., Ishida M., Nakajima T., Honda Y., Kitao O., Nakai H., Vreven T., Montgomery Jr. J.A., Peralta J.E., Ogliaro F., Bearpark M., Heyd J.J., Brothers E., Kudin K.N., Staroverov V.N., Keith T., Kobayashi R., Normand J., Raghavachari K., Rendell A., Burant J.C., Iyengar S.S., Tomasi J., Cossi M., Rega N., Millam J.M., Klene M., Knox J.E., Cross J.B., Bakken V., Adamo C., Jaramillo J., Gomperts R., Stratmann R.E.,

Yazyev O., Austin A.J., Cammi R., Pomelli C., Ochterski J.W., Martin R. L., Morokuma K., Zakrzewski V.G., Voth G.A., Salvador P., Dannenberg J.J., Dapprich S., Daniels A.D., Farkas O., Foresman J.B., Ortiz J.V., Cioslowski J., Fox D. J.: Gaussian 09, Revision B.01, Gaussian, Inc., Wallingford, CT 2010.

16. Li W. D., Ran G. X., Teng H. L., Lin Z. B.: Acta Pharmacol. Sin. 23, 752 (2002).

17. Castell J.V., Gomez-Lechon M. J., David M., Hirano T., Kishimoto T., Heinrich P.C.: FEBS Lett. 232, 347 (1998).

18. Ryng S., Zimecki M., Mączyński M., Chodaczek G., Kocięba M.: Pharmacol. Rep. 57, 195 (2005).

19. Zimecki M., Ryng S., Mączyński M., Chodaczek G., Kocięba M., Kuryszko J., Kaleta K.: Pharmacol. Rep. 58, 236 (2006).

NATURAL DRUGS

PHYTATE, INORGANIC AND TOTAL PHOSPHORUS AND THEIR RELATIONS TO SELECTED TRACE AND MAJOR ELEMENTS IN HERBAL TEAS

PAWEŁ KONIECZYŃSKI and MAREK WESOŁOWSKI*

Department of Analytical Chemistry, Medical University of Gdansk,
Gen. J. Hallera 107, 80-416 Gdańsk, Poland

Abstract: Phytate phosphorus in 59 samples of herbal teas was determined within the range of 2.44-36.90 µg/mL. Extraction yield was statistically higher in extracts from the leaves than that found in extracts from other plant organs. Average total level of trace elements determined in medicinal herbs follows the order: Fe > Mn > Zn > Cu, for major elements the order is: Ca > Mg > Na > K. Correlation analysis revealed that relations of phytate P to other phosphorus forms and metals were statistically insignificant. However, there were several characteristic relations of inorganic phosphorus to water-extractable K, Zn and total Zn. Furthermore, positive relations were found between total and water-extractable fractions of metals. Principal component analysis grouped the samples into separate clusters. It was also found that inorganic P, as well as water-extractable Zn and Na, had a huge impact on differentiation of the studied plant material.

Keywords: phytate phosphorus, anti-nutrient component, medicinal herbal teas, trace and major elements, inter-elemental relations

Phosphorus (P), among other major and trace elements, is one of the most important indispensable constituents of all living organisms. This non-metallic element contributes to the biochemical transitions, which are necessary for vital processes through creating highly energetic bonds in molecules of ATP and ADP. It is a constituent of DNA and RNA, amino acids and peptides. As phosphates, P plays a crucial role in acid-base homeostasis by regulating the buffer properties of blood (1).

Total phosphorus (total P), along with the trace and major elements level in medicinal herbs, has been reported in many studies, and it varied within the range of mg/g of dry plant tissue (2, 3). The concentration of inorganic phosphate (inorganic P) in aqueous extracts from medicinal herbs has also been studied. It was found that this fraction of P occurs over the range of 53 to 63% of the total P in the plant material (4, 5). Inorganic P has also a positive effect on the synthesis of secondary metabolites of medicinal plants (6).

However, the inorganic P is not only a single chemical species, in which this element occurs in a plant material. It has also been found that several

plant materials and foods of plant origin, including cereals and legumes, contain P in a phytate form (7-9). The content of phytates in food of plant origin can vary depending on various processing and cooking procedures (10).

The phytate form of phosphorus consists of phytic acid (phytate; *myo*-inositol 1,2,3,4,5,6-hexakisphosphate) (Fig. 1), which is the primary source of inositol and the principal storage form of P in plant seeds contributing between 50 and 80% of total P (11). This is important for health, because phytate P can bind certain elements, such as Fe or Mg, making them less available for humans (11). In this context, the phytate P can be regarded as an anti-nutrient component. However, there is also information in the literature that phytates play a beneficial role in prevention of different types of cancer, as well as they have antioxidant properties (12, 13). It has also been reported that the diet high in phytic acid can have protective effect against heavy metals, like cadmium (14).

A previous study has shown that inorganic P is often correlated to total level of this element, and with several metallic elements occurring in medici-

nal plants, e.g., with Mg (4). These relations can be explained by the fact that P, Mg and Fe have a synergistic effect in plant metabolic processes (15). A literature review has shown that phytate P level in medicinal herbs has not been widely studied. However, the contents of phytic acid was analyzed in several African medicinal plants and it was found within the range of 0.89 – 2.55 mg/g (16). The

analysis of phytates is crucial for patients drinking herbal teas, because phytate P can chelate certain metals, such as Mg, Ca, K or Fe, thus lowering their bioavailability for humans. Therefore, the objective of this study was to determine the phytate P in herbal teas and to investigate its relation to total P, inorganic P, and selected trace and major elements in herbal teas prepared from different morphological parts of medicinal plants.

EXPERIMENTAL

Plant material

The studied medicinal herbal materials comprised herbs (sample numbers are given in parenthesis): *Herba Euphrasiae* (*1* and *2*), *Millefolii* (*3* and *4*), *Equiseti* (*5-7*), *Hyperici* (*8-10*) and *Violae tricoloris* (*11* and *12*); leaves: *Folium Salviae* (*13-16*), *Sennae* (*17-19*) and *Urticae* (*20* and *21*); flowers: *Inflorescentia Tiliae* (*22-25*), *Crataegi* (*26-29*), *Flos Sambuci* (*30* and *31*), *Anthodium Calendulae* (*32-34*) and *Chamomillae* (*35-38*); fruits: *Fructus Anisi* (*39-41*), *Crataegi* (*42-45*), *Foeniculi* (*46-48*), *Rubi* (*49* and *50*), *Sorbi* (*51*), *Rosae* (*52*), *Aroniae* (*53*), *Sambuci* (*54*), *Myrtilli* (*55*) and *Pericarpium Phaseoli* (*56*); seeds: *Semen Sylibi mariani* (*57, 58*) and *Psylli* (*59*).

All samples were taken from Polish herbal firms. Most of them originated from "Kawon",
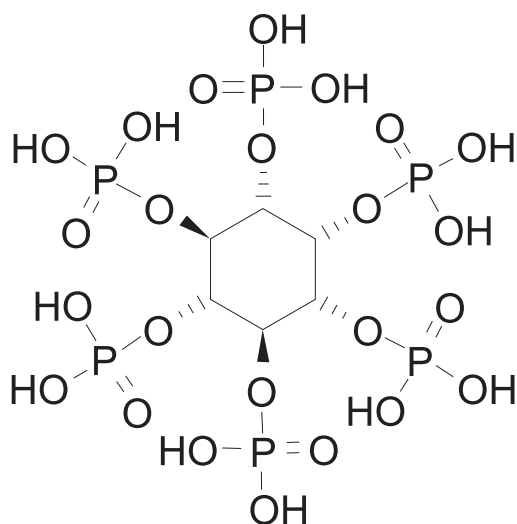

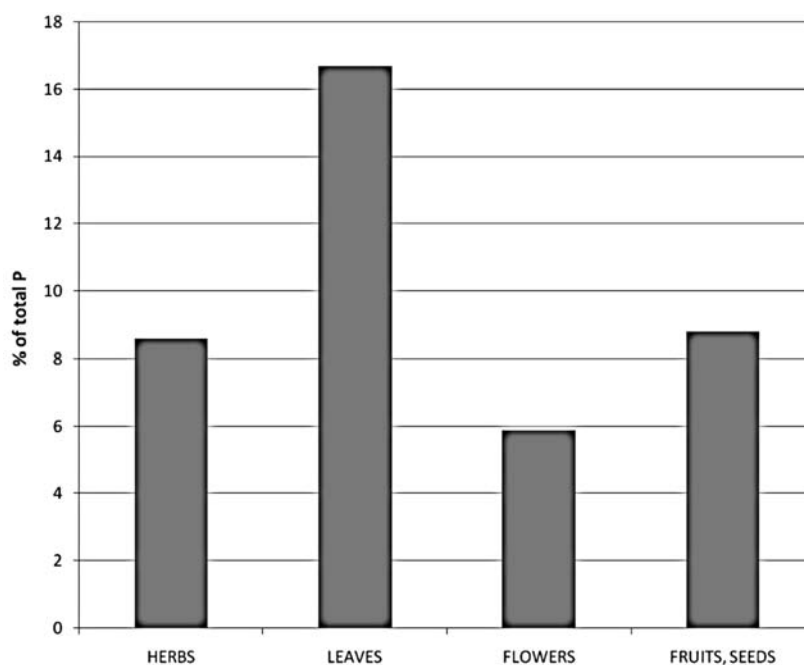Figure 1. Chemical structure of phytic acid. From www.http://chemistry.about.com

Figure 2. The average extraction yield of phytate P (% of total P) obtained for different morphological parts of medicinal plants

Table 1. Recovery and precision (n = 6) of the methods tested on the Certified Reference Material: Mixed Polish Herb (INCT-MPH-2).

Element (total concentration)	Declared contents (mg/kg d.w.)	Determined ± SD (mg/kg d.w.)	Recovery (%)	Precision as CV
P	2.50*	2.16 ± 0.06*	86.4	2.8
Fe	460.00	360.00 ± 4.41	78.3	1.2
Zn	33.50	37.72 ± 1.39	112.6	3.7
Mn	191.00	219.04 ± 8.56	117.5	3.8
Cu	7.77	7.59 ± 0.22	97.7	2.9
Mg	2.92*	3.32 ± 0.03*	113.7	0.9
Ca	10.8*	10.0 ± 0.01*	92.6	0.1
Na	350.00	359.90 ± 2.50	102.8	0.7
K	19.1*	16.8 ± 0.04*	88.0	0.2

* (mg/g d.w.), CV – coefficient of variation, d.w. – dry weight
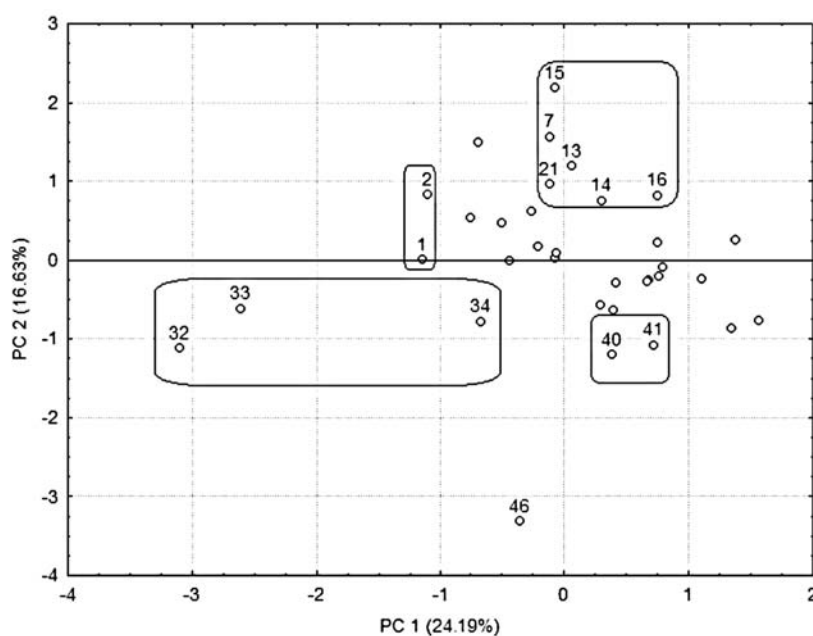
Figure 3. Distribution of the analyzed samples of medicinal herbal materials in two-dimensional plot of PC1 *vs.* PC2. Sample numbers correspond to herbal materials characterized in the Experimental part and in Table 2

samples No. *22, 43* and *59* were from "Herbapol", *49* and *51* from "Dary Natury", *57* from "Herbavita", and sample No. *58* from ZPH "ASZ" herbal firms.

Digestion of plant samples

The quantification of total level of P and metallic elements was proceeded by microwave digestion of the analyzed herbal material. The samples were placed in teflon vessels, and a mixture of HNO_3 (65% Selectipur solution) and H_2O_2 (30% solution) (3 + 5, v/v) (Merck, Germany) was added. Then, the samples were digested in a Uniclever BM-1z mineralization device (Plazmatronika, Poland). The following parameters of microwave digestion were applied: pressure over the range of 31 to 45 atm., temperature between 250 and 350°C, the power of microwaves set to 85% of the maximum value, time of digestion 7 min, time of cooling 5 min. After digestion, the samples were transferred into volu-

Table 2. Results of determination of phytate phosphorus, total phosphorus and inorganic phosphorus in the studied medicinal plant samples.

Sample No.	Phytate P (µg/mL)			Total P	P-PO$_4$	P-PO$_4$/ total P (%)
	Range	Mean ± SD	Phytate P/ total P (%)	mean (mg/g)		
Herbs (Herba)						
1	10.46 – 12.13	11.44 ± 0.87	3.9	2.71	2.28	84.1
2	28.06 – 29.46	28.95 ± 0.77	7.5	3.56	1.63	45.8
3	10.79 – 14.19	12.77 ± 1.76	3.9	2.86	1.86	65.0
4	13.73 – 15.33	14.37 ± 0.84	4.8	2.66	2.42	91.0
5	25.52 – 27.06	26.04 ± 0.88	12.6	1.79	1.24	69.3
6	21.59 – 23.66	22.64 ± 1.03	11.4	1.82	0.98	53.8
7	22.73 – 27.59	26.08 ± 2.09	10.1	2.15	1.62	75.3
8	n.d.	n.d.	n.d.	2.37	1.72	72.6
9	20.72 – 23.06	21.50 ± 1.30	8.3	2.48	2.05	82.7
10	24.39 – 25.19	24.77 ± 0.40	10.4	2.20	1.16	52.7
11	19.66 – 21.59	20.75 ± 0.99	8.5	2.34	1.19	50.9
12	23.79 – 25.39	24.61 ± 0.80	12.9	1.88	1.51	80.3
Leaves (Folium)						
13	10.86 – 12.13	11.68 ± 0.71	6.5	2.17	1.46	67.3
14	15.13 – 17.19	16.37 ± 1.09	13.0	2.11	1.43	67.8
15	19.13 – 20.13	19.71 ± 0.51	18.5	1.25	1.01	81.5
16	22.26 – 23.79	23.13 ± 0.78	17.6	1.72	1.25	72.7
17	36.26 – 37.66	36.90 ± 0.70	48.3	0.73	0.17	23.3
18	34.93 – 35.06	35.02 ± 0.07	19.9	1.55	0.74	47.7
19	19.33 – 23.19	20.62 ± 2.23	18.8	1.75	0.42	24.0
20	22.33 – 24.79	23.22 ± 1.36	4.1	4.58	0.79	17.2
21	15.13 – 17.13	16.26 ± 1.02	3.5	4.22	0.73	17.3
Flowers (Flos, Inflorescentia, Anthodium)						
22	12.19 – 14.19	12.86 ± 1.15	7.8	2.28	1.31	57.5
23	17.00 – 17.93	17.62 ± 0.53	8.5	1.98	1.13	57.1
24	17.46 – 18.00	17.64 ± 0.31	6.6	2.48	1.20	48.4
25	13.33 – 14.59	14.08 ± 0.66	7.0	1.93	0.82	42.5
26	14.80 – 15.93	15.55 ± 0.65	5.3	2.77	1.27	45.8
27	19.46 – 20.59	20.26 ± 0.69	8.6	2.24	0.94	41.9
28	17.53 – 19.86	19.00 ± 1.27	8.7	2.19	0.85	38.8
29	12.86 – 16.13	14.17 ± 1.72	5.9	2.23	0.64	28.7
30	22.33 – 24.13	23.37 ± 0.93	6.2	3.77	1.09	28.9
31	20.39 – 21.79	21.26 ± 0.75	4.8	4.36	1.10	25,2
32	18.79 – 21.46	19.75 ± 1.48	7.6	4.10	3.57	87.1
33	18.99 – 24.46	20.84 ± 3.13	7.6	4.50	2.31	51.3
34	7.53 – 10.00	8.73 ± 1.23	2.1	2.78	1.31	47.1
35	4.86 – 7.19	6.24 ± 1.22	3.4	2.99	0.84	28.1
36	4.53 – 5.53	4.97 ± 0.50	1.9	3.68	0.83	22.6
37	n.d.	n.d.	n.d.	2.82	1.14	40.4
38	4.26 – 9.19	5.90 ± 2.84	2.0	3.53	2.34	66.3

Table 2. cont.

Sample No.	Phytate P (µg/mL)			Total P	P-PO$_4$	P-PO$_4$/ total P (%)
	Range	Mean ± SD	Phytate P/ total P (%)	mean (mg/g)		
Fruits, seeds (*Fructus, Semen*)						
39	17.79 – 17.93	17.86 ± 0.07	8.3	3.11	0.41	13.2
40	8.79 – 10.79	9.90 ± 1.01	2.9	3.21	0.33	10.3
41	2.26 – 4.60	3.71 ± 1.26	10.0	1.16	0.56	48.3
42	19.06 – 20.33	19.48 ± 0.73	2.5	1.37	0.82	59.9
43	7.33 – 8.33	7.97 ± 0.55	10.5	1.27	0.49	38.6
44	1.53 – 3.53	2.44 ± 1.01	5.2	1.19	0.79	66.4
45	18.59 – 19.93	19.22 ± 0.67	0.4	3.52	0.50	14.2
46	10.79 – 13.06	11.66 ± 1.22	4.5	4.01	0.65	16.2
47	15.72 – 16.53	16.06 ± 0.43	2.6	3.83	1.05	27.4
48	21.46 – 23.73	22.39 ± 1.18	10.0	1.55	0.54	34.8
49	17.00 – 18.93	18.11 ± 0.99	13.4	1.66	0.74	44.6
50	9.06 – 11.66	10.24 ± 1.31	7.7	1.40	0.16	11.4
51	30.26 – 31.32	30.90 ± 0.56	7.5	1.37	0.43	31.4
52	2.67 – 3.67	3.27 ± 0.52	26.9	1.02	0.11	10.8
53	10.00 – 12.33	11.51 ± 1.30	1.0	2.70	0.65	24.1
54	21.86 – 23.46	22.73 ± 0.80	10.2	1.04	n.d.	n.d.
55	n.d.	n.d.	n.d.	3.65	0.50	13.7
56	17.00 – 17.10	17.11 ± 0.11	41.7	0.82	0.25	30.5
57	5.10 – 5.30	5.22 ± 0.10	0.5	3.03	0.24	7.9
58	13.26 – 13.73	13.48 ± 0.25	4.4	3.06	1.24	40.5
59	8.46 – 10.86	9.84 ± 1.23	5.3	4.00	n.d.	n.d.

n.d. – not detected (below detection limit)

metric flasks and diluted up to 50 mL with redistilled water (Heraeus Quarzglas, Switzerland).

Extraction/tea brewing procedure

The dry sample of a medicinal herb (a bag of 1-2 g) was placed in a 250 mL beaker, and 100 mL of boiling redistilled water was added. Then, the sample was brewed during 15 min under glass cover and the bag was removed from the extract, which was transferred into a volumetric flask and diluted up to 100 mL with redistilled water.

Determination of phytate phosphorus

Phosphate P was determined spectrophotometrically with the Wade reagent (9). To 2 mL of the aqueous extract (tea) of a medicinal herb, 10 mL of the Wade reagent consisting of a 0.03% FeCl$_3$ solution and a 0.25% 5-sulfosalicylic acid solution, 3 + 1 (v/v) was added. Then, the sample was diluted up to 25 mL with redistilled water and

the absorbance was measured at 500 nm using a UV/Vis spectrophotometer (Metertek SP-870, South Korea).

The calibration curve was characterized by regression equation: y = 0.6879 – 0.015x for the range of 5.33-40 µg/mL (r = 0.9899). The method was validated (17) by determining limits of detection (1.6 µg/mL) and quantification (5.33 µg/mL). The accuracy (recovery) of the method was evaluated by the standard addition method as 80%.

Determination of total and inorganic phosphorus

Total P in the digested herbal samples and inorganic P in the aqueous extracts of medicinal herbs were determined based on phospho-molybdenum blue reaction (4). The absorbance was measured at 650 nm. The accuracy and precision of the method were checked using the Certified Reference Material: Mixed Polish Herb (INCT-MPH-2). These values are shown in Table 1.

Table 3. Results of determination of trace and major elements in the studied medicinal plant samples.

Trace elements (mg/kg)			
Element	Range	Mean ± SD	Median
Fe total	27.49 – 408.64	131.00 ± 90.60	105.91
Fe extr.	1.78 – 31.39	6.85 ± 5.04	5.48
Zn total	4.56 – 85.36	39.86 ± 18.36	40.43
Zn extr.	0.35 – 49.35	12.21 ± 10.22	8.91
Mn total	7.41 – 243.01	75.53 ± 63.5	45.96
Mn extr.	0.34 – 92.05	24.15 ± 24.81	16.10
Cu total	3.48 – 56.85	10.43 ± 7.61	8.92
Cu extr.	0.25 – 23.93	4.06 ± 4.32	3.44
Major elements (mg/g)			
Mg total	0.79 – 11.42	3.84 ± 2.89	2.85
Mg extr.	0.09 – 10.85	1.44 ± 1.52	1.12
Ca total	1.39 – 133.89	31.48 ± 29.30	25.09
Ca extr.	0.09 – 76.01	8.92 ± 13.72	3.89
Na total	0.24 – 6.84	2.16 ± 1.88	1.19
Na extr.	0.02 – 0.62	0.10 ± 0.11	0.07
K total	0.27 – 1.70	0.73 ± 0.25	0.70
K extr.	0.04 – 0.57	0.26 ± 0.13	0.22

extr. – water extractable form of the element

Table 4. Statistically significant correlations indicating high correlation ($r > 0.5$; $\alpha < 0.05$) between elements in the studied medicinal plant samples.

Pair of elements	r	p
$P\text{-}PO_4$ – K extr.	0.52	0.000044
$P\text{-}PO_4$ – Zn total	0.50	0.000062
$P\text{-}PO_4$ – Zn extr.	0.60	0.000001
Ca total – Ca extr.	0.72	0.000000
Na total – Na extr.	0.67	0.000000
K total – K extr.	0.76	0.000000
Zn total – Zn extr.	0.51	0.000058
Mn total – Mn extr.	0.80	0.000000
Cu total – Cu extr.	0.81	0.000000

extr. – water extractable forms, p – significance level calculated by *Statistica* program

Determination of metallic elements

Total concentrations and the water-extractable forms of Fe, Zn, Mn, Cu, Mg, Ca, Na and K were determined by AAS in the digested medicinal plants, and in herbal teas. The 250 Plus Atomic Absorption Spectrometer (Varian, Australia) was used. The standard analytical parameters were as follows: air/acetylene flame, the analytical wavelengths (in nm): Fe (248.3), Zn (213.9), Mn (279.5), Cu (324.8), Mg (285.2), Ca (422.7), Na (589.0), and K (766.5). The accuracy and precision of the method were checked using the Certified Reference Material: Mixed Polish Herb (INCT-MPH-2), and these values are listed in Table 1.

Statistical evaluation of the results

The program Statistica 7.1 (Statsoft, Poland) was applied for all statistical calculations. The start-

ing database for PCA had the dimensions of 19 × 59, i.e., the concentrations of phytate P, inorganic P, total P, as well as total and water-extractable forms of Mg, Ca, Na, K, Fe, Zn, Mn, and Cu (19 parameters), determined in 59 analyzed samples.

RESULTS AND DISCUSSION

Phytate phosphorus

Phytate P in herbal teas fell in the range of 2.44-36.90 μg/mL, as shown in Table 2. The average level of extraction yield obtained for the aqueous extracts from different plant parts, ranged from 5.9% of total P in flowers to 16.7% of total P in leaves (Fig. 2). As only two samples of the seeds were analyzed, the fruits and seeds were treated as one group in statistical evaluation. The differences in the extraction yield of phytate P in the herbal teas are statistically significant only for the leaves, as confirmed by the Student's t-test (t = 2.18, p = 0.04, $\alpha < 0.05$).

As compared to the literature data, the phytate P level in the studied medicinal plants is much lower than that in the bean, lentil and legumes samples (7-9). It appears, according to our findings, that medicinal plants, in spite of containing quite high levels of total and inorganic P, in the order of mg/g d.w. (4, 5), don't have comparable levels of phytate P. However, when comparing our results of phytate P determination with the data obtained for African

medicinal plants (16), the level of phytate P appears in the similar range of concentrations.

Relating the concentration of phytate P recalculated in mg/kg d.w., to total P level in the same samples, as shown in Table 2, it is on average about 8% of total P. This is in contrast to the level of inorganic P, which constitutes much higher part of total P, on average 44.6%.

Inter-elemental relations

The results of quantification of metallic elements in the plant samples are shown in Table 3. The average total level of trace elements follows the order: Fe > Mn > Zn > Cu, while for the major elements: Ca > Mg > Na > K. When considering the median values this order remains the same. These results are compatible with the literature data (4, 18).

A correlation analysis enabled to recognize relations among phytate P, total and inorganic P, as well as among the trace and major elements in the studied medicinal herbs and teas obtained from them. From 210 calculated correlation coefficients, only 51 were statistically significant ($\alpha < 0.05$). The values of r > 0.5 were considered as a high correlation, and they are presented in Table 4. Surprisingly, the relations of phytate P to other P forms were below the significance level, similarly as the relations of phytate P to metallic elements. However, there are several characteristic relations of inorganic
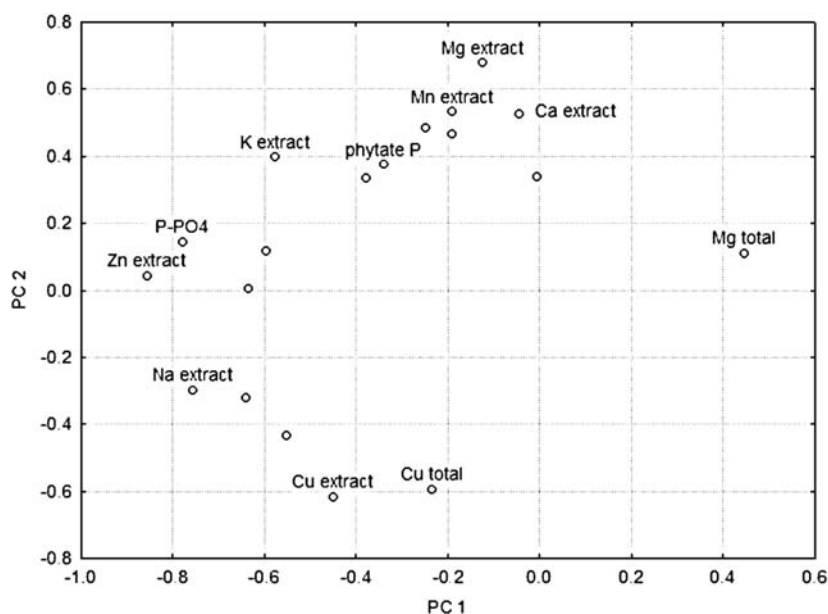

Figure 4. The two-dimensional loading plot of PC1 *vs.* PC2 obtained for medicinal herbal materials. Term "total" denotes the total content of essential elements in herbal materials and term "extract" refers to the content of water extractable forms

P to water extractable K, Zn, and total Zn, which can reveal a synergistic interaction between them. Also positive relations between total and water extractable amounts of the metallic elements were found.

Principal Component Analysis

One of the pattern recognition methods widely used for interpretation of experimental results is Principal Component Analysis, PCA (19). This statistical method is particularly useful in situations, when an experimental database comprises multivariate data describing a number of analyzed samples. The most important advantage of PCA is reducing the multidimensionality and the possibility to extract those factors, which influence the variability of the studied samples. These arguments have led us to application of PCA to the experimental results.

The results of PCA calculations revealed that first three principal components (PCs) explain together 54% of the variability among the studied medicinal plant samples, and first two PCs 40.8%. Therefore, a two-dimensional plot of first two PCs was used. A graphical interpretation of the PCA results (Fig. 3) shows that there are several characteristic groups of the studied plant samples. For example, in the left area of the plot there is a group of three samples of *Calendulae Flos* (*32-34*, sample numbers given in parenthesis). They all have a similar PC2 value, but the PC1 value differentiates one of them (*34*) from the remaining two representing the same plant species. Two samples of *Euphrasiae Herba* (*1* and *2*) are grouped in the central zone of the plot. In the right area there are also two characteristic clusters. Underneath there is one group of *Anisi Fructus* (*40* and *41*), and below a single sample of *Foeniculi Fructus* (*46*). In the upper right area of the plot, there is one cluster grouping all four samples of *Salviae Folium* (*13-16*), as well as one sample of *Hyperici Herba* (*7*) and one of *Urticae Herba* (*21*). Such a location of the samples given above as examples is caused by similar concentration of several elements in them or water extractable forms of the elements.

The loading plot of first two PCs, presented in Figure 4, shows which elements or their water extractable species have the highest impact on the distribution of the analyzed plant samples in a two-dimensional space. Total Mg concentration is positively correlated to PC1, but a stronger negative correlation of water-extractable Zn, inorganic P and of water extractable Na, can be seen. Regarding the correlation of PC2 with original parameters, one can notice that it is positively correlated to water

extractable Mg, as well as to water extractable species of Mn and Ca. On the other hand, PC2 is negatively correlated to total and water extractable levels of Cu. After PCA calculation, it was also found that PC3 was negatively related to water-extractable form of Mn, but this could not be shown on the 2D plot.

CONCLUSIONS

It was found that herbal teas contained phytate P at a relatively low level, of the order of μg/mL. The extraction yield for phytate P obtained from the leaves of medicinal plants was the highest in comparison with the other analyzed plant organs. The flowers represented the lowest extraction yield for phytate P among all the studied plant organs. It was also found that no statistically significant relations occurred between phytate P and the analyzed trace and major elements. However, inorganic P concentration in herbal teas was positively correlated to water extractable K, Zn, and total Zn, which reveals a synergistic interaction between these essential elements.

PCA was a helpful multivariate statistical method, which enabled the analyzed samples to be grouped based on similarity of their elemental contents, as well as to state that inorganic P, water extractable Zn and Na, had a crucial impact on differentiation of the studied plant materials.

REFERENCES

1. Murray R.K., Granner D.K., Mayes P.A., Rodwell V.W.: Harper's Biochemistry, 25th edn.; McGraw-Hill, New York 2000.
2. Lemberkovics E., Czinner E., Szentmihalyi K., Balazs A., Szoke E.: Food Chem. 78, 119 (2002).
3. Kalny P., Fijalek Z., Daszczuk A., Ostapczuk P.: Sci. Total Environ. 381, 99 (2007).
4. Konieczynski P., Wesolowski M.: Food Chem. 103, 210 (2007).
5. Konieczynski P., Wesolowski M., Radecka I., Rafalski P.: Chem. Spec. Bioavail. 23, 61 (2011).
6. Liu S., Zhong J.J.: Proc. Biochem. 33, 69 (1998).
7. Urbano G., Lopez-Jurado M., Aranda P., Vidal-Valverde C., Tenorio E., Porres J.: J. Physiol. Biochem. 56, 283 (2000).
8. Coelho C.M.M., Santos J.C.P., Tsai S.M., Vitorello V.A.: Braz. J. Plant Physiol. 14, 51 (2002).

9. Norhaizan M.E., Nor Faizadatul Ain A.W.: Mal. J. Nutr. 15, 213 (2009).

10. Duhan A., Khetarpaul N., Bishnoi S.: Food Chem. 78, 9 (2002).

11. Thavarajah D., Thavarajah P., See C.T., Vandenberg A.: Food Chem. 122, 254 (2010).

12. Moorty H.K., Venugopal P.: Indian J. Urol. 24, 295 (2008).

13. Ali M., Shuja M.N., Zahoor M., Qadri I.: African J. Biotechnol. 9, 1551 (2010).

14. Daley T., Omoregie S.N., Wright V., Omoruyi F.O.: Biol. Trace Elem. Res. 151, 400 (2013).

15. Mehra A., Farago M.E.: Metal ions and plant nutrition, in Plants and the Chemical Elements: Biochemistry, Uptake, Tolerance and Toxicity, Farago M.E. Ed., pp. 32-66, VCH, Weinheim 1994.

16. Ekpa O.D.: Food Chem. 57, 229 (1996).

17. Konieczka P., Namieśnik J.: Assessment and quality control of results of analytical measurements (Polish), WNT, Warszawa 2009.

18. Malik J., Szakova J., Drabek O., Balik J., Kokoska L.: Food Chem. 111, 520 (2008).

19. Otto M.: Chemometrics. Statistics and computer application in analytical chemistry, Wiley-VCH, Weinheim 1999.

PHARMACEUTICAL TECHNOLOGY

STATISTICAL OPTIMIZATION AND *IN-VITRO* EVALUATION OF HOLLOW MICROCAPSULES OF AN ANTI-HYPERTENSIVE AGENT

TUSHAR A. PREMCHANDANI* and BHAKTI B. BARIK

Department of Pharmaceutics, Utkal University, Vani Vihar, Bhubhaneshwar, Orissa, India

Abstract: The present work attempts to formulate and evaluate hollow microcapsules of an antihypertensive drug - ramipril, which will remain in vicinity of absorption site. The emulsion diffusion solvent evaporation method was employed for preparation of microspheres using Eudragit E100. Glycerol monostearate and sodium lauryl sulfate were used as surfactants, which showed good effect of film integrity. The different proportion of Eudragit E100 and ramipril at varying speed were employed for formulating hollow microspheres using 3^2 full factorial design. The formulated microspheres were subjected to evaluation of various parameters such as particle size analysis using motic microscope, drug loading efficiency and *in vitro* drug release. The main effect plot showed negative impact of polymer concentration and drug complex concentration, whereas positive impact of rotation speed on the % release of drug and drug encapsulation efficiency. The optimized batch of microcapsules was formulated as a hard gelatine capsule dosage form containing loading (plain drug) as well as sustained fraction of drug in form of microcapsules. It was found that dosage form also showed good *in vitro* release profile.

Keywords: ramipril, hollow microcapsules, emulsion diffusion, solvent evaporation, Eudragit E100

Ramipril is angiotensin converting enzyme inhibitor and mainly used in treatment of hypertension (1, 2). Microspheres are discrete multiparticulate delivery systems and are prepared for prolonged drug delivery, to improve bioavailability or stability and to get a site specific drug delivery. Microspheres can also offer advantages like reducing side effects, decreasing dosing frequency and improving patient compliance as well as limiting fluctuation within therapeutic range (3-5). Eudragit polymers are series of acrylate and methacrylate polymers available in different ionic forms. Eudragit E100 is insoluble in aqueous media but is permeable and have pH-dependent release profile (6-8). The aim of this study was to prepare Eudragit microspheres containing ramipril to achieve a sustained drug release profile suitable for peroral administration. The work started by investigating some formulation variables (polymer type, polymer : drug ratio, stirring speed) to obtain spherical particles. Then, the yield of production, particle size distribution, encapsulation efficiency, surface properties and ramipril release rate from microspheres were investigated. The influences of formulation variables on the microsphere properties were examined by employing full factorial design using Eudragit E100 (0.75, 1.5 g), ramipril complex (0.75, 1.5 g) and stirring speed (900, 1500 rpm)

MATERIALS AND METHODS

Chemicals and reagents

Ramipril was obtained as generous gift sample from Ajantha Pharmaceuticals, Mumbai, Eudragit E 100 was obtained as gift sample from Evonik Industries, Mumbai, glycerol monosterate, dichloromethane, polyvinyl alcohol, Tween 20, sodium lauryl sulfate and all other chemicals used were of analytical grade.

Preparation of floating microspheres of ramipril by emulsion diffusion solvent evaporation technique

Floating microspheres containing ramipril were prepared using emulsion solvent diffusion technique (9, 10). For the preparation of floating
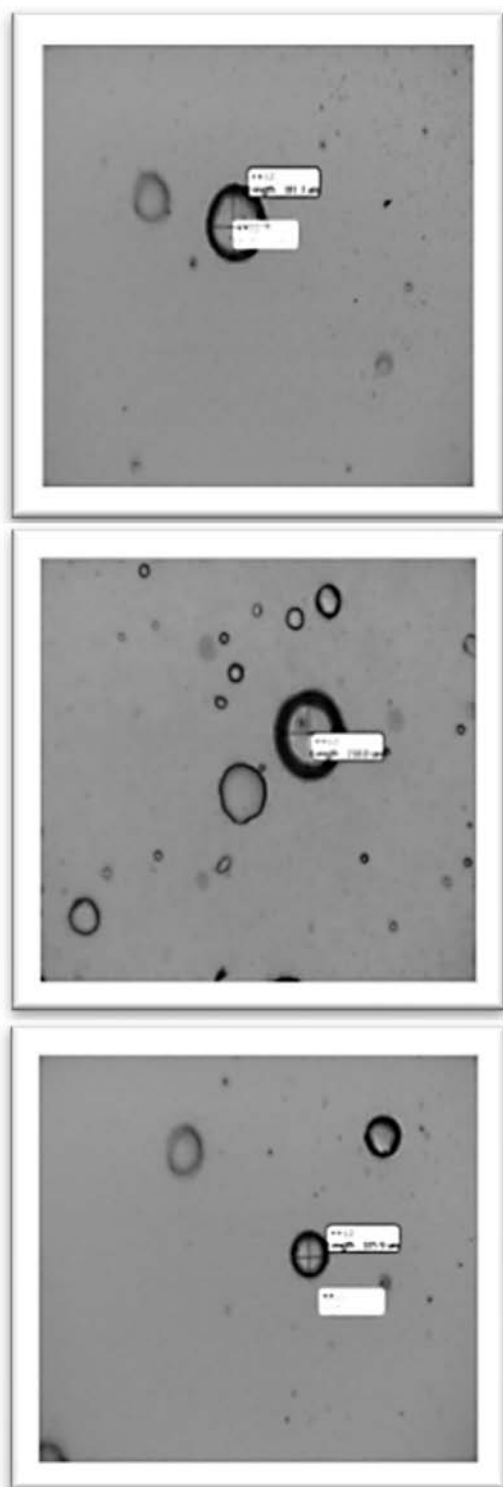

Figure 1. Motic pictures of ramipril hollow microspheres (oil immersion microscopy)

microspheres, employing design of experiment, the release controlling polymer used was Eudragit E100 in varying concentration.

Table 2 provides different proportion of drug complex and polymer concentration used at varying speed for preparation of microspheres. Glycerol monosterate and SLS were added as a stabilizer in the solution of drug and polymer. The following method was adopted for preparation of hollow microspheres.

The required quantity of drug and polymer was dissolved in a mixture of dichloromethane and ethanol (1 : 1, v/v, 80 mL). To this, glycerol monosterate (1.5 g) was added. The above mixture was dropped in a solution of polyvinyl alcohol (0.5%, 200 mL) by adding sodium lauryl sulfate (1%). The resultant solution was stirred with a mechanical stirrer for 1 h at different rotation conditions mentioned in Table 1. The formed floating microspheres were filtered and washed with water, dried at room temperature and stored in a desiccator until further use.

Particle size analysis

Particle size analysis was done by oil immersion microscopy (11, 12). Hollowness and release pattern are the basic attraction of the hollow microsphere so these are the very important evaluation parameters and motic images are recorded and shown in Table 2.

Drug encapsulation efficiency

The various batches of the floating microspheres were subjected to estimation of drug content (8, 13, 14). The floating microspheres equivalent to 50 mg of ramipril from all batches were accurately weighed and crushed. The powdered microspheres were dissolved in methanol (10 mL) in volumetric flask (100 mL) and made the volume with 1.2 pH buffer. This solution was then filtered through Whatman filter paper No. 44. After filtration, from this solution accurate quantity (10 mL) was taken and diluted up to 100 mL with pH 1.2 buffer. From this solution, accurate volume (2 mL) was pipetted out and diluted up to 10 mL with pH 1.2 buffer and the absorbance was measured at 210 nm against 1.2 pH buffer as a blank. All determinations were done in triplicate. The percentage drug entrapment was calculated as follows:

$$\% \text{ Drug entrapment} = \frac{\text{Calculated drug concentration}}{\text{Theoretical drug concentration}} \times 100$$

Percentage yield

The percentage yield of different formulations was determined by weighing the floating microspheres after drying. The percentage yield was calculated as follows.

$$\% \text{ Yield} = \frac{\text{Total weight of floating microspheres}}{\text{Total weight of drug and polymer}} \times 100$$

Table 1. Formulation matrix using Minitab.

Formulation code	Eudragit E100 (g)	Ramipril (g)	Rotation speed (rpm)	% Drug encapsulation efficiency	% Yield
F1	0.75	0.75	1500	76.12 ± 2.32	75.78 ± 2.67
F2	1.50	1.50	1500	52.86 ± 1.56	68.60 ± 3.89
F3	1.5	0.75	900	50.23 ± 3.67	65.90 ± 2.12
F4	0.75	1.50	1500	64.86 ± 3.14	54.65 ± 1.09
F5	1.50	1.50	900	48.16 ± 2.19	67.98 ± 2.92
F6	0.75	0.75	900	72.16 ± 4.56	72.67 ± 1.56
F7	1.50	0.75	1500	68.11 ± 1.56	63.77 ± 1.98
F8	0.75	1.50	900	50.19 ± 2.56	61.89 ± 1.54

± indicates n = 3

Table 2. Mean particle size of different batches of hollow microcapsules.

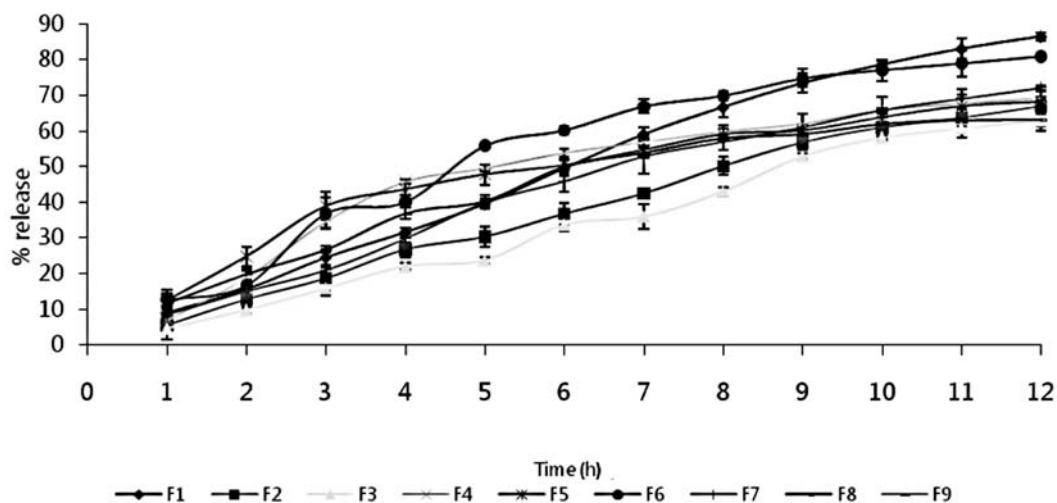| No.	Formulation code	Particle size (micrometers)
1	F1	206.7 ± 0.74
2	F2	282.6 ± 0.75
3	F3	318.4 ± 6.61
4	F4	338.3 ± 7.14
5	F5	319 ± 5.89
6	F6	213 ± 4.89
7	F7	298 ± 7.99
8	F8	308 ± 5.98

± indicates n = 3

Figure 2. *In-vitro* drug release profile of batches F1 to F8, 1.2 pH buffer

Table 3. Kinetics of drug release from formulated batches F1-F8.

Batch No.	Best fit model	r^2	k
F1	Zero order	0.995	2.109
F2	Zero order	0.996	1.409
F3	Zero order	0.995	-0.990
F4	Higuchi	0.977	2.553
F5	Higuchi	0.989	0.958
F6	Higuchi	0.979	3.161
F7	Zero order	0.988	4.176
F8	Higuchi	0.986	2.324

Table 4. Formulation composition for hard gelatin capsules

No.	Ingradient	Quantity for 20 capsules of weight 150 mg
1.	Ramipril (plain)	100 mg
2.	Ramipril (microspheres)	150 mg
3.	Avicel PH 101	2.0 g
4.	Lactose	750 mg
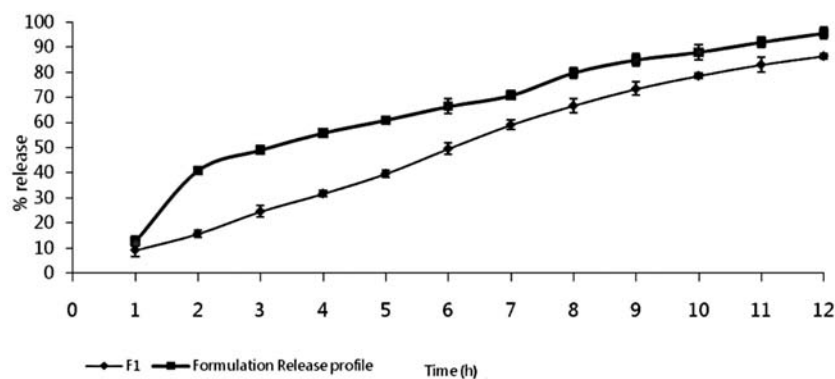
Figure 3. *In vitro* drug release profile of batch F1 and hard gelatin capsule

Shape and surface characterization of floating microspheres by scanning electron microscopy

The size and surface morphology of floating microspheres were examined by scanning electron microscopy as shown in Figures 4 and 5. These figures illustrate the microphotographs of batch F1. The floating microspheres were spherical with no visible major surface irregularity. Few wrinkles and inward dents at the surface and some crystal shape particles were appeared. It may be due to collapse of floating microspheres during the *in situ* drying process.

***In-vitro* release studies**

In-vitro release of ramipril from floating microspheres was carried out using the USP dissolution test apparatus (Type-II) (15). A weighed amount of floating microspheres equivalent to 50
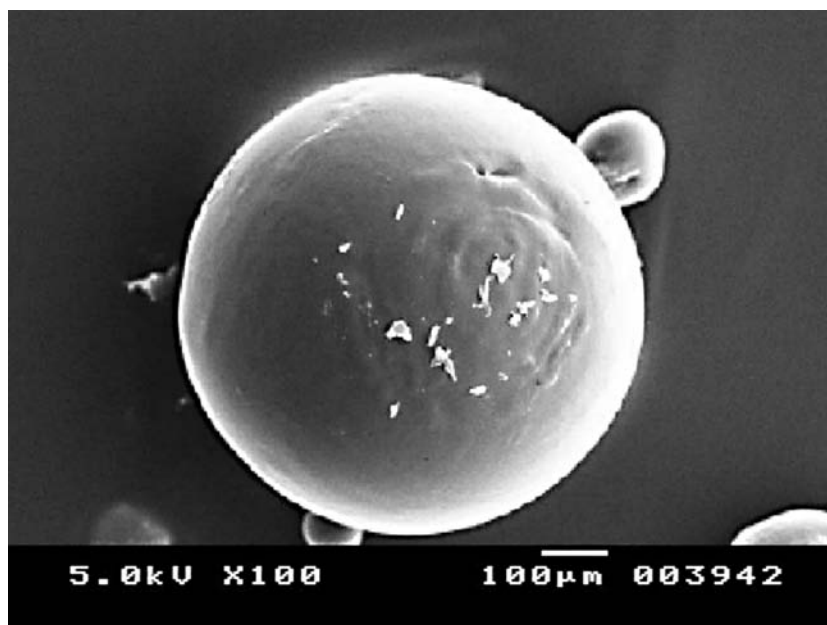
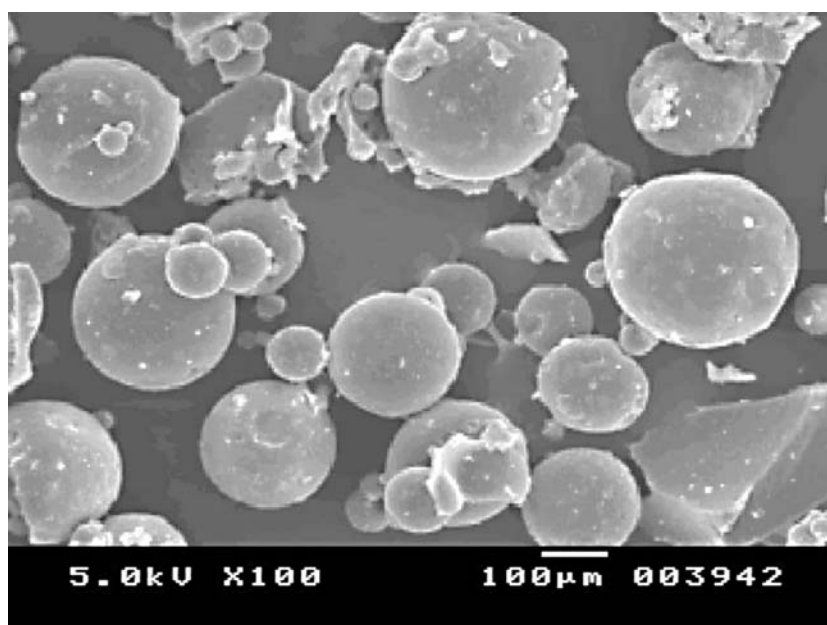Figure 4. Scanning electron microphotograph of formulation F1

Figure 5. Scanning electron microphotograph of formulation F1

mg of drug were filled into a muslin cloth and tied to the paddle. Dissolution medium used was 900 mL of pH 1.2 buffer maintained at $37 \pm 0.5^{\circ}$C and stirred at 50 rpm. At predetermined time intervals, 5 mL samples were withdrawn and replaced with equal amount of pH 1.2 buffer. The collected samples were filtered and suitably diluted with media and analyzed spectrophotometrically at 210 nm to determine the amount of drug released in the dissolution medium. The *in vitro* drug release is shown in Figure 2.
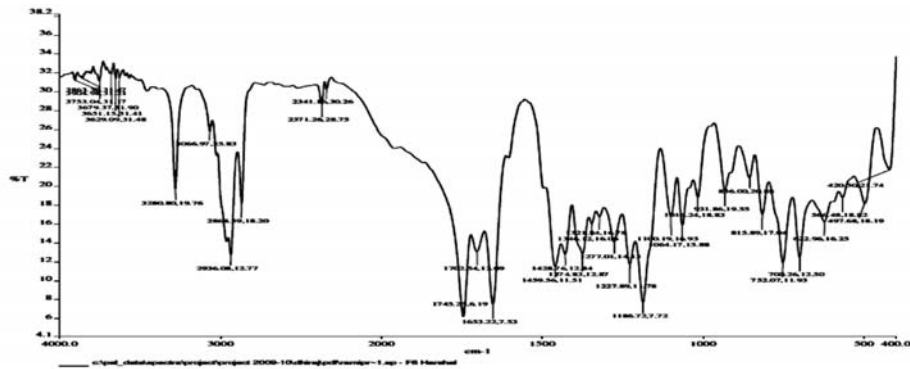
Figure 6. IR-spectrum of ramipril API
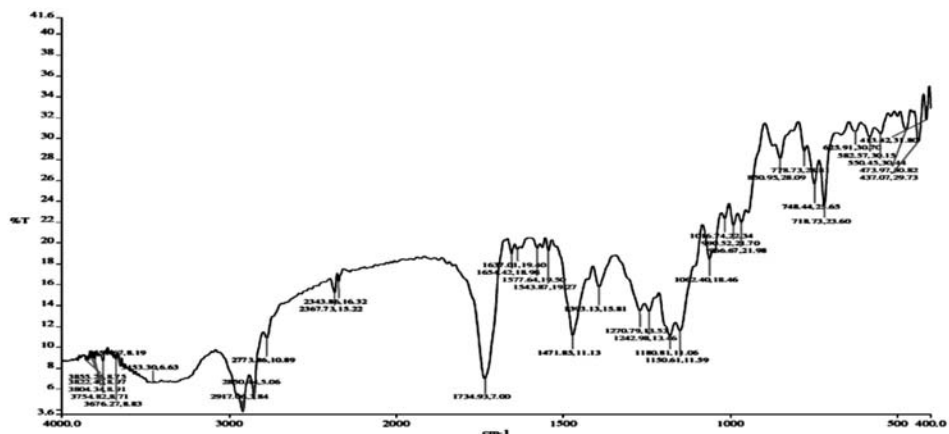
Figure 7. IR spectrum of batch F1
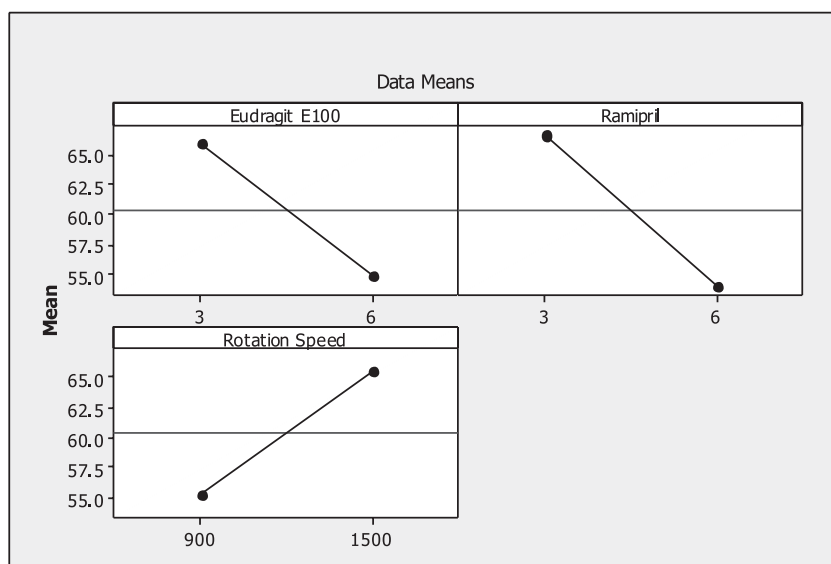
Figure 8. Main effect plot showing effect of Eudragit E100, ramipril and rotation speed on % drug encapsulation efficiency
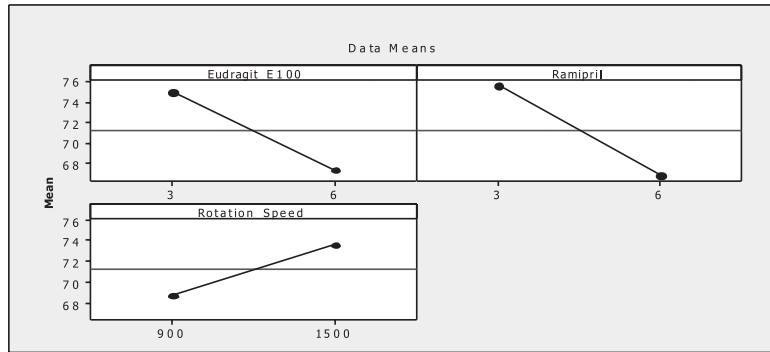
Figure 9. Main effect plot showing effect of Eudragit E100, ramipril and rotation speed on drug release after 12 h
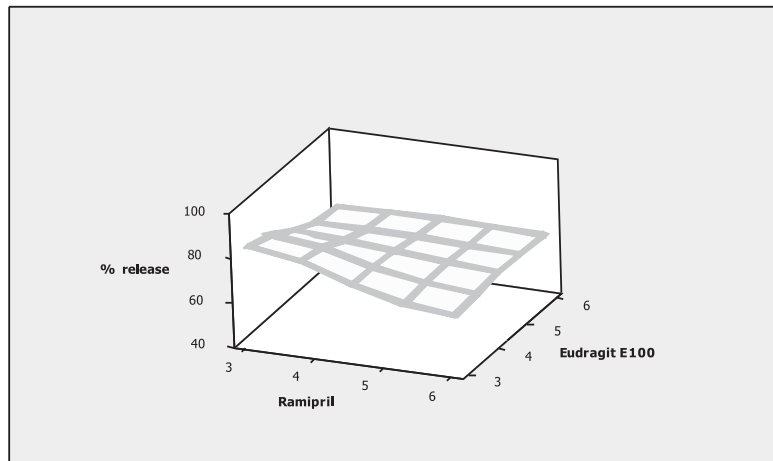
Figure 10. Surface plot showing effect of Eudragit E100 and ramipril on % release of ramipril
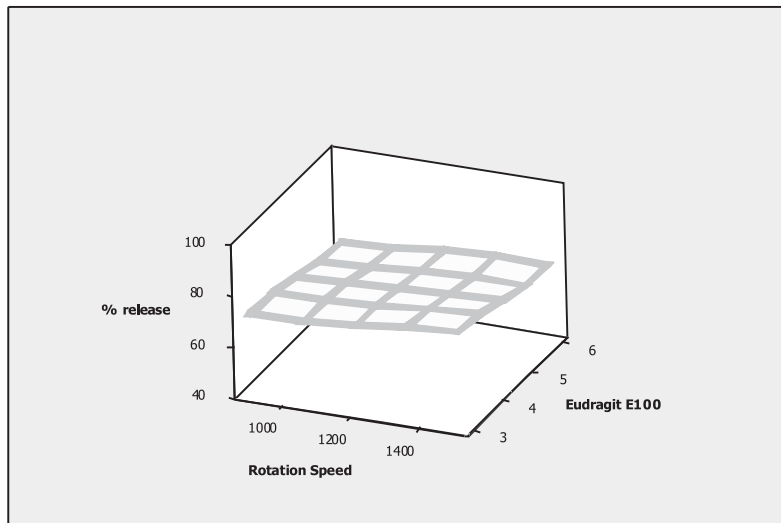
Figure 11. Surface plot showing effect of Eudragit E100 and rotation speed on % release of ramipril

Figure 12. Surface plot showing effect of ramipril concentration and rotation speed on % release of ramipril

Figure 13. Surface plot showing effect of ramipril concentration and rotation speed on % DEE (drug encapsulation efficiency)

Figure 14. Surface plot showing effect of ramipril and Eudragit E100 on % DEE (drug encapsulation efficiency)

Figure 15. Surface plot showing effect of drug rotation speed and Eudragit E100 on % DEE (drug encapsulation efficiency)
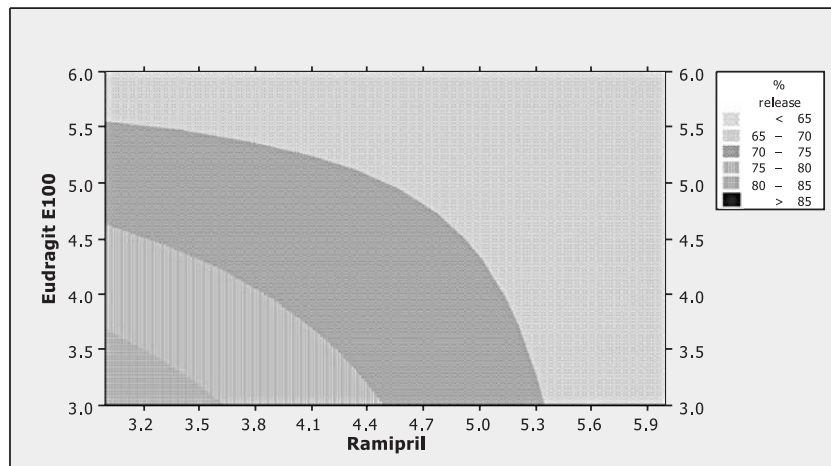
Figure 16. Contour plot showing effect of Eudragit E100 and ramipril on % release of ramipril

Figure 17. Contour plot showing effect of Eudragit E100 and rotation speed on % release of ramipril

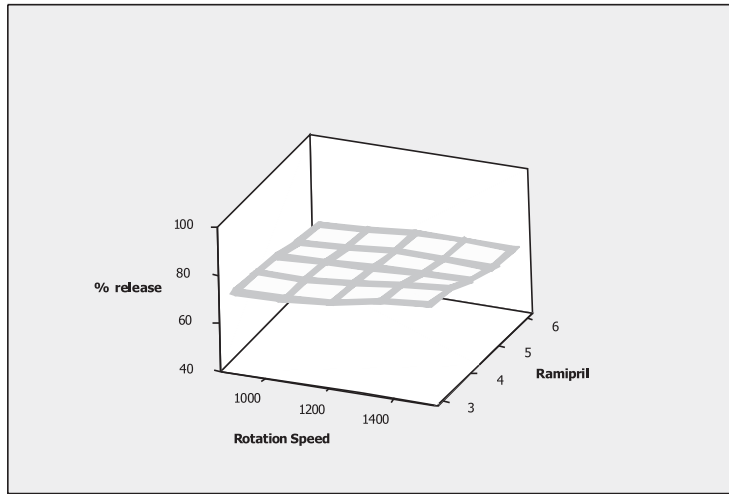Figure 18. Contour plot showing effect of ramipril concentration and rotation speed on % release of ramipril
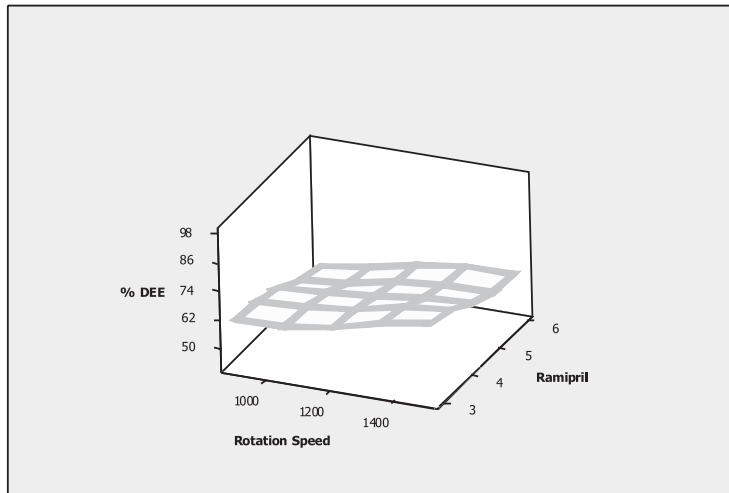

Figure 19. Contour plot showing effect of ramipril concentration and rotation speed on % DEE (drug encapsulation efficiency)
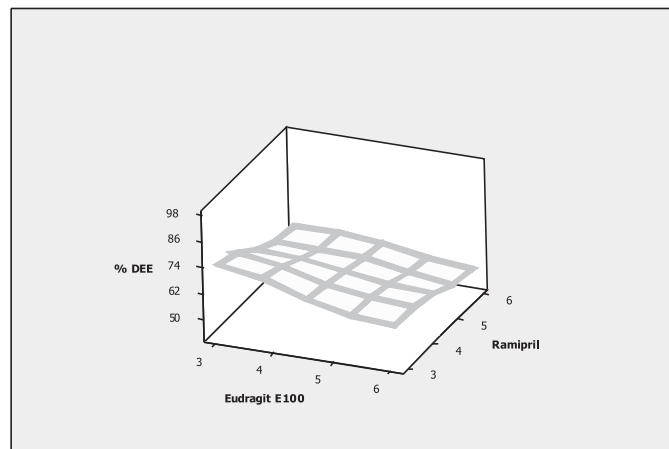

Figure 20. Contour plot showing effect of ramipril and Eudragit E100 on % DEE (drug encapsulation efficiency)
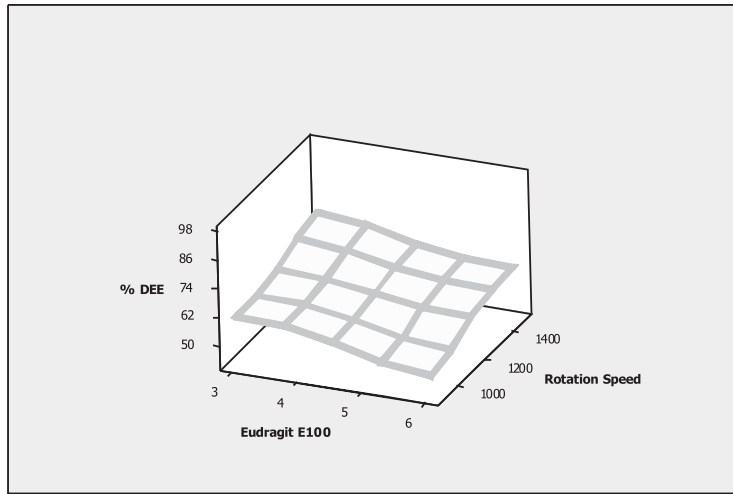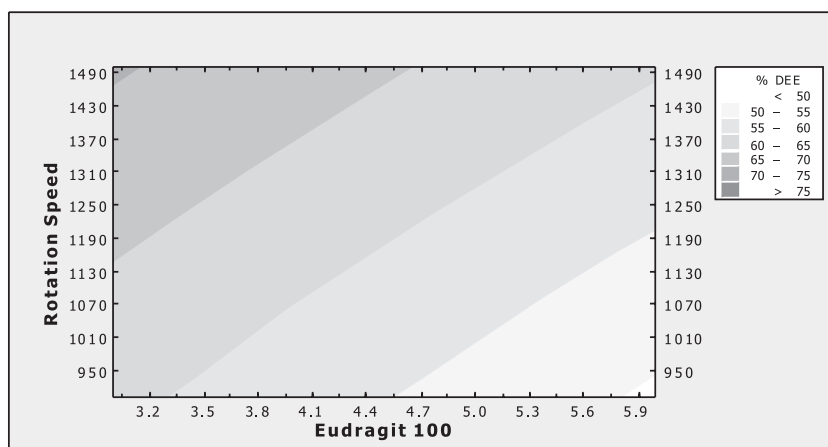
Figure 21. Contour plot showing effect of drug rotation speed and Eudragit E100 on % DEE (drug encapsulation efficiency)
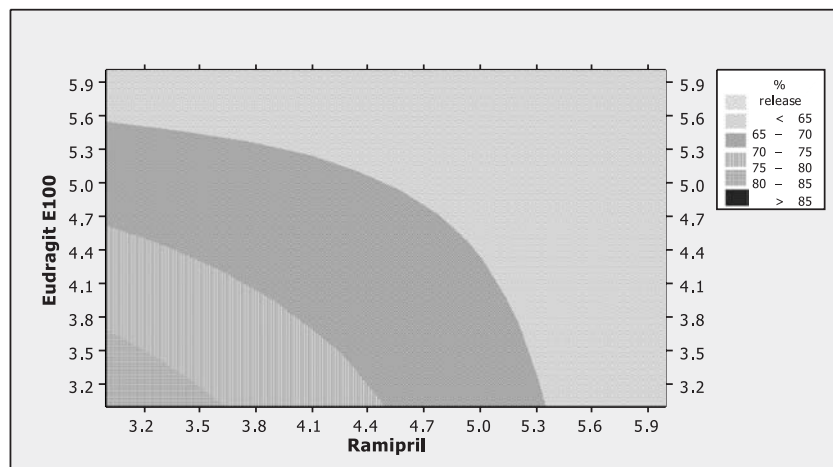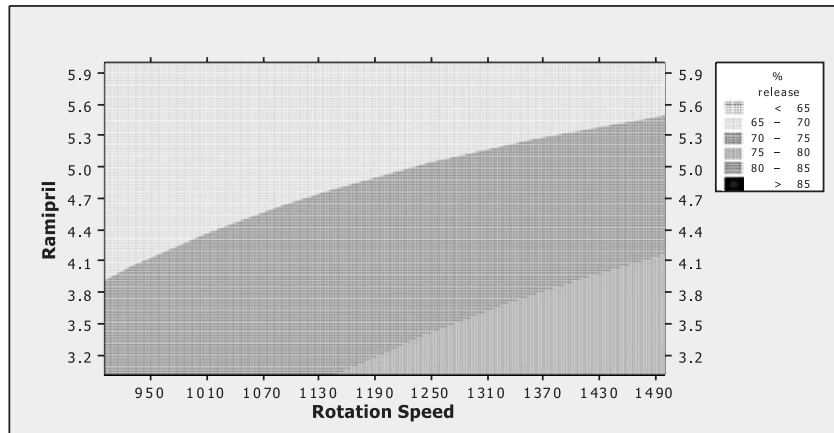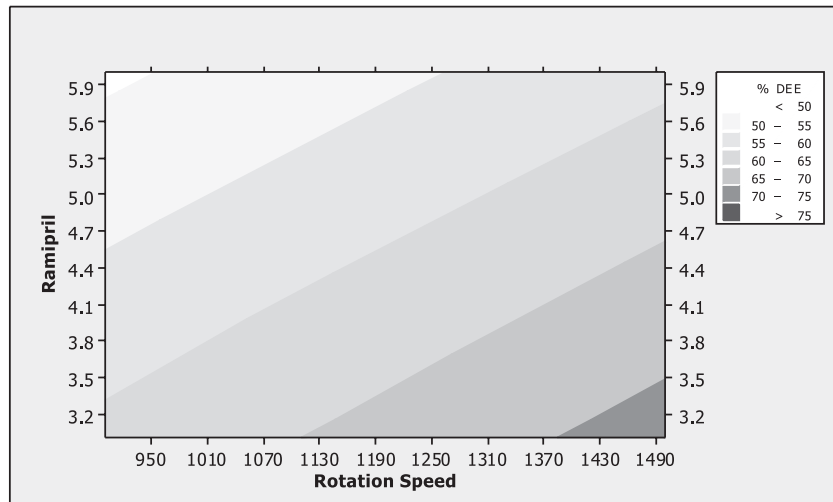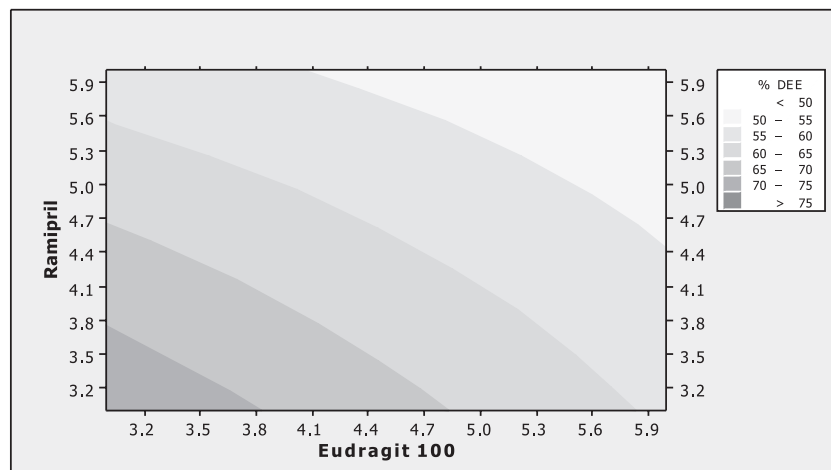
Fourier transforms infra-red spectroscopy (FT-IR) analysis

The Fourier transform infra-red analysis was conducted for the analysis of drug polymer interaction and stability of drug during microencapsulation process. The IR spectra of ramipril, Eudragit E100 and optimized batch F1 floating microspheres were recorded. The IR results are shown in Figures 6 and 7.

Analysis of results by Minitab

The full factorial design was setup to study the effect of various input variables (Eduragit 100, drug complex and stirring speed) on % drug encapsulation efficiency and % release of drug. The polynomial equation for the generalized linear model for 1st order can be depicted as follows:

$$Y = b0 + b_1X1 + b_2X2 + b_3X3\ b_{12}X1X2$$
$$+ b_{23}X2X3 + b_{13}X1X3 + b_{123}X1X2X3$$

where, Y is the dependent variable, b0 is the arithmetic mean response of the 9 runs, and b1, b2 and b3 are the estimated coefficients for factors X1, X2 and X3. The main effects (X1, X2 and X3) represent the average result of changing one factor at a time from its low to high value. The interaction terms (X1X2X3) show how the response changes when 3 factors are simultaneously changed. The polynomial terms (X1X2, X2X3 and X1X3) are included to investigate nonlinearity.

The polynomial equation for % drug encapsulation efficiency is:

$$Y = 71.23 + 3.73X1 + 4.38X2 - 2.47X3 +$$
$$4.39X1X2 - 0.45X2X3 - 1.25X1X3 +$$
$$15.13X1X2X3$$

The polynomial equation for % drug release is:

$$Y = 60.33 + 5.50X1 + 6.31X2 - 5.15X3 +$$
$$1.98X1X2 + 0.49X2X3 - 0.30X1X3 +$$
$$71.34X1X2X3$$

The interaction plots and main effect plots show relationship of selected variables with the selected observable output variables.

Formulation of suitable dosage form (hard gelatin capsule)

From various evaluation parameters it was found that batch F1 containing low amount of drug as well as polymer at high rotational speed gave optimal drug release in 12 h. So, suitable dosage form, hard gelatin capsule was formulated employing loading dose as well as sustained hollow microcapsules were incorporated as in Table 4 and were subjected to *in vitro* release profile for which the results are shown in Figure. 3

RESULTS AND DISCUSSION

Ramipril is ACE inhibitor which works by reducing load on the heart. In present attempt, the novel approach hollow microspheres were tried for delivery of sustained delivery of ramipril and final delivery in the form of hard gelatin capsule. For formulation of hollow microspheres the full factorial design was employed using three key input variables at two levels i.e., amount of Eudragit (0.75 and 1.50 g), amount of Ramipril (0.75 and 1.5 g) and rotation speed (900 and 1500 rpm). Glyceryl monostearate was used to prevent aggregation of formed microspheres as it may help in formation of

thin layer around the formed membrane of microcapsules.

The formed microcapsules were evaluated for various parameters such as % drug encapsulation efficiency, particle size and *in vitro* drug release which was found to be highest for batch containing low concentration of drug complex and low concentration of Eudragit E100 at high rotation speed. The 3D surface plot, main effect plots and contour plots also confirm high encapsulation efficiency and high release of the drug. From main effect plot it can be observed that maximum encapsulation is seen at low concentration of polymer and drug complex and high stirring speed. The % release results were also similar to the results for % drug encapsulation efficiency. The optimized batch F1 was selected for further incorporation into the suitable dosage form and hard gelatin capsule was formulated which was also evaluated and showed satisfactory release when compared with batch F1.

The surface characterization was done by using SEM and it shows uniformity in size and shape of microcapsules. Further, the FTIR spectra reveal that there does not exist interaction between components used.

CONCLUSION

The formulation of hollow microspheres for ramipril is a challenging task. The wise selection of formulation ingredients as well as selection of surfactants can provide effective way of preparing them at laboratory level. The full factorial experimental design provides key input variables necessary for providing stable hollow microspheres.

REFERENCES

1. Tortora G.J., Grabowaski S.R.: Principles of Anatomy and Physiology, "Physiology of Stomach",10th edn., pp. 70-80, J. Wiley and Sons, New York 2003.
2. Hajare A.A., Shetty Y.T.: Res. J. Pharm. Technol. 1, 52 (2008).
3. Fursule R.A., Patra C.N., Kosalge S.B., Pati D.D., Deshmukh P.K.:. Int. J. Health Res. 1, 241 (2008).
4. Kale R.D., Tayade P.T.: Indian J. Pharm. Sci. 69, 120 (2007).
5. Shishu, Gupta N., Agrawal N.: AAPS PharmSciTech. 8(2), 48 (2007).
6. Jain S.K., Agrawal G.P., Jain N.K.: AAPS PharmSciTech. 7(4), 90 (2006).
7. Yoo H.S.: Colloids Surf. B Biointerfaces 52, 47 (2006).
8. Basavaraj B.V., Deveswaran R., Bharath S., Abraham S., Furtado S., Madhavan V.: Pak. J. Pharm. Sci. 21, 451 (2008).
9. Sato Y., Kawashima Y., Takeuchi N.: Eur. J. Pharm. Biopham. 55, 297 (2003).
10. Ali J., Khar R.K., Ahuja A.: Biopharmaceutics and Pharmacokinetics. 1st edn., pp. 27-29, Birla Publications, New Delhi 2001.
11. Tanwar Y.S.: Floating microspheres: Development, characterization and application. 4(3) 2006, www.pharmainfo.net , accessed on internet 12. 04. 2010.
12. Gaba P.: Floating microspheres: a review. 6(5), 2008. www.pharmainfo.net, accessed on internet 2. 2. 2010.
13. Pawar A.P., Sher P.: Eur. J. Pharm. Biopharm. 65, 85 (2007).
14. Srivastava, A. K., Ridhurkar, D. N., Wadhwa, S.: Acta Pharm. 55, 277 (2005).
15. Sato Y., Kawashima Y., Takeuchi N.: Eur. J. Pharm. Biopham. 55, 297 (2003).

MATERIAL AND TABLETING PROPERTIES OF *AZADIRACHTA INDICA* GUM WITH REFERENCE TO OFFICIAL ACACIA GUM

ABAYOMI T. OGUNJIMI and GBENGA ALEBIOWU*

Department of Pharmaceutics, Obafemi Awolowo University, Ile-Ife, Nigeria

Abstract: This study determined the material and tableting properties of *Azadirachta indica* gum (NMG) relative to acacia gum (ACA). The morphological properties were assessed with size and shape factors of aspect ratio, roundness, irregularity and equivalent-circle-diameter. The tableting properties of the gums were determined using compressional characteristics, tensile strength (TS), brittle fracture index (BFI) and crushing-strength-friability/disintegration-time ratio (CSFR/DT). The results suggest that NMG possesses larger, irregular and more elongated particles than ACA. The onset and amount of plastic deformation occurring in NMG was faster and higher, respectively, than in ACA. The result shows that, although ACA tablets were stronger, their tendency to cap/laminate was higher than in NMG tablets. The NMG tablets possess lower DT than those of ACA, while the CSFR/DT result suggests that a better balance exists between the strength and weakness of NMG tablets. The study concluded that NMG can be a useful excipient in tablet formulation.

Keywords: neem gum, acacia gum, tensile strength, brittle fracture index, disintegration, crushing strength-friability/disintegration-time ratio

In the production of pharmaceutical tablets, one or more excipients are needed to facilitate the production of good quality tablets, particularly for active pharmaceutical ingredients (API) that have little or no directly compressible properties. One of these excipients is a binder, which is employed in pharmaceutical tablet formulation to provide adequate mechanical properties by promoting the bonding properties existing between the different components of a powder mix in a formulation (1, 2). Various substances such as starches, celluloses and gums have been employed in pharmaceutical tablet formulations as binders (3). Gums have been used in pharmaceutical solid dosage formulations mainly as binders and directly compressible excipients.

Azadirachta indica gum, which belongs to the family of galactan gums (4) is a very complex condensate of heteropolysaccharides and proteins. The proteins are tightly linked to the polysaccharides, which constitute the major component. Drastic degradation of a smaller gum complex component shows that it contains D-glucose, D-glucuronic acid, L-arabinose, L-fucose, mannose and xylose. Investigation of the amino acid composition of the gum shows aspartic acid as the most abundant (5). Acacia gum (gum Arabic) consists of a group of macromolecules characterized by a high proportion of carbohydrates (approximately about 97%), which are predominantly composed of D-galactose and L-arabinose units and a low proportion of proteins (< 3%) (6, 7). However, neem gum has unusual structural features in that it contains appreciable amount of D-glucosamine and proteins (8) unlike other plant gums. Although studies have been done on the characterization and mechanical properties of various gums in pharmaceutical tablet formulations (3, 9–11), not much work has been done on the characterization and suitability of neem gum in tablet formulations.

In the present study, the morphological, compressional, disintegrant and mechanical properties of neem gum (NMG) obtained from the trunk of *Azadirachta indica* (A. Juss) tree were evaluated in comparison with a standard gum binder, acacia BP. The morphological properties were determined using shape factors of aspect ratio, roundness, irregularity and equivalent circle diameter (ECD). The compressional properties were determined by the Heckel and Kawakita equations, whereas its tableting properties were assessed with the aid of tensile strength (T), brittle fracture index (BFI), and the crushing strength – friability/disintegration time ratio (CSFR/DT).

* Corresponding author: e-mail: gbengaalaba@gmail.com, galebiowu@yahoo.co.uk; phone: +2348069384107

Although, researchers have carried out studies to elucidate the chemical compositions of neem gum (4, 5, 8), however, no study is available in the literature to specifically evaluate the safety profile of the gum exudate. Thus, this work includes the acute toxicity profile of neem gum using the Lorke's method (12).

EXPERIMENTAL

Materials

The materials used were *Azadirachta indica* gum obtained from the trunk of *Azadirachta indica* (A. Juss) tree and processed as described by Ogunjimi and Alebiowu (2), acetone and 99.8% ethanol (Sigma-Aldrich Laborchemikalien GmbH, Seelze, Germany), and acacia gum BP.

METHODS

Acute toxicity testing

The acute toxicity test on the *Azadirachta indica* gum was carried out using the Lorke's method (12). The toxicity was carried out in two phases using 13 experimental animals (rats). The animals were divided into three groups consisting of three animals per group. In the first phase, neem gum at doses of 10, 100, 1000 mg/kg body weight were administered orally in order to establish the range of doses that could produce toxic effects. The animals were observed for mortality within 24 h of administration. The second phase involved repeating the 1000 mg/kg body weight and new doses of 1600, 2900 and 5000 mg/kg body weight, which were administered orally (n = 1) and were observed for 24 h for mortality. The result obtained was used to determine the LD_{50} of the neem gum.

Particle shape and size characterization

This was determined by optical microscopy (LEICA DM 750 Research Microscope with an integrated icc50 camera, LEICA Microsystems GmbH, Germany). The images were then transferred to a personal computer for analysis. Approximately 300 particles picked randomly in the optical field for each sample were analyzed using the Image Pro Premier software (MediaCybernetics, Bethesda, MD, USA) to determine the particle descriptors of major and minor axis length, perimeter and projected area from which shape factors of aspect ratio, roundness, irregularity and equivalent circle diameter were determined according to the following equations (13):

$$Aspect\ ratio = \frac{b}{l} \qquad \text{Eq. 1}$$

$$Roundness = \frac{4 \times \pi \times A}{p^2} \qquad \text{Eq. 2}$$

$$Irregularity = \frac{p}{l} \qquad \text{Eq. 3}$$

$$Equivalent\ circle\ diameter = 2 \times \sqrt{\frac{A}{\pi}} \qquad \text{Eq. 4}$$

where b = length of the minor axis (minimum Feret diameter), l = length of major diameter (maximum Feret diameter), A = projected area of the particle, p = perimeter.

The aspect ratio varies between 0 and 1, with a low value indicative of an elongated particle and a perfect circle having an aspect ratio of 1. Roundness is a measure of how closely the projected area of the powder resembles a circle; a perfect circle has a roundness value of 1. Irregularity measures the surface area compared to the size of the particle; in this case, a perfect circle has an irregularity of p. Equivalent circle diameter (ECD) is a measure of size; it is the diameter of a sphere with the same cross-sectional area as the powder. The higher the equivalent circle diameter, the larger the mean particle size (13).

Determination of swelling capacity of gum

The method described by Bowen and Vadino (14) was used. Five grams of each powdered gum was poured gently into a 100 mL measuring cylinder and the bulk volume (V_0) was measured. Distilled water was added to disperse the gum (at room temperature), and subsequently, made up to the 100 mL mark. The dispersion was allowed to stand for 24 h when the volume (V_1) of the swollen gum was read. The swelling index was calculated as V_1/V_0. The determination was done in triplicate.

Determination of moisture content and sorption (hygroscopicity) of the gum

The moisture content of 10 g each of the gum was determined with an Ohaus moisture balance, model 6010H (Ohaus Scale Corporation, New Jersey, USA) set to emit 2 watts of heat for 2 min, while the moisture sorption of the gum was determined by exposing 1 g of the gum (previously dried at 50°C to a constant weight) to a constant relative humidity of 75% for a period of 72 h. Samples (1 g each) were placed in glass cups of uniform internal dimensions and kept in hygrostats prepared using standard solution of sodium chloride in wells of glass desiccators (15). Percent moisture (M_p) absorbed was determined from the weight gained at the end of 72 h according to equation Eq. 5. The determination was done in triplicate.

$$M_p = (\frac{W_2 - W_1}{W_1}) \times 100 \qquad \text{Eq. 5}$$

where W_1 is the initial weight of sample (1 g) and W_2 is the weight of sample after 72 h.

Determination of density parameters of gum

The apparent particle density of the gum was determined by the pycnometer method using acetone as displacement fluid. The bulk density of each gum powder at zero pressure (loose density) was determined by pouring the powder at an angle of 45° through a funnel into a glass measuring cylinder with a diameter of 22 mm and a volume of 50 mL (16). The relative density, D_o, of each gum powder was obtained from the ratio of its loose density to its particle density. The Hausner`s ratio determined as the ratio of the initial bulk volume to the tapped volume, was obtained by applying 100 taps to 30 g of each gum powder in a graduated cylinder at a standardized rate of 38 taps per minute (17). The Carr's index (CI) was obtained from the relationship:

[(Tapped density – Bulk density)/Tapped density] × 100 Eq. 6

All determinations were performed in quadruplicate.

Determination of angle of repose

The angle of repose was determined by measuring the radius "r" of the base and the height "h" of the conical heap formed by pouring 30 g each of the gum through a glass funnel held at 5 cm from the horizontal onto a flat base. The angle of repose (θ) was calculated as a mean of four determinations as:

$$\theta = \tan^{-1}(\frac{h}{r}) \qquad \text{Eq. 7}$$

Determination of flow rate

The flow rate (F_r) of the powdered gum was determined from the time "t" it took 30 g of the gum to pass through the orifice of an Erweka flow rate meter. The flow rate was calculated as a mean of four determinations as:

$$F_r = \frac{30\,g}{t} \qquad \text{Eq. 8}$$

Determination of compressional properties

The Heckel equation is widely used for relating the relative density, D, of a powder bed during compression to the applied pressure, P. It is written as:

$$\ln[(1/1 - D)] = k_P + A \qquad \text{Eq. 9}$$

The slope of the straight-line portion, K, is the reciprocal of the mean yield pressure, P_y, of the material. From the value of A, the intercept, the relative density, D_a, can be calculated using the following equation (18):

$$D_A = 1 - e^{-A} \qquad \text{Eq. 10}$$

The relative density of the powder at the point when the applied pressure equals zero, D_o, is used to describe the initial rearrangement phase of densification as a result of die filling. The relative density, D_b, describes the phase of rearrangement at low pressures and is the difference between D_A and D_O.

$$D_b = D_A - D_O \qquad \text{Eq. 11}$$

The Kawakita equation is used to study powder compression and the degree of volume reduction, C. It is written as:

$$C = \frac{(v_o - v_P)}{v_o} = abp/(1 + bp) \qquad \text{Eq. 12}$$

The equation in practice can be rearranged to give P/C = P/a + 1/ab, where V_o is the initial bulk volume for granular materials and V_p is the bulk volume after compression. The constant "a" is equal to the minimum porosity of the material before compression, while the constant "b" is related to the plasticity of the material. The expression $(1 - a)$ gives the initial relative density of the material, D_i which has been shown to provide a measure of the packed initial relative density of tablets with the application of small pressure or what may be referred to as tapping. The reciprocal of b gives a pressure term, P_k, which is the pressure required to reduce the powder bed by 50% (16, 19, 20).

Preparation of gum tablets

Tablets (500 mg) were prepared from the gum powder by compressing them using a 12.5 mm die and flat faced punches for 30 s with predetermined loads on a model C, hydraulic hand press (Carver Inc., Menomonee Falls, USA). Tablets with a hole (1.5 mm diameter) at their center were made using an upper punch with a hole and a lower punch with a pin (21). After ejection, the tablets were stored in a desiccator for 24 h to allow for elastic recovery and hardening in order to prevent false low yield values. The tablets weights and dimensions were determined to within ±1 mg and 0.01 mm, respectively, and their relative densities (*D*) were calculated using the equation:

$$D = m/V_t\rho_s \qquad \text{Eq. 13}$$

where m is the weight of the tablets (g), V_t is the volume of tablets and ρ_s is the particle density of the powders.

Determination of mechanical properties

The tensile strength of the normal tablets (T) and of apparent tensile strength (To) of those containing a hole, were determined at room temperature by

diametral compression (22) using a digital Erweka hardness tester and by applying equation Eq. 14:

$$T = 2F/\pi dt \qquad \text{Eq. 14}$$

where T (or To) is the tensile strength of the tablet (MNm^{-2}), F is the load (MN) needed to cause fracture, d is the tablet diameter (m), and t is tablet thickness (m). Results were taken from tablets, which split cleanly into two halves without any sign of lamination. All measurements were made in quadruplicate. The BFI of the tablets were calculated using Eq. 15:

$$BFI = 0.5 \, (T/T_o - 1) \qquad \text{Eq. 15}$$
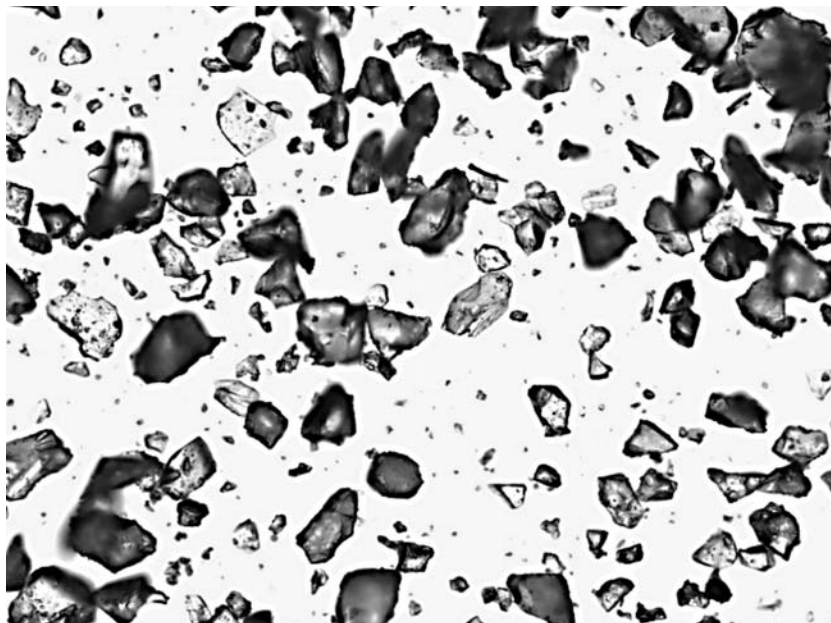
Figure 1. Photomicrograph of neem gum powder (100×)
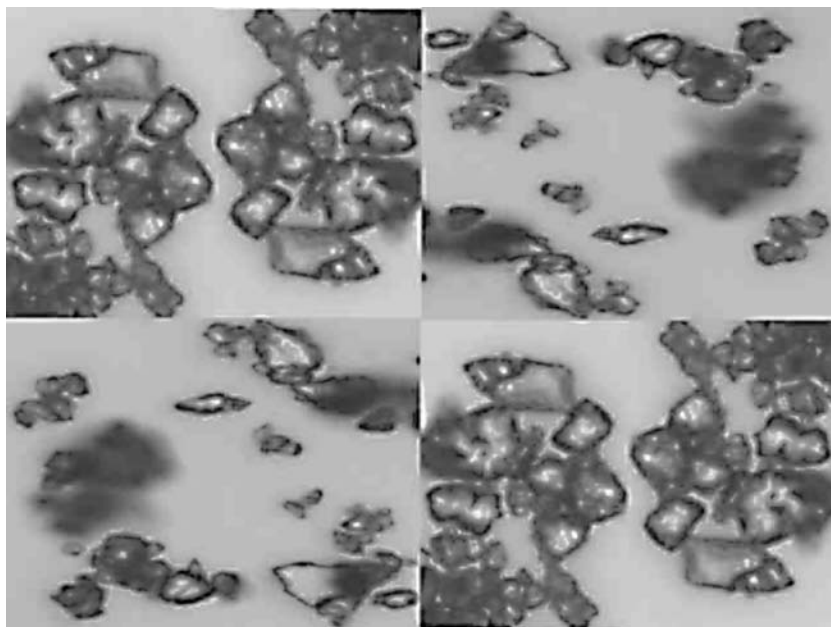
Figure 2. Photomicrograph of acacia gum powder (400×)
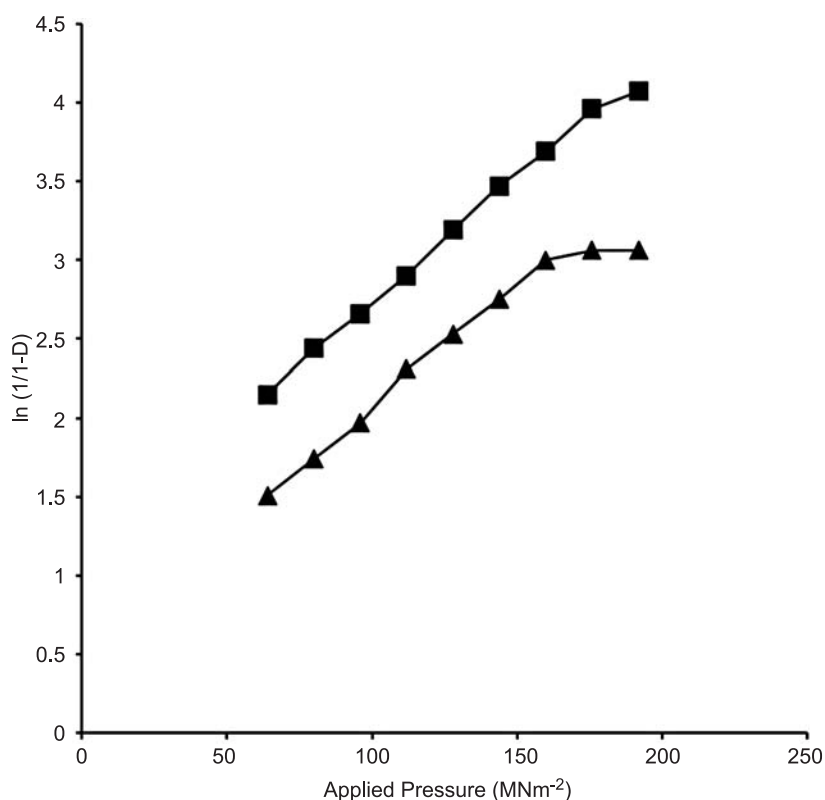
Figure 3. Heckel plots for tablets made from the gums. ■ NMG, ▲ ACA

Determination of tablet crushing strength and friability

A digital Erweka hardness tester was used at room temperature to determine the load required to diametrically break the tablet (crushing strength) into two equal halves. Tablets with signs of lamination and capping were not used. The friability of the tablets was determined using a Roche friabilator (Erweka Apparatebau, Germany) operated at 25 rev/min for 4 min. Ten tablets were used at each relative density. The mean of four determinations was taken for the crushing strength and friability values.

Disintegration test

The disintegration time (DT) of the gum tablet was determined in distilled water at $37 \pm 0.5^{\circ}C$ in a BP Manesty six station disintegration test unit (Manesty Machines Ltd., Liverpool, UK). Tablets were placed on the wire mesh just above the surface of the distilled water in the tube. The time taken for each tablet to disintegrate and all the granules to go through the wire mesh was recorded. Results were expressed as an average of three determinations.

RESULTS AND DISCUSSION

The acute toxicity results show that the LD_{50} of neem gum is higher than 5000 mg/kg, which suggests that neem gum exudate is safe as there were no deaths recorded at this dose (12).

The photomicrographs (Figs. 1 and 2) show the shape of NMG and ACA, respectively. Both gums are polygonal in shape; however, ACA exists as aggregates. The morphological and physical properties are as presented in Table 1. The result showed that the aspect ratio and roundness of NMG particles were lower than those of ACA, implying that NMG is more elongated than ACA, while the projected area of ACA is closer to a perfect circle. The result also showed that NMG had particle size (ECD) that is larger and more irregular than that of ACA. The flow and packing properties of powder blends have been shown to depend to a large extent on their particle shape and sizes (23, 24). The swelling index result showed that NMG swelled 1.04 times its weight while ACA was soluble in distilled water. The moisture content values of NMG and ACA suggest that their use in formulations containing moisture sensi-

Table 1. Morphological and physical properties of neem and acacia gums.

Properties	Neem gum	Acacia gum
Aspect ratio	0.57	0.62
Roundness	0.44	0.68
Irregularity	3.34	2.75
ECD (mm)	18.90	14.30
Swelling Index	1.040 ± 0.012*	Soluble
Moisture content	7.540 ± 0.214	5.810 ± 0.132
Moisture Sorption	14.500 ± 0.105	7.400 ± 0.201
Particle density	1.476 ± 0.012	1.479 ± 0.015
Bulk density	0.690 ± 0.010	0.708 ± 0.021
Porosity (%)	53.252	52.130
Hausner's Ratio	1.207	1.395
Carr's Index	17.167	28.340
Angle of Repose	22.692	34.994
Flow Rate	3.229 ± 0.020	2.890 ± 0.050

* Mean ± SD, n = 3

Table 2. Parameters obtained from Heckel and Kawakita plots for neem and acacia gum.

	Parameters	Neem gum	Acacia gum
Heckel analysis	P_y (MNm^{-2})	62.112	68.027
	D_o	0.310	0.401
	D_A	0.451	0.678
	D_B	0.141	0.277
Kawakita analysis	D_i	0.348	0.435
	P_k (MNm^{-2})	11.236	14.231

tive active ingredients should be done with caution. However, the result also showed that the moisture content of NMG is higher than that of ACA, which might have resulted from the appreciable amount of polysaccharide and proteins present in neem gum unlike in acacia gum. It could also be due to the tight link between the polysaccharides and the protein (11).

The values of particle and bulk densities obtained for ACA were higher than those of NMG. This could be due to the regularity of ACA, which form fewer arches and bridges than NMG, hence an increase in packing per unit space suggesting that the particle shape has an influence on the density properties of the powders. The result also showed that the porosity of NMG was higher than that of ACA. This could also be due to the regularity of ACA. It has been observed that because of particle geometry, mechanical forces may exist in particles, which tends to influence their packing (25).

Hausner's ratio provides an indication of degree of densification of powders/granules that could result from vibration of the feed hopper e.g., during tableting, with values of above 1.2 indicating considerable amount of densification, while Carr's compressibility index (26) is a direct measure of the potential powder/granule arch or bridge strength and stability; a less than 20% standard value suggests free-flowing powder/granules. The HR, CI and angle of repose (a characteristic of internal friction or cohesion of particles) values of NMG were lower than those of ACA suggesting that NMG possesses a higher flow that could be useful in direct compression. These results could be due to the particle size of NMG, which was higher than that of ACA. A decrease in powder particle size has been shown to cause an increase in the surface area per unit mass thus leading to an increase in the cohesive strength of the powder bed thereby reducing flowability [27].
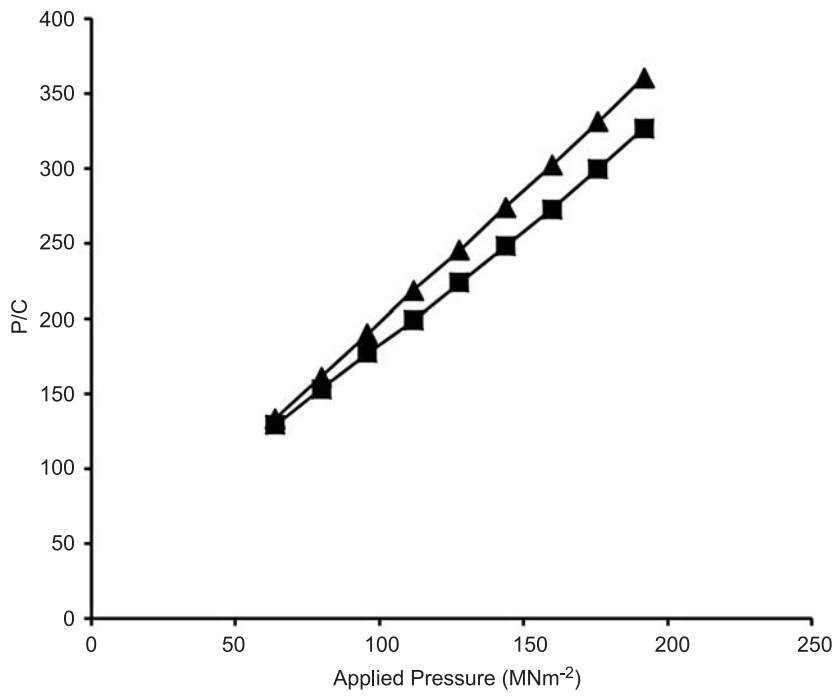
Figure 4. Kawakita plots for tablets made from the gums. ■ NMG, ▲ ACA
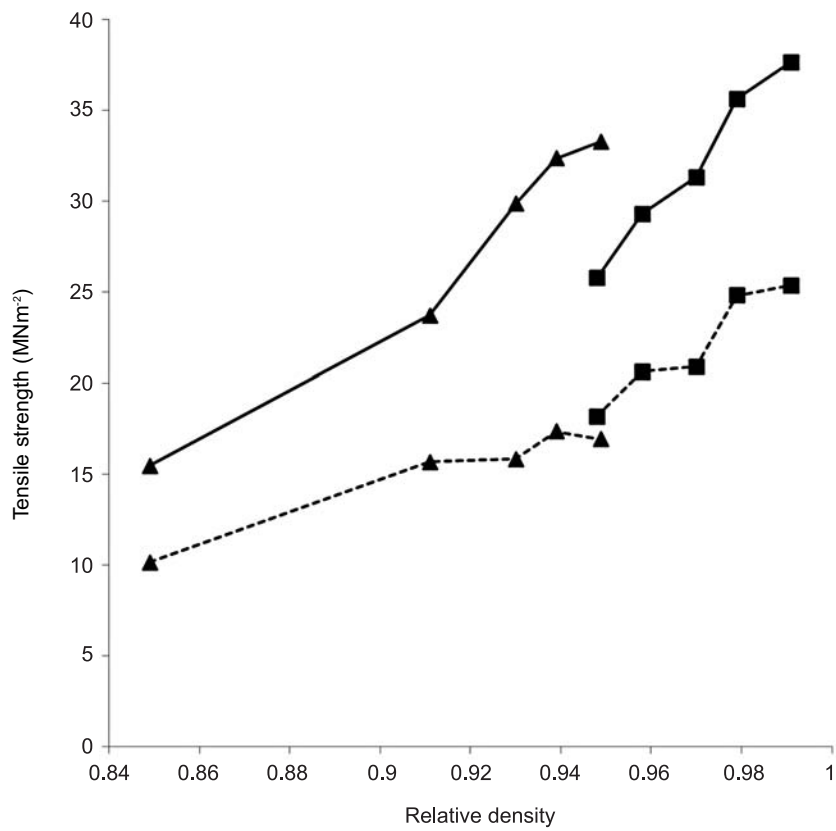
Figure 5. Plot of tensile strength *versus* relative density for gum tablets. ■ NMG, ▲ ACA. (———) Tablets without holes and (– – – –) tablets with holes
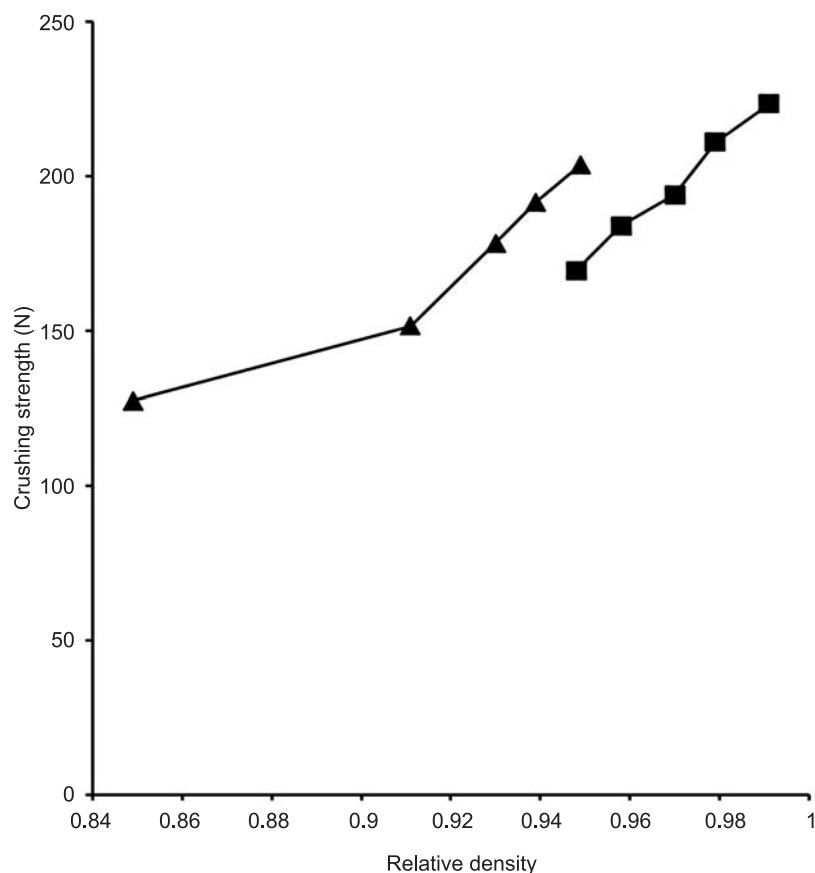
Figure 6. Plot of crushing strength *versus* relative density for gum tablets. ■ NMG, ▲ ACA

Table 3. Values of tensile strength (T or T_o), brittle fracture index (BFI), crushing strength (CS), disintegration time (DT), friability (FR) and crushing strength-fraiblity/disintegration time ratio (CSFR/DT) of gum tablets at relative density of 0.90.

Properties	Neem gum	Acacia gum
T (MN/m^{-2})	13.85 (0.12)*	25.95 (0.18)
T_o (MN/m^{-2})	8.943 (0.08)	14.631 (0.20)
BFI	0.270 (0.01)	0.390 (0.02)
CS (N)	105.001 (2.64)	165.540 (4.26)
FR (%)	1.020 (0.03)	1.303 (0.02)
DT (min)	15.603 (0.35)	32.195 (0.42)
CSFR/DT	6.598	3.946

* Mean ± SD, n = 3

The flow rate result also suggests that NMG has a higher flow than ACA. This result could be due to the same reason given above.

Figure 3 shows the Heckel plot for neem and acacia gums. Values of mean yield pressure, P_y, were calculated from region of the plots showing the highest correlation coefficient of linearity. The intercept, A, was determined from the extrapolation of the region for calculating P_y, while the values of D_A and D_B were calculated from Eq. 2 and 3, respectively. The values of P_y, D_o, D_A and D_B are shown in Table 2.
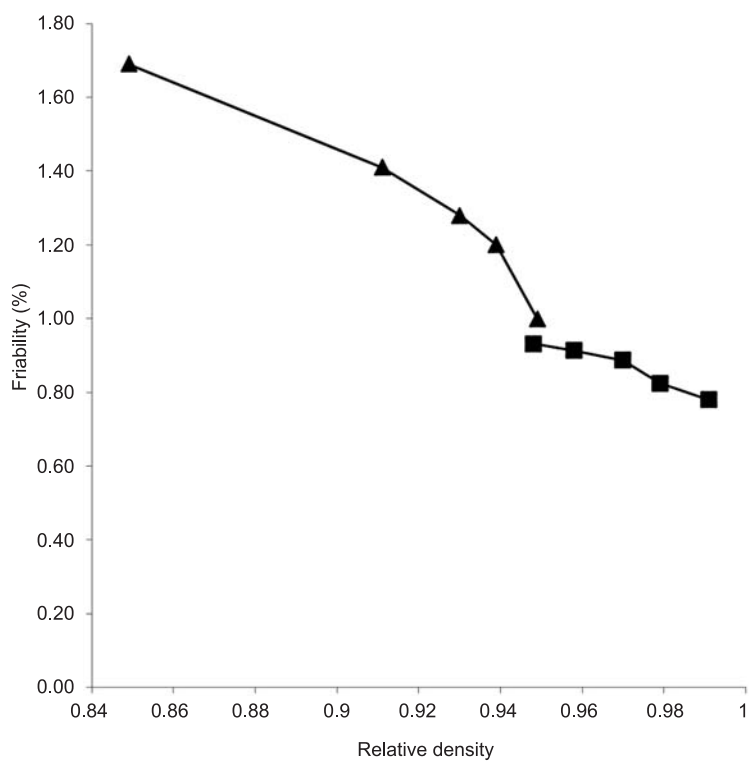
Figure 7. Plot of friability *versus* relative density for gum tablets. ■ NMG, ▲ ACA
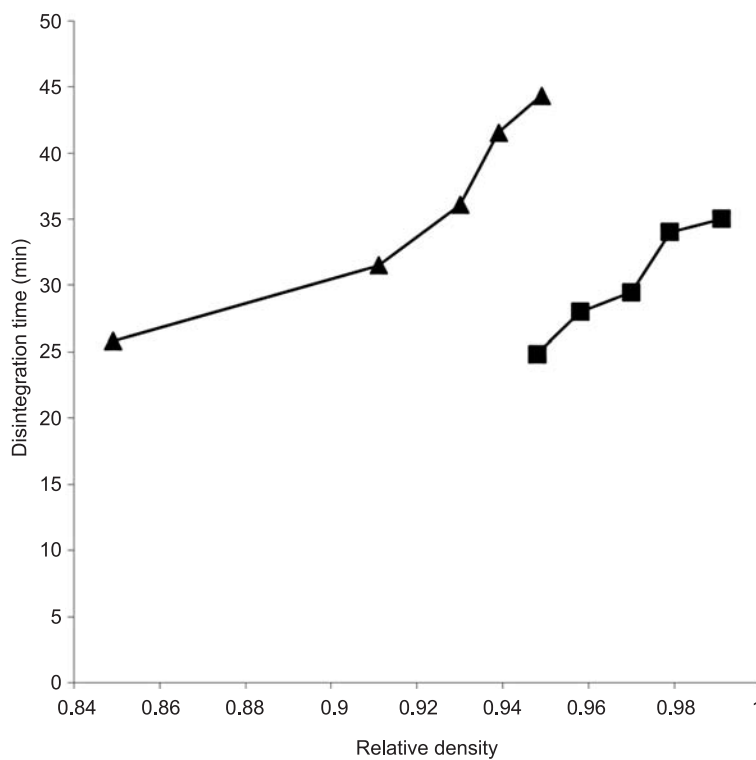
Figure 8. Plot of disintegration time *versus* relative density for gum tablets. ■ NMG, ▲ ACA

The result shows that the D_o value of ACA was higher than that of NMG. This suggests more initial packing of ACA in the die as a result of die filling than NMG. This result could be due to the regularity and smaller particle size of ACA when compared to NMG. D_B represents the phase of rearrangement of particles at low pressure. The result shows that the D_B value of NMG was lower than that of ACA. This suggests more fragmentation of ACA particles at low pressures than NMG. The D_A value of ACA, which represent the total degree of packing at zero and low pressures, was higher than that of NMG.

The mean yield pressure, P_y, is inversely related to the ability of the material to deform plastically under pressure. The value of P_y for ACA was higher than that of NMG. This implies that the onset of plastic deformation in ACA occurred at a higher pressure.

The Kawakita plots of neem and acacia plots are shown in Figure 4. A linear relationship was obtained at all compression pressures used with a correlation coefficient of 0.999 for the gums, thus, the Kawakita equation was used to predict the densification mechanism of the two gums. Values of a and ab were obtained from the slope and intercept of the plots, respectively.

The D_i value of ACA was higher than that of NMG. The D_i values are also seen to be higher than the values of D_o. Bearing in mind that the methods of determination of D_o and D_i have their limitations, (28), the differences in the values of D_o and D_i are probably due to the fact that while D_o describes the loose initial relative density of the batches due to die filling, D_i provides a measure of the packed initial relative density of the batches with the application of small pressure or what may be referred to as tapping of the granules (20).

The P_k is an inverse measure of the amount of plastic deformation occurring during compression, with low values depicting materials that are soft and readily deform under pressure. Table 2 shows that NMG exhibited the highest amount of plastic deformation when compared to ACA. Odeku and Itiola (29) have shown that P_y is different from P_k in that while the P_y value relates essentially to the onset of plastic deformation during compression, the P_k value appears to relate to the total amount of plastic deformation occurring during the compression process. Thus, the present result showed that NMG had a faster onset of plastic flow and a higher of amount of plastic deformation when compared to ACA.
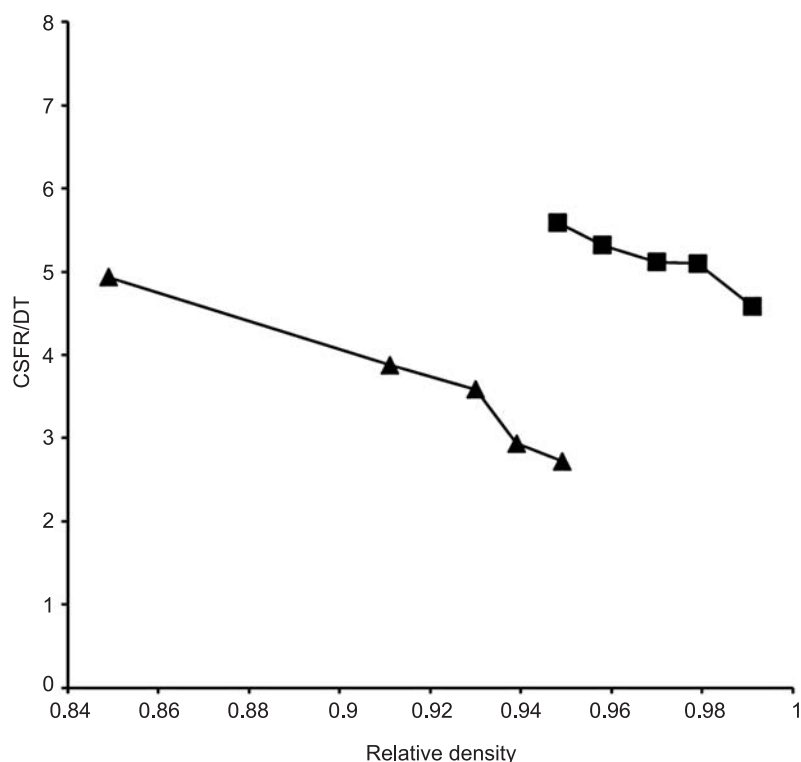

Figure 9. Plot of CSFR/DT *versus* relative density for gum tablets. ■ NMG, ▲ ACA

The result of tensile strength test on the gum tablets generally fits the equation:

$$T \ or \ T_o = AD + B \ .... \quad (Eq. \ 15)$$

with correlation coefficient of > 0.927. A and B are constants, which depend on the nature of the gum and on whether the tablet had a hole in it or not. Plots of tensile strength *versus* relative density of NMG and ACA are presented in Figure 5. It can be seen that at all relative densities the tensile strength (T) of a tablet with a hole was lower than that of the same without a hole, the hole acting as a stress concentrator (21, 30).

The value of T and BFI of the gum tablet at a relative density of 0.90 are presented in Table 3. The result shows that ACA has a higher T and BFI when compared to NMG. This suggests that ACA produced stronger gum tablets; however, the tendency of ACA tablets to cap or laminate is also higher when compared to NMG.

Although low P_k values of powders have been shown to be responsible for high T values, as higher total plastic deformation would lead to more contact points for interparticulate bonding (31), the result showed that ACA which had a slightly higher P_k value (Table 2) than NMG had a higher T. This result could be due to the brittleness (BFI) (Table 3) of ACA, which caused more breakages in the material on application of pressure, and this would lead to creation of more contact points for bonding, thus making the ACA tablets to have a higher T.

Crushing strength provides a measure of strength while friability measures the weakness of a tablet (3). Plots of crushing strength *versus* relative density of NMG and ACA gum tablets are shown in Figure 6. It is observed from the figure that as the relative density increased, the crushing strength of the tablets also increased. This could be due to the decrease in porosity and subsequent increase in the number of contact points, hence, an increase in the degree of bonding between the particles (21). It can also be seen from the result (Table 3) that the crushing strength of ACA tablets was higher than that of NMG tablets. This could be due to the brittleness of ACA gum, which caused more breakages and consequent creation of more particle-particle contact points, hence leading to higher crushing strength values.

Figure 7 shows the plot of friability *versus* relative density for gum tablets of NMG and ACA. It is observed that friability decreased with an increase in relative density for both gum tablets. At a relative density of 0.90 (Table 3), the friability of ACA tablet was higher than that of NMG. This result could be due to the brittleness of ACA gum, which caused more breakage and chipping off in the friabilator drum.

The disintegration time of the gum tablets obtained generally increased with an increase in relative density of the tablets as shown in the plots of disintegration time against relative density for gum tablets of NMG and ACA (Fig. 8). With an increase in relative density, there is usually an accompanying decrease in porosity (32), which consequently slows down water penetration into tablets. Also, when porosity decreases, more solid bridges are formed, making destruction of interparticulate forces difficult (33, 34). The result also showed that at a relative density of 0.90 (Table 3), the disintegration time of ACA tablets was significantly higher than that of NMG tablets. This could be due partly to the brittleness of ACA gum, which caused more breakages and consequent creation of more particle-particle contact points thereby reducing the rate of liquid penetration into the micropores of ACA gum tablets.

The crushing strength friability/disintegration time ratio (CSFR/DT) has been suggested as a better index for measuring tablet strength (crushing) and weakness (friability), it simultaneously evaluates all negative effects of these parameters on disintegration time (35). A higher value of CSFR/DT ratio indicates a better balance between binding and disintegration properties. The values of CSFR/DT for NMG and ACA gum tablet at a relative density of 0.90 are as shown in Table 3. Higher values of CSFR/DT obtained for NMG gum tablet suggests that NMG gum tablets will produce a better balance between the mechanical and disintegration properties of tablets when used in directly compressible formulations. This could be due to the high CS of ACA tablets which ultimately led to longer DT of the tablets.

CONCLUSION

The results obtained from the present work showed that:
- the morphology of a gum powder material influences its tableting properties;
- the NMG powder would lead to the production of tablets with lower TS and lower tendency to cap or laminate when used in a directly compressible formulation relative to ACA gum powder;
- the NMG powder is more likely to produce tablets with a better balance between mechanical and disintegration properties than that of ACA powder as reflected in the CSFR/DT values when used in direct compression.

REFERENCES

1. Joneja S.K., Harcum W.W., Skinner G., Barnum P.E., Guo J.H.: Drug Dev. Ind. Pharm. 25, 1129 (1999).
2. Ogunjimi A.T., Alebiowu G.: Braz. J. Pharm. Sci. 46, 205 (2010).
3. Adetogun E.A., Alebiowu G.: Acta Pol. Pharm. Drug Res. 66, 433 (2009).
4. Aspinal G.O.: Advances in carbohydrate chemistry and biochemistry. Wolfrom M.L., and Tipson R.S. Eds., Vol. 24, p. 333, Academic Press, New York 1969.
5. van der Nata J.M., van der Siuisa W.G., de Silvab K.T.D., Labadie R.P.: J. Ethnopharmacol. 35, 1 (1991).
6. Islam A.M., Phillips G.O., Sljivo A., Snowden M.J., Williams P.A.: Food Hydrocolloid., 11, 493 (1997).
7. Montenegro M.A., Boiero M.L., Valle L., Borsarelli C.D.: Gum Arabic: more than an edible emulsifier. In Products and Applications of Biopolymers, pp. 3-24, Johan Verbeek Ed., Intech, Rijeka 2012.
8. Ushalakshmi S., Pattabiraman, T.N.: Indian J. Biochem., 4, 181 (1967).
9. Kulkarni G.T., Gowthamarajan K., Suresh B.: Indian Drugs 39, 422 (2002)
10. Odeku O.A., Itiola O.A.: Drug Dev. Ind. Pharm. 28, 329 (2002).
11. Panda D.S., Choudhury N.S.L., Yedukondalu M., Si S., Gupta R.: Indian J. Pharm. Sci. 70, 614 (2008).
12. Lorke D.: Arch. Toxicol. 54, 275(1983).
13. Bodhmage A.: M.Sc. Thesis, Saskatchewan University, Canada (2006) (unpublished).
14. Bowen F.E., Vadino W.A.: Drug Dev. Ind. Pharm. 10, 505 (1984).
15. Nyqvist H.: Int. J. Pharm. Technol. Prod. Manuf. 4, 47 (1983).
16. Alebiowu G., Osinoiki K.A.: Farmacia 58, 341 (2010).
17. British Standard 1460. British Standard Institution, London 1970.
18. Humbert-Droz P., Gurny R., Mordier D., Doelker E.: Int. J. Pharm. Tech, Prod. Manuf. 4, 29 (1983).
19. Lin C., Cham T.: Int. J. Pharm. 118, 169 (1995).
20. Podczeck F., Sharma M.: Int. J. Pharm. 137, 41 (1996).
21. Alebiowu G., Itiola O.A.: Drug Dev. Ind. Pharm. 28, 663 (2002).
22. Fell J.T., Newton J.M.: J. Pharm. Sci. 59, 688 (1970).
23. Johansson B., Nicklasson F., Alderborn G.: Int. J. Pharm. 163, 35 (1998).
24. Itiola O.A., Odeku O.A.: Trop. J. Pharm. Res. 4, 363 (2005).
25. Harwood C.F., Pilpel N.: J. Pharm. Sci. 57, 478 (1968).
26. Carr R.L.: Chem. Eng. 72, 163 (1965).
27. Sameh A., Firas A., Gabrielle B.: Int. J. Pharm. 413, 29 (2011).
28. Celik M.: Drug Dev. Ind. Pharm. 18, 767 (1992).
29. Odeku O.A, Itiola O.A.: Pharm. Pharmacol. Commun. 4, 183 (1998).
30. Hiestand E.N., Wells J.F., Poet C.B., Ochs J.F.: J. Pharm. Sci. 66, 510 (1977).
31. Itiola O.A., Pilpel N.: J. Pharm. Pharmacol. 43, 145 (1991).
32. Zhang Y., Law Y., Chakrabarti S.: AAPS PharmSciTech. 4, article 62 (2003).
33. Bi Y., Yonezawa Y., Sunada H.: J. Pharm Sci. 88, 1004 (1999).
34. Gohil U.C., Podzeck F., Turnbull N.: Int. J. Pharm. 285, 51 (2004).
35. Upadrashta S.M., Katikaneni P.R., Nuessla N.O.: Drug Dev. Ind. Pharm. 18, 1701 (1992).

SURFACE ACTIVITY OF NOVEL SURFACE ACTIVE COMPOUNDS, PRODUCTS OF CATALYTIC OXYETHYLATION OF CHOLIC ACID AND THEIR MICELLAR ADDUCTS WITH SELECTED LIPOPHILIC THERAPEUTIC AGENTS

MICHAŁ KRZYSZTOF KOŁODZIEJCZYK[1*], MICHAŁ JAKUB NACHAJSKI[1], MAREK LUKOSEK[2] and MARIAN MIKOŁAJ ZGODA[1]

[1]Chair of Applied Pharmacy, Medical University of Lodz, Muszyńskiego 1, 90-151 Łódź, Poland
[2]Surface-Active Agent Plant "ICSO Blachownia", Energetyków 9, 47-225 Kędzierzyn Koźle, Poland

Abstract: The aim of this study was to determine the surface activity parameters of novel surface active compounds, products of catalytic oxyethylation of cholic acid, and their micellar adducts with selected lipophilic therapeutic agents (diclofenac, loratadine, naproxen and rutin). High solubility of lipophilic naproxen was observed in the environment of aqueous solutions of the cholic acid oxyethylation products as suggested by determined factual solubility and the value of micellar partition coefficient (K_w^m). Determined surface activity of surfactants described by various physicochemical characteristics (γ_{cmc}^{25}, cmc, ΔG_m^o and A_m) suggested their compatibility with physiological values of the surface activity of plasma (48.0-52.0 mJ/m²) and lacrimal fluid (46.0-52.0 mJ/m²). Calculated values of HLB^1_{HNMR} and n_{TE} of the micellar adduct in solid phase (solid dispersion) corresponded to an increase in its hydrophilicity, and, therefore, suggested possible mechanisms and site of diclofenac, loratadine, naproxen and rutin solubilization in the micellar structure (core or palisadic layer).

Keywords: solubilization, surface activity, diclofenac, loratadine, naproxen, rutin, ethoxylation products of cholic acid

Products of the catalytic oxyethylation of cholic acid in molecular fragmentation state, a new group of novel surface-active compounds, are characterized by marked physicochemical compatibility with bile "A" (duodenal content). Additionally, these compounds are not recognized as xenobiotics by the human immune system (1-7).

As was confirmed previously *in vitro*, the marked solubilizing properties of the lipophilic therapeutic agents exhibited by the cholic acid oxyethylates have substantiated further preformulation research on the possible implementation of these derivatives as formulations in the solid oral drug forms. Following the disintegration, further dissolving and effective transport of such formulation could occur independently from the physiological value of the lithogenolithic index of bile "A" (duodenal content) (8-13).

Previous viscosity (η) analyses and determination of the surface activity (γ) of bile "A" in healthy subjects and patients with various biliary tract disorders (4) constituted a base for further studies of the surface activity of the aqueous solutions of the cholic acid oxyethylates with n_{TE} = 20-70, (n_{TE} = number of oxyethylene segments) and their micellar adducts with lipophilic therapeutic agents (BCS class II and IV) (14).

Determination of selected parameters: critical micelle concentration - cmc, thermodynamic potential of micelle formation - ΔG_m^o, the size of the lipophilic core uplift above the phase boundaries - A_m, surface tension at the critical area - γ_{cmc}^{25}, characterizing surface activity of the novel class of nonionic surfactants and their adducts with the lipophilic therapeutic agents enabled the assessment of their potential application in solid oral drug formulations and injections (15, 16).

The aim of this study was to determine the surface activity parameters of novel surface active compounds, products of the catalytic oxyethylation of cholic acid, and their micellar adducts with selected lipophilic therapeutic agents. The results of this

---

* Corresponding author: e-mail: michal.kolodziejczyk@umed.lodz.pl

study may constitute a base for further original and novel research on formulating solid oral forms of drugs (non-coated tablets, prolonged release tablets, matrix tablets with variable core viscosity) or parenteral formulations (injections, intravenous infusions). These formulations should be characterized by established, stable pharmaceutical and biological availability independent of pathological changes in the solubilizing properties of bile "A" (duodenal content).

EXPERIMENTAL

Materials

Diclofenac; 2-{2-[(2,6-dichlorophenyl)amino]phenyl}acetic acid, pure for analysis (Sigma, Germany); rutin (rutoside), pure for analysis (Sichuan Xieli Pharmaceutical Co. Ltd., China); loratadine, pure for analysis (Zydus Cadila – Cadila Healtcare Ltd., India); naproxen, pure for analysis, serial no. 381936 (Medana, Poland); products of the
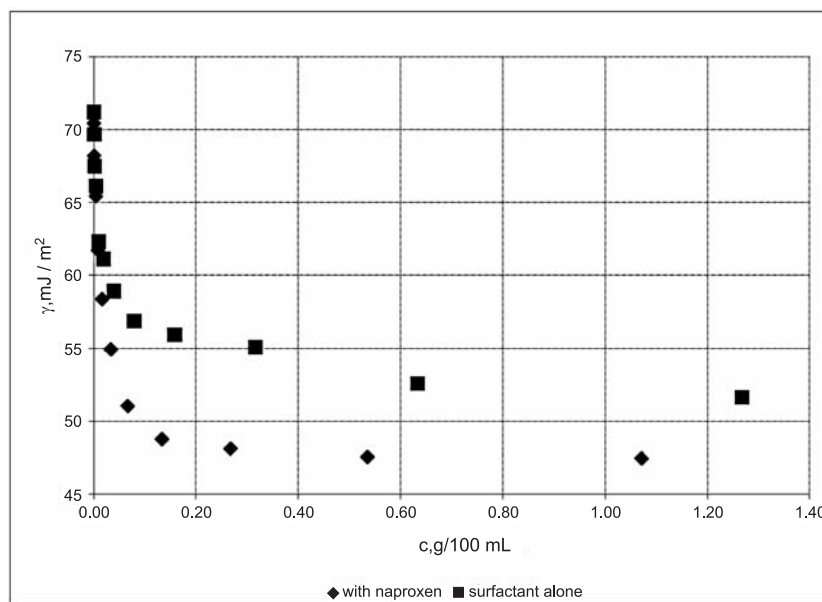

Figure 1. Relationship between the surface activity (g, mJ/m²) and the concentration of surfactant (c, g/100 mL; oxyethylated cholic acid $n_{TE} = 50$)
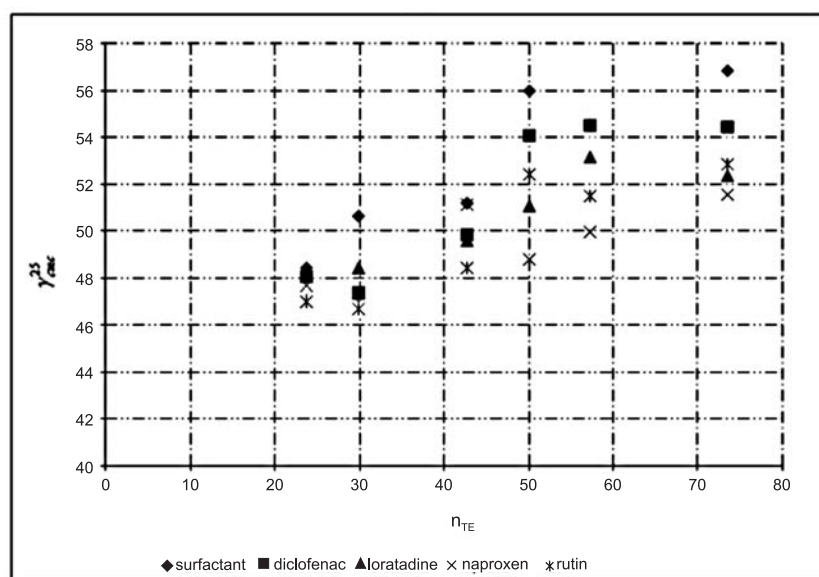
Figure 2. Relationship between surface activity in "critical area" (γ_{cmc}^{25}) and the number of oxyethylated segments (n_{TE}) in surfactant

Table 1. Basic viscosity and hydrodynamic characteristics of the aqueous solutions of cholic acid oxyethylation products solubilizing naproxen[1,2].

Cholic acid oxyethylation roduct Mη	C_{exp} [g × 100 cm⁻³]	GLL [η]	$M_{η\,adduct}$	$R_o × 10^{-7}$ [cm]	$R_{obs} × 10^{-8}$ [cm]	$Ω × 10^{-20}$ [cm]	$c/n_J/*$ [mg × dm⁻³]	K_w^{m*}
1. Cholic acid n_{TE} = 20 Mη = 1981.7	1.0220	0.0835679	1826.6	3.5427	1.5011	1.0137	534.42	32.61
2. Cholic acid n_{TE} = 30 Mη = 1877.5	1.0274	0.0854125	1879.5	3.6026	2.9414	1.0661	556.99	34.03
3. Cholic acid n_{TE} = 40 Mη = 2108.5	1.0119	0.0928375	2157.6	3.8785	3.1667	1.3302	528.78	32.25
4. Cholic acid n_{TE} = 50 Mη = 2730.7	1.0711	0.1115816	2925.6	4.5642	3.7266	2.1679	675.51	41.48
5. Cholic acid n_{TE} = 60 Mη = 2662.15	1.0075	0.1126817	2973.5	4.6041	3.7591	2.2251	782.73	48.22
6. Cholic acid n_{TE} = 70 Mη = 3011.1	1.0103	0.1280905	3676.4	5.1572	4.2107	3.1274	816.59	50.35

[1] theoretical solubility in water $c_{t(o)}$ = 51.0 mg/dm³; [2] determined solubility in water $c_{/n/}$ = 15.9 mg/dm³; * – calculated in relation to the determined solubility $\sim c_{/n/}$

catalytic oxyethylation of cholic acid in molecular fragmentation state with declared molar content of ethylene oxide, n_{TE} = 20-70.

Structural characteristics of the novel class of surfactants were described in our previous publication (12).

Determination of oxyethylated segment content (n_{TE}) and hydrophilic-lipophilic balance $HLB_{'HNMR}$ of dry adduct (solid dispersion) after micellar solubilization in equilibrium

The ¹HNMR spectra of the adduct of lipophilic therapeutic agents after micellar solubilization in equilibrium in solid phase (solid dispersion) were obtained as described previously (1, 3, 5, 8).

They were used to calculate the hydrophilic-lipophilic balance on the basis of the following equation:

$$HLB_{'HNMR} = \frac{15 \cdot A_h}{0.05\,(15 \cdot A_h + 10 \cdot A_l)} \quad (1)$$

Where A_h = number of hydrophilic protons, A_l = number of lipophilic protons

Determination of the overall number of lipophilic protons $\Sigma\,^1H$ = 36 in the structure of the molecule of cholic acid made it possible to calculate the content of oxyethylated segments in dry micellar adduct after solubilization in equilibrium, on the basis of the following equation:

$$n_{TE} = \frac{(36 \cdot \frac{A_h}{A_l} - 3)}{4} \quad (2)$$

Surface activity and viscosity of aqueous solutions of the products of cholic acid oxyethylation and their adducts resulting from micellar solubilization in equilibrium

The surface activity of aqueous solutions of the products of cholic acid oxyethylation and their micellar adducts with the lipophilic therapeutic agents was determined with the stalagmometric method in accordance with the Polish Standard (17).

Determined value of critical micellar concentration (cmc) enabled the calculation of the thermodynamic potential of micelle formation (ΔG_m^o) based on the following equation:

$$\Delta G_m^o = 2.303 \cdot RT \log cmc \quad (3)$$

where: ΔG_m^o = the thermodynamic potential of micelle formation, R = gas constant (8.314J/mol·K), T = temperature.

The numerical value of the decrease in the surface activity coefficient in critical area (γ_{cmc}^{25}) enabled the calculation of the "average area per

surfactant molecule" on phase boundary (minimal value of A_m per 1 molecule corresponds to approximately 20×10^{-16} cm^2) on the basis of the equation:

$$f(\pi) \cdot A_m = k \cdot T, \qquad (4)$$

where: $f(\pi) = \gamma_{H_2O}^{25} - \gamma_{cmc}^{25}$ (5), A_m = the size of the lipophilic core uplift above the phase boundaries, $\gamma_{H_2O}^{25}$ = the surface tension of water, γ_{cmc}^{25} = the surface tension at the critical area, k = constant, T = temper-

ature which was further transformed into the following application version:

$$A_m = \frac{k \cdot T}{\gamma_{H_2O}^{25} - \gamma_{cmc}^{25}}. \qquad (6)$$

This aforementioned relationship results from the mathematical transformation of Gibbs formula:

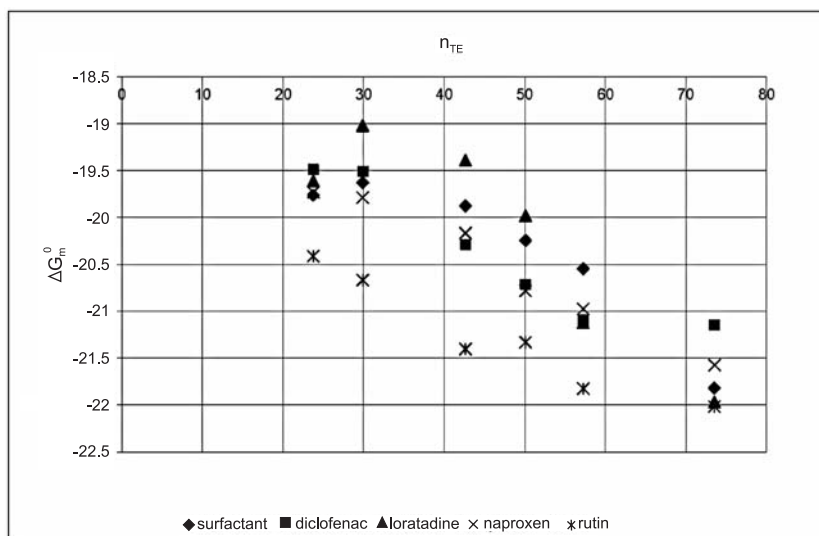$$T = \frac{c}{RT} \cdot \frac{\pi}{c}, \qquad (7)$$

Figure 3. Relationship between the thermodynamic potential of micelle formation (ΔG_m^o) and the number of oxyethylated segments (n_{TE}) in surfactant
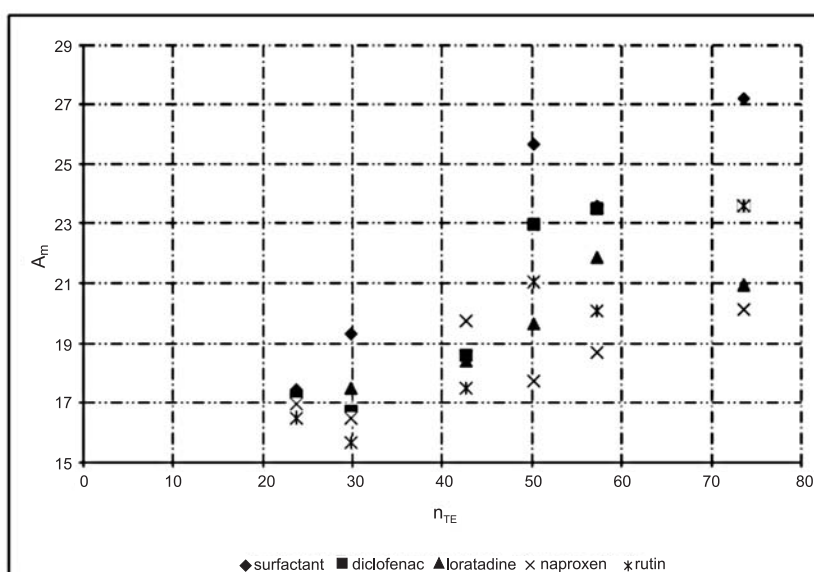

Figure 4. Relationship between the surface of lipophilic core upthrust over the phase boundary (A_m) and the number of oxyethylated segments (n_{TE}) in surfactant

Table 2. Basic surface activity characteristics of novel surface active compounds, products of catalytic oxyethylation of cholic acid and their micellar adducts with selected lipophilic therapeutic agents.

Surfactants	γ^{25}_{cmc} [mJ × m^{-2}]	cmc [g × 100 cm^{-3}]	cmc × 10^{-4} [mol × dm^{-3}]	ΔG^{o}_{m} [kJ × mol^{-1}]	A_m × 10^{-20} [m^2]
1. Cholic acid n_{TE} = 20	48.41	5.0243 × 10^{-2}	3.4514	-19.7647	17.4646
2. Cholic acid n_{TE} = 30	50.65	6.2741 × 10^{-2}	3.6374	-19.6345	19.2985
3. Cholic acid n_{TE} = 40	51.16	7.5306 × 10^{-2}	3.2915	-19.8823	19.7714
4. Cholic acid n_{TE} = 50	55.94	7.4248 × 10^{-2}	2.8381	-20.2497	25.6634
5. Cholic acid n_{TE} = 60	54.52	7.3762 × 10^{-2}	2.5158	-20.5486	23.5897
6. Cholic acid n_{TE} = 70	56.85	5.4959 × 10^{-2}	1.5059	-21.8211	27.2069
Diclofenac					
1. Cholic acid n_{TE} = 20	48.05	7.0487 × 10^{-2}	3.8519	-19.4925	17.2018
2. Cholic acid n_{TE} = 30	47.35	7.3248 × 10^{-2}	3.8199	-19.5131	16.7129
3. Cholic acid n_{TE} = 40	49.86	7.4628 × 10^{-2}	2.7845	-20.2899	18.6094
4. Cholic acid n_{TE} = 50	54.07	7.5247 × 10^{-2}	2.3528	-20.7147	22.9838
5. Cholic acid n_{TE} = 60	54.47	7.6124 × 10^{-2}	2.0166	-21.0969	23.5089
6. Cholic acid n_{TE} = 70	54.53	8.9918 × 10^{-2}	1.9766	-21.1467	23.5897
Loratadine					
1. Cholic acid n_{TE} = 20	47.07	7.0487 × 10^{-2}	3.6696	-19.6127	16.5251
2. Cholic acid n_{TE} = 30	48.42	7.5006 × 10^{-2}	4.6528	-19.0241	17.4720
3. Cholic acid n_{TE} = 40	49.60	7.5663·× 10^{-2}	4.0067	-19.3948	18.3850
4. Cholic acid n_{TE} = 50	51.05	7.9244 × 10^{-2}	3.1596	-19.9836	19.6675
5. Cholic acid n_{TE} = 60	53.14	7.2758 × 10^{-2}	1.9934	-21.1257	21.8493
6. Cholic acid n_{TE} = 70	52.33	6.0724 × 10^{-2}	1.4185	-21.9692	20.9486
Naproxen					
1. Cholic acid n_{TE} = 20	47.69	6.3875 × 10^{-2}	3.4969	-19.7322	16.9469
2. Cholic acid n_{TE} = 30	47.01	6.4215 × 10^{-2}	3.4166	-19.7898	16.4854
3. Cholic acid n_{TE} = 40	51.13	6.3243 × 10^{-2}	2.9311	-20.1698	19.7429
4. Cholic acid n_{TE} = 50	48.77	6.6943 × 10^{-2}	2.2881	-20.7838	17.7355
5. Cholic acid n_{TE} = 60	49.95	6.2968 × 10^{-2}	2.1176	-20.9758	18.6854
6. Cholic acid n_{TE} = 70	51.54	6.1144 × 10^{-2}	1.6631	-21.5748	20.1389
Rutin					
1. Cholic acid n_{TE} = 20	47.01	10.5487 × 10^{-2}	2.6668	-20.4149	16.4854
2. Cholic acid n_{TE} = 30	46.67	7.5062 × 10^{-2}	2.3962	-20.6694	15.6458
3. Cholic acid n_{TE} = 40	48.42	7.0486 × 10^{-2}	1.7821	-21.4035	17.4720
4. Cholic acid n_{TE} = 50	52.41	7.1248 × 10^{-2}	1.8345	-21.3331	21.0342
5. Cholic acid n_{TE} = 60	51.48	7.2758 × 10^{-2}	1.5019	-21.8277	20.0801
6. Cholic acid n_{TE} = 70	52.85	6.7438 × 10^{-2}	1.3921	-22.0174	23.5897

where: c = the molar concentration of the solute, T = surface concentration
and Szyszkowski formula:

$$\pi = \gamma_o - \gamma = a \cdot (1 + b \cdot c), \qquad (8)$$

with the resulting following equation:

$$\pi \cdot A_m = R \cdot T. \qquad (9)$$

This aforementioned equation is the "surface equation of state". After the bilateral dividing by the Avogadro constant, it can be transformed into the following equation:

$$f = (\pi) \cdot A_m = k \cdot T. \qquad (10)$$

The estimated and calculated values are summarized in Table 2.

The limiting viscosity number (LVN, η) of aqueous solutions after micellar solubilization of naproxen by the cholic acid oxyethylation products was estimated on the basis of the Polish Standard by means of the Ubbelohde viscosimeter (18). The estimated LVN was used to calculate several viscosity parameters: viscosity average molar masses - M_η, the end of mean square distance between chain terminals - R_o, hydrodynamic value of micelle radius - R_{obs}, and effective volume - Ω. The results are summarized in Table 1.

RESULTS AND DISCUSSION

Micellar solubilization of lipophilic therapeutic agent in equilibrium in the environment of aqueous solutions of cholic acid oxyethylation

The formerly described spectroscopic method (11-13) was employed to determine the amount of

Table 3. Content of oxyethylated segments (n_{TE}) and the value of hydrophilic-lipophilic balance (HLB_{HNMR}) of micellar adduct in solid dispersion determined by means of ^1H NMR.

Surfactant	Determined n_{TE}	HLB^1_{HNMR}	Micellar adduct of cholic acid n_{TE} = 20-70							
			Diclofenac		Loratadine		Naproxen		Rutin	
			HLB^1_{HNMR}	$n_{TE(X)}$	HLB^1_{HNMR}	$n_{TE(X)}$	HLB^1_{HNMR}	$n_{TE(X)}$	HLB_{HNMR}	$n_{TE(X)}$
1. Cholic acid n_{TE} = 20	23.77	12.85	15.57	20.37	15.85	22.21	16.66	19.22	14.63	15.59
2. Cholic acid n_{TE} = 30	29.88	13.14	16.54	28.01	16.85	31.39	16.74	30.09	16.22	25.05
3. Cholic acid n_{TE} = 40	42.66	15.01	17.38	39.11	17.58	42.98	17.44	40.77	17.30	37.82
4. Cholic acid n_{TE} = 50	50.11	16.59	17.95	51.85	17.64	51.99	17.64	51.01	17.74	46.54
5. Cholic acid n_{TE} = 60	57.28	17.79	18.12	57.22	18.09	56.28	18.11	56.61	18.19	59.86
6. Cholic acid n_{TE} = 70	73.57	19.22	18.37	67.09	18.42	69.81	18.33	65.29	18.33	65.44

lipophilic therapeutic agent solubilized in equilibrium conditions in aqueous solutions of novel surface active agents with $c_{exp} \geq cmc$.

Approximation equation describing the relationship between the concentration of the therapeutic agent (naproxen; c, mg × 100 cm^{-3}) and the measured value of absorbance (A) at λ = 262 nm wavelength, p = 0.05 and r = 0.9982, i.e.:

$$A = 0.0923 + 0.1722 \cdot C, \qquad (11)$$

and the following transformation of the equation:

$$c = A - \frac{0.0923}{0.1722}, \qquad (12)$$

made it possible to calculate the amount of the solubilized therapeutic agent.

The results of the calculation were used to estimate the value of the micellar partition coefficient (K_w^m, Table 1).

Hydrodynamic parameters characterizing the process of naproxen solubilization in equilibrium (Table 1) suggest that their progression occurs proportionally to the value of micellar partition coefficient (K_w^m).

These aforementioned findings suggest that population based content of naproxen (250 mg or 500 mg per drug unit; tablet or suppository) in combination with approximately 1% of the content of the cholic acid oxyethylation products in these formulations, enable the complete solubilization of the active substance irrespective of the physiological value of the lithogenolithic index of bile "A" (duodenal content).

Similarly to previous studies (1, 3, 5, 8), the value of cmc was determined based on the formulation:

$$\gamma_{cmc}^{25} = (c, g/100\ cm^3, Fig. 1), \qquad (13)$$

along with the decrease in the value of surface activity coefficient in the critical region (γ_{cmc}^{25}).

Table 2 summarizes the values of surface activity of aqueous solutions of the cholic acid oxyethylation products and their micellar adducts with lipophilic therapeutic agents (diclofenac, loratadine, naproxen and rutin).

The observed relationship between γ_{cmc}^{25} and n_{TE} (Fig. 2) suggests that the surface activity coefficient in the critical area (cmc) does not decrease below 46 mJ/m^2.

Conferring observed values of γ_{cmc}^{25} to the physiological range of the surface activity of body fluids (γ = 46.0 (48.0) − 52 mJ/m^2) suggests potential safety of the cholic acid derivatives used as excipients in drug formulation technology (solid oral forms, eye drops, infusions and injections). This finding is particularly interesting since the structure of cholic acid is not recognized as xenobiotic by the human immune system.
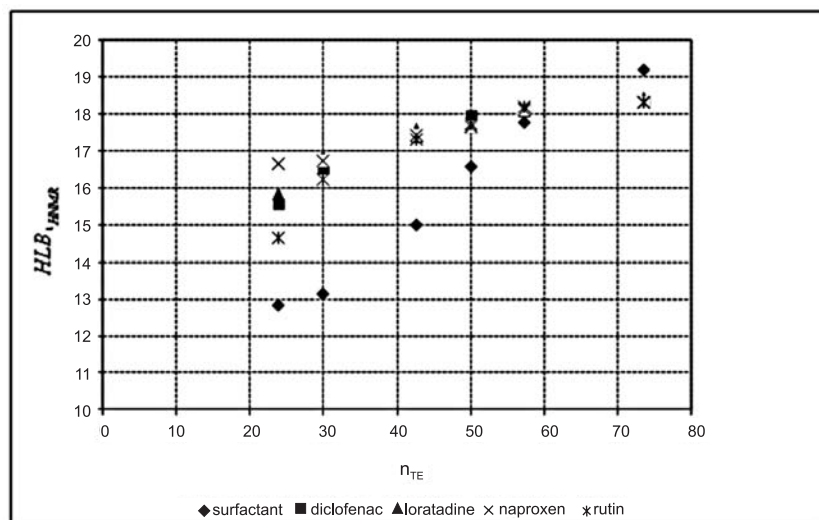
Figure 5. Relationship between micellar level of hydrophilic-lipophilic balance of adduct and solubilizer and the number of oxyethylated surfactant segments determined in equilibrium

Table 4. Approximation equations describing the relationship: $\Delta G_m^o = f(n_{TE})$ for the cholic acid derivatives and their micellar adducts.

Solubilizer	Type of equation	"r"	Directional coefficients	
Micellar adduct			"a"	"b"
1. Cholic acid*	y = a + bx	0.9246	-18.4256	-4.0949×10^{-2}
	1/y = a + bx	0.9324	-5.3725×10^{-2}	9.5953×10^{-5}
2. Cholic acid + diclofenac	y = a + bx	0.9394	-18.6459	-3.8233×10^{-2}
	y = a + b/x	0.9641	-22.0796	66.6786
3. Cholic acid + loratadine	y = a + bx	0.8996	-17.6089	-5.5745×10^{-2}
	1/y = a + bx	0.8974	-5.5801×10^{-2}	1.3272×10^{-4}
4. Cholic acid + naproxen	y = a + bx	0.9862	-18.6832	-3.9409×10^{-2}
	1/y = a + bx	0.9861	-5.3122×10^{-2}	$9.3072 \cdot 10^{-5}$
5. Cholic acid + rutin	y = a + bx	0.9629	-19.7440	-3.3186×10^{-2}
	y = a + blogx	0.9818	-15.7254	-3.3972

* cholic acid n_{TE} = 20-70

Analyzing the relationship between the calculated value of the thermodynamic potential of micelle formation by solubilizer (ΔG_m^o) or its adducts with lipophilic therapeutic agents, and the determined content of oxyethylated segments (n_{TE}): $\Delta G_m^o = f(n_{TE})$ revealed significant variability of changes of various adducts in comparison to the ΔG_m^o of solubilizer whose homologous line was characterized by specific content of n_{TE} (Fig. 3). This finding indicates the necessity of further detailed analysis of the course of relationship $\Delta G_m^o = f(n_{TE})$ for analyzed lipophilic therapeutic agents.

The course of relationship between the surface of lipophilic core upthrust over the phase boundary (A_m) and the number of oxyethylated segments (n_{TE}) in surfactant (solubilizer, Fig. 4) is specific for the site and topologic micellar structure of adduct's solubilizer.

As suggested by the course of this relationship, solubilized adduct is more hydrophilic (as confirmed by significant decrease in the value of A_m) than the micellar structure of surfactant (solubilizer).

This finding was additionally confirmed by the fact that the calculated values of A_m for solubilizer

Table 5. Approximation equations describing the relationship between $HLB_{^1HNMR}$ of dry adduct and solubilizer as a function of n_{TE}* by $p = 0.05$:$HLB_{^1HNM}$ = f(n_{TE}).

Solubilizer	Type of equation	"r"	Directional coefficients	
Micellar adduct			"a"	"b"
1. Cholic acid**	$y = a + bx$	0.9896	9.3678	0.1384
	$\log y = a + b\log x$	0.9853	0.5658	0.3837
	$\log y = a + b/x$	0.9559	1.3504	6.3006
2. Cholic acid + diclofenac	$y = a + bx$	0.9651	14.7713	5.8039×10^{-2}
	$\log y = a + b/x$	0.9995	1.2946	-2.1034
3. Cholic acid + loratadine	$y = a + bx$	0.9608	15.0441	5.1573×10^{-2}
	$\log y = a + b/x$	0.9916	1.2919	-2.0530
4. Cholic acid + naproxen	$y = a + bx$	0.9655	15.8221	3.8736×10^{-2}
	$1/y = a + bx$	0.9643	6.2739×10^{-2}	-1.2746×10^{-4}
5. Cholic acid + rutin	$y = a + bx$	0.9478	14.1899	6.8998×10^{-2}
	$\log y = a + b/x$	0.9992	1.2923	-2.0039

* n_{TE} was determined in total solids left after evaporating water from the solution of solubilizer and micellar adduct; ** cholic acid n_{TE} = 20-70

(Fig. 4) were located under the plot of function $A_m = f(n_{TE})$.

Surprisingly, this finding was also confirmed by the course of relationship between micellar level of hydrophilic-lipophilic balance of adduct and solubilizer, calculated by means of ^{1}HNMR method (HLB^1_{HNMR}) and the number of oxyethylated surfactant segments determined in equilibrium: $HLB_{^1HNMR} = f(n_{TE})$ (Fig. 5).

The values of $HLB_{^1HNMR}$ and n_{TE} for solubilizer and studied adducts are summarized in Table 3.

Approximation equations presented in Table 4, describing the relationship between ΔG_m^o and determined content of n_{TE} by $p = 0.05$, suggest that the "a" coefficient for solubilizers ($\Delta G_{m(aprox)}^o = -18.4256$ kJ/mol) is comparable to those for micellar adducts with diclofenac (– 18.6459 kJ/mol) and naproxen (– 18.6832 kJ/mol).

Slight decrease in micellar stability of adduct was observed in case of loratadine ($\Delta G_{m\ (aprox)}^o = -17.6039$ kJ/mol), whereas the micellar stability of rutin adduct ($\Delta G_{m(aprox)}^o = -19.7440$ kJ/mol) increased surprisingly despite a significant rise in the effective molecular volume.

The ΔG_m^o value for adduct, as well as quantitative characteristics of solubilization by homologous structures of the new class of surfactants, raises the possibility of formulating model preparations for parenteral use.

Gradients of lines that illustrate the relationship between HLB^1_{HNMR} along with the number of oxyethylated segments (n_{TE}, Table 5) for solubilizers and their micellar adducts suggest that (by $n_{TE} = 0$) the value of $HLB_{HNMR(0)}$ for molecular adducts of cholic acid derivatives with diclofenac, loratadine, naproxen and rutin ranges from 14.1899 (rutin) to 15.8221 (naproxen). This in turn, suggests their surprisingly high solubility in water and isotonic solutions when compared to cholic acid whose $HLB_{^1HNMR(0)}$ (by $n_{TE} = 0$) was found to be 9.3698.

The increase in HLB_{HNMR} value of adduct that was observed in this study suggests indirectly the possible mechanism and site of diclofenac, loratadine, naproxen and rutin solubilization by the micelle of cholic acid oxyethylation products. Moreover, it suggests that structural and quantitative characteristics of this process depend on the amount of oxyethylated segments (n_{TE}) in the molecule of surfactant.

CONCLUSIONS

High solubility of lipophilic naproxen was observed in the environment of aqueous solutions of the cholic acid oxyethylation products as suggested by determined factual solubility and the value of micellar partition coefficient (K_w^m).

Determined surface activity of surfactants (new class of derivatives) described by various physicochemical characteristics (γ_{cmc}^{25}, cmc, ΔG_m^o and A_m) suggests their compatibility with physiological values of the surface activity of plasma (48.0-52.0 mJ/m^2) and lacrimal fluid (46.0-52.0 mJ/m^2). This finding establishes the possible application of the

cholic acid oxyethylation products as excipients (solubilizers) in formulations of solid drug forms containing lipophilic therapeutic agents.

Calculated values of HLB_{HNMR} and n_{TE} of the micellar adduct in solid phase (solid dispersion) corresponded with an increase in its hydrophilicity (Table 3), and, therefore, suggested possible mechanisms and site of diclofenac, loratadine, naproxen and rutin solubilization in the micellar structure (core or palisadic layer).

Acknowledgment

REFERENCES

1. Brzeski Z., Sodolski W.: Przeg. Lek. 63, 521 (2006).
2. Forster W.A., Zabkiewicz J.A., Liu Z.: Pest. Manag. Sci. 62, 664 (2006).
3. Liu Z.Q., Gaskin R.E., Zabkiewicz J.A.: Weed Research. 44, 237 (2004).
4. Nasal A., Buciński A., Bober L., Kaliszan R.: Int. J. Pharm. 159, 43 (1997).
5. Oleszczuk P.: Biotechnologia 76, 9 (2007).
6. Reschly E.J., Krasowski M.D.: Curr. Drug Metab. 7, 349 (2006).
7. Stieger B., Meier P.J.: Curr. Opin. Cell Biol. 10, 462 (1998).
8. Wiedmann T.S., Kamel L.: J. Pharm. Sci. 91, 1743 (2002).
9. Zgoda M.M., Karczewski T.: Diagn. Lab. 29, 163 (1993).
10. Zgoda M.M., Karczewski T.: Acta Pol. Pharm. Drug Res. 47, 61 (1990).
11. Zgoda M.M., Lukosek M., Nachajski M.J.: Polim. Med. 36, 13 (2006).
12. Zgoda M.M., Nachajski M.J., Kolodziejczyk M.K., Woskowicz M.H., Lukosek M.: Polim. Med. 37, 21 (2007).
13. Zgoda M.M., Nachajski M.J., Kolodziejczyk M.K., Woskowicz M.H., Lukosek M.: Polim. Med. 37, 39 (2007).
14. Linderberg M., Kopp S., Dressman J.B.: Eur. J. Pharm. Biopharm. 58, 265 (2004).
15. Bettinetti G.P., Mura P., Liguori A., Bramanti G., Giordano F.: Farmaco Prat. 43, 331 (1988).
16. Bhat P.A., Rather G.M., Dar A.A.: J. Phys. Chem. B 113, 997 (2009).
17. Polish Standard PN-90/C-04809 (ISO 304 i 6889). Surface active agents. The determination of surface tension (γ_s) and interfacial tension (γ_i)"].
18. Polish Standard PN-93/C-89430 (ISO 1628/1:1984). Methods of testing plastics. Rheological properties. Determination of viscosity number: general conditions.

NANOPRECIPITATION WITH SONICATION FOR ENHANCEMENT OF ORAL BIOAVAILABILITY OF FUROSEMIDE

BHANU P. SAHU[1]* and MALAY K. DAS [2]

[1]GIPS, Gauhati University, Azara, Guwahati, India
[2]Department of Pharmaceutical Sciences, Dibrugarh University, Dibrugarh, India

Abstract: Furosemide is a weakly acidic diuretic indicated for treatment of edema and hypertension. It has very poor solubility but high permeability through stomach and upper gastrointestinal tract (GIT). Due to its limited solubility it has poor and variable oral bioavailibility of 10–90%. The aim of this study was to enhance the oral bioavailibilty of furosemide by preparation of nanosuspensions. The nanosuspensions were prepared by nanoprecipitation with sonication using DMSO (dimethyl sulfoxide) as a solvent and water as an antisolvent (NA). The prepared nanosuspensions were sterically stabilized with polyvinyl acetate (PVA).These were characterized for particle size, ζ potential, polydispersity index, scanning electron microscopy (SEM), differential scanning calorimetry (DSC), X-ray diffraction (XRD) pattern and release behavior. The average particle size of furosemide nanoparticles were found to be in the range of 150–300 nm. This was further confirmed by SEM photograph. The particle size varies with an increase in concentration of drug and stabilizer. The preparations showed negative ζ potential and polydispersity index in the range of 0.3 ± 0.1. DSC and XRD studies indicated that the crystalline furosemide drug was converted to amorphous form upon precipitation into nanoparticles. The saturation solubility of prepared furosemide nanoparticles markedly increased compared to the original drug in simulated gastric fluid. The release profiles of nanosuspension formulation showed up to 81.2% release in 4 h. It may be concluded that the nanoprecipitation with ultrasonication have potential to formulate homogenous nanosuspensions with uniform sized amorphous nanoparticles of furosemide. Polyvinyl acetate can be used as a suitable steric stabilizer to prepare stable furosemide nanosuspensions. The enhanced saturation solubility in simulated gastric fluid may lead to enhanced absorption of furosemide.

Keywords: nanosuspension, nanoprecipitation, furosemide, bioavailability

Furosemide is a powerful diuretic used in edemas and chronic hypertension (1). Furosemide is a BCS (Biopharmaceutics Classification System) class IV drug due to its low water solubility (5–20 µg/mL) and low permeability (2). It has a very variable bioavailibity of 10–90% due to its low solubility in the stomach. However, furosemide is preferentially absorbed in the stomach and upper intestine where it has good permeability, but due to its low solubility in this conditions its absorption is very poor and variable (3). Altough it has good solubility in intestinal fluid, being a BCS Class IV drug it has very poor permeability through intestinal region. Hence, improving the solubility in gastric fluid becomes important to increase the systemic absorption of furosemide from stomach region and upper GIT, where it has better permeability and may result in improved bioavailability. The improvement of the bioavailability of poorly water soluble drugs has

been of major concern during the last decades. Altough in order to increase the dissolution rate of furosemide several attempts were carried out in the past (4–8), however, most of these techniques require a large amount of additives limiting their use from the safety perspective. So far, no attempts have been reported on enhancement of dissolution by reduction in particle size of furosemide using nanosuspensions.

Recently, the nanosuspension technology has been successfully applied to tackle the formulation issue of several poorly soluble drugs. Nanosuspensions are carrier-free colloidal drug delivery system containing minimum additives (9, 10). These preparations have several advantages and results in considerable increase in drugs saturation solubility. The preparations are more homogenous and have good dispersity and scale up features (11, 12). The methods of preparation of nanosuspenisons are simple and universal in approach (13, 14).

* Corresponding author: GIPS, Hathkhowapara, Azara, Guwahati-17, India; e-mail: pratapsuman2004@yahoo.co.in

Nanosuspensions can be prepared either by top-down or bottom-up processes. The top-down process involves particle size reduction of large drug particles into smaller particles using various techniques such as: media milling, microfluidization and high pressure homogenization. However, all these processes involve high energy input and are highly inefficient. In the bottom-up approach, the drug is dissolved in an organic solvent and is then precipitated on addition of an antisolvent in the presence of a stabilizer. The precipitation method results in smaller size and homogenous particles. Besides, it may lead to amorphous drug nanoparticles which have higher saturation solubility and dissolution rate (15, 16). Various adaptations of this approach include: (i) solvent–anti-solvent method, (ii) supercritical fluid processes, (iii) spray drying, (iv) emulsion–solvent evaporation and (v) ultrasonication (17, 18). Hence, in the present study, the method of precipitation was explored for the preparation of nanosuspensions. The precipitation was combined with sonication to get more homogenous and smaller particles.

The nanosuspensions can be stabilized by electrostatic or steric stabilization or a combination of both. However, steric stabilization is more advantageous than electrostatic stabilization as the latter may be lost in the variable pH condition of the GIT and is effected by electrolytes. The stability of sterically stabilized nanosuspensions depends on the property of the drug like enthalpy and logP as well as the hydrophobicity of the stabilizer (19, 20).

The aim of this study was to enhance the saturation solubility of furosemide in gastric fluid and thereby oral bioavailability of the drug by preparation of nanosuspension. The possibility of producing a stable nanosuspension of furosemide by controlled precipitation with sonication using steric stabilizer has been investigated. The impact of various experimental parameters on particle formation including solvent–antisolvent ratio, diffusing drug concentrations, type and concentration of stabilizer and stir-
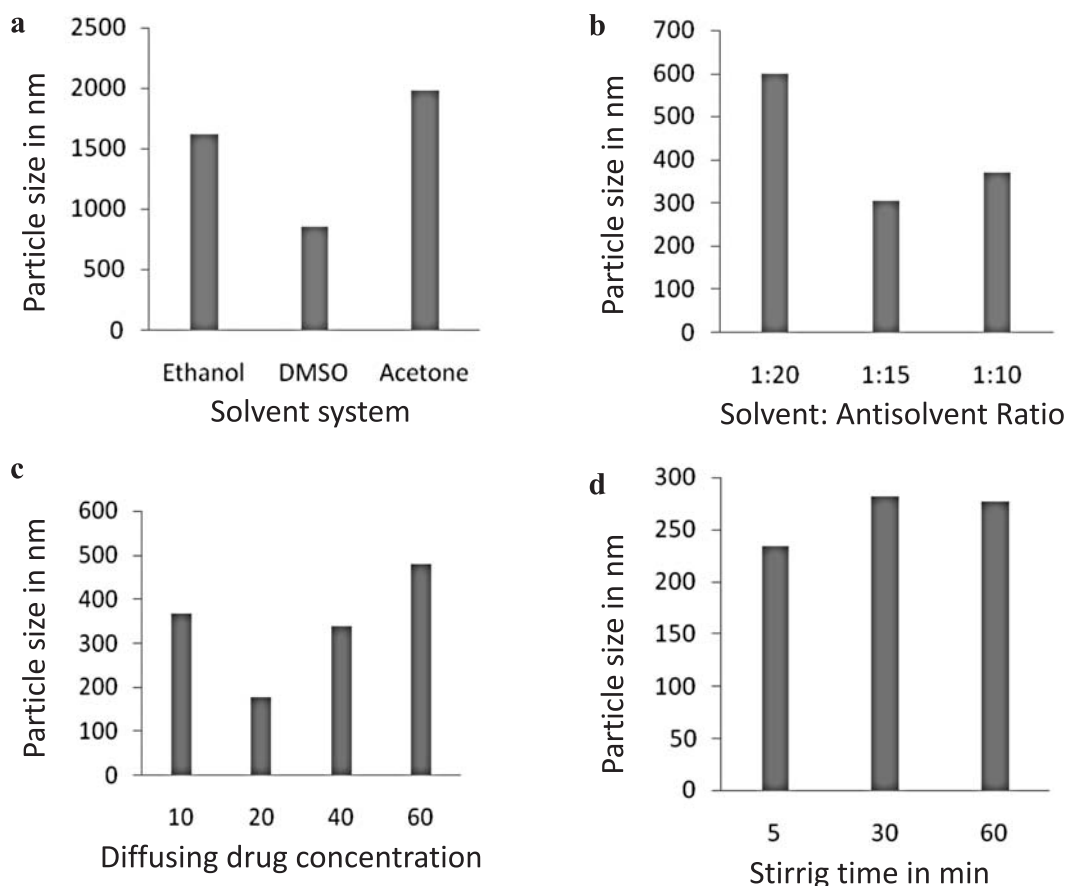
Figure 1. Effect of (**a**) solvent system, (**b**) solvent : antisolvent ratio, (**c**) diffusing drug concentration, (**d**) stirring time on mean particle size
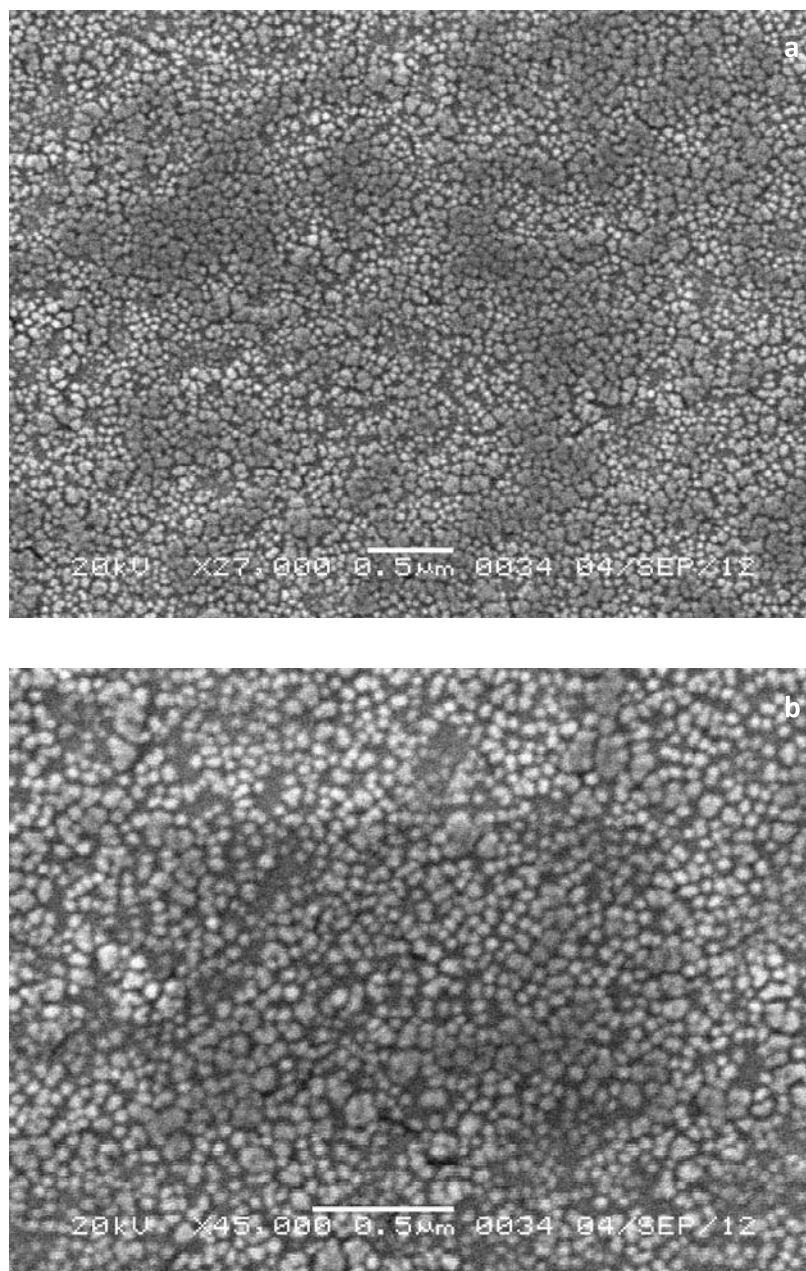
Figure 2. **a**) SEM photomicrograph of furosemide nanoparticles (27,000×); **b**) (45,000×). Scale bar = 0.5 μm

ring time were studied. Characterization and physical stability of the obtained nanosuspension were also carried out.

MATERIALS AND METHODS

Preparation of nanoparticles

Furosemide nanoparticles were produced by precipitation–ultrasonication technique (21). The required amount of drug was dissolved in water-miscible solvent (DMSO). Different concentrations of drug in solvent (5, 10, 25, 40 mg/mL) were used. The obtained drug solution was then injected into the water containing stabilizer (PVA) with stirring. The suspension was then ultrasonicated under cold condition. The preparations were then lyophilized using freeze dryer.

Size measurement and ζ potential analysis

The particle size and the polydispersity index (PI) of the precipitated nanoparticles were measured immediately by dynamic laser light scattering method using (Zetasizer Ver. 6.11 Malvern). The ζ potential of the preparations was also measured using (Zetasizer Malvern).

Scanning electron microscopy (SEM)

The morphology of the dried nanoparticles was observed using scanning electron microscopy (SEM) JSM-6360 (JEOL Inc., Japan). Small drop of the nanosuspension was air dried followed by oven drying and were fixed on an SEM stub using double-sided adhesive tape and coated with Au at 20 mA for 6 min through a sputter-coater (Ion sputter JFC 1100, Japan). A scanning electron microscope with a secondary electron detector was used at an accelerating voltage of 15 kV (22).

Determination of saturation solubility

The saturation solubility of furosemide was evaluated by dispersing lyophilized powder in 20 mL of simulated gastric fluid pH 1.2 to obtain 2 mg/mL of drug suspension. This was placed on a shaking water bath for 48 h to ensure that the solubility equilibrium had been reached. The samples were centrifuged and the resulting supernatant was analyzed by UV spectrophotometer at 274 nm.

X-ray diffraction studies (XRD)

The effect on crystallinity of precipitated furosemide nanopartilces was observed by X-ray diffraction using a XRD-6000 diffractometer (Shimadzu, Japan). The powder was placed in a glass sample holder. CuK radiation was generated at 30 mA and 40 kV and samples were scanned from 5 to 90° with a step size of 0.02°.

Fourier transforms infrared spectroscopy (FT-IR)

Drug excipients interactions were studied by FTIR spectroscopy (23). FTIR spectra were recorded for furosemide, PVA and the dried nanoparticles. Samples were prepared in KBr discs (2 mg drug in 8 mg KBr) with a hydrostatic press at a force of 8 t cm^{-2} for 2 min. The scanning range was 450–4000 cm^{-1} and resolution was 2 cm^{-1}.

Differential scanning calorimetry (DSC)

The DSC analysis of pure drug, PVA and the dried nanoparticles was carried out using Mettler Toledo (Model SW 810) to observe any possible drug-excipients interaction. Samples (5.5–8 mg) were weighed accurately using a single pan elec-
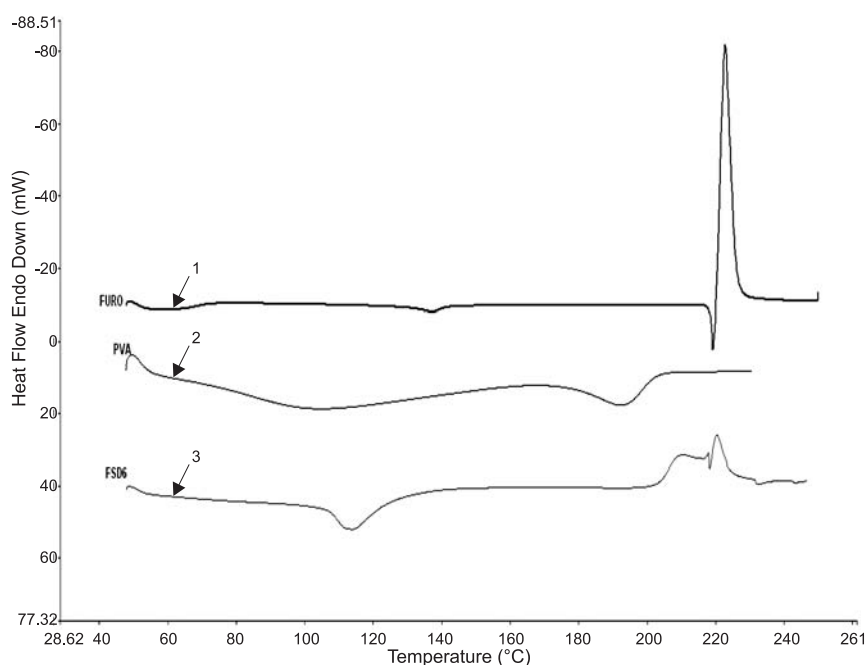
Figure 3. DSC thermogram of (1) pure drug furosemide (Furo), (2) PVA; (3) precipitated furosemide nanoparticles (FSD6)
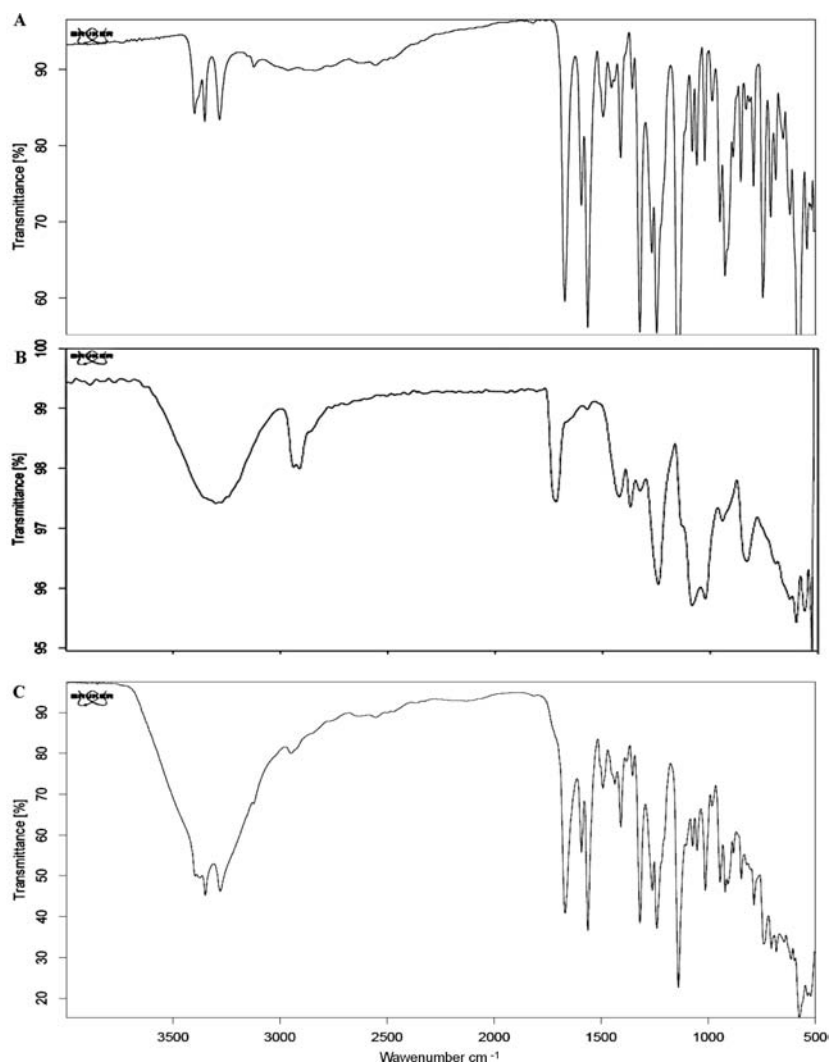
Figure 4. FTIR spectra of (**A**) pure drug furosemide; (**B**) PVA; (**C**) precipitated furosemide nanoparticles

tronic balance and heated in sealed aluminum pan at rate of 5°C/min from 25 to 450°C temperature range under a nitrogen flow of 35 mL/min (24).

In vitro release kinetic experiments

In vitro drug release of the nanosuspensions was determined by the dialysis membrane diffusion technique in phosphate buffer (PB) 6.5 + 0.5% SLS (sodium lauryl sulfate). One milliliter of nanosuspension was placed in the dialysis membrane (M.w. cut off 12000–14000, HiMedia, India), fixed in an apparatus of surface area 1.76 cm^2 and receptor volume of 20 mL. The entire system was kept at 37°C with continuous magnetic stirring. Samples (1 mL) were withdrawn from the receptor compartment at predetermined time intervals and replaced by fresh

medium. The amount of drug dissolved was determined UV spectrophotometrically at 277 nm.

Physical stability study

The physical stability of the nanosuspensions on storage was studied at 4°C (refrigerator), room temperature and 40°C (stability chamber) for 6 months. Particle size diameter (PSD) measurements were selected as suitable parameter for evaluation of physical stability (25).

RESULTS AND DISCUSSION

Preparation of nanoparticles

Furosemide nanoparticles were produced by precipitation–ultrasonication technique. The aque-

ous phase containing a suitable stabilizer have been used as the antisolvent and the use of different water miscible solvents (ethanol, acetone, dimethyl sulfoxide DMSO) having good solubility of furosemide has been explored as solvents. The effect of various variables like diffusing drug concentration, solvent : antisolvent ratio, type of stabilizer, concentration of stabilizer, stirring time and ultrasonication have been observed. Ethanol, DMSO and acetone have been tried as solvent for the preparations. These preparations gave particle size of 1617, 856 and 1980 nm, respectively, as shown in Fig 1a. Hence, DMSO was selected as solvent as it produced nanoparticles of smaller size of furosemide on precipitation.

From the preliminary studies, the effect on particle sizes of different solvent : antisolvent ratios (1 : 20, 1 : 15, 1 : 10) was observed, which produced particles of 600, 304, 369 nm, respectively. As such, formulation with S : NS 1 : 15 showing smaller particle size was selected for the preparation as suitable S : NS ratio. The selection of proper S : NS ratio is important for the formulation as it effects the extent of supersaturation and thereby effects the size of the precipitated furosemide particles.

The effect of stirring time (5, 30 and 60 min) on the particle size was studied, which showed particle size of 233.6, 281.2 and 276.9 nm, respectively, when prepared by precipitation with ultrasonication. No sign of aggregation due to stirring have been observed and the particle size doesn't show dependence on stirring time.

In the present study, suitability of steric stabilizer alone for stabilization of the nanosuspension have been investigated. The logP of furosemide is 2.3, hence, moderately hydrophobic stabilizer (HPMC and PVA) have been selected for the preparation. Since the stability of the nanosuspensions depends on the hydrophobicity of the drug and stabilizer, a similar hydrophobicity should result in better surface coverage thereby providing better steric stabilization. HPMC and PVA have been used as stabilizers for the preparations at various concentrations. PVA based formulations at various concentrations 0.15, 0.25 and 0.5% showed particle size 288, 239, and 156 nm, respectively, which were comparatively smaller than HPMC based formulations. Hence, from the preliminary studies, PVA at concentration of 0.5% was found to be optimum stabilizer concentration.

The effect of diffusing drug concentration on the particle size was studied. The nanosuspensions were made with different diffusing drug concentrations 10, 20, 40 and 60 mg/mL. The particle size varies with the change in drug concentration as shown, giving particle size of 366, 179, 339 and 478 nm, respectively. Preparations with 20 mg/mL diffusing drug concentration were found to be optimum for PVA based formulations and were selected for further studies. The study indicates that sufficient supersaturation is required for diffusing drugs to get precipitate in nanoparticulate range due to the enhanced rate of crystal nucleation and growth. But at very high concentration, the particle size increases, as very high supersaturation increases the parti-
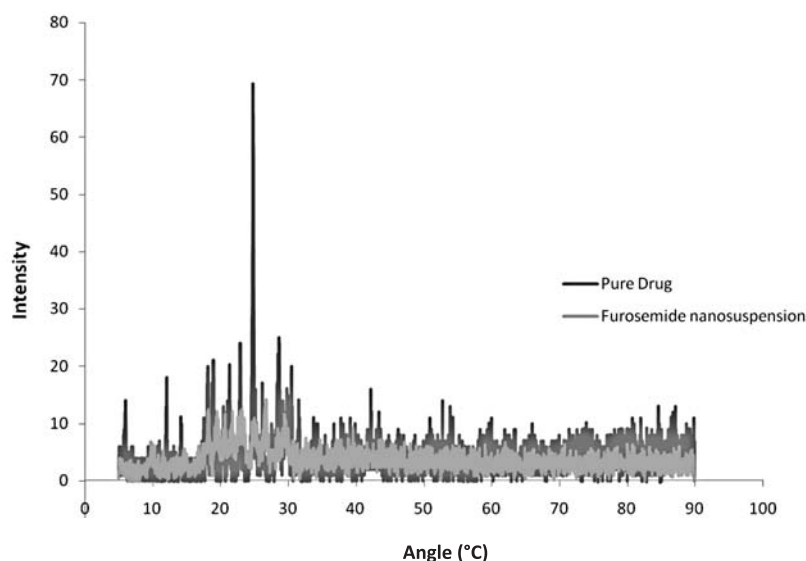

Figure 5. X-ray diffraction patterns of pure furosemide drug precipitated PVA based furosemide nanoparticles
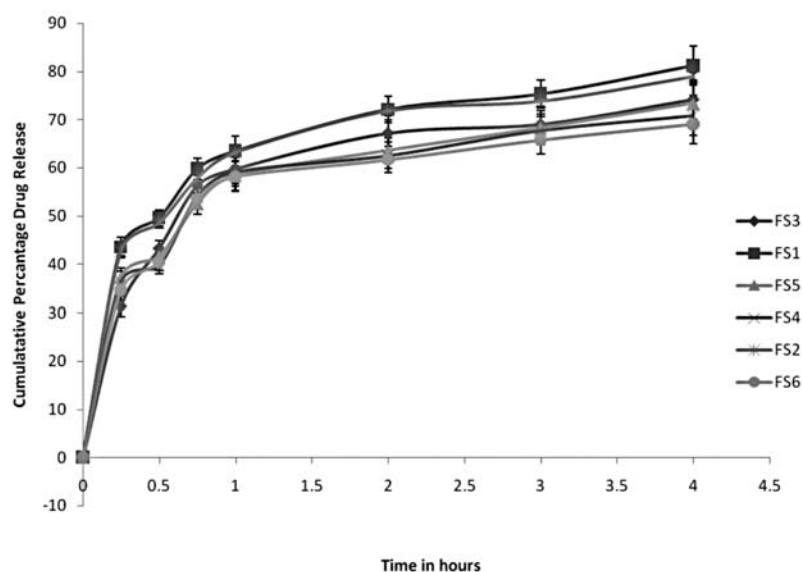
Figure 6. Cumulative percentage of furosemide released from various formulations

cle growth by promoting condensation/coagulation The effect of ultrasonication on the size of the precipitated particles was observed. The particle size was found to be 733 nm in precipitation alone with higher polydispersity index. The particle size was considerably decreased and more uniform in case of precipitation with ultrasonication for 15 min under cold condition showing particle size of 557.5 nm. Application of sonication during precipitation assists in the diffusion of solvent in the antisolvent and results in smaller and more homogenous dispersions. Hence, precipitations with ultrasonication have been used for the further preparations of nanoparticles of furosemide.

After proper selection of the different variables, the furosemide nanosuspensions were prepared and suitably characterized.

Size measurement and ζ potential analysis

The average particle size of furosemide nanoparticles were found to be in the range of 100–300 nm. The particles were homogeneous as indicated by polydispersity index of 0.3 ± 0.1. The ζ potential of the nanoparticles was found to be negative which may be due to the presence of terminal carboxylic groups.

Scanning electron microscopy (SEM)

Morphology of precipitated drug particles in the suspension after air drying followed by oven drying is shown in Figures 2a and 2b. The drug par-

ticles precipitated with the PVA as stabilizer are spherical in shape and the size ranges from 100 to 300 nm. The particles are discrete and uniform in size and there is no sign of agglomerations.

Differential scanning calorimetry (DSC)

The DSC analysis of pure drug, PVA and the dried nanoparticles was carried out. The DSC thermogram of furosemide shows a characteristic, sharp exothermic melting point peak at 229.8°C, which indicates the crystalline nature of the drug. The peak corresponding to the melting point of furosemide in the precipitated nanoparticles is broader indicating a decline in the crystallinity of furosemide in nanosuspension. The result is shown in Figure 3. This result was further confirmed by XRD analysis.

X-ray diffraction studies (XRD)

The representative X-ray diffraction patterns of the pure furosemide powder and oven dried nanosuspensions are shown in Figure 4. The figures indicated changes in the drug crystal structure. The X-ray patterns of the pure furosemide displayed the presence of numerous distinct peaks at 6.01°, 12.09°, 18.13°, 18.17°, 24.81°, 24.85°, 24.89° and 28.65°, which suggested that the drug was in crystalline form. The precipitated nanoparticles samples showed diminished peaks suggesting the conversion of crystalline furosemide drug into amourphous form upon precipitation into nanoparticles. The result is shown in Figure 4.

Saturation solubility

The results of saturation solubility of pure drug and lyophilized furosemide nanosuspensions revealed a saturation solubility of 12.0 μg/mL and 438.32 μg/mL in simulated gastric fluid of pH 1.2, respectively. The saturation solubility of furosemide in nanosuspension increased 36-fold than that of pure furosemide. The substantial increase in the saturation solubility may be due to the increased surface area of the small sized nanoparticles. The formation of amorphous particles may also have resulted in this increase in solubility.

Fourier transform infrared spectroscopy (FT-IR)

The IR (infra red) spectra of furosemide in pure drug and in the precipitated nanoparticles were comparable and found to be intact. The spectrum of pure furosemide shows the characteristic peaks at 3647.51 cm^{-1} (O-H stretch), 3286.81 cm^{-1} (N-H stretch), 3147.05 cm^{-1} (C-H stretch), 1568.18 cm^{-1} (C=O stretch), 1672.34 cm^{-1} (N-H bending), and 1263.44 cm^{-1} (S=O asymmetric stretch). FT-IR spectra of precipitated nanoparticles of furosemide showed no substantial shifting of the position of functional groups. The peaks indicated no major

interactions between furosemide and PVA in the formulation. The result is shown in Figure 5.

In vitro release kinetic experiments

The release profile of furosemide nanosuspensions in PB 6.5 + 0.5% SLS shows up to 81.2% release in 4 h. The drug release of prepared furosemide nanoparticles markedly increased as compared to the original drug. This enhancement in the drug release may be attributed to the enhanced solubility of drug due to an increase in the surface area. The comparative release results of selected formulations have been shown in Figure 6.

Physical stability study

Recently it has been reported that amorphous particles are more prone to aggregation. Hence, the nanoparticles were stabilized by steric hindrance by sufficient surface coverage using polymeric stabilizer PVA. The physical stability on storage was therefore observed after 6 months. The formulations at 4°C, room temperature and at 40°C remained stable after 6 months. The polymeric stabilizer PVA at 0.5% concentration was found to be sufficient to provide proper steric coverage to keep the amor-

Table 1. Effect of drug concentration and surfactant concentration on mean particle size, polydispersity index and drug release.

Formulation code	Diffusing drug concentration mg/mL	PVA concentration %	Z average (diameter in nm)	Drug release % (PI)	Polydispersity index
FS$_1$	25	0.5	179.2	81.2	0.395
FS$_2$	25	1.0	188.6	78.9	0.401
FS$_3$	40	0.15	339.5	74.2	0.424
FS$_4$	10	0.15	366.6	70.9	0.385
FS$_5$	45	0.5	378.4	73.4	0.45
FS$_6$	5	0.5	382.6	69.1	0.424
FS$_7$	10	0.75	387.2	71.3	0.412
FS$_8$	25	0.25	198.4	80.4	0.412
FS$_9$	25	0.5	179.2	81.2	0.395
FS$_{10}$	40	0.75	345.6	76.8	0.422

Table 2. Physical stability evaluation of the furosemide nanosuspensions.

Formulations	Storage temperature conditions	Initial particle size	Particle size after 6 months
FS16	4°C	156.7	158.5
	R T		162.2
	40°C		172.5

phous nanoparticles stable. The stability of the nanosuspensions may also be due to the method of precipitation which, in comparision to top down approaches, involves lesser involvement of energy. Moreover, the process results in more homogenous dispersions as indicated by the narrow polydispersity index of 0.3, which may be responsible for the absence of Ostwald ripening on storage generally associated with amorphous particles. The particle size diameter (PSD) data on storage are given in Table 2. Sedimentation was observed in all the conditions but the preparations were easily redispersed on shaking.

CONCLUSION

From the study it may be concluded that stable nanosuspension can be prepared for furosemide by precipitation with ultrasonication. The nanoprecipitation of furosemide results in smaller particles in 150–350 nm range with increased surface area and results in amorphization of the drug. This results in considerable increase in saturation solubility in simulated gastric fluid, which may enhance the oral systemic absorption of furosemide from stomach region where it has better permeability. The polymeric stabilizer PVA was found to be efficient in providing proper steric coverage to the amorphous nanoparticles. The preparation was found to be stable and compatible.

REFERENCES

1. Boles Ponto L.L., Schoenwald R.D.: Clin. Pharmacokinet. 18, 381 (1990).
2. Lindenberg M., Kopp S., Dressman J.B.: Eur. J. Pharm. Biopharm. 58, 265 (2004).
3. Davis S.S.: Drug Discov. Today 10, 249 (2005).
4. Ozdemir N., Ordu S.: Farmaco 52, 625 (1997).
5. Chul S.S., Kim J.: Int. J. Pharm. 251, 79 (2003).
6. Akinlade B., Elkordy A.A., Essa E.A., Elhagar S.: Sci. Pharm. 78, 325 (2010).
7. Chaulang G., Patel P., Hardikar S., Kelkar M., Bhosale A., Bhise S.: Trop. J. Pharm. Res. 8, 43 (2009).
8. Patel R.C., Keraliya R.A., Patel M.M., Patel N.M.: J. Adv. Pharm. Technol. Res. 1, 180 (2010).
9. Keck C.M., Müller R.H.: Eur. J. Pharm. Biopharm. 62, 3 (2006).
10. Gao L., Zhang D., Chen M.: J. Nanopart. Res. 10, 845 (2008).
11. Horn D., Rieger J.: Angew. Chem. Int. Ed. Engl. 40, 4331 (2001).
12. Rogers T.L., Gillespie I.B., Hitt J.E., Fransen K.L., Crowl C.A., Tucker C.J., Kupperblatt G. B. et al.: Pharm. Res. 21, 2048 (2004).
13. Schwitzera J.M., Achleitner G., Pomperb H., Müller R.H.: Eur. Pharm. Biopharm. 58, 615 (2004).
14. Pu X., Sun J., Wang Y., Wang Y., Liu X., Zhang P., Tang X. et al.: Int. J. Pharm. 379, 167–173 (2009).
15. Kesisoglou F., Panmai S., Wu Y.: Adv. Drug Deliv. Rev. 59, 631 (2007).
16. Mueller R.H., Keck C.M.: Eur. J. Pharm. Sci. 34 Suppl., S20 (2008).
17. Patravale V.B., Date A.A., Kulkarni R.M.: J. Pharm. Pharmacol. 56, 827 (2004).
18. Rabinow B.E.: Nat. Rev. Drug Discov. 3, 785 (2004)
19. Matteucci M.E., Brettmann B.K., Rogers T.L., Elder E.J., Williams R.O., Johnston K.P.: Mol. Pharm. 4, 782 (2007).
20. George M., Ghosh I.: Eur. J. Pharm. Sci. 48, 142 (2013).
21. Sahu B.P., Das M.K. (2013) Nanosuspension for enhancement of oral bioavailability of felodipine. Appl. Nanosci. DOI 10.1007/s13204 -012-0188-3
22. Dong Y, Ng W.K., Hu J., Shen S., Tan R.B.H.: Int. J. Pharm. 386, 256 (2010).
23. Zhang H.-X., Wang J.X., Zhang Z.B., Le Y., Shen Z.G., Chen J.F.: Int. J. Pharm. 374, 106 (2009).
24. Ali H.S.M.., York P., Blagden N.: Int. J. Pharm. 375, 107 (2009).
25. Eerdenbrugh B.V., Froyen L., Humbeck J.V., Martens J.A., Augustins P., Mooter G.V.: Eur. J. Pharm. Sci. 35, 127 (2008).

INTERACTION ANALYSIS OF ASPIRIN WITH SELECTIVE AMINO ACIDS

GHULAM MURTAZA[1]*, SABIHA KARIM[2], MUHAMMAD NAJAM-UL-HAQ[3], MAHMOOD
AHMAD[4], TARIQ ISMAIL[1], SHUJAAT ALI KHAN[1], MUHAMMAD HASSHAM HASSAN BIN ASAD[1]
and IZHAR HUSSAIN[1]

[1]Department of Pharmaceutical Sciences, COMSATS Institute of Information Technology,
Abbottabad, Pakistan
[2]University College of Pharmacy, University of the Punjab, Lahore, Pakistan
[3]Department of Chemistry, Bahauddin Zakariya University, Multan, Pakistan
[4]Faculty of Pharmacy and Alternative Medicines, The Islamia University of Bahawalpur,
Bahawalpur, Pakistan

Abstract: This study was conducted to assess the compatibility of aspirin with selective amino acids by study-
ing the effect of amino acids on the solubility of aspirin, so that the attention could be paid towards the use of
proteinous foods along with aspirin. Two different types of dissolution media, i.e., 0.5% solution of each amino
acid and 100 mL of distilled water (100 mL each), were prepared. Then, 1 g of aspirin was added in both media
and shaked gently. Ten milliliters of sample was withdrawn at different time intervals, i.e., 10, 20, 30, 40, 50
and 60 min and analyzed spectrophotometrically at 265 nm. It is evident from results that the absorbance of
aspirin increased with the addition of amino acids and this increase was significant ($p < 0.05$). Absorbance after
adding amino acid like glycine, tyrosine, glutamic acid, tartaric acid and aspartic acid was observed to be 2.98,
2.96, 2.92, 3.23 and 3.28, respectively, as compared to that of aspirin alone. The increase in absorbance of
aspirin in the presence of tartaric acid and aspartic acid was non-significantly ($p > 0.05$) greater than that in the
presence of other amino acids like glycine, tyrosine and glutamic acid. The absorbance of aspirin in the pres-
ence of tartaric acid and aspartic acid was 3.23 and 3.28, respectively, while the absorbance of aspirin in the
presence of glycine, tyrosine and glutamic acid was 2.98, 2.96 and 2.92, respectively. This study elaborates that
the solubility of aspirin increases with concomitant administration of amino acids, thus the use of amino acids
(proteinous foods) with aspirin should be prohibited or low dose of aspirin should be recommended in such sit-
uation.

Keywords: aspirin, amino acids, solubility, bioavailability, interaction

Aspirin is the acetate ester of salicylic acid
(Fig. 1) (1). Aspirin is an acronym for acetyl (a por-
tion of the chemical), spir from spirea (an ornamen-
tal plant) and as in salicin (the compound from
which aspirin is derived) (2). The chemical formula
of aspirin is $C_9H_8O_4$. Aspirin is colorless, odorless
and white crystalline powder (3–5). Molecular mass
of aspirin is 180.16 g/mol. Its melting point is
135°C. Its 1 g dissolves in 300 mL of water at 25°C
and in 100 mL of water at 37°C (6). It is stable in
air but gradually hydrolyses on contact with mois-
ture to acetic and salicylic acids. Aspirin is also
unstable in solutions of alkali hydroxides and car-
bonates (pKa 3.49 at 25°C) (7). Another aspect is
the poor water solubility of aspirin, which eventual-
ly results into local irritation of stomach mucosa
after oral administration (8). Aspirin exerts most of
its effect by inhibiting cyclooxygenase enzymes
(COX) thus suppressing the formation of
prostaglandins (PGs).

Aspirin inhibits both COX-1 and COX-2
enzyme but the effect on former is more pro-
nounced. Inhibition of COX enzyme is irreversible.
The reduction in the formation of prostaglandins
diminishes the sensitivity of the nerve fibers to pain
producing substances such as serotonin (5-HT) and
bradykinin, thus increasing pain threshold (9).

About 10% of a pre-dissolved 250 mg dose of
aspirin is absorbed from an acidic solution in the
stomach though the main absorption site is upper

* Corresponding author: e-mail: gmdogar356@gmail.com; mobile: 923149293393; fax: 92992383441
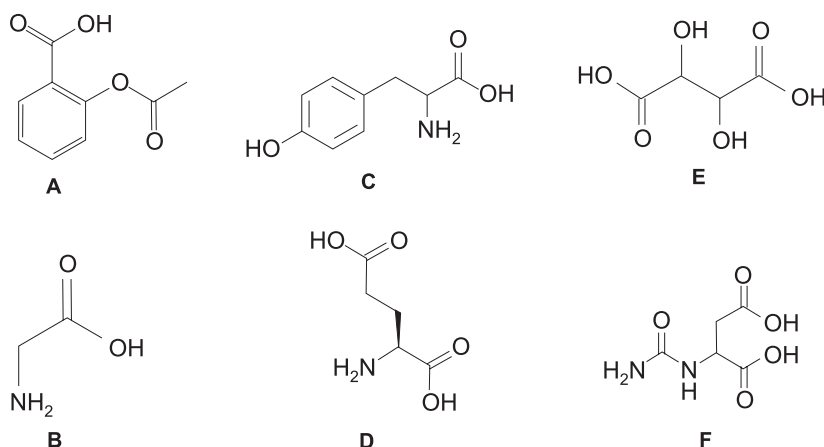
Figure 1. Chemical structures of aspirin (A), glycine (B), tyrosine (C), glutamic acid (D), tartaric acid (E) and aspartic acid (F)

intestine. This is partially because of poor solubility of compound at the strong acidic pH but also the comparably small absorption surface of the stomach mucosa (7).

Like most of other drugs, aspirin is mainly absorbed in upper intestine by passive diffusion of the non-ionized form (5).

Amino acids (AA) are the basic building blocks of proteins. Fundamentally, AA are joined together by peptide bonds to form the basic structure of proteins. AA are organic compounds that contain the basic amine group, NH_2 and acid carboxyl group, COOH.

AA are classified into different ways based on polarity, structure, nutritional requirement, and metabolic fate. Generally used classification is based on polarity. The nature of R-group attached to AA determines the their polar nature. The classification of AA on the basis of polarity is as follows: non-polar AA, polar AA with no charge, polar AA with positive charge and polar AA with negative charge. Non-polar AA are neutral (R-group is chargeless), hydrophobic and possess equal number of amino and carboxyl groups. The amino acid in this group includes glycine. Polar AA with no charge possess no charge on the 'R' group and undergo participation in hydrogen bonding of protein structure. The AA in this group include tyrosine. Polar AA with positive charge possess positive charge on the R-group and have greater number of amino groups as compared to carboxyl groups, which makes it basic, for example arginine. Polar AA with negative charge (dicarboxylic mono-AA) possess negative charge on the R-group and have greater number of carboxyl groups as compared to amino groups which makes them acidic, for example aspartic acid and glutamic acid (4).

This study was conducted to assess the effect of AA on the solubility of aspirin, so that the attention could be paid towards the use of proteinous foods along with aspirin. Literature survey has elaborated that no such study has been conducted previously. This study will help in the future to avoid any biological incompatibility, i.e., incompatibility between drug and food, particularly in the development of total parenteral nutrition containing aspirin.

EXPERIMENTAL

Materials

Aspirin (99.6% purity) was gifted by Mega Pharmaceuticals, Sheikhupura, Pakistan. Glycine, tartaric acid, L-aspartic acid, L-tyrosine, glutamic acid and phenol red were purchased from Pak Chemical Traders, Lahore, Pakistan. Sodium hydroxide (NaOH) was procured from Merck, Darmstadt, Germany. Double distilled water using glass apparatus was prepared in our laboratory.

Methodology

First of all, two different types of dissolution media i.e., 0.5% solution of each amino acid and 100 mL of distilled water (100 mL each), were prepared. Then, 1 g of aspirin was added in both media and shaked for 5 min. The sample (10 mL) was withdrawn at different time intervals, i.e., 10, 20, 30, 40, 50 and 60 min and analyzed spectrophotometri-

cally at 265 nm (10) using double beam spectrophotometer (1601, Shimadzu, Japan). Each sample was compensated with an equal volume of dissolution medium.

Using calibration curve, concentration of drug was determined for each sample. The value of regression coefficient (R^2) for aspirin was 0.9925, which indicated a good correlation between the concentration and absorbance within the concentration range (2–64 µg/mL) tested. The Y-equation for aspirin was y = 0.042x – 0.004. Each experiment was conducted three times.

Statistics

One way ANOVA was applied to elaborate the significance of difference between various parameters. The level of significance was set at 0.05.

RESULTS AND DISCUSSION

Glycine is an organic compound with the formula, NH_2CH_2COOH (Fig. 1). With a hydrogen substituent as its 'side chain', glycine is the smallest of the 20 AA commonly found in proteins. It is unique among the proteinogenic AA in that it is not chiral (11).

Plasma levels of aspirin > 300 µg/mL are considered obviously toxic. Severe toxic consequences are correlated with plasma concentrations > 400 µg/mL. A single poisonous dose of aspirin in adults is not recognized with confidence but death may be anticipated at a dose ≥ 30 g. The blood salicylate levels are measured to determine the severity of aspirin intoxication (12, 13). Thus, it is very important to determine the agents which interact with aspirin and ultimately potentiate or diminish its plasma concentration to avoid any undesired situation. In this context, present study was designed to elaborate the possible interaction between AA and aspirin.

It is evident from results that the absorbance of aspirin increased with the addition of amino acids and this increase was significant (p < 0.05). This increase in absorbance represents the increase in the ionization and thus enhanced solubility of aspirin. Absorbance after adding amino acid like glycine, tyrosine, glutamic acid, tartaric acid and aspartic acid was observed to be 2.98, 2.96, 2.92, 3.23 and 3.28, respectively, as compared to that of aspirin alone (Tab. 1). The possible reason of increase in aspirin solubility in the presence of these selective AA could be due to the coating of aspirin particles by amino acid particles forming capsule-like structure and thus masking its hydrophobic properties, imparting hydrophilic properties and preventing the aggregation of aspirin particles (14).

This reason could be responsible for the enhanced wettability of aspirin, which ultimately improves its solubility (14). This phenomenon not only increases the solubility of aspirin, but also protects the mucosal membrane from the irritation of aspirin due to the application of coating of AA on the surface of aspirin. It reduces the contact between aspirin and mucosal membrane (15). It has also been proposed that carboxylic acid group interacts with the gastric mucosa, which is responsible for gastric irritation. AA bear the free amino group which reacts with the carboxylic acid group of aspirin instead of reacting with that of gastric mucosa (16). Thus gastric irritation can be minimized by concomitant administration of aspirin with the selected AA.

However, this increase in solubility of aspirin in the presence of AA also exhibits increased solubility of aspirin itself. It would result in the increased bioavailability and thus therapeutic toxic

Table 1. Influence of various amino acids on the solubility of aspirin (Results are expressed as the mean ± standard deviation, n = 3).

Time (min)	Absorbance of aspirin	Absorbance of aspirin after adding various amino acids				
		Glycine	Tyrosine	Glutamic acid	Tartaric acid	Aspartic acid
10	0.95 ± 0.02	2.97 ± 0.25	2.90 ± 0.23	2.91 ± 0.11	3.21 ± 0.41	3.13 ± 0.54
20	0.96 ± 0.04	2.97 ± 0.31	2.91 ± 0.32	2.92 ± 0.19	3.22 ± 0.38	3.22 ± 0.33
30	0.97 ± 0.04	2.97 ± 0.29	2.93 ± 0.37	2.92 ± 0.39	3.22 ± 0.52	3.25 ± 0.40
40	0.98 ± 0.03	2.97 ± 0.30	2.94 ± 0.18	2.92 ± 0.32	3.22 ± 0.35	3.26 ± 0.49
50	0.99 ± 0.01	2.97 ± 0.21	2.95 ± 0.20	2.92 ± 0.28	3.22 ± 0.50	3.28 ± 0.22
60	0.99 ± 0.02	2.98 ± 0.27	2.96 ± 0.26	2.92 ± 0.20	3.23 ± 0.47	3.28 ± 0.26

Table 2. General properties of selective amino acids.

Name	Solubility (g/100 mL of water at 25°C)
Aspirin	0.0032
Glycine	24.9910
Tyrosine	0.0453
Glutamic acid	0.8641
Tartaric acid	0.1002
Aspartic acid	0.7781

ity can be observed. It is therefore suggested to the prescribers, to instruct the patients to avoid the use of amino acids along with these selective AA (5).

It is also evident from the results that the increase in absorbance of aspirin in the presence of tartaric acid and aspartic acid was non-significantly ($p > 0.05$) greater than that of other AA like glycine, tyrosine and glutamic acid. The absorbance of aspirin in the presence of tartaric acid and aspartic acid was 3.23 and 3.28, respectively, while the absorbance of aspirin in the presence of glycine, tyrosine and glutamic acid was 2.98, 2.96 and 2.92, respectively (Tab. 1). The possible reason for this increased absorbance by aspirin in the presence of tartaric acid and aspartic acid could be due to the presence of high number of hydroxyl groups present in these amino acids (Fig. 1).

This study is interesting not only for pharmacists but also for nutritionists, rather for clinical nutritionists dealing with parenteral feeding. There are several studies in the literature in which interaction of aspirin with high protein products of vegetable or animal origin has been discussed. Odou et al. found significant ($p < 0.05$) effect of concomitantly administered beverages (milk, spirit, and beer) on the pharmacokinetics of orally administered aspirin in healthy human volunteers (17). Yoovathaworn et al. (18) and Thithapandha (19) also determined the influence of caffeine on the pharmacokinetic parameters of aspirin in twelve healthy male human. Both research groups observed that caffeine significantly ($p < 0.05$) increased the rate of aspirin absorption (18, 19).

LIMITATION OF STUDY

In a normal diet for a healthy person or patient (except for parenteral nutrition), amino acids are not generally present as a single molecule, they must compete with many other components. This study should therefore, be expanded to a complex system of nutrients.

CONCLUSION

This study elaborates that the solubility of aspirin increases with concomitant administration of AA, thus the use of AA (proteinous foods) with aspirin should be prohibited or low dose of aspirin should be recommended in such situation. The results of this study will help in prescribing aspirin with these selective AA to avoid any biological incompatibility, i.e., incompatibility between drug and food.

REFERENCES

1. Schror K.: Acetylsalicylic acid. 4th edn., p. 25, Ameer Publishers, Canada 2006.
2. Enger E.D., Ross F.C., Bailey D.B.: Concepts in biology. 12th edn., McGraw-Hill, Boston 2007.
3. IARC Working Group on the Evaluation of Cancer Preventive Agents, International Agency for Research on Cancer, Non-steroidal Anti-inflammatory Drugs, Spain.
4. Stoker H.S.: General, Organic, and Biological Chemistry. 5th edn., p. 15, Huvian Publishers, Amsterdam 2002.
5. Connors K.A., Connors K.A., Amidon G.L.: Chemical Stability of Pharmaceuticals. 2nd edn., p. 222, Saber Publishers, Barcelona 2005.
6. Saeb K.: Instant pharmacology. p. 187, Nui Publishers, Auckland 2003.
7. Seager S.L., Slabaugh M.R.: Chemistry for Today: general, organic and biochemistry. 3rd edn., p. 203, Saber Publishers, Barcelona 1996.
8. Stolerman L.P.: Encyclopedia of Psychopharmacology. 7th edn., p. 1, Nevian Publishers, Sydney 1994.
9. Fried B., Sherma J.: Thin layer chromatography. vol. 4, p. 289, SRS Publishers, Kolkata 1999.
10. Murtaza G., Khan S.A., Shabbir A., Mahmood A., Asad M.H.H.B., Farzana K., Malik N.S., Hussain I.: Sci. Res. Essays 6, 417 (2011).
11. Agarkar P.H., Maheshwari V.L., Kulkarn Y.A.: Biochemistry for Nursing. 3rd edn., p. 3, CBC Publishers, Mumbay 1987.
12. The Merck Index, Merck & Co., Inc., Whitehouse Station, NJ 1996.
13. Gupta V.: Handbook of Chemistry and Physics. p.58, CRC Press, Cleveland 1977.

14. Agarkar P.H., Maheshwari V.L., Kulkarn Y.A.: Biochemistry for Nursing. 5th edn., p. 3, CBC Publishers, Mumbay 1992.

15. Rasool F., Ahmad M., Khan H.M.S., Khan S.A., Murtaza G.: Asian J. Chem. 23, 3815 (2011).

16. Murtaza G.: Latin Am. J. Pharm., 30, 1389 (2011).

17. Odou P., Barthelemy C., Robert H.: J. Clin. Pharm. Therap. 26, 187 (2001).

18. Yoovathaworn K.C., Sriwatanakul K., Thithapandha A.: Eur. J. Drug Metab. Pharmacokinet. 11, 71 (1986).

19. Thithapandha A.: J. Med. Assoc. Thai. 72, 562 (1989).

THE IMPACT OF LIPOSOMES ON TRANSDERMAL PERMEATION OF NAPROXEN – *IN VITRO* STUDIES

DOROTA SZURA[1], ŁUKASZ OZIMEK[1], MAGDALENA PRZYBYŁO[1], KATARZYNA KARŁOWICZ-BODALSKA[2], EWA JAŹWIŃSKA-TARNAWSKA[3]*, ANNA WIELA-HOJEŃSKA[3] and STANISŁAW HAN[2]

[1]NOVASOME Research & Development Centre, Olsztyńska St. 5, 51-423 Wrocław, Poland;
[2]Wrocław Medical University, Department of Industrial Pharmacy,
Borowska St. 211A, 50-556 Wrocław, Poland
[3]Wrocław Medical University, Department of Clinical Pharmacology,
Bujwida St. 44, 50-345 Wrocław, Poland

Abstract: The possibility of applying liposomes as a topical drug delivery system is still a matter of intensive research. The purpose of this study was to determine the suitability of liposomes as carriers of naproxen and to prove their impact on the effectiveness of transdermal permeation of an active substance. The study was conducted with the use of Franz Diffusion Cell System by comparing the efficacy of a preparation containing 20% of phosphatidylcholine (PC) and 10% of naproxen with reference preparations, i.e., a formulation containing 10% of naproxen without PC and the commercial product Naproxen 10%, gel. The largest transdermal penetration flux of naproxen and the highest efficacy of naproxen permeation were obtained for the formulation containing 10% of naproxen and 20% of PC. The study of the influence of liposomes size and topology on the transdermal diffusion of naproxen (large unilamellar vesicle, LUV, multilamellar vesicle, MLV) showed that there was no statistically significant difference in the flux or total amounts of transdermally diffused naproxen between compared formulations. In conclusion, liposomes present in a formulation double the efficacy of the transdermal permeation of naproxen *in vitro* compared to reference preparations containing no carriers. Better permeation effect of a formulation was not related to the liposome type (LUV or MLV).

Keywords: naproxen, liposomes, phosphatidylcholine, transdermal permeation.

The most popular forms of administration for naproxen (non-steroidal anti-inflammatory drug – NSAID) (1) are oral and transdermal. Oral administration is limited by the potential risk of adverse effects (AE) affecting primarily the gastrointestinal tract (2, 3). Therefore, the tolerance for classical oral forms of NSAIDs (including naproxen) is often poor and in some patients their use may lead to many unwanted symptoms, such as: nausea, vomiting, indigestion, pain, diarrhoea and constipation (4), as well as gastric ulcer and gastrointestinal bleeding (5). Because of these adverse effects, associated with the oral NSAIDs delivery, alternative routes of naproxen administration were introduced, such as transdermal preparations. The transdermal route is more and more often used for products containing NSAIDs in the local treatment of pain associated with muscle and joint inflammation (6). Contemporary pharmaceutical technology has enabled topical drug administration to provide systemic effects (7). Transdermal systems of drug administration have many advantages compared to traditional routes, including small but long-lasting and stable release of an active substance to the system and fewer adverse effects associated with medication. In 1994, Singh et al. showed that local concentration of NSAIDs, including naproxen, in the subcutaneous tissues is proportional to the transdermal permeation rate of the active substance (6). However, due to the protective function of the skin, there are in its structure many barriers restricting possible ways of drug delivery to and through the skin. Therefore, many strategies are still under investigation with the aim to increase the potential of the transdermally delivered substances to permeate the skin.

There are two main reasons for low efficacy of transdermal preparations containing naproxen: poor

---

* Corresponding author: e-mail: tje1@wp.pl

solubility of naproxen in the aqueous phase (water solubility approximately 15.9 mg/L at 25°C, logP = 3.18 (8, 9), which explains why it is frequently used in preparations in a form of crystals, and high resistance of the stratum corneum (SC) of the skin to external factors. The efficacy of a naproxen containing product could be ameliorated by improving the solubility of naproxen in a formulation and by applying the, so called, permeation enhancers. However, substances used as permeation enhancers, e.g.: surfactants, organic solvents or substances altering skin permeability, give rise to adverse effects themselves (10). Transdermal drug permeation enhancers may cause local irritation or erythema, therefore, intensive search is carried on for efficient and safe carrier systems (11-13). Different nanoparticles have been tested, which could be used as a transdermal carrier system. For example, Kirjavainen et al. have shown that phospholipids (liposomes) used as a carrier system increase the level of estradiol, progesterone and propanolol penetration to the lipid layer of SC (14). There are many advantages of applying liposomes since phospholipids which build liposomes are non-toxic, non-immunogenic, biocompatible and biodegradable. Yokomizo et al. showed that phospholipids containing unsaturated fatty acids are strong promoters of transdermal permeation for some topically applied drugs (15), while Valjakka-Koskela et al. proved that phospholipids and other co-solvents (ethanol and propylene glycol) help to increase the transdermal penetration flux of naproxen (16). Other studies evaluated the influence of phospholipids and unsaturated fatty acids on the increased transdermal permeation of naproxen (17, 18). It was shown that liposomes built of phospholipids containing unsaturated fatty acids induced increased transdermal drug permeation and its distribution into tissues to higher degree than its accumulation in the skin.

Liposomal delivery systems (LDSs) are carrier systems which encapsulate or attach a hydrophobic or hydrophilic substance (e.g., a drug) and thereby change its pharmacokinetic properties. The use of phospholipids in pharmaceutical preparations and their influence on the skin has been discussed in many publications (19-21). Liposomes may impact the kinetics of a given drug in many ways, which largely depend on composition and physicochemical properties of liposomes (22-24). When applied to the skin, liposomes may either increase the local concentration of a drug by streaming the active substance into target tissues, or decrease the intensity of side effects, or increase the amount of the active substance to be delivered to the system (25, 26).

Four major mechanisms have been described for the liposomal enhancement of the transdermal permeation of an active substance. They are: the impact on the diffusion of a free drug, the impact on increased transdermal permeation, the impact on the fusion with SC, and, the most controversial one, the impact on the permeation of intact liposomes (together with the active substance encapsulated within liposome) (25-27). The mechanism of liposomal influence on drug activity may depend on size, structure and composition of liposomes, and also on the route of administration (occlusive or nonocclusive technique) (23).

The purpose of the study conducted and presented here was to demonstrate the suitability of liposomes as naproxen carriers.

MATERIALS AND METHODS

Materials

The permeability of formulations being compared was tested *in vitro* using the Franz diffusion cell system on the pig ear skin, which is well recognized substitute for human skin (the test material was obtained from animals from the Institute of Animals of the Wrocław University of Environmental and Life Sciences; according to Resolution 22/2006 of the National Ethic Committee for Experimental Animals of 7 November 2006, § 1 p. 2b no local ethic committee's consent is required to conduct such experiments.

The permeation efficacy of the drug from various formulations was compared for the experimental formulation containing 10% of naproxen and 20% of phosphatidylcholine (PC) in a form of liposomes and for the reference formulations: a naproxen product having the same composition but no PC and the commercial product Naproxen 10%, gel. The study of the effect of size and topology of liposomes on the efficacy of permeation was tested comparing the rate of transdermal diffusion of naproxen from a formulation containing calibrated, large unilamellar vesicles (LUV) of 125 ± 10 nm diameter, PDI = 0.150 and from a formulation containing multilamellar vesicles (MLV).

Reagents

The following reagents were used: phosphatidylcholine (PC) (Phospholipon 90NG) from Phospholipid (Colony, Germany), propylene glycol (PGly) from DOW Europe (Frankfurt a/M, Germany), naproxen from Zhejiang Charioteer Pharmaceutical (Shanghai, China), phosphate buffer

(PBS) from Sigma-Aldrich (Steinheim, Germany). The remaining reagents (acetonitrile, KH_2PO_4, orthophosphoric acid, ethanol) were analytically pure and they were obtained from Chempur (Piekary Śląskie, Poland).

Test formulations containing naproxen

1. 10% of naproxen, 20% of PC, 20% of PGly, 50% of PBS; 2. 10% of naproxen, 20% of PGly, 70% of PBS; 3. a commercial gel, containing 10% of naproxen (Hasco-Lek, Poland); 4A. 2.8% of naproxen, 20% of PC (MLV), 20% of PGly, 57.2% of distilled water; 4B. 2.8% of naproxen, 20% of PC (LUV), 20% of PGly, 57.2% of distilled water.

Methods
The preparation and characteristics of liposomes

In order to prepare the formulation containing naproxen, the adequate amount of lipid (depending on the test formulation) was dissolved in propylene glycol. The solution was stirred intensively at 50°C. Then, powdered naproxen was added. A clear, light-yellow solution was obtained and mixed with water/buffer. This produced multilamellar vesicles (MLV) which were then calibrated through two polycarbonate membranes with pore diameter of 100 nm (Nucleopore, Whatman, England) using the Avestin Emulsiflex C50 extruder (Avestin, Ottawa, Canada) to obtain large unilamellar vesicles (LUV) of 125 ± 10 nm diameter, PDI = 0.150. The size of liposomes was determined using the dynamic light scattering technique (Zetasizer Nano S, Malvern Instruments, Malvern, England).

The transdermal diffusion testing (diffusion method)

The Franz diffusion test was used to measure the transdermal permeation of naproxen (PermeGear, Hellertown, USA). The Franz diffusion cell system is composed of the donor and acceptor compartments, and the skin is attached between them. The skin patches were cut out from the dorsal area of a pig's ear. They were physically removed from defrosted pig ears using a scalpel. The skin was then cut into smaller patches of approximately 1 cm in diameter, and hair was removed using scissors. The quality and intactness of each skin patch was checked by measuring impedance ($k\Omega/cm^2$) according to the method described in detail in (28). The patches for which the value of impedance was greater than or equal to 27 $k\Omega$ (MT 4090 LCR Meter, Motech Instruments, Tainan, Taiwan) were used for further tests. Patches so prepared were stored at –20°C and defrosted immediately before testing. Round skin fragments were gently placed on the receptor compartment of the diffusion cell so that the epidermis was facing the donor compartment. The receptor compartment was filled with PBS and the cells were then incubated at 32°C (which corresponded to the temperature of human skin) using an external water coat. After 30 min of conditioning of the pig skin with receptor solution, approximately 50 mg of the test formulation was applied onto the donor compartment of each cell using a plastic syringe. The receptor solution was continuously stirred throughout the experiment by a magnetic stirrer at 400 rpm. After 20 h of incubation, the diffused cells were carefully disassembled. Transdermal permeation of naproxen was calculated on the basis of its concentration in the acceptor compartment. The accuracy of calculations was confirmed by determining the total recovery of naproxen from each compartment. Only these results were used for further calculations for which the total recovery of naproxen was from 90 to 100%. Each experiment with Franz diffusion cells was performed using 9 cells for each formulation.

HPLC analysis

The concentration of naproxen in the acceptor compartments was determined spectrophotometrically, using the high performance liquid chromatography. The HPLC analysis was carried out using the Agilent 1200 system chromatograph (Agilent Technologies) with a UV-VIS (254 nm) detector and a column thermostat (50°C). The stationary phase was a chromatographic column filled with LiChrospher® 100, 250 × 4.6 mm, RP-18 and pore diameter of 5 μm from Merck (Germany). The mobile phase was composed of a mixture of 10 mM KH_2PO_4 pH 2.0 and acetonitrile 58 : 42 (v/v), injected in isocratic conditions onto the column at the rate of flow of 1.5 mL/min.

The method was validated for specificity, linearity, precision, accuracy, robustness, limit of detection and quantitation (29). The accuracy of the method was between 96.8–101.3% (average 99.1%, RSD = 1.5%) and the calibration curve was linear (R^2 = 0.99) over naproxen concentrations ranging from 35.8 to 86.4 μg/mL. The limit of detection (LOD) and limit of quantitation (LOQ) were 7.81 ng/mL and 26.00 ng/mL, respectively. The method was found to be specific, precise, accurate, and reproducible.

The results were statistically analyzed using Student *t*-test and Snedecor F test. The statistical significance of difference for the Snedecor F test was estimated at p = 95% (31).
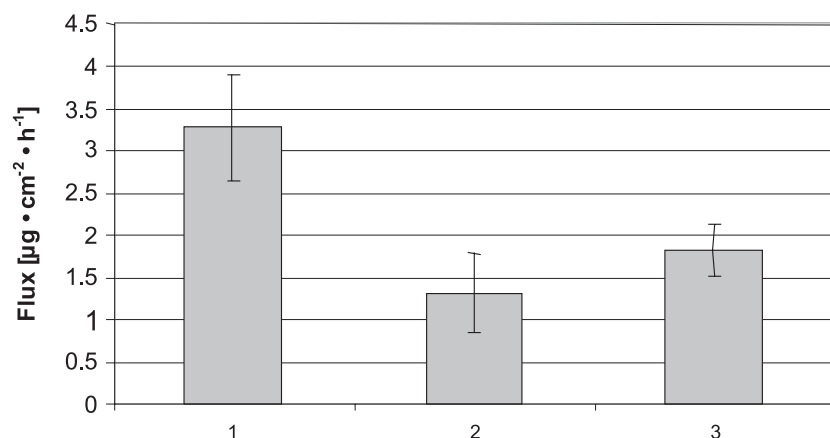
Figure 1. Average values of naproxen flux for three test formulations. Error posts indicate standard deviation. 1 – formulation containing 10% of naproxen and 20% of PC; 2 – formulation containing 10% of naproxen and no PC; 3 – commercial product Naproxen 10%, gel
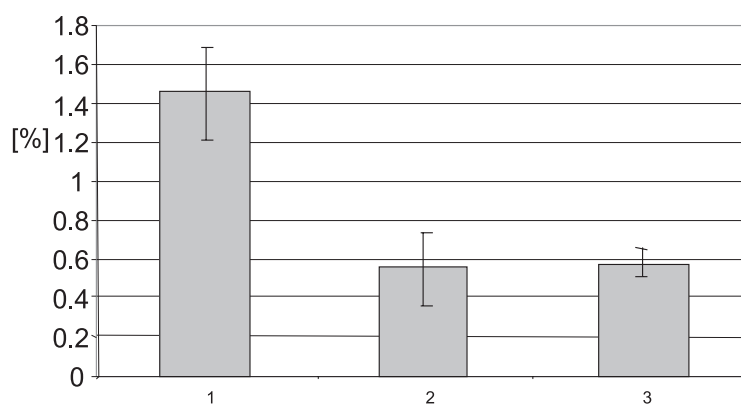
Figure 2. The fraction of the active substance transported across the skin under the experimental conditions, expressed as a percentage of naproxen applied to the skin. 1 – formulation containing 10% of naproxen and 20% of PC; 2 – formulation containing 10% of naproxen and no PC; 3 – commercial product Naproxen 10%, gel

RESULTS

The influence of liposomes on the transdermal permeation of naproxen

The influence of liposomes on the naproxen transport across the skin of pig's ear was analyzed by comparing for various formulations the amount of the active substance that passed through the skin from the test formulations to the acceptor compartment of the diffusion cell.

Results were presented as the total amount of naproxen [μg] transported across 1 cm² of skin as a function of time (flux). The average values of naproxen flux obtained in 9 repetitions of the experiment are presented in Figure 1.

The greatest transdermal flux of naproxen was obtained for the formulation containing 10% of naproxen and 20% of PC. When compared to other formulations, the difference was statistically significant.

The efficacy of transdermal permeation of naproxen can also be expressed as the ratio of the amount of naproxen transported across the skin to the amount of naproxen applied to the skin (in %). The average values obtained in 9 repetitions were: 1.45 ± 0.4% for formulation (1), 0.55 ± 0.18% for formulation (2), and 0.58 ± 0.07% for formulation (3). The formulation (1) which contained liposomes was found to be much more efficient that the other two, and the difference was statistically significant (Fig. 2).

Table 1. The flux and the fraction of transdermally diffused naproxen to the total amount of naproxen applied to the skin.

Naproxen formulation	Flux [μg / cm² / h]	Percentage [%]
(A)	4.58 ± 2.83	6.35 ± 2.82
(B)	3.95 ± 2.13	4.88 ± 1.91

(A) – formulation containing MLV liposomes; (B) – formulation containing LUV liposomes

The results have shown that the efficacy (measured as the permeability rate) of the preparation containing 10% of naproxen with the addition of liposomes was two times higher than that of the test reference preparations containing no PC.

The influence of the liposome size on the transdermal permeability of naproxen

The influence of the liposome size on the transdermal diffusion of naproxen was tested by comparing the efficacy *in vitro* of two formulations containing 2.8% of naproxen and 20% of PC, where one formulation contained large unilamellar vesicles (LUV) (4B) and the other multilamellar vesicles (MLV) (4A). The average values from the repeated experiments, expressed as a fraction of naproxen applied to the skin which passed to the receptor compartment was 6.35 ± 2.82% for formulation A and 4.88 ± 1.91% for formulation B. The results have shown that there is no statistically significant difference between both formulations when the fluxes or the amounts of transdermally diffused naproxen are compared (Table 1).

DISCUSSION

Transdermal delivery of systemic drugs is a way to avoid factors which impact the gastrointestinal absorption of an active substance, such as pH, food or motor behavior of the gastrointestinal tract. Moreover, skin application of a drug is advantageous for drugs with little bioavailability as the so called first-pass effect can be eliminated (31). Unfortunately, transdermal drug administration is problematic as skin permeability for both hydrophobic and hydrophilic substances is small due to the fact that skin is the natural protective barrier (31). The major barrier for exogenic substances is the external epidermal layer (SC) (32). It is built of a highly ordered lipid structure localized between corneocytes (33). Therefore, in order to increase the intensity of the transdermal permeation of drugs, and to increase the efficacy of these drugs, a variety of modifiers are used enhancing skin permeability (14).

Naproxen is an anti-inflammatory drug sparingly soluble in water. As the gradient of concentration between the formulation and epidermis is low, the transport of naproxen across the skin after topical application is also small. Low gradient is caused by low concentration of naproxen in the formulation. The majority of commercial formulations contain naproxen in the form of crystals that are unable to pass through the skin barrier (no results are presented here). One of possibilities of improving the transdermal transport of naproxen is to increase its solubility. This can be done by using complex macromolecular mixtures containing for example cyclodextrins, hydrophilic polymers (34), amino acids (35) or polyvinylpyrrolidone (PVP) (36, 37). In their work, Zerrouk et al. have tested the ability of PVP and chitosan to increase the solubility and absorption of naproxen. They showed that both these ingredients increased the solubility of the drug (27, 38).

The use of micelles, microemulsion or liposomes as drug carriers largely contributes to the increased stability and bioavailability of the drug and reduces the risk of adverse effects. Micelles and microemulsions have already been used to enhance naproxen solubility. Poloxamer gel 409 (PF-127) significantly increased solubility of naproxen by spontaneous formation of micelles containing naproxen. Due to this effect the amount of naproxen in a non-crystalline form significantly increases resulting in the rise of its effective concentration, which should facilitate the transdermal permeation. This effect is a linear function of PF-127 concentration (16). In another example, Correa et al. showed that better solubility of naproxen in the presence of an emulsion stabilized by hexadecyltrimethylammonium bromide, containing isopropyl myristate or butyl stearate, is directly proportional to the volume of the microemulsion phase and that it depends on pH (39).

The purpose of the study presented here was to obtain a naproxen containing formulation for transdermal administration with the efficacy better than traditional ointments or gels. In this context, drug

efficacy is understood as its ability to pass through the skin of pig ear, which was tested using the Franz diffusion cell method. In order to improve solubility of naproxen and to enhance the skin permeability liposomes were added to the formulation base.

Liposomes are more and more frequently used as efficient drug carriers. They have also been the subject of studies which have recently gained in intensity. The structure of liposomes is such that they encapsulate drug particles inside a vesicle or build particles into their membrane. In addition to that, liposomes as skin modifiers enhance the transdermal transport of an active substance and skin absorption, which makes them efficient and popular drug carriers. There are many examples in the literature of the influence of liposomes on the enhanced transdermal permeation and absorption of different active substances (40–42). In the studies discussed here, the transdermal transport of naproxen in the presence of liposomes was two times higher compared to the reference formulations.

These experiments were conducted using liposomes built of natural phosphatidylcholine. The most recent studies on this type of liposomes have shown that in the majority of cases the classic liposomes fail to pass into the lower parts of skin intact, and that their activity is rather limited to the superficial layers of SC (43). We suggest three possible mechanisms of liposomal activity used in our studies: (i) liposomes improve solubility of naproxen, (ii) liposomes act directly on SC by lowering the natural permeability barrier, and (iii) phospholipids form a thin film on the skin surface, which facilitate the transport of the drug from the formulation into the skin.

The transport of an active substance from liposomes across the skin is determined by such factors as: the composition of lipids, the lamellar structure and the liposomal surface charge. Little is known about the effect the liposome size has on the transdermal permeability and absorption of drugs. The correlation between these parameters has not yet been established. Du Plessis et al. compared effects of topical administration of lipophilic substances: cyclosporine and cholesterol sulfate in the presence of liposomes of various size (44). They showed that medium size liposomes (300 nm, 600 nm) are better absorbed to the SC than the small ones (60 nm), but do not permeate to the deeper skin layers. Michel et al. have proved that there was an insignificant difference in the amount of the lipophilic drug that passed through the skin when SUVs ((small, unilamellar vesicles, < 50 nm) or MLVs (> 130 nm) were used as a carrier (34). The studies of the influ-

ence of the liposome size on the transport of hydrophilic substances were conducted by Šentjurc et al. (45). Their results show that the transdermal transport of a drug is independent of the size of liposomes, irrespective of the type or composition of the test liposomes and niosomes, as long as their diameter is less than 200 nm. For smaller nanoparticles, transport is significantly decreased. They also proved that small liposomes are unstable and decompose immediately upon contact with various surface types (44). Other studies, conducted by Verma et al. focused on the effect the size of carrier particles has on the transport of two marked fluorescent substances across the human skin. Their data confirmed that liposomes of 120 nm diameter improve the transport of carboxyfluorescein to the skin compared to larger liposomes (24).

The results above clearly show that the type of liposomes added to the formulation (MLV or LUV) is insignificant as far as the effect on the transdermal transport of naproxen is concerned. The *in vitro* studies showed that the formulation containing naproxen encapsulated in liposomes built of phosphatidylcholine significantly improved the transdermal transport of the drug. Under the experimental conditions, the amount of naproxen that passed through the skin was two times greater compared to the reference formulation containing the same amount of naproxen but no liposomes. Probably the same effect will be obtained *in vivo*, but further studies still need to be conducted. It is suggested that the mechanism of liposomal activity is complex and multileveled. This could be explained by the fact that liposomes act as co-solvents and/or skin modifiers. A complete understanding of the actual mechanism of these phenomena should help to design new and more efficient formulations containing naproxen.

Acknowledgment

REFERENCES

1. Rainsford K.D.: Subcell. Biochem. 42, 3 (2007).
2. Bensen W., Weaver A., Espinoza L., Zhao W.W., Riley W., Paperiello B., Recker D.P.: Rheumatology 41, 1008 (2002).
3. Lane M.E., Kim M.J.: J. Pharm. Pharmacol. 58, 1295 (2006).

4. Castellsague J., Riera-Guardia N., Calingaert B., Varas-Lorenzo C., Fourrier-Reglat A., Nicotra F., et al.: Drug Saf. 35, 1127 (2012)

5. Castellsague J., Pisa F., Rosolen V., Drigo D., Riera-Guardia N., Giangreco M., Clagnan E., et al.: Pharmacoepidemiol. Drug Saf. 22, 365 (2013).

6. Singh P., Roberts M.S.: J. Pharmacol. Exp. Ther. 268, 144 (1994).

7. Cevc G., Blume G., Schätzlein A., Gebauer D., Paul A.: Adv. Drug Deliv. Rev. 18, 349 (1996).

8. Hansch, C. Leo A., Hoekman D.: in Exploring QSAR Hydrophobic, Electronic, and Steric Constants, p. 23, American Chemical Society, Washington, DC 1995.

9. Yalkowsky S.H., Dannenfelser R.M.: Aquasol. Database of Aqueous Solubility. Version 5. College of Pharmacy, University of Arizona at Tucson, AZ 1992.

10. Barry B.W., Bennett S.L.: J. Pharm. Pharmacol. 39, 535 (1987).

11. Kanikkannan N.: BioDrugs 16, 5, 339 (2002).

12. Gao Y., Liang J., Liu J., Xiao Y.: Int. J. Pharm. 377, 128 (2009).

13. Ammar H.O., Salama H.A., El-Nahhas S.A., Elmotasem H.: Curr. Drug Deliv. 5, 290 (2008).

14. Kirjavainen M., Monkkonen J., Saukkosaari M., Valjakka-Koskela R., Kiesvaara J., Urtti A.: J. Control. Release 58, 207 (1999).

15. Yokomizo Y., Sagitani H.: J. Control. Release 42, 37 (1996).

16. Suh H., Jun H.W.: Int. J. Pharm. 129, 13 (1996).

17. Puglia C., Bonina F., Rizza L., Cortesi R., Merlotti E., Drechsler M., Mariani P. et al.: J. Pharm. Sci. 99, 2819 (2010).

18. Ustündağ Okur N., Apaydın S., Karabay Yavaşoğlu N.Ü., Yavaşoğlu A., Karasulu H.Y.: Int. J. Pharm. 416, 136 (2011).

19. Foldvari M., Gesztes A., Mezei M.: J. Microencapsul. 7, 479 (1990).

20. Ganesan M.G., Weiner M.D., Flynn G.L. Ho N.F.H.: Int. J. Pharm. 20, 139 (1984).

21. Kirjavainen M., Urtti A., Jääskeläinen I., Suhonen T.M., Paronen P., Valjakka-Koskela R., Kiesvaara J., Mönkkönen J.: Biochim. Biophys. Acta 1304, 179 (1996).

22. Langner M.: Pol. J. Pharmacol. 52, 3 (2000).

23. Pérez-Cullell N., Coderch L., de la Maza A., Parra J.L., Estelrich J.: Drug Deliv. 7, 7 (2000).

24. Verma D.D., Verma S., Blume G., Fahr A.: Int. J. Pharm. 258, 141 (2003).

25. El Maghraby G.M., Barry B.W., Williams A.C.: Eur. J. Pharm. Sci. 34, 203 (2008).

26. El Maghraby G.M., Williams A.C., Barry B.W.: J. Pharm. Pharmacol. 58, 415 (2006).

27. Zerrouk N., Mennini N., Maestrelli F. Chemtob C., Mura P.: Eur. J. Pharm. Biopharm. 57, 93 (2004).

28. Karande P., Jain A., Mitragotri S.: J. Control. Release 110, 307 (2006).

29. Note for guidance on validation of analytical procedures: Text and methodology. CPMP/ICH/381/95 EMEA (1995).

30. Konieczko P., Namieśnik J.: Evaluation and quality control of analytical measurements results (Polish). WTN, Warszawa 2007.

31. Honeywell-Nguyen P.L., Bouwstra J.A.: Drug Deliv. Today: Technologies 2, 67 (2005).

32. Kielhorn J.M-K.S, Mangelsdorf I.: in Environmental Health Criteria, p. 253, Raport of World Health Organization, 2006.

33. Elias P.M., Friend D.S.: J. Cell Biol. 65, 180 (1975).

34. Michel C., Purmann T., Mentrup E., Seiller E., Kreuter J.: Int. J. Pharm. 84, 93 (1992).

35. Faucci M.T., Mura P.: Drug Dev. Ind. Pharm. 27, 909(2001).

36. Cirri M., Maestrelli F., Corti G., Furlanetto S., Mura P.: J. Pharm. Biomed. Anal. 42, 126 (2006).

37. Mura P., Faucci M.T., Bettinetti G.P.: Eur. J. Pharm. Sci. 13, 187 (2001).

38. Mura P., Zerrouk N., Mennini N., Maestrelli F., Chemtob C.: Eur. J. Pharm. Sci. 19, 67 (2003).

39. Correa M.A., Scarpa M.V., Franzini M.C., Oliveira A.G.: Colloids Surf. B: Biointerfaces 43, 108 (2005).

40. Elmoslemany R.M., Abdallah O.Y., El-Khordagui L.K., Khalafallah N.M.: AAPS PharmSciTech. 13, 723 (2012).

41. Song Y.K., Hyun S.Y., Kim H.T., Kim C.K., Oh J.M.: J. Microencapsul. 28, 151 (2011).

42. Dubey V., Mishra D., Nahar M., Jain V., Jain N.K.: Nanomedicine 6, 590 (2010).

43. Elsayed M.M.A., Abdallah O.Y., Naggar V.F., Khalafallah N.M.: Int. J. Pharm. 332, 1 (2007).

44. Du Plessis J., Ramachandran C., Weiner N., Müller D.G.: Int. J. Pharm. 103, 277 (1994).

45. Sentjurc M., Vrhovnik K., Kristl J.: J. Control. Release 59, 87 (1999).

CHARACTERIZATION OF GLICLAZIDE RELEASE FROM ISABGOL HUSK HYDROGEL BEADS BY VALIDATED HPLC METHOD

VIPIN K. SHARMA[1]* and B. MAZUMDAR[2]

[1]Department of Pharmaceutical Sciences, Faculty of Ayurved and Medical Sciences
Gurukul Kangri University, Haridwar-249404, Uttarakhand, India
[2]Department of Pharmaceutical Sciences, Dibrugarh University, Dibrugarh-786004, Assam, India

Abstract: *Isabgol* husk, a medicinally important natural polysaccharide was applied for fabrication of hydrogel beads by ionic gelation method to incorporate gliclazide. Different strengths of *Isabgol* husk and sodium alginate were utilized for assessing the process variables on formulation performance. Aqueous solution of calcium chloride in 2, 5 and 8% w/v strength was used as cross-linker for polymeric blends of *Isabgol* husk and sodium alginate. The formulations were characterized for various parameters such as particle size, swelling index, entrapment efficiency, *in vitro* release, and release kinetics. The quantification of gliclazide throughout the study was performed by HPLC method which was validated according to ICH guidelines for system suitability, linearity, accuracy, sensitivity, precession, robustness, and ruggedness. The surface morphology of beads was observed by scanning electron microscopy. The formed beads were brown, free flowing, spherical, and irregular in structure. The size in different formulations varied from 752.83 ± 0.630 to 838.62 ± 0.741 μm. The beads remained for 2–3 h in alkaline phosphate buffer (pH 7.4), after that they showed disintegration. The formulations released up to 95% of loaded gliclazide in phosphate buffer (pH 7.4) within 8 h. No significant difference was observed in parameters studied such as particle size, entrapment efficiency and swelling index for hydrogel beads during accelerated stability study (p > 0.05). The regression equation developed by HPLC method was linear (r^2 > 0.9990) over the range 2.5 to 10 μg/mL. The limit of detection (LOD) and limit of quantification (LOQ) were 0.037619 μg/mL and 0.113997 μg/mL, respectively. The observed values for number of theoretical plates (N ≥ 2000), tailing factor (T ≤ 2), asymmetry factor (AF ≤ 1), and relative standard deviation (RSD ≤ 1%) of applied method showed the reliability for gliclazide estimation in *Isabgol* husk hydrogel beads.

Keywords: validation, *Isabgol* husk, cross-linking, *in vitro* release

The pharmaceutical formulations such as conventional and controlled release are prepared by using different excipients with drug(s) and are used to solve the main aim of making the incorporated drug(s) available at desired site of action in required quantity. In conventional dosage forms, the fluctuations of drug concentration in blood occur that sometimes create the available dose level of drug below and upper to the therapeutic window. Amongst different categories of drug delivery devices, solid formulations are administered through oral route and follow a certain rate to achieve therapeutic drug concentration. Before absorption, these formulations undergo disintegration and dissolution in gastrointestinal fluid. This step of absorption from gastrointestinal tract (GIT) affects the bioavailability of the formulations. The fluctuations in bioavailability are considered mainly due to insufficient dissolution and subsequent absorption of the drug from the GIT. In case of water insoluble drugs, these factors have more impact on desired therapeutic level of the drug. In sustained release dosage forms, the release of drug is slow and compatible with the rate of absorption that results minimal loss of drug in GIT by presystemic metabolism. Hence, it becomes necessary to a drug delivery device to release the incorporated drug(s) in required manner to attain a desired concentration for a desired time in systemic circulation (means bioavailability) so that it may achieve the therapeutic goal, e.g., therapeutic efficacy. In sustained release formulations, special attention is given to microparticulate drug delivery devices due to their efficient volume to surface area ratio, small spherical size and retention to desired sites in the body in case of technically modified surface.

The applicability of different fabrication techniques depends upon the active pharmaceutical

* Corresponding author: e-mail: sharmadibru@gmail.com

ingredient (API) and polymeric carrier. The performance of the formulation to achieve the desired goal of therapeutics is also governed by polymeric network. The drug carrier of natural origin such as gums, mucilage, resins, latex etc., have been applied in development of conventional and modified drug delivery devices and draw a marked consideration due to their eco-friendly nature, low cost, safety, biocompatibility, and availability for development of novel drug delivery systems (1).

Isabgol husk is obtained from epidermal and collapsed adjacent layers removed from the seeds of *Plantago spp.* and is well known for enormous water holding capacity in contact with water for forming mucilage. It is widely used for its different therapeutic effects, e.g., ulcerative colitis, hemorrhoids, constipation, hypercholesterolemia, diabetes mellitus, colorectal cancer etc. (2). *Isabgol* husk has been used for the development of hydrophilic matrix and microparticulate system for different drugs (3). Grafted *Isabgol* structure with polyacrylamide and polyacrylonitrile have been reported for the use in flocculation study (4). Alginates are also naturally occurring polysaccharides obtained from marine brown-algae consisting of two monomeric units; β-D-mannuronic acid (M) and α-L-guluronic acid (G). These residues are arranged in homopolymeric blocks (GG, MM) and in heteropolymeric blocks (MG). Sodium alginate shows gelling properties in the presence of multivalent cations such as Ca^{2+}, Ba^{2+}, Al^{3+} etc. The cross-linked structure has marked swelling in water and acidic environment but it is sensitive towards the alkaline phosphate condition as the egg-box like structure of cross-linked alginates ruptures.

Gliclazide is an oral hypoglycemic second generation sulfonyl urea, which is useful for long term treatment of non-insulin dependent diabetes mellitus (NIDDM) (5). Previous studies showed that gliclazide possesses good general tolerability, low incidence of hypoglycemia, and low rate of secondary failure (5). For a hypoglycemic drug to be effective, rapid absorption from the gastrointestinal tract is required. However, the absorption rate of gliclazide from the gastrointestinal tract is slow and varied amongst subjects. Several studies on healthy volunteers and diabetic patients revealed that the time to reach plasma concentration (t_{max}) ranged from 2 to 8 h following a single oral administration of 80 mg of gliclazide tablet (5). The slow absorption has been suggested to be due to either hydrophobic nature or poor permeability of the drug across the GI membrane. Due to this, controlled release formulations of the said drug are available in the market as incorpo-

ration of gliclazide in such preparations may control its absorption from gastrointestinal tract and overcome the variability problems.

The present study was undertaken to assess the participation of *Isabgol* husk with sodium alginate in controlling gliclazide release from hydrogel beads and the impact of process variables on entrapment efficiency, *in vitro* release and other formulation related factors. Due to insoluble nature of gliclazide in water, aqueous ionic gelation-cross-linking technique may be an appropriate method for sustained release formulation development of gliclazide.

Besides the release of incorporated drug from drug delivery devices, the quantification of drug by suitable and routine analytical technique becomes necessary. The selective and sensitive analytical methods for quantitative determination of drugs and their metabolites are essential for successful evaluation of clinical pharmacology, pharmacokinetics (PK), bioavailability (BA) and bioequivalence (BE) studies. In this study, HPLC method was used for gliclazide quantification. The proposed method was validated for the parameters like system suitability, linearity, accuracy, sensitivity, precision, robustness and ruggedness according to ICH guidelines (6). The linearity of an analytical method is its ability to elicit that test results are proportional to the concentration of drug in samples within a given range. It is generally determined by constructing calibration curve. The accuracy is the closeness of agreement (degree of scatter) between a series of measurements obtained from multiple samplings of the same homogenous sample under prescribed conditions. It is determined by calculating % RSD of various measurements at different time, equipment or analyst.

EXPERIMENTAL

Materials

Isabgol husk, as readymade herbal remedy (Sidhpur, Gujarat), was procured from local market. Gliclazide was obtained as gift sample from Comed Pharmaceuticals Ltd., Baroda. HPLC grade methanol, water and acetonitrile were procured from Rankem, New Delhi. All other regents and chemicals were of analytical grade and used without further purification and modification.

Methods
Formation of hydrogel beads of *Isabgol* husk by aqueous ionic gelation cross-linking technique (7)

Hydrogel beads of gliclazide composing of *Isabgol* husk and sodium alginate were fabricated by

using *Isabgol* husk in different strength for facilitating the spherical beads formation. Sodium alginate was added for its hardening effect during cross-linking with calcium chloride. About 3% w/v dispersion of *Isabgol* husk and sodium alginate was prepared in distilled water and gliclazide was added in dispersion, which was homogenized at 500 rpm at room temperature. The dispersion containing gliclazide was added *via* 23-gauge needle-syringe into a gently agitated 5% w/v calcium chloride solution. The droplets instantaneously gelled into discrete, free flowing, brown colored beads upon contact with calcium chloride solution. These whitish and spherical beads were left for 30 min in cross-linker solution for curing and hardening. After curing, calcium chloride solution was decanted and each batch was washed three times successively with 500 mL of distilled water for removing unreacted calcium chloride from the surface and the beads were dried at 60°C for 10 h. Different variables such as calcium chloride concentration and sodium alginate to *Isabgol* husk ratio were studied to analyze the effect of these factors on particle size, swelling behavior, drug entrapment efficiency, *in vitro* release and release kinetics.

Particle size determination

The particle size of beads was measured microscopically by observing about 250–300 particles on a glass slide under optical microscope (Olympus, Japan) at 5× magnification. In microscopic observation, the divisions in eye piece covered by particles were counted and by multiplication with least count of ocular micrometer, the size range of particles was determined.

Swelling index

Swelling of formulations was measured gravimetrically by taking initial weight and weighing after complete swelling in swelling media on single pan electronic balance with least count of 0.1 mg. The swelling media used for swelling were distilled water, 0.1 M HCl and phosphate buffer (pH 7.4). The swelling index was calculated by following expression:

$$\text{Swelling index}(\%) = \frac{\text{Weight after swelling} - \text{Initial weight}}{\text{Initial weight}} \times 100$$

HPLC method development and optimization

The HPLC system used in the study was of CECIL (UK) CE 4200 with UV detector CE 4201; HPLC pump; injector loop Rheodyne (Model No. 2767, 20 µL volume loop). Data acquisition was performed by the POWERSYSTEM software.

Chromatographic analysis was performed on a C-18 column (250 × 4 × 60 mm, 5 µm, Luna 5u, Phenomenex). The mobile phase consisted of phosphate buffer (pH 3.4) : acetonitrile (20 : 80 v/v) and the flow rate was set at 1 mL/min. The mobile phase was filtered through 0.45 µm filter under vacuum and untrasonicated before pumping into HPLC system. The column was maintained at ambient temperature and equilibrated by pumping the mobile phase through the column for at least 30 min prior to the injection of the drug solution. The absorbance of the effluent was monitored by UV detection at 227 nm.

Drug entrapment efficiency

About 50 mg formulation was taken into 50 mL media composed of 30 mL of phosphate buffer (pH 7.4) and 20 mL methanol taken in 100 mL volumetric flask for 48 h with occasional shaking. After it, the beads with media were disintegrated for 30 min in ultrasonicator, crushed in pestle mortar and then filtered through Whatman filter paper. The filtrate following suitable dilution was analyzed by HPLC at 227 nm. The drug entrapment efficiency was determined by the following relation (7):

$$\text{Drug entrapment efficiency (\%)} = \frac{\text{Practical drug content}}{\text{Theoretical drug content}} \times 100$$

Surface morphological study

It was performed by scanning electron microscope (ZIESS EVO 40EP, Carl Zeiss, Cambridge, UK) for formulations prepared by sodium alginate, and *Isabgol* husk-sodium alginate combination. The surface study was also performed for the formulation remained after dissolution to assess the impact of dissolution on beads.

Dissolution test

The dissolution test was performed in basket type dissolution test apparatus (Model: DR-08, Campbell Electronics, Mumbai) in six replicates for each formulation at 50 rpm. The dissolution media used in the study were: distilled water, 0.1 M HCl and phosphate buffer (pH 7.4). The dissolution media were maintained at 37.5 ± 0.5°C. The sampling was performed by withdrawing 5 mL of the sample at preset time interval such as 0, 15, 30, 45, 60, 75, 90, 105, 120, 150, 180, 210, 240, 300 and 480 min and the dissolution medium was replenished by pre-warmed dissolution medium to maintain the volume constant. The samples after suitable dilution were analyzed by determining absorbance at 227 nm by HPLC method. The respective concentration of gliclazide in dissolute samples was calculated from the calibration curve obtained from

pure sample of gliclazide. The dilution factor was applied as follows to determine the accurate concentration of gliclazide in each sample withdrawn:

$$C_n = O_n[\frac{V_1}{V_t - Vs}] \times [\frac{C_{n-1}}{O_{n-1}}]$$

where C_n is the corrected concentration of nth sample, O_n is the original concentration of the nth sample, V_t is the volume of the dissolution medium, Vs is the volume of the sample withdrawn, C_{n-1} is the corrected concentration of the $(n-1)^{th}$ sample and O_{n-1} is the original concentration of the $(n-1)^{th}$ sample.

Release kinetics analysis

The release behavior of gliclazide in different media was analyzed by zero order, first order, Korsmeyer-Peppas, Higuchi and Hixon-Crowell models by using the following expressions (8):

Zero order : $M_t = K_o t$
First order : $\log M_t = \log M_o - K_1 t / 2.303$
Korsmeyer-Peppas : $\ln M_t = n \ln t + \ln K$
Higuchi : $M_t / M_\alpha = K_h \cdot t^{1/2}$
Hixon-Crowell : $M_t^{1/3} = M_o^{1/3} - kt$

In above equations, M_t is the amount of drug released at time t and K_0, K_1 and K_H are the coefficient of respective equations.

Stability study

The accelerated stability testing of incorporated gliclazide in hydrogel was performed at 40°C and 75% RH in stability chamber (NSW-175, New Delhi) up to six months. About 100 mg of each formulation was kept in open mouth HPTE bottles at preset experimental conditions for 6 months. After 1, 3, and 6 months, the formulations were analyzed for particle size, drug content, swelling behavior and scanning of gliclazide by validated HPLC method.

Statistical analysis

In all cases, the experimentation was performed in triplicate (n = 3) where the number of studies are not mentioned. Significance of results was tested by ANOVA using Sigma State software (Sigma State 2.03, SPSS, Chicago, USA). Significance of differences was defined at p < 0.05.

RESULTS AND DISCUSSION

The beads formed after hydrogelation of *Isabgol* husk and sodium alginate were spherical in shape with irregular surface that may be due to drying effect of hydrogel at surface. The drug crystals observed on the surface were probably formed as a result of their migration along with water to the surface during drying. Similar results were also observed by Fathy et al. (9) for alginate beads composed of tiaramide. The SEM photographs of the preparations formed by *Isabgol* husk-sodium alginate and sodium alginate are shown in Figure 1. The formulations prepared with their characteristics are summarized in Table 1. The particle size of *Isabgol* husk-sodium alginate (1 : 2) beads prepared in 2% w/v calcium chloride solution was found to be 825.47 ± 1.149 μm, which decreased in 8% w/v strength of calcium chloride to 790.41 ± 1.201 μm. The effect of calcium ions on particle size was also observed in higher ratio of *Isabgol* husk to sodium alginate (3 : 4). In 2% w/v strength, the particle size was measured as 872.03 ± 0.2933 μm which was decreased to 810.33 ± 0.5533 μm in 8% w/v strength of calcium chloride. The decrement in particle size emphasized the role of calcium in tight junction formation in cross-linked polymeric network resulting smaller in size. The smaller bead size e.g., 872.03 ± 0.2933 μm on higher concentration of *Isabgol* husk on applying similar calcium ion strength for low *Isabgol* husk ratio revealed the participation of *Isabgol* husk in cross-linking. Similarly, on increasing the strength of calcium chloride from 2 to 8% w/v, the particle size was also decreased from 804.63 ± 1.4278 μm to 790.21 ± 1.201 μm and from 813.41 ± 0.9233 μm to 790.12 ± 0.241 μm in sodium alginate beads, respectively. The particle size of different formulations is shown in Table 1.

The swelling index (%) of beads in distilled water has also been summarized in Table 1. In formulations of 1 : 2 *Isabgol* husk-sodium alginate prepared in 2 to 8% w/v calcium chloride strength, the swelling index (%) decreased from 354 ± 4.71 to 296 ± 3.42, while in 3 : 4 *Isabgol* husk-sodium alginate formulations, it decreased from 426 ± 3.54 to 176 ± 1.23. Similarly, in sodium alginate formulations such as AA, AA/2 and AA/4, it decreased from 406 ± 2.43 to 352 ± 1.12. Here, it was considered due to more involvement of calcium in cross-linking resulting in tight network of polymer that may create hindrance in water diffusivity to cross-linked *Isabgol* husk-sodium alginate beads. Secondly; on increasing the concentration of cross-linking agent, reduction in the mobility of the polymer chains and consequently, a decrease in porosity may occur resulting in slow swelling. The results also showed that the swelling was related to the polymer concentration because more swelling was observed on increased polymer content. The loading efficiency of the majority of the systems prepared was high

Table.1 Formulations of *Isabgol* husk-sodium alginate beads fabricated by aqueous ionic gelation-crosslinking technique.

	Formulation code	Conc. of sodium alginate (g)	Conc. of *Isabgol* husk (g)	Conc. of CaCl$_2$ (% w/v)	Particle size (μm ± S.D.)	Entrapment efficiency (%)	Swelling index (%)
1.	A/2	1	0.5	2	825.47 ± 1.149	89.54 ± 1.26	354 ± 4.71
2.	A	1	0.5	5	813.78 ± 0.7485	93.45 ± 0.134	326 ± 2.34
3.	A/4	1	0.5	8	794.41 ± 0.7485	94.16 ± 1.23	296 ± 3.42
4.	AA/2	1	Ż	2	804.63 ± 1.4278	88.41 ± 0.07	406 ± 2.43
5.	AA	1	Ż	5	781.57 ± 0.4872	87.65 ± 0.118	342 + 1.21
6.	AA/4	1	Ż	8	790.21 ± 1.201	90.06 ± 2.34	352 ± 1.12
7.	BB/2	0.75	Ż	2	813.41 ± 0.9233	83.14 ± 0.12	376 ± 1.78
8.	BB	0.75	Ż	5	752.83 ± 0.6300	83.46 ± 0.031	330 ± 3.56
9.	BB/4	0.75	Ż	8	790.12 ± 0.241	95.78 ± 1.23	291 ± 2.23
10.	B/2	1	0.75	2	872.03 ± 0.2933	91.66 ± 0.89	426 ± 3.54
11.	B	1	0.75	5	838.62 ± 0.7412	95.12 ± 1.112	338 ± 1.23
12.	B/4	1	0.75	8	810.33 ± 0.5533	96.10 ± 1.16	176 ± 1.23

*Values shown in parentheses are the S.D. of three successive results

Table 2. Results of the system suitability studies.

Property	Mean ± S.D.*	% RSD	Required limits
Retention time (t$_R$) (s)	161.2 ± 1.13	0.7045	RSD ≤ 1%
Theoretical plates (N)	7281.058 ± 7.67	0.1053	N ≥ 2000
Tailing factor (F)	1.66 ± 0.01	0.6024	T ≤ 2
Asymmetry factor (AF)	0.766 ± 0.005	0.7530	AF ≤ 1

*Average of six determinations

Table 3. Calibration data of gliclazide by HPLC method.

No.	Concentration (μg/ mL)	Peak area (mV.S) (Mean ± S.D.)*	%RSD
1.	2.5	1303.533 ± 7.902742	0.606255
2.	5.0	2624.233 ± 5.772844	0.219982
3.	7.5	3975.203 ± 4.87455	0.122624
4.	10.0	5393.233 ± 5.997077	0.111196

* The mean of six successive readings

Table 4. Accuracy of method in terms of recovery results.

Sample %	Area (mV.s) (Mean* ± SD)	Initial amount (μg/mL)	Amount added (μg/mL)	Amount recovered (μg/mL)	Recovery %	% RSD
80	5337.908 ± 2.265582	2	8	9.98	99.99672	0.042443
90	5863.704 ± 6.813041	2	9	10.95	100.061	0.127635
100	6364.534 ± 1.4851	2	10	11.89	99.97656	0.023334
110	6951.695 ± 0.956106	2	11	12.98	99.98622	0.013754
120	7562.257 ± 3.567373	2	12	14.12	99.94802	0.047173

* Average of six successive determinations
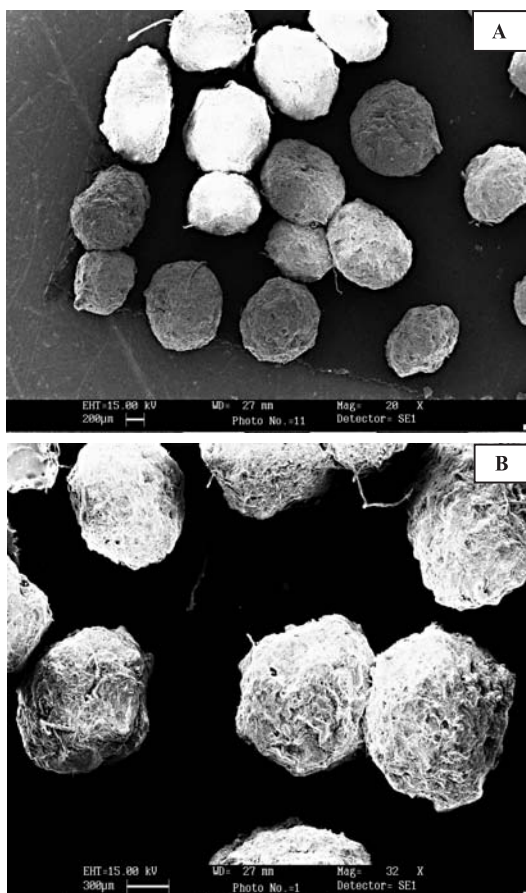
Figure 1. Photomicrographs of gliclazide loaded hydrogel beads of (**A**) sodium alginate and (**B**) *Isabgol* husk-sodium alginate

owing to the low water solubility of gliclazide in water and the minimum loss of the drug during preparation of the beads as well as in washings with water prior to drying. A relation with increment of entrapment efficiency with decrement in particle size was observed that may be due to more cross-linking resulting in less loss of drug in dispersed media during fabrication

Figure 2. Chromatogram of peak width at 50% height (w_1) and 10% height (w_2), retention time (rt), and peak height (h) of gliclazide

Figure 3. Unimodel, positively skewed chromatographic peak of gliclazide in mobile phase of phosphate buffer (pH 3.4) and acetonitrile (20 : 80 v/v)

Table 5. Linear regression characteristics parameters of gliclazide by HPLC method.

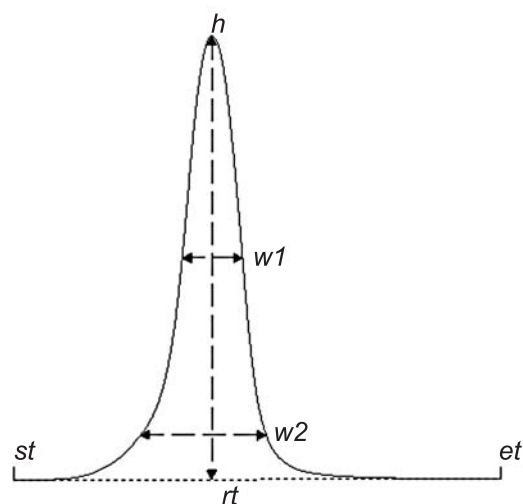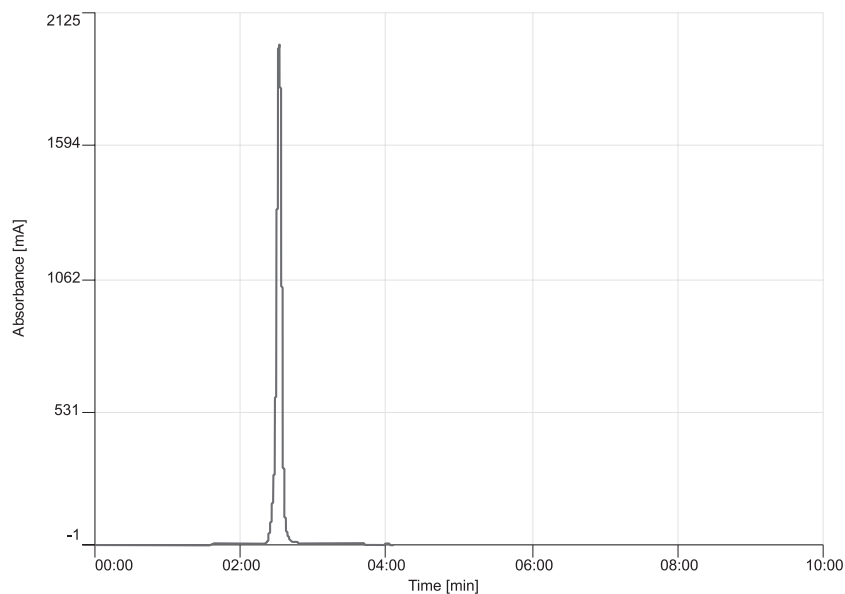| Parameters	HPLC method
Calibration range (µg/mL)	2.5–10
Detection wavelength	227 nm
Mobile phase, phosphate buffer (pH 3.4) : acetonitrile) v/v	20 : 80
Regression equation (Y)	y = 538.19x – 33.053, R^2 = 0.9997
Retention time (s)	160.4
Slope (m)	538.19
Intercept (c)	33.053
Correlation coefficient (r^2)	0.9997
Limit of detection (LOD) (µg/mL)	0.037619
Limit of quantification (LOQ) (µg/mL)	0.113997

Table 6. Intra-day precision results of gliclazide.

No.	Concentration (µg/mL)	Retention time (s)	Area (mV.s)
1.	15	160.3	8041.95
2.	15	160.8	8038.721
3.	15	161.2	8036.03
4.	15	161.3	8043.564
5.	15	160.4	8037.106
6.	15	160.7	8036.03
7.	15	160.9	8041.95
8.	15	161.1	8044.103
9.	15	161.8	8043.564

Table 7. Inter-day precession results of gliclazide determination by HPLC method.

No.	Concentration (µg/µL)	Retention time (s)	Area (mV.s)
1.	15	161.2	8040.335
2.	15	161.5	8039.259
3.	15	161.8	8038.721
4.	15	160.9	8038.182
5.	15	160.8	8036.03
6.	15	161.3	8037.106
7.	15	161.7	8042.488
8.	15	160.4	8044.641
9.	15	160.2	8038.721

Table 8. Robustness study of HPLC method for gliclazide estimation.

No.	Flow rate (mL/min)	Peak area (Mean ± S.D.)	Retention time (s) (Mean ± SD)*	Mean % RSD (for retention time)	Mean % RSD (for area)
1.	0.5	4287.711 ± 26.92009	160.125 ± 0.330404	0.206341	0.627843
2.	1	4286.635 ± 27.8305	160.25 ± 0.896289	0.559306	0.649239
3.	1.5	4307.899 ± 29.60815	161.175 ± 0.670199	0.415821	0.687299

*Average of six successive determinations

Table 9. Ruggedness studies of HPLC method for gliclazide determination.

Injection number	User-1			User-2		
	Area (mV.s)	Retention time (s)	Theoretical plates (N)	Area (mV.s)	Retention time (s)	Theoretical plates (N)
5 µg/mL	2627.66	161.2	7115.519	2622.78	160.8	6775.759

Table 10. Release behavior of hydrogel beads of sodium alginate and *Isabgol* husk-sodium alginate in distilled water, 0.1 M HCl, and phosphate buffer (pH 7.4)

No.	Formulation code	Time (min) required for 50% release of loaded gliclazide ($t_{50\%}$)		
		In distilled water	In 0.1 M HCl	In phosphate buffer (pH 7.4)
1.	A/2	741.0642	466.6285	256.4819
2.	A	922.0937	478.5284	286.9242
3.	A/4	988.0937	478.5284	315.9242
4.	AA/2	620.7927	375.3471	249.835
5.	AA	688.8649	397.5341	283.3517
6.	AA/4	728.8649	417.5341	323.3517
7.	BB/2	598.9712	342.1793	213.3317
8.	BB	694.9605	357.4922	243.0078
9.	BB/4	724.9605	371.4922	253.0078
10.	B/2	912.112	524.1456	248.8384
11.	B	963.931	596.5950	283.1824
12.	B/4	1058.612	648.2974	323.1824

Validation of HPLC method

In the study, the determination of gliclazide in all samples was performed by HPLC method that was carried out according to the recommendations for analytical method validation.

System suitability

System suitability tests are an integral part of method development and are to ensure adequate performance of the chromatographic system. Retention time (t_r), number of theoretical plates (N), asymmetry factor (AF), and tailing factor (F) were evaluated by applying following expressions for six replicate injections of the drug at a concentration of 5 µg/mL. The presentation of peak width at 50% and 10% height is shown in Figure 2. The numbers of theoretical plates (N) are also countable for assessing the column efficiency. The mathematical concept of theoretical plates was applied by using half peak height method as following:

$$N = 5.545 \, (\frac{t_R}{W_h})^2$$

Table 11. Release kinetics parameters of sodium alginate and *Isabgol* husk-sodium alginate beads crosslinked by calcium chloride.

Formulation code	Name of kinetic models									
	Zero order		Korsmeyer-Peppas		First order		Higuchi		Hixon-Crowell	
	k	r²	n	r²	k	r²	k	r²	k	r²
In distilled water										
B	0.0508	0.9111	0.5453	0.9787	-0.0003	0.9264	1.2317	0.986	-0.004	0.5797
AA/2	0.0411	0.9168	0.5087	0.9861	-0.0002	0.9331	0.9991	0.9899	-0.0036	0.555
In 0.1 M HCl										
B	0.1142	0.956	0.6664	0.9788	-0.0007	0.9682	2.6497	0.9814	-0.0057	0.6954
AA/2	0.1135	0.7847	0.6497	0.9641	-0.0008	0.8431	2.9038	0.9792	-0.0048	0.4742
In phosphate buffer (pH 7.4)										
B	0.1425	0.8205	0.6735	0.951	-0.0012	0.9325	3.626	0.9717	-0.0051	0.463
AA/2	0.1456	0.7095	0.6797	0.909	-0.0015	0.8727	3.8806	0.9726	-0.0051	0.463

where N is a number of theoretical plates; t_R = retention time, and 'W_h' = peak width at half height (in units of time). Columns with high plate numbers are considered to be more efficient, that is, have higher column efficiency, than columns with a lower plate count. A column with a high number of theoretical plates will have a narrower peak at a given retention time than a column with a lower theoretical plates number. High column efficiency is beneficial in case of less peak separation (meaning lower α value) and on the other hand, more efficient columns are needed. Column efficiency is a function of the column dimensions (diameter, length and film thickness), the type of mobile phase and its flow rate, nature of compound to be separated, and its retention.

The tailing factor was determined by using the following formula:

$$T = (\frac{a + b}{2a})$$

where T is the tailing factor (measured at 10% of peak height), b = distance from the point at peak midpoint to the trailing edge and a = distance from the leading edge of the peak to the midpoint. The peak asymmetry was calculated using the following equation:

$$Asymmetry = \frac{N_{10}}{N_{50}}$$

where N_{10} is the plate efficiency at 10% of the peak height and N_{50} is the plate efficiency at 50% of the peak height. Here, the plate efficiency at 10 and 50% of the peak height was determined by the following formulae:

$$\text{Plate efficiency @50%} = 05.54 \left(\frac{\text{Retention time}}{w_1}\right)^2$$

$$\text{Plate efficiency @10%} = 18.55 \left(\frac{\text{Retention time}}{w_2}\right)^2$$

The results are shown in Table 2. The number of theoretical plates (N) was greater than 2000 (N ≥ 2000) and the tailing factor was less than 2 (T ≤ 2). Similarly, the asymmetry factor was less than 1 (AF ≤ 1). In all six replicates of the experimentation according to ICH guidelines, the % RSD was also less than one (RSD ≤ 1%). All these results indicated the suitability of the applied HPLC method for gliclazide estimation. It was found that the regression coefficient for linear curve fitting for calibration was 0.9997 (r^2 > 0.9990). The higher value of regression coefficient 'r' indicated the linear kinetics as best curve fitting model for developed HPLC method. The unimodel, sharp, and pointed chromatographic peak of gliclazide in mobile phase of

Table 12. Stability study analysis of *Isabgo*l husk hydrogel beads.

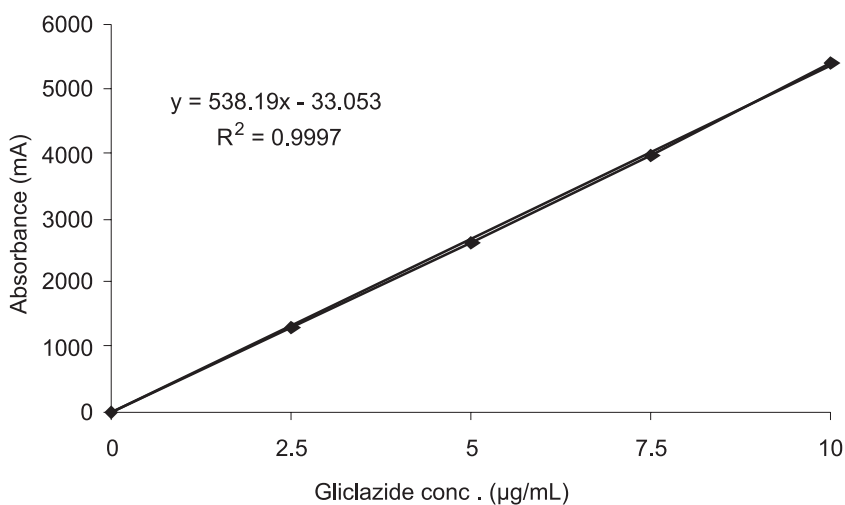| Formulation code	Time (months)	Particle size (µm)	Entrapment efficiency (%)	Swelling index (%)
A	1	814.26 ± 0.26	92.66 ± 0.631	331 ± 0.42
	3	816.14 ± 1.45	93.04 ± 0.12	335 ± 1.43
	6	815.12 ± 0.89	92.98 ± 1.78	334 ± 1..98
A/2	1	820.05 ± 2.02	89.88 ± 0.87	359 ± 2.23
	3	823.18 ± 1.45	90.42 ± 2.56	358 ± 3.12
	6	826.23 ± 0.59	90.12 ± 1.72	361 ± 0.59
A/4	1	797.45 ± 1.22	95.53 ± 0.45	299 ± 1.38
	3	799.89 ± 2.55	94.89 ± 1.23	301 ± 0.58
	6	803.23 ± 0.87	95.67 ± 2.14	298 ± 1.22

Figure 4. Calibration curve of gliclazide through HPLC method in mobile phase

phosphate buffer (pH 3.4) and acetonitrile (20 : 80 v/v) is shown in Figure 3.

Linearity

Several aliquots from the standard stock solution of gliclazide (10 mg/mL) in different strengths such as 2.5, 5, 7.5 and 10 µg/mL were prepared in the mobile phase. The detection of gliclazide was performed by UV at 227 nm. The peak was recorded for all samples and calibration graph was obtained by plotting peak area *versus* concentration of gliclazide. The plot of peak area against concentration of gliclazide was found to be linear in the range of 2.5 to 10 µg/mL with the correlation coefficient of 0.9997. The calibration data of gliclazide are given in Table 3 and the calibration curve of gliclazide is shown in Figure 4.

Accuracy

The accuracy was performed in triplicate after spiking pure drug equivalent to 80, 90, 100, 110 and 120% of the standard concentration of gliclazide (10 µg/mL). The results obtained after drug analysis are shown in Table 4. The results indicated the excellent recovery of gliclazide. In all the samples, the recovery of the drug was not less than 99.94%. The recovery results indicated that the method is highly accurate for determination of gliclazide.

Sensitivity

The limit of detection (LOD) and limit of quantification (LOQ) were determined from standard deviation and slope method according to ICH guidelines. The LOD was found to be 0.037619 µg/mL and LOQ was found to be 0.113997 µg/mL.

The results of linear regression with LOD and LOQ are presented in Table 5.

Precision

The precision of the method was demonstrated by intra-day and inter-day variation studies.

Intra-day precision

In the intra-day studies, six injections of the standard solution (15 µg/mL) were injected into the chromatographic system in different time interval within a day. The results of gliclazide potency in the samples are shown in Table 6 with % RSD.

Inter-day precision

In the inter-day variation studies, six injections of standard solution (15 µg/µL) were injected at different days. The results of gliclazide potency in samples are shown in Table 7 with % RSD.

Robustness

Robustness of the method was determined by making slight changes in chromatographic condi-
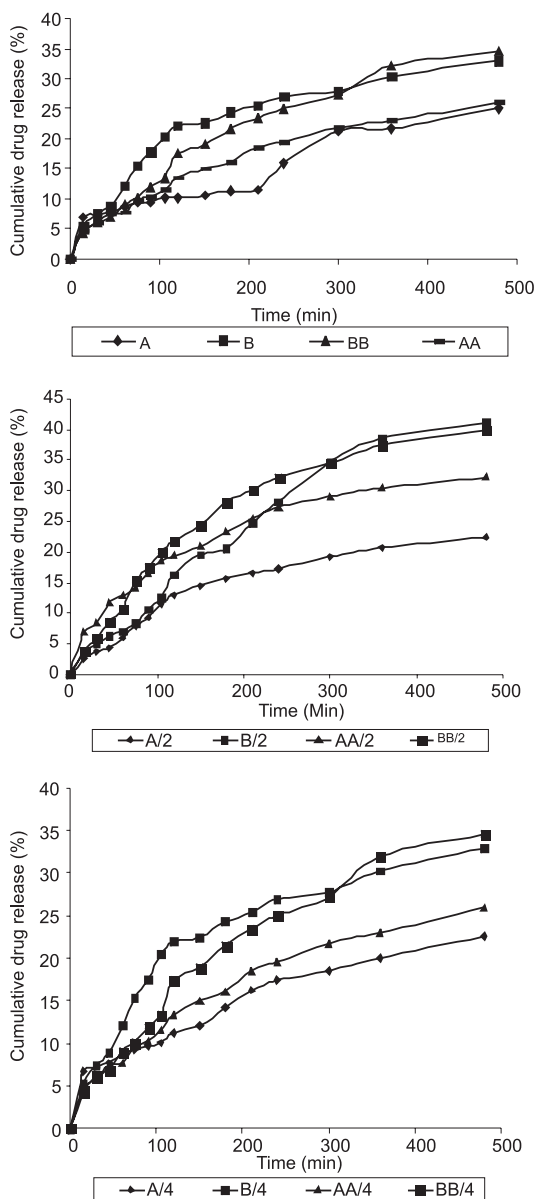

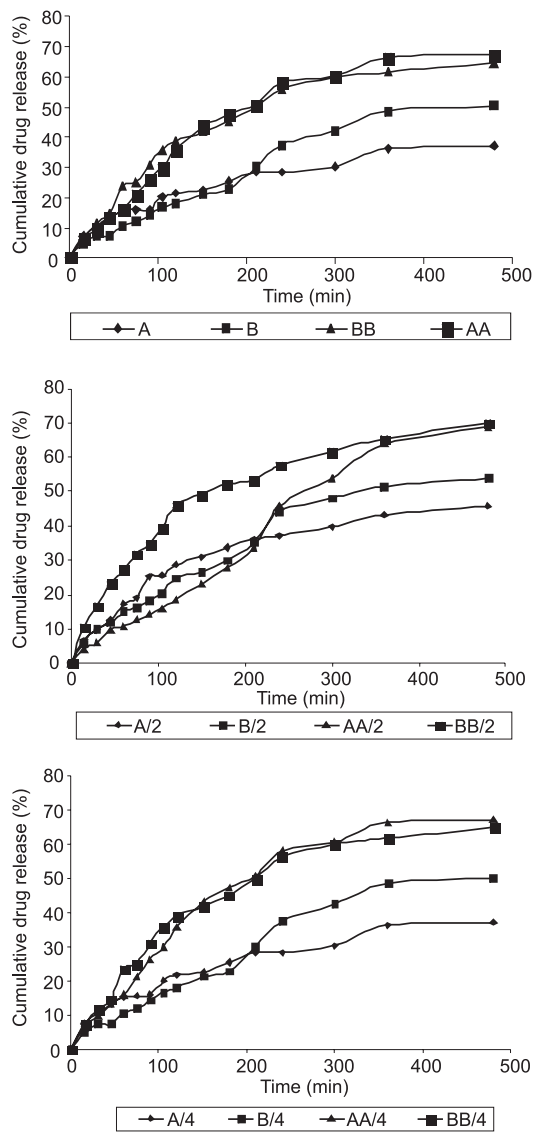Figure 5. (i). Dissolution pattern of different formulations in distilled water

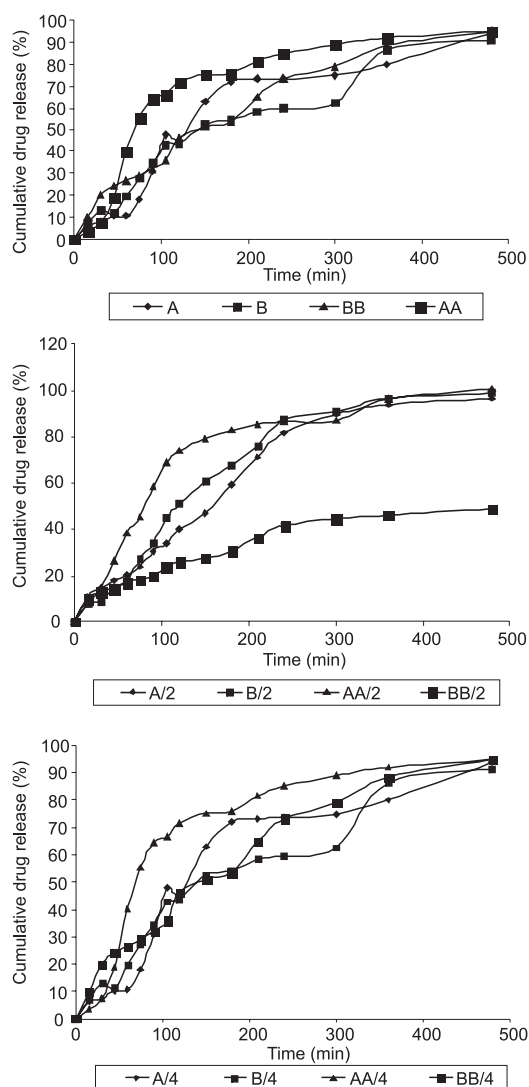Figure 5. (ii). Dissolution pattern of different formulations in 0.1 M HCl

Figure5. (iii). Dissolution pattern of formulations in phosphate buffer (pH 7.4)

tions such as change in flow rate from 0.5 to 1.5 mL/min. It was observed that there were no marked changes in the chromatograms, which demonstrated that the method applied for determination of gliclazide is robust. The results of robustness of the method are represented in Table 8.

Ruggedness

It was analyzed by determining precession on the same instrument but by the different user. Results of the reproducibility of the method are shown in Table 9.

In vitro **drug release**

The release pattern of formulations in distilled water, 0.1 M HCl and phosphate buffer (pH 7.4) has

been shown Figure 5 (i, ii, and iii). Due to sensitivity of *Isabgol* husk-sodium alginate cross-linked beads towards ionic media, the release pattern of beads was different in distilled water, 0.1 M HCl and phosphate buffer ($p < 0.05$). The time required for 50% release of loaded gliclazide from formulations has been summarized in Table 10. It was found that $t_{50\%}$ value was lower in phosphate buffer (pH 7.4) than in distilled water and 0.1 M HCl for all formulations. It indicated the faster drug release in phosphate buffer (pH 7.4) than in 0.1 M HCl and distilled water. The slow release of gliclazide at pH 1.2 has been observed due to the stability of alginate at low pHs and the conversion of calcium alginate to the insoluble but swelling alginic acid (10, 11). In phosphate buffer (pH 7.4), the rapid swelling and erosion of the beads has also been observed in swelling study that may greatly contribute in facilitating the fast release. The value of $t_{50\%}$ was comparatively larger for formulations containing more *Isabgol* husk (B/2, B, and B/4) than those containing less amount of *Isabgol* husk (A/2, A, and A/4). Here, it was inferred that more amount of *Isabgol* husk may provide the thicker hydrogel coating on gliclazide dispersed in beads and hence resulting in slow release.

Release kinetics of gliclazide

The release kinetics of sodium alginate and *Isabgol* husk-sodium alginate beads has been summarized in Table 11. In B and AA/2 formulations, the value of 'n' was greater than 0.5 (n > 0.5) that indicated anomalous drug diffusion mechanism. In case of formulation B, it was found that 'n' was 0.6664 and 0.6735 in 0.1 M HCl and phosphate buffer (pH 7.4) dissolution media, respectively. Similarly, for the formulation AA/2, the value of 'n' was found to be 0.6497 and 0.6797 in 0.1 M HCl and phosphate buffer (pH 7.4) dissolution media, respectively. The increment in 'n' value in 0.1 M HCl and phosphate buffer (pH 7.4) was considered due to swelling controlled diffusion of gliclazide from sodium alginate and *Isabgol* husk-sodium alginate polymeric network cross-linked by calcium chloride. It was observed that the value of regression coefficient 'r' was closer towards '1' in case of Higuchi model that indicated the diffusion of drug followed by relaxation of polymeric network of the beads. As the penetration of swelling media causes the swelling, the channels of cross-linked matrix start to open and cause the drug release.

The diffusion of drug from beads has also been shown in photomicrographs taken by SEM in Figure 6. The surface was found porous and hard. Some

of the drug particles were also seen on the surface as well as nearby to the pores boundary. This porous structure on the surface may develop due to diffu-

sion of drug from the matrix. The surface of *Isabgol* husk-sodium alginate beads was more rigid as these were formed by possible involvement of polymeric structure of *Isabgol* in cross-linking that resulted in hard surface structure

The hydrogel beads of gellan gum cross-linked by calcium chloride and zinc sulfate also showed the non-fickian release of cephalexin due to relaxation of polymeric chains in dissolution media (12). Similar mechanism of gliclazide release from gliclazide/metformin tablets fabricated by using Eudragit NE30D in wet granulation method has been observed by Arno et al. (13).

During stability testing study, it was observed that swelling index (%) of beads varied from 331 ± 0.42 to 335 ± 1.43, 358 ± 3.12 to 361 ± 0.59, and 298 ± 1.22 to 301 ± 0.58, for A, A/2 and A/4, respectively. The variation in particle size was also observed i.e., 814.26 ± 0.26 to 816.14 ± 1.45 μm, 820.05 ± 2.02 to 826.23 ± 0.59 μm and 797.45 ± 1.22 to 803.23 ± 0.87 μm for A, A/2 and A/4, respectively. For the formulations A, A/2 and A/4 undergone stability study, the entrapment efficiency (%) varied from 92.66 ± 0.631 to 93.04 ± 0.12, 89.88 ± 0.87 to 90.42 ± 2.56, and 94.89 ± 1.23 to 95.67 ± 2.14, respectively. However, variation in results of entrapment efficiency, swelling index and particle size was not statistically significant from the initial values for these parameters ($p > 0.05$). When the entrapped gliclazide in spinking media containing mobile phase was scanned at 227 nm during stability study of A, A/2 and A/4 formulations, a uni-model sharp peak was obtained for each formulation
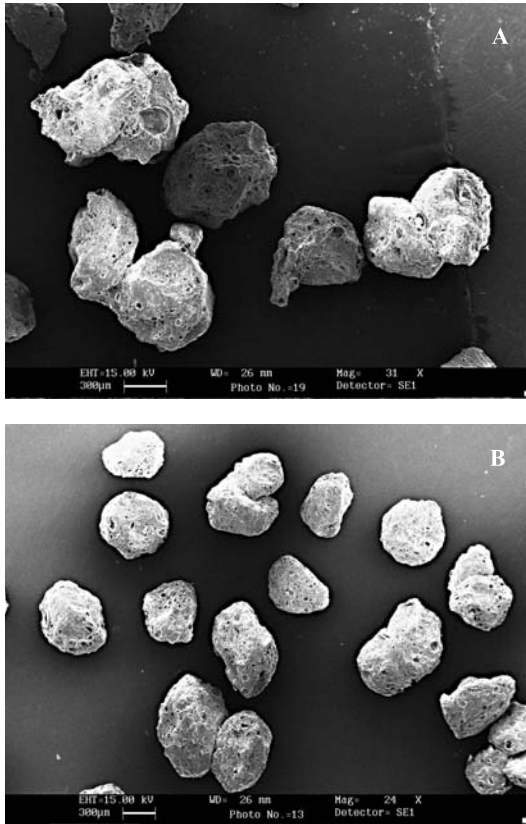

Figure 6. Photomicrographs of gliclazide loaded hydrogel beads (A) after dissolution in distilled water (B) after dissolution in 0.1 M HCl
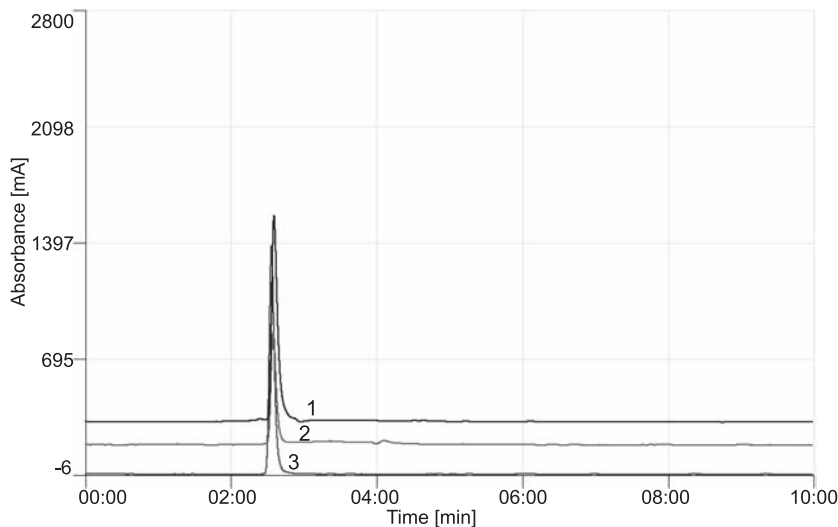

Figure 7. Chromatograms of gliclazide through stability study of A (1), A/2 (2), and A/4 (3)

166 VIPIN K. SHARMA and B. MAZUMDAR

at every time of the study and the peak can be overlaid to one another as shown in Figure 7.

CONCLUSION

The formulations prepared with high concentration of calcium chloride strength were more spherical and smaller size and showed marked effect on gliclazide entrapment and its release in dissolution media. Due to aldobiouronic content, *Isabgol* may participate in complex formation with Ca²⁺ ions. Due to chelation with phosphate in alkaline phosphate buffer (pH 7.4), the beads were unstable. The stability of formulations in terms of swelling index, particle size and entrapment efficiency revealed the reliability and suitability of the fabrication technique for sustained release gliclazide beads development of *Isabgol* husk. The study also revealed that the polymers have their significant impact on drug release from drug delivery devices and it is more effective in sustained release formulations. The release behavior followed by gliclazide in all dissolution media was diffusion followed by relaxation of the polymer chains. The release mechanism of gliclazide from beads may be fruitful as the initial fast release and then slow release, as shown in Higuchi model, will increase the absorption content and hence bioavailability of the drug. The quantification of gliclazide in formulations by HPLC method indicated high degree of regression coefficient (r < 0.9990) and relative standard deviation (%RSD < 1). The results of limit of detection (LOD) and limit of quantification (LOQ) were also of significant importance. All other results of applied HPLC method such as selectivity, sensitivity, precession, accuracy, ruggedness, and robustness indicated the applicability of this method in gliclazide determination in pure form and in formulations.

REFERENCES

1. Soppimath K.S., Aminabhavi T.M., Dave A.M., Kumbar A.G., Rudzinski W.E.: Drug Dev. Ind. Pharm. 28, 974 (2002).
2. Marlett J.A., Kajs T.M., Fischer M.H.: Am. J. Clin. Nutr. 72, 789 (2000).
3. Maurya D.P., Yasmin Sultana Y., Aquil1 M., Kumar D., Chuttani K., Ali A., Mishra A.K.: J. Microencap. 28, 482 (2011).
4. Mishra A., Srinivasan R., Gupta R.: Colloidal Polym. Sci. 281, 191 (2003).
5. Delrat P., Paraire M., Jochemsen R.: Biopharm. Drug Dispos. 23, 157 (2002).
6. International Conference on Harmonization, Draft Guideline on Validation of Analytical Procedures, Definitions and Terminology, Federal Register Vol. 60, Issue 40 (March 1, 1995).
7. Sa B., Halder A., Mukherjee S.: J. Microencap. 22, 80 (2005).
8. Sharma V.K., Bhattacharya A.: Indian Drugs 46, 868 (2009).
9. Fathy M., Safwat S., El-Shanawany M., Shawky Tous N., Otagiri M.: Pharm. Dev. Technol. 3, 10 (1998).
10. Yotsuyanagi T., Ohkubo T., Ohhashi T., Ikeda K.: Chem. Pharm. Bull. 35, 1563 (1987).
11. Hodson A., Mitchell J., Davies M., Melia C.: J. Control. Release 33, 152(1995).
12. Agnihotri S.A., Jawalakar S.S., Aminabhavi T.M.: Eur. J. Pharm. Biopharm. 63, 261 (2006).
13. Arno E.A., Anand P., Bhaskar K., Ramachandran S., Saravanan M., Vinod R.: Chem. Pharm. Bull. 50, 498 (2002).

STABILITY EVALUATION OF THERMOSENSITIVE DRUG CARRIER SYSTEMS BASED ON PLURONIC® F-127 POLYMER

KAMIL P. GRELA[1]*, DOMINIK M. MARCINIAK[2] and JANUSZ PLUTA[2]

[1]Student Scientific Organisation at the Department of Drugs Form Technology,
Wroclaw Medical University, Borowska 211A, 50-556 Wrocław, Poland
[2]Department of Drugs Form Technology, Faculty of Pharmacy, Wroclaw Medical University,
Borowska 211A, 50-556 Wrocław, Poland

Abstract: The aim of this study was to evaluate the stability of thermosensitive systems based on Pluronic® F-127 polymer, in aspects of their possible application in novel drug technology. A formulation was prepared without any active ingredient, consisting of 16% (w/w) of polymer dissolved in aqueous medium. Such preparation was autoclaved and then subjected to 3-month conditioning at elevated (40°) and reduced (5°C) temperature. Rheological parameters: viscosity, consistency and sol-gel transition characteristics were studied in 1-month interval. The significance of measured changes was evaluated by proper statistical analyses. Significant changes exceeding the established criteria (±10% of every initial value) were observed during the study. Furthermore, total involution of sol-gel transition phenomenon was observed in samples stored at 40°C. Results indicate the lack of stability in tested formulation at both of storage conditions. However, some regularity indicates that the stability at reduced temperature could be confirmed, if only the concentration of polymer and the measurements schedule were slightly modified.

Keywords: Poloxamer P 407, Pluronic® F-127, thermosensitive drug carriers, stability

Poloxamers, known by their commercial names Pluronic® or Kolliphor® are linear, triblock copolymers of ethylene oxide (EO) and propylene oxide (PO) (1). They are used as excipients in the cosmetics and food industry, but also in drug formulation technology (2). Their monographs are present for example in European (3), American (4), British (2) and Polish (5) pharmacopoeias. Poloxamers exist in more than 30 varieties, varying in average molecular mass and reciprocal proportions of PEO and PPO blocks. Those differences are responsible for their physical properties, such as state of matter, HLB value or ability to set thermosensitive systems.

Due to the presence of both hydrophilic (poly-PE) and lipophilic (poly-PO) blocks in every single molecule, Pluronics possess amphiphilic properties and act as surface acitive agents. These features allow them to be used as emulsifiers, solubilizers or stabilizers in solutions, suspensions or even micro- and macromolecular therapeutical dispersions (9, 10). An additional feature, typical only for varieties of high molecular mass and significant content of hydrophillic blocks, is their ability to form thermosensitive systems in water solutions (1, 11). In such systems, rapid viscosity growth with formation of a semisolid gel is observed as a reaction to heating of the solution, but only if a high enough concentration of proper polymer is used.

Regarding literature reports describing the relation between poloxamers structure and their potential toxicity as well as efficiency in thermosensitive systems (1), it is practical to choose Pluronic® F-127 as it is the most efficient and at the same time the least toxic. The simplicity of obtaining thermosensitive systems with this certain variety of Pluronic® (F-127) has resulted in newly invented formulations which remain liquid at room or decreased temperature, but form a gel *in situ*, in the place and time of administration. Attempts have been made to prepare such formulations intended to be administered externally (e.g., topical, upon thermal burns, ophthalmic and rectal) (9, 12-14) or by injection (intramuscular, intratumoral, intraocular, intraarterial) (9, 15). Nevertheless, no preparation using Pluronics' thermogelling mechanism is com-

* Corresponding author: e-mail: kamgrela@gmail.com; dominik.marciniak@umed.wroc.pl; phone: 71 784 03 22

mercially available. Although some data about stability of Pluronic-based formulations could be found (16, 17), they concern complex formulations with additional excipients (e.g., polyethyleneglycol, polysorbate, ethanol). Investigation (e.g., in MEDLINE, Scopus, Elsevier, Springer and Web of Knowledge databases) showed a lack of any former studies covering stability of thermosensitive formulations based on pure Pluronic® F-127 or even of the polymer in aqueous media by itself.

The aim of this study was to evaluate the stability of thermosensitive systems based on Pluronic® F-127 polymer, during storage at different conditions, by the measurements of their rheologic parameters, i.e., viscosity, hardness, cohesiveness and phase transition characteristics.

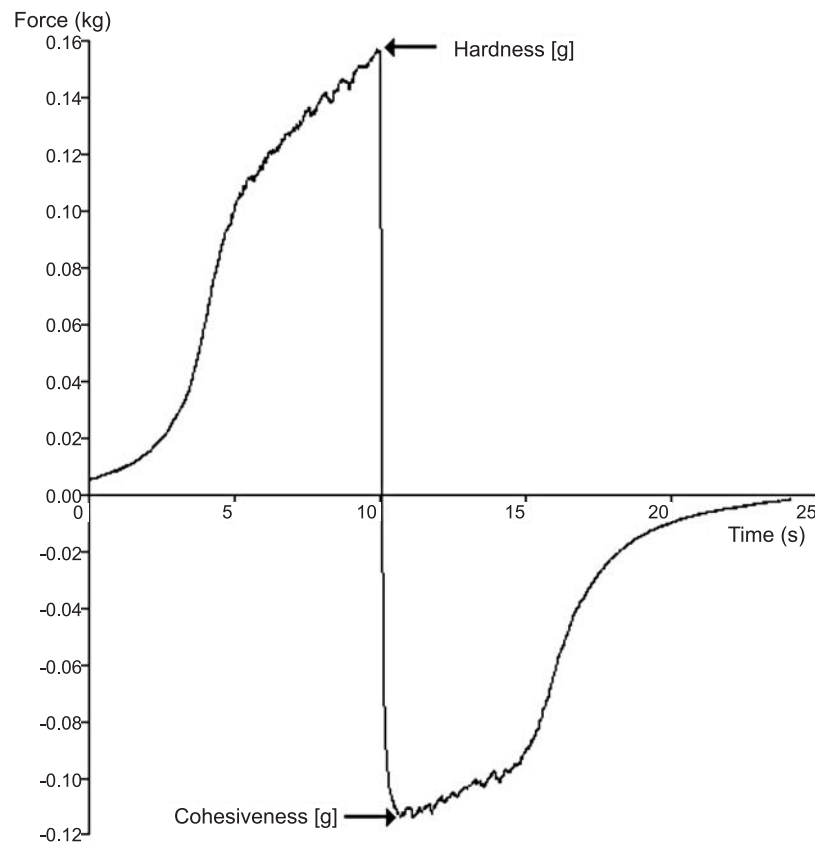Figure 1. An example plot of force *versus* time. showing the effects of consistency analysis and explaining the method of determination of the hardness and the cohesiveness values

Table 1. Identification of data points.

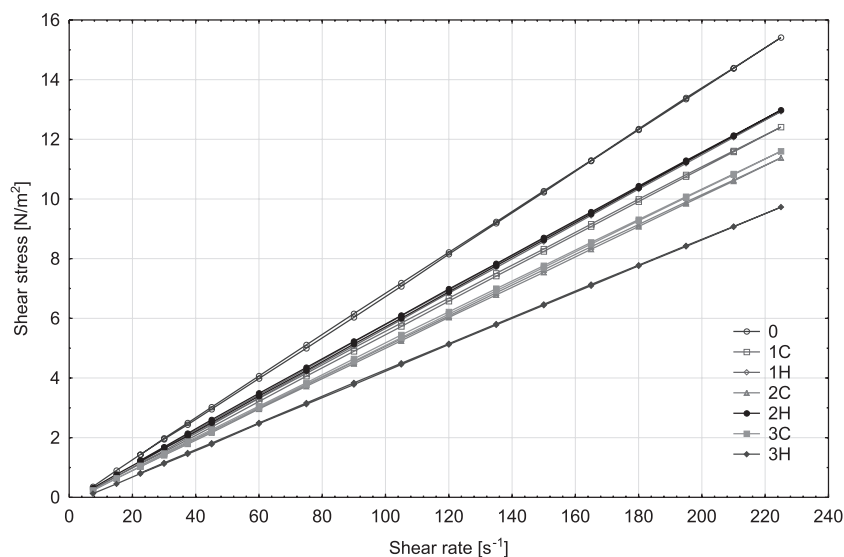| Sample name	Conditioning time [months]	Temperature °C
0	Zero point	
1C	1	5
1H	1	40
2C	2	5
2H	2	40
3C	3	5
3H	3	40

Figure 2. Mean flow curves measured at 25°C. All samples

MATERIALS AND METHODS

Materials

To prepare the formulation, polymer Pluronic® F-127 (BASF, USA) and purified water according to Aqua purificata monograph (FP IX) were used. All ingredients were weighed upon OHAUS Pioneer PA213CM/1 electronic scale (OHAUS Corporation, USA). Conditioning took place in KBF LQC-240 climatic chamber (BINDER GmbH, Germany). Rheologic parameters were measured with Brookfield RVDV III+ CP cone-plate rheometer (Brookfield Engineering Inc., USA) and TA.XT Plus Texture Analyser textuometer (Stable Micro Systems, Great Britain).

Methods

Preparation and conditioning of formulation

The aim was to prepare a formulation, which should remain liquid at room temperature, form a gel at 30-35°C and persist in the plateau of its maximal viscosity at 37°C, which is the human body temperature. According to literature (12) and manufacturer data (19), 16.0% (w/w) concentration was chosen. Initial measurements confirmed this choice as satisfying the above criteria.

Dispersion of Pluronic® F-127 was prepared according to the cool method (11). At first, proper quantities of ingredients were weighed out. About half of the necessary water amount was placed in a glass beaker, then the polymer was besprinkled upon its surface and the rest of the necessary water was added. The beaker was covered and put in the refrigerator overnight; the next day it was a clear solution inside. To ensure the homogeneity of dispersion, it was agitated with a mechanic stirrer for about 20 min. Prepared solution was split into adequate number of infusion-type hermetic glass bottles in a volume of 100 mL. Afterwards, samples filled and closed in bottles were autoclaved for 30 min at controlled temperature of 105°C.

Solutions were kept under following conditions: 1. climatic chamber: temperature 40 ± 2°C, relative humidity 75 ± 5%; 2. refrigerator: temperature 5 ± 3°C. According to the European Medicines Agency (EMA) guideline, these conditions were exact for: general accelerated stability evaluation and long-term stability evaluation specific for formulations intended to be stored in refrigerator (18). Samples were protected from direct or reflected sunlight and artificial light.

Study schedule and identification of data points

Formulation was examined and analyzed at the zero point (subsequent day after sterilization), and then in 1-month intervals at the time of 1, 2 and 3 months (± 2 days). Every time a new and freshly opened container of formulation was used. To every sample, a fixed name was given, indicating the length of the storage period (numbers 0-3) and used storage conditions (letters C/H). Details are shown in Table 1.

Table 2. Changes of dynamic viscosity $\eta_{dyn,25}$ [mPas] and apparent viscosity $\eta_{app,37}$ [mPas] values in tested samples.

Sample	Dynamic viscosity $\eta_{dyn,25}$ [mPas]				Apparent viscosity $\eta_{app,37}$ [mPas]			
	Mean	Percent	±95% c.i.	RSD	Mean	Percent	±95% c.i.	RSD
0	69.15	100.0%	1.46	2.0%	7594.40	100.0%	679.718	8.53%
1C	55.80	80.7%	2.32	4.0%	6282.64	82.7%	491.369	7.45%
1H	58.27	84.3%	1.51	2.5%	8412.09	110.8%	790.238	8.95%
2C	51.20	74.0%	1.18	2.2%	6351.68	83.6%	631.293	9.47%
2H	58.20	84.2%	0.99	1.6%	5505.94	72.5%	472.293	8.17%
3C	52.23	75.5%	0.53	1.0%	5786.42	76.2%	461.648	7.60%
3H	44.17	63.9%	0.86	1.8%	104.05	1.4%	19.373	17.74%

±95% c.i. – 95% confidence interval; RSD – relative standard deviation.

Table 3. Sol-gel transition temperature $T_{sol \to gel}$ [°C] in tested samples.

Lower sol-gel transition temperature $T_{sol \to gel}$ [°C]						
0	1C	1H	2C	2H	3C	3H
31.5	32.5	33.0	33.5	34.0	34.0	(38.0)

Table 4. Changes of hardness Hd_{25} [g] and cohesiveness Coh_{25} [g] values in tested samples.

Sample	Hardness Hd_{25} [g]				Cohesiveness Coh_{25} [g]			
	Mean	Percent	±95% c.i.	RSD	Mean	Percent	±95% c.i.	RSD
0	8.17	100.0%	0.046	0.54%	3.74	100.0%	0.052	1.33%
1C	8.41	103.0%	0.062	0.70%	3.66	97.8%	0.067	1.73%
1H	8.45	103.4%	0.053	0.60%	3.68	98.4%	0.038	0.99%
2C	8.71	106.6%	0.045	0.49%	3.57	95.5%	0.034	0.91%
2H	8.37	102.5%	0.053	0.61%	3.78	101.0%	0.032	0.82%
3C	8.61	105.4%	0.037	0.41%	3.68	98.4%	0.069	1.79%
3H	8.28	101.4%	0.028	0.32%	3.80	101.6%	0.030	0.76%

±95% c.i. - 95% confidence interval; RSD - relative standard deviation.

Measurements

Viscosity. Flow curves were designated at two different temperatures: 25.0°C and 37.0°C. Measurements of shear stress were done with constantly increasing and then decreasing shear rates, in the ranges of 7.5-225.0 s⁻¹ (25°C) and 3.84-15.36 s⁻¹ (37°C). Flow curves were used to estimate the viscosities: dynamic viscosity $\eta_{dyn,25}$ [mPas] at temp. 25°C and also apparent viscosity $\eta_{app,37}$ [mPas] measured at temp. 37°C and shear rate of $\gamma = 15.36$ s⁻¹. All measurements were repeated six times for every sample at both temperatures.

Sol-gel transition characteristics. To determinate the transition characteristics, a method similar to those found in the literature (15, 18) was used. A rheometer was used to measure the changes of apparent viscosity of formulation observed during the linear increase of temperature. Certain conditions were: shear rate: $\gamma = 0.38$ s⁻¹, temperature range: 23-43°C, temperature increase rate: 0.75°C/min, viscosity measurement interval: 0.5°C. Data were presented as a plot of viscosity versus temperature. The temperature corresponding to the first observed change of viscosity was interpreted as the sol-gel transition temperature, $T_{sol \to gel}$ (gelation temperature).

Consistency. Measurements were taken with a textuometer. Default probe was used, tipped with flat plastic disc (diameter = 35 mm, height = 5 mm),
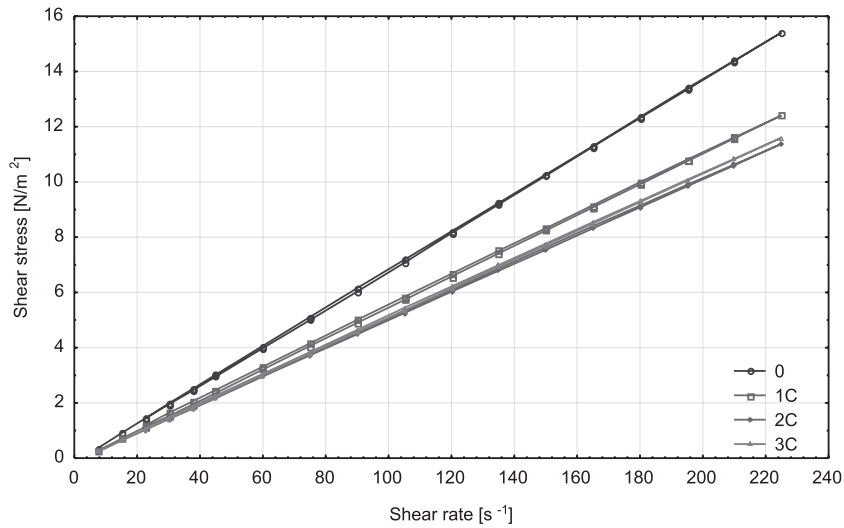
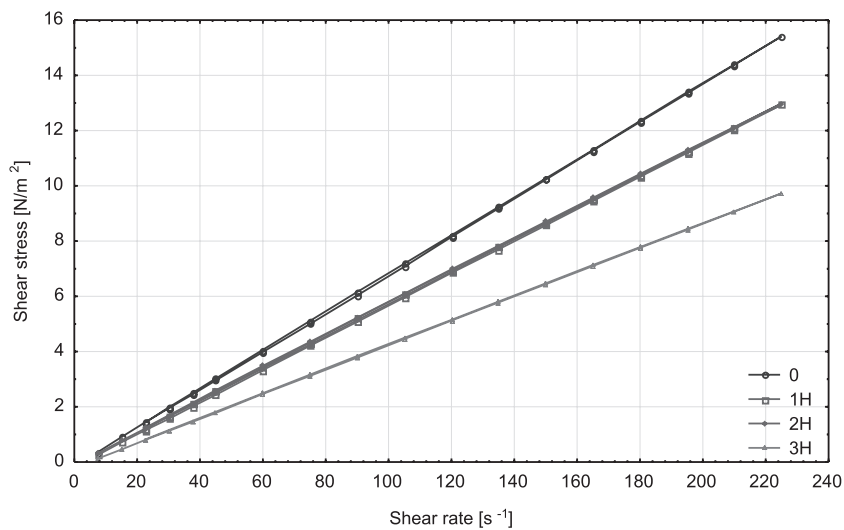Figure 3. Mean flow curves measured at 25°C. Samples conditioned at 5°C

Figure 4. Mean flow curves measured at 25°C. Samples conditioned at 40°C

provided by the manufacturer. The process of this study was to measure the forces acting on the probe, when it was consecutively immersed and emerged in/from the container with the formulation. The probe was immersed to a given depth of 20 mm below the formulation surface and then emerged to the starting position, which was always about 15 mm over the surface. The position of the first contact with formulation surface was determined by the trigger force of 5.0 g. The vertical velocity of the probe in both directions was set to 2.0 mm/s.

Data were acquired as a plot of force against time and were used to analyze the extreme absolute values of forces noticed during every measurement cycle. The maximum positive value observed during the immersion phase was treated as hardness (Hd_{25}/Hd_{40} [g]), while the extreme absolute value in the emersion phase was treated as cohesiveness (Coh_{25}/Coh_{40} [g]) of the examined substance (see Fig. 1). The study was performed for every sample in the state of sol and gel, respectively, at 25.0 and 40.0°C. Measurement cycle was performed six
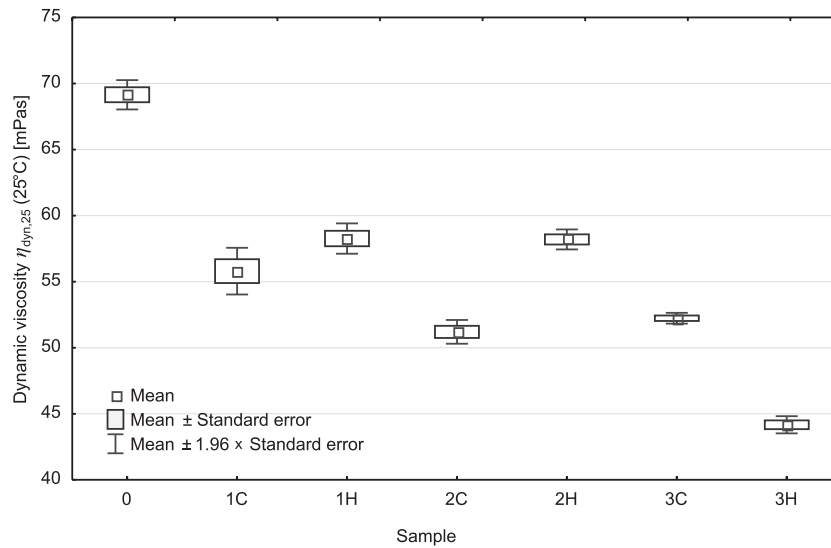
Figure 5. Box plot of average values of dynamic viscosity $\eta_{dyn,25}$ [mPas] in tested samples

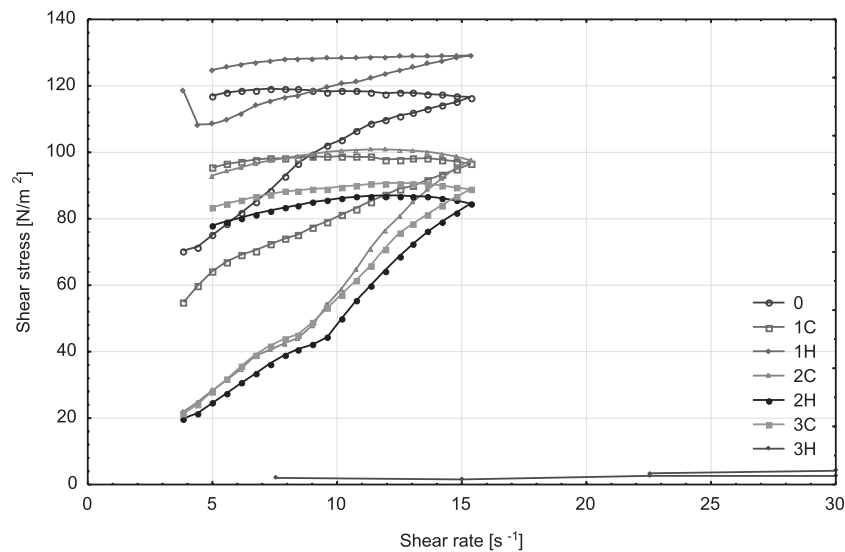Figure 6. Mean flow curves measured at 37°C. All samples

times for every examined sample at both temperatures.

Methods for data analysis

Raw data obtained from studies of viscosity and texture were transformed logarithmically. Mean values of analyzed parameters were evaluated by ANOVA parametric analysis of variance followed by two *post-hoc* tests: NIR (LSD: Lowest Significant Difference) and Levene's test. The normality of distribution of transformed data was checked by three different statistical tests: Kolmogorov-Smirnov,

Lilliefors and Shapiro-Wilk, while the homogeneity of variance was evaluated by Levene's and Brown-Forsythe tests. Correlations between some parameters were evaluated by the lowest quarter method, through the estimation of best-fit linear plot, also with care of Pearson's correlation coefficient and the confidence level, estimated by t test. In every performed analysis, the level of significance was set at 0. Statistical analysis was made with STATISTICA 10.2 PL software.

Significant changes less than ± 10% of the initial value were considered as acceptable and allowed to state the stability of the analyzed parameter.

RESULTS

Viscosity

Flow curves designated at 25°C (Figures 2-4) showed Newtonian flow characteristics. This observation was confirmed by estimation of linear equation for every obtained curve:

$$\tau = \eta \times \gamma + b$$

where: τ = shear stress [N/m²], η = dynamic viscosity [mPas], γ = shear rate [s-1], b = yield stress/measurement error [N/m²].

Using the above equation, it was possible to get the η dynamic viscosity value of every sample, with mean correlation coefficient reaching 0.99993 and mean error b = -0.1171 N/m². This value was relatively small and of negative sign, what allowed to treat it rather as negligible measurement inaccuracy in Newtonian flow model than as a yield stress typical for plastic flow model.

During the three months period, a significant decrease of dynamic viscosity was observed, reaching the level of 75.5% (3C) and 63.9% (3H) of ini-
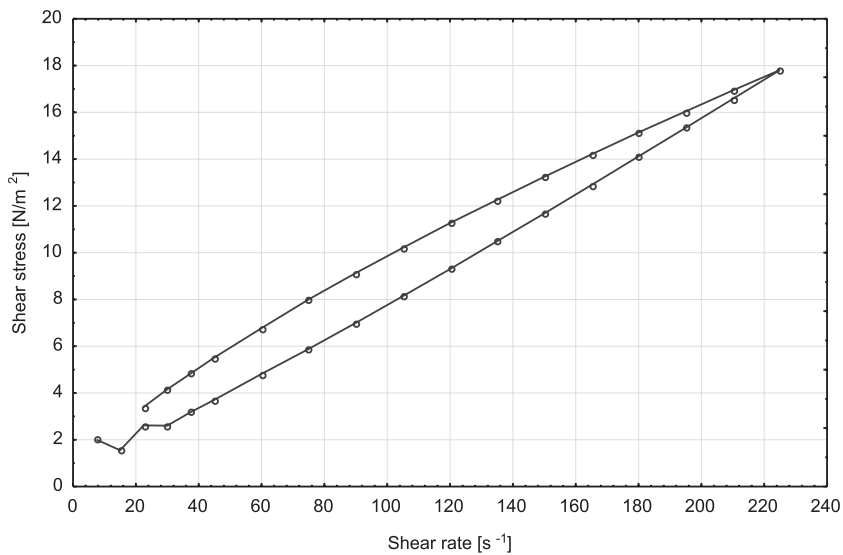

Figure 7. Mean flow curve of sample 3H measured at 37°C
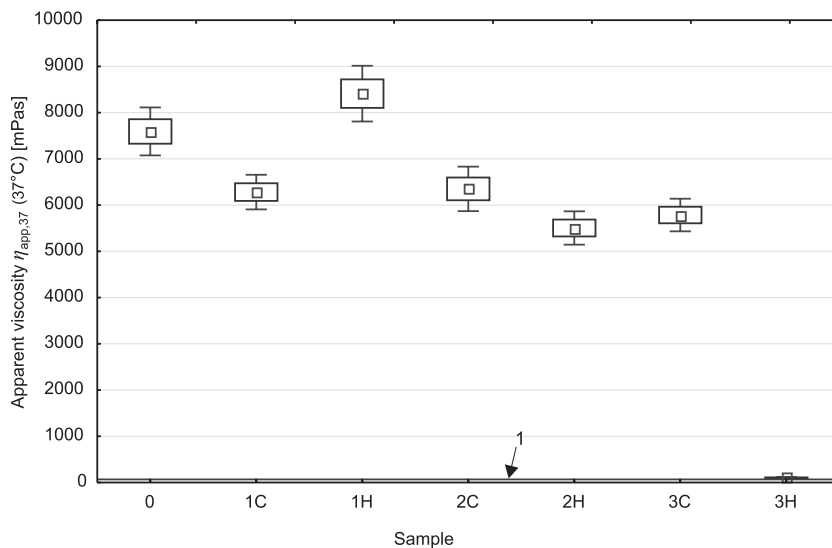
Figure 8. Box plot of average values of apparent viscosity $\eta_{app,37}$ [mPas] in tested samples. Horizontal line (1) refers to mean dynamic viscosity $\eta_{dyn,25}$ [mPas] in "zero point" sample, measured at 25°C
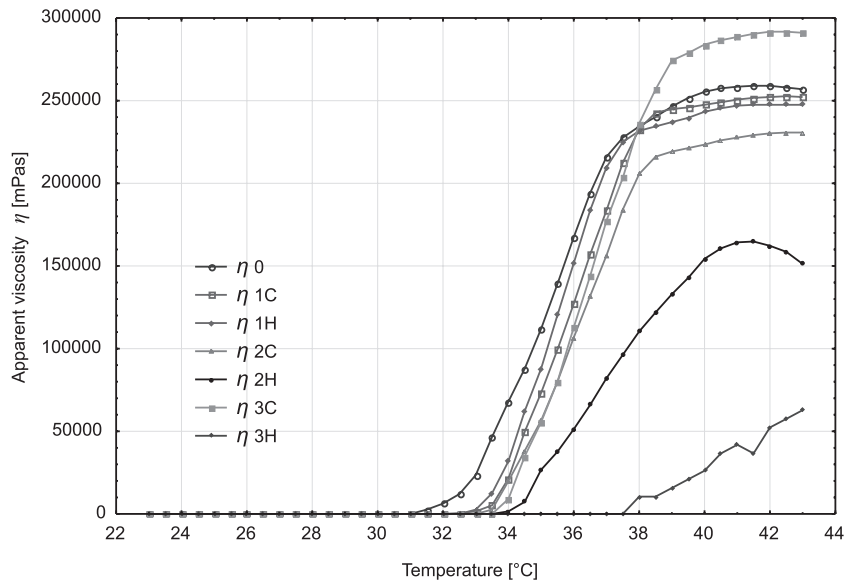
Figure 9. Phase transition characteristics in tested samples
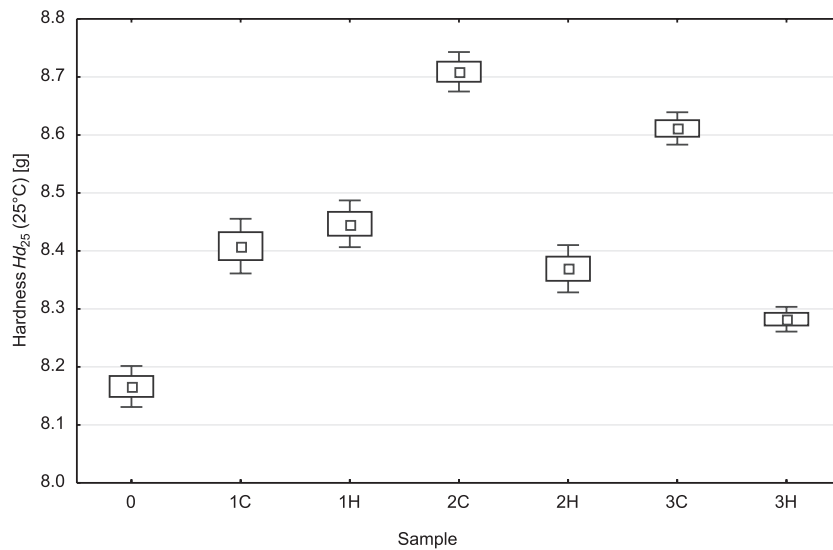
Figure 10. Box plot of average values of hardness Hd_{25} [g] in tested samples

tial value. In the first and second month, the viscosity of samples stored at elevated temperature was significantly higher than of analogical ones; in the third month the situation has inverted due to a considerable decrease of viscosity in elevated-temperature samples. Overall changes showed stronger decrease of the viscosity during storage at elevated temperature.

Flow curves designated at 37°C (Figs. 6, 7) showed explicit non-Newtonian flow characteris-

tics. Ascending parts of curves laid concave. which showed a decrease in viscosity with increasing of the shear rate; thus pseudoplastic flow was observed. Descending parts of the same curves laid almost horizontally and higher than ascending ones. This proved that viscosity was increasing due to the process (time) of shearing, thus rheopexy (negative thixotropy) was also observed. The exception of this rule was observed in sample 3H, where the degradation of structure was so intensive. that its rheologi-

cal behavior has changed into slightly dilatant flow with lower rheopexy (Fig. 7). In this case, the apparent viscosity $\eta_{app,37}$ at 37°C reached almost the level typical for dynamic viscosity at 25°C (see: horizontal line in Fig. 8). These dramatic changes have forced a modification of measurement conditions (extension of used shear rate range). to avoid the inaccuracy that might came from improper usage of the apparatus' scope.

During three months, a statistically significant decrease of apparent viscosity had been observed, which was intensified by the elevated storage temperature. Exceptionally high degradation was observed in the third month of study, in sample stored at elevated temperature. In samples stored in the refrigerator, only moderate changes occurred in the months 2-3, despite the significant change in the first month.

Sol-gel transitions characteristics

Both the sol-gel transition temperature (gelation temperature) $T_{sol \to gel}$ and the maximal viscosity
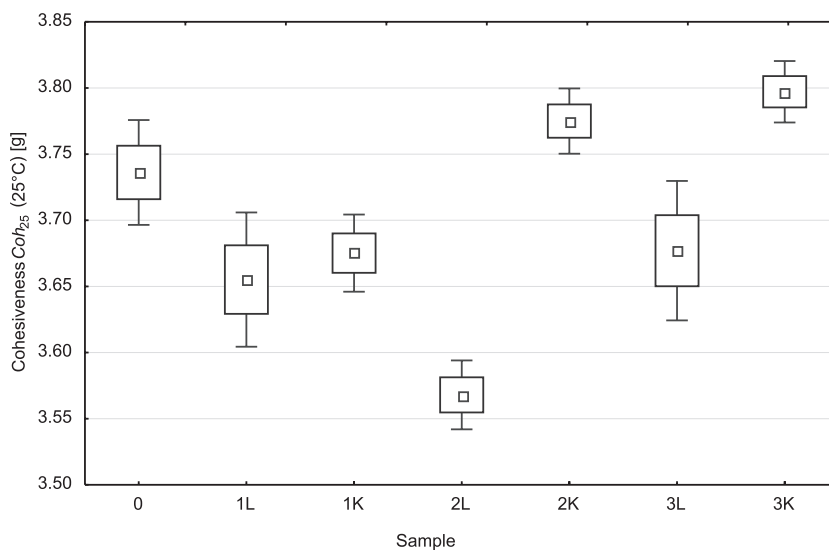

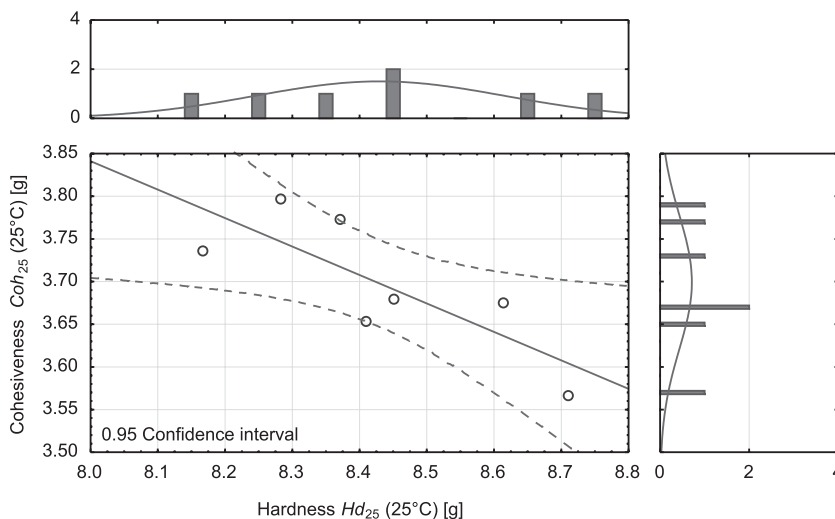Figure 11. Box plot of average values of cohesiveness Coh_{25} [g] in tested samples

Figure 12. Correlation plot: cohesiveness (6.51 - 0.334) as a function of hardness (25°C), correlation r = -0791

Table 5. Correlation parameters between mean hardness and cohesiveness; both analyzed at 25°C.

Analyzed correlation	$Coh_{25} = f(Hd_{25})$
Corelation coefficient r	-0.791
Determination coefficient r^2	0.626
Statistics t	-2.90
Confidence level p	0.0341
Number of cases n	7
Intercept b	6.51
Slope a	-0.334

Table 6. Changes of hardness Hd_{40} [g] and cohesiveness Coh_{40} [g] values in tested samples.

Sample	Hardness Hd_{40} [g]				Cohesiveness Coh_{40} [g]			
	Mean	Percent	±95% c.i.	RSD	Mean	Percent	±95% c.i.	RSD
0	133.72	100.0%	3.612	2.57%	97.17	100.0%	1.314	1.29%
1C	123.80	92.6%	1.181	0.91%	90.86	93.5%	0.921	0.97%
1H	126.76	94.8%	1.254	0.94%	91.08	93.7%	1.271	1.33%
2C	151.06	113.0%	3.882	2.45%	111.14	114.4%	2.506	2.15%
2H	21.41	16.0%	0.845	3.76%	8.60	8.9%	0.288	3.19%
3C	128.50	96.1%	3.585	2.66%	90.42	93.1%	1.993	2.10%
3H	13.54	10.1%	0.488	3.44%	4.66	4.8%	0.240	4.90%

±95% c.i. - 95% confidence interval; RSD - relative standard deviation.

Table 7. Correlation parameters between mean *hardness* and *cohesiveness* values, both analyzed at 40°C.

Analyzed correlation	$Coh_{40} = f(Hd_{40})$
Corelation coefficient r	0.999
Determination coefficient r^2	0.999
Statistics t	70.3
Confidence level p	1.11E-08
Number of cases n	7
Intercept b	-6.96
Slope a	0.777

observed in this transition have significantly changed during the study, as shown in Figure 9 and Table 3.

Samples stored in the refrigerator showed the increase of $T_{sol \rightarrow gel}$ of about 2.5°C, but the maximal viscosity changed only slightly. In samples stored at climatic chamber, parameters deteriorated significantly after the first month. Exceptionally high degradation was observed in sample 3H: the curve showed almost linear character; area of the steep slope and the plateau in upper part of plot were not present at all (Fig. 9). The transformation observed in this case could not be called *sensu stricto* a sol-gel transition.

Consistency

Consistency studies performed at 25°C showed statistically significant differences between most of the samples. Changes of the hardness Hd_{25} [g] consisted of an initial increase followed by a
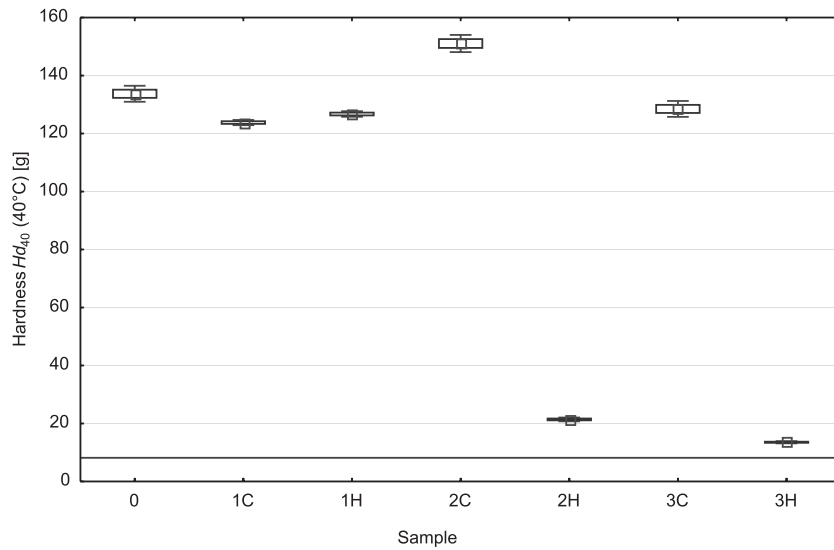
Figure 13. Box plot of average values of hardness Hd_{40} [g] in tested samples. Horizontal line refers to mean hardness Hd_{25} [g] in "zero point" sample at 25°C
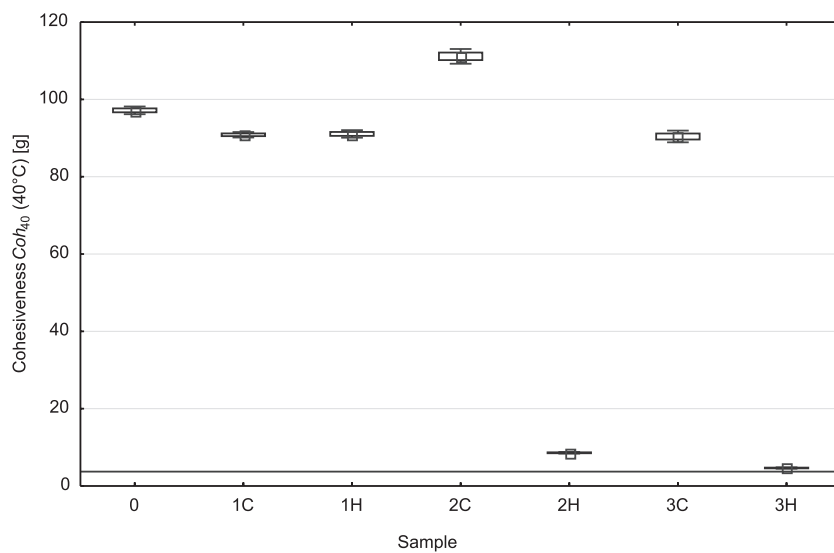
Figure 14. Box plot of average values of cohesiveness Coh_{40} [g] in tested samples. Horizontal line refers to mean cohesiveness Coh_{25} [g] in "zero point" at 25°C

moderate decrease with time (see: Fig. 10. Tab. 4). The lowest value was noticed in the zero point sample and the following measurements showed values between 101.4 and 106.6% of the initial one. In the second and third month, the hardness of samples stored in the refrigerator was significantly higher than of the analogical samples, stored at elevated temperature.

Cohesiveness studies performed at 25°C showed an exactly opposite direction of changes:

initial decrease, followed by an increase with time. up to more than 100% of initial value (Fig. 11. Tab. 4). Values obtained in the second and third month were at 95.5 to 101.6% of the initial value. In the second and third month, the cohesiveness of samples stored at elevated temperature was significantly higher than of analogical samples stored in the refrigerator.

Changes observed in cases of hardness and cohesiveness. both measured at 25°C - even if they
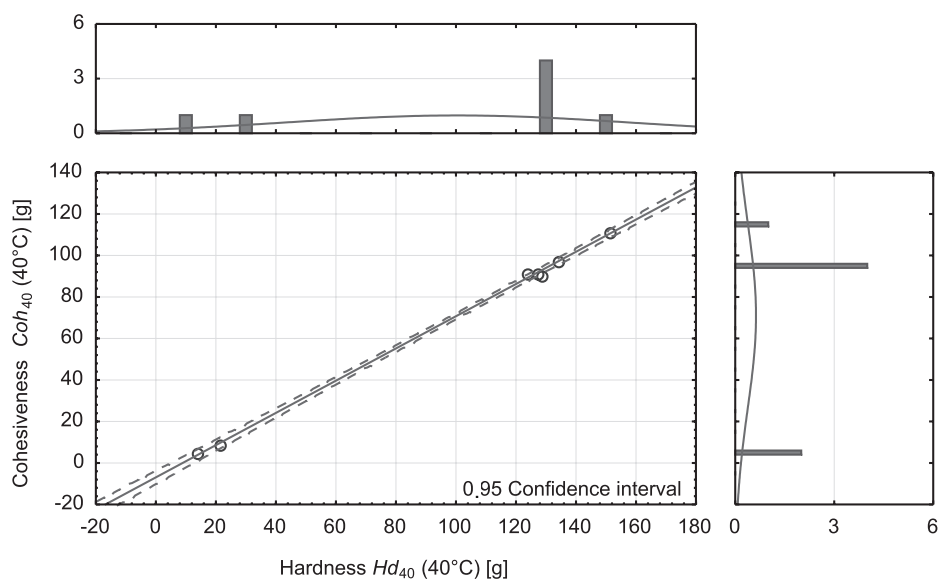
Figure 15. Correlation plot: cohesiveness (-6.995 + 0.77652) as a function of hardness (40°C), correlation r = 0.99949

were statistically significant - did not exceed the ± 10% of initial value, thus stability of those parameters under conditions used was confirmed.

Statistically significant correlation was observed between values of hardness and cohesiveness, measured at 25°C. Parameters of this correlation are presented in Table 5, correlation plot is shown in Figure 12.

Consistency studies performed at 40°C showed exceptional degradation of gel structure in the second and third month, in samples stored at elevated temperature. The direction and level of changes of both hardness and cohesiveness were similar; even a statistically highly significant correlation was observed between those parameters (Fig. 15. Tab. 7). In both cases, the changes observed during the first month did not exceeded ± 10% of initial value,but later a significant and very considerable degradation of gel structure appeared in samples stored at elevated temperature (see Figs. 13, 14. Tab. 6). Hardness and cohesiveness of samples 2H and 3H reached almost the levels typical for a temperature of 25°C.

DISCUSSION

Parameters of consistency measured at 25°C: hardness Hd_{25} [g] and cohesiveness Coh_{25} [g] remained stable during the whole period of study, in all samples and regardless to their storage conditions. Though observed changes were in general sta-

tistically significant, none of them exceeded the range ± 10% of initial value. Between hardness Hd_{25} and cohesiveness Coh_{25}. a statistically significant correlation was observed.

Dynamic viscosity $\eta_{dyn,25}$ in every sample underwent statistically significant changes, leading to a decrease in the value below the given criteria. In samples stored at elevated temperature, the changes during the 3 months were more intensified and clearly progressive. Sample stored at 5°C showed a decrease to about 80% of initial value. but in the subsequent months this value remained constant and any changes did not exceed ± 10%. This regularity suggests that the parameter could be considered as stable, if the measurement schedule was slightly modified to introduce the time needed for the formulation structure to stabilize. It is possible that leaving a gap of 5-10 days between the sterilization of the samples and making the first measurements might bring a change leading to an overall improvement in the results of the stability evaluation of the considered parameter.

Here it should be noted that even if measurements performed at room temperature provided many information about stability, they only covered those parameters, which are important at the moment of storage and preceding the administration. Changes analyzed above, although significant, may affect only the process of administration, but they have nothing in common with effectiveness and safety of already applied preparation. Their impor-

tance should be considered in terms of being enough to state the overall lack of stability. Better information, explaining the changes in application-related behavior, could be obtained through analysis of data from tests performed at elevated temperatures, closer to that of the human body. Proper analyses are shown below.

Hardness Hd_{40} [g] and cohesiveness Coh_{40} [g] (at 40°C) in samples stored in the refrigerator remained relatively constant. only in one case (2C) exceeding the acceptance criteria. It must be noted that due to the direction of this single change, no degradation of structure could be stated. In samples conditioned at elevated temperature, the changes in hardness Hd_{40} and cohesiveness Coh_{40} were exceptionally intensified in the second and third month of study. Values of those parameters reached nearly the level typical for them when measured at room temperature (see Fig. 10, 11, 13, 14 and Tabs. 4, 6), which shows severe degradation of structure and weakening of the sol-gel transition phenomenon. The level of those changes indicated the absolute uselessness of samples 2H and 3H as a thermosensitive drug bases, intended to form a gel *in situ* at human body temperature.

Apparent viscosity $\eta_{app,37}$ [mPas] of samples stored at elevated temperature underwent substantial and statistically significant changes, leading to a value many times lesser than the initial one. In samples stored in the refrigerator, changes were less explicit and of a different nature: there was a decrease to level 82.7% of initial value in the first month, but this level remained constant for the rest of the study. Furthermore, any changes between the values from the first, second and third month were not statistically significant. Here it may be assumed as earlier (as in the case of dynamic viscosity $\eta_{dyn,25}$) that the parameter could be considered as stable, if the measurement schedule would be slightly modified to introduce an additional time between sterilization and first measurements.

Analysis of the sol-gel transition characteristics confirmed the remarks about stronger degradation of formulation's structure during storage at elevated temperature. Weakening of the sol-gel transition scale (sample 2H), leading to even a disappearance of this phenomenon (sample 3H), was clearly visible. Acquired transition curves allowed also to notice that temperature of apparent viscosity measurements (37.0°C) did not refer to the plateau of viscosity (which was achieved during the sol-gel transition). but only to the upper part of the steep slope area. This situation might have generated additional inaccuracy of measurements and thus might have

been responsible for the relatively large standard deviations of measured $\eta_{app,37}$ values. Such situation should be avoided in further studies.

Analysis of the sol-gel transition temperatures, $T_{sol \rightarrow gel}$, showed a progressive increase of this temperature, appearing regardless of the storage conditions. In planning of any further studies, this phenomenon should also be considered. It is necessary to find a proper concentration of polymer, allowing for the temperature to change, but still leaving a safety margin for this parameter.

Even if the results of the above analyses showed a lack of stability, they seemed optimistic in the case of refrigerator-stored samples. Evaluation of acquired data and attempt of discovering any relations or regularities within them led to a conclusion that stability during storage at 5°C could be easily confirmed, if the polymer concentration were slightly modified and/or excipients were added, to keep the plateau of viscosity in the temperature typical for the area of application and measuremets.

CONCLUSIONS

During the study, progressive degradation of formulation's structure was observed and confirmed, regardless of the storage conditions. Observed changes debar the possibility of using it as a medicinal preparation, for which stability of rheological parameters is absolutely required.

Analysis of acquired data, performed according to given methods and criteria, allowed to declare stability only in cases of hardness Hd_{25} and cohesiveness Coh_{25}, both measured at 25°C. Stability of those parameters was observed in every sample, regardless of the storage conditions.

Conditioning at elevated temperature exerted strong, negative impact on stability of examined parameters, which led to the conclusion that Pluronic® F-127 dispersions need to be stored in a refrigerator.

Observations on changes in dynamic viscosity $\eta_{dyn,25}$ and apparent viscosity $\eta_{app,37}$ in refrigerator-stored samples during the first month of study suggest that a modification of measurements schedule is necessary. Introducing a few days of "gap" after sterilization or some additional measurement points in the first month should be considered.

Stability of thermosensitive formulation based on Pluronic® F-127 could be proved if formulations were stored at decreased temperature and the proper concentration of polymer and/or excipients were chosen, with consideration to results of above and similar studies.

REFERENCES

1. Schmolka I.R.: J. Biomed. Mater. Res. 6, 571 (1972).
2. Collett J.H.: in Handbook of pharmaceutical excipients. 6th edn.. Rowe R., Sheskey P, Weller P. Eds., p. 506. Pharmaceutical Press, Grayslake 2009.
3. European Pharmacopoeia 7.0 supplement 8, p. 2751. European Directorate for the Quality of Medicines and HealthCare, Strasbourg 2013.
4. United States Pharmacopeia 26 - National Formulary 21, p. 1492, The United States Pharmacopeial Convention, Maryland 2003.
5. Polish Pharmacopeia IX, p. 3092, Polish Pharmaceutical Society, Warszawa 2013.
6. BASF - Product Information. The Chemicals Catalog - Pluronic®. Internet: http://worldaccount.basf.com/wa/NAFTA~en_US/Catalog/ChemicalsNAFTA/pi/BASF/Brand/pluronic (accessed: 4. 07. 2013).
7. Reintjes T.: in Solubility Enhancement with BASF Pharma Polymers. Solubilizer Compendium. Reintjes T. Eds., p. 103, BASF SE, Lampertheim 2011.
8. Kabanov A.V., Batrakova E.V., Alakhov V.Y.: J. Control. Release 82, 189 (2002).
9. Dumortier G., Grossiord J.L., Agnely F., Chaumeil J.C.: Pharm. Res. 23, 2709 (2006).
10. Antunes F.E., Gentile L., Rossi C.O., Tavano L., Ranieri G.A.: Colloid. Surface B. 87, 42 (2011).
11. Kolliphor® P Grades Technical Information. BASF Corporation, New Jersey 2013.
12. Dumortier G., El Kateb N., Sahli M., Kedjar S., Boulliat A. et al.: Drug Dev. Ind. Pharm. 32, 63 (2006).
13. Ricci E.J., Lunardi L.O., Nanclares D.M.A., Marchetti J.M.: Int. J. Pharm. 288, 235 (2005).
14. Edsman K., Carlfors J., Petersson R.: Eur. J. Pharm. Sci. 6, 105 (1998)
15. Karolewicz B., Pawlik-Gałczyńska A., Pluta J., Ryszka F.: Polim. Med. 41, 35 (2011).
16. Shawesh A., Kallioinen S., Antikainen O., Yliruusi J.: Pharmazie 57, 690 (2002).
17. El-Houssieny B., Hamouda H.: Drug Discov. Therap. 4, 33 (2010).
18. ICH Topic Q1E: Evaluation of Stability Data (CPMP/ICH/420/02). European Medicines Agency, London 2003.
19. Pluronic® F127 Surfactant Viscosity As a Function of Temperature & Concentration. Technical Bulletin. BASF Corporation, New Jersey 2006.
20. Charrueau C., Tuleu C., Astre V., Grossiord J.L., Chaumeil. J.C.: Drug Dev. Ind. Pharm. 27, 351 (2001)

GENERAL

LEGAL INSTRUMENTS SUPPORTING THE DEVELOPMENT OF ORPHAN MEDICINAL PRODUCTS IN THE EUROPEAN UNION

KATARZYNA MIASKOWSKA-DASZKIEWICZ*

Faculty of Law, Canon Law and Administration, Department of European Union Law,
The John Paul II Catholic University of Lublin, Collegium Iuridicum, 1 Spokojna St. 20-074 Lublin, Poland

Abstract: Securing the freedoms of the Internal Market by the European Union entails an obligation to implement such mechanisms so that medicinal products placed on the market could be, on the one hand, widely available to the citizens of Member States and, on the other, so that medicinal products could be both safe and effective. The first aspect involves acting towards the improvement of public health and the prevention of human diseases and troubles, while the second – removing the sources of danger to human health. From this perspective, we need to highlight the problem of a deficit in the development, and thus a deficit in the availability of medicinal products authorized for marketing, which are intended for use in rare diseases. This paper aims to analyze the European Union pharmaceutical law in order to establish whether, and if yes – how the EU legal regulations support the development and availability of orphan medicinal products on the Internal Market.

Keywords: orphan medicinal product, rare disorders, marketing authorization, industrial property rights

Considering the protection of public health, the European law establishes a rule that no medicinal product can remain on the market without a valid authorization issued by an appropriate authority. Depending on which authority issues the authorization, one can distinguish between a national procedure: the authorization is issued by an administrative authority of a Member State (in Poland, since 1 May 2011 it is the President of the Office for Registration of Medicinal Products, Medical Devices and Biocids) or a central procedure: the regulator is the European Union, which resolves disputes on the basis of an evaluation report of the European Medicines Agency. The basic EU regulation in this respect is the Directive of the European Parliament and of the Council 2001/83/EC of 6 November 2001 on the Community code relating to medicinal products for human use (OJ L 311, 28. 11. 2001, p. 67 (hereinafter Directive 2001/83/EC), along with its most important revision – the Directive of the European Parliament and Council 2004/27/EC of 31 March 2004 (OJ L 136, 30. 04. 2004, p. 1; hereinafter Directive 2004/27/EC), as well as the

Regulation (EC) 726/2004/EC of 31 March 2004, laying down Community procedures for the authorization and supervision of medicinal products for human and veterinary use and establishing a European Medicines Agency (OJ L 136, 30. 04. 2004, p. 1; hereinafter Regulation (EC) 726/2004/EC).

The marketing authorization of medicinal products is performed on the basis of an appropriate administrative procedure and an application that meets detailed criteria. Marketing authorization for a medicinal product is issued on the basis of an evaluation of the product's safety, its therapeutic efficacy and quality.

The protection of health plays a significant role in the policy of the EU; it is a part of many areas of the *acquis*, and its realization, according to the Treaty on the Functioning of the European Union (hereinafter referred to as TFEU), is multi-sectoral. This means analyzing each EU policy with regard to the realization of health protection, which has the highest priority according to Art. 168 of the TFEU. The principle indicated in the cited Treaty provision is sometimes described as a 'cross-section clause' as its content can be defined as an order, formulated in

* Corresponding author: e-mail: kamias@kul.lublin.pl

a positive manner, extracted from the entire activity of the European Union (1).

The specificity of the orphan medicinal products on the market

The notion of an "orphan drug" was first used in 1983 to describe treatment recommended to patients with rare diseases. That year, the United States of America announced the *Orphan Drug Act* (2). The law aimed at creating favorable conditions for the research and development of "orphan drugs" used in the treatment of rare diseases.

The Community programme for rare diseases, including genetic ones, defines the frequency of rare diseases as affecting no more than 5 of every 10,000 people in the EU (3). Regardless of the fact that rare diseases occur infrequently, the total number of people affected with such diseases in the EU ranges from 27 to 36 million. Most cases concern diseases that occur rarely and affect a maximum of 1 per 100,000 people (4). From the point of view of large pharmaceutical companies, orphan drugs are hardly profitable as they are intended for a small number of patients, i.e., finally, for a small percentage of purchasers. Therefore, one faces a dilemma: on the one hand, the number of recipients is insufficient to consider manufacture as profitable but on the other, these medicines are often the only possibility to save patients' life and health. Thus, orphan drugs remain products developed mostly by small, innovative laboratories, generally remaining of little interest to the global pharmaceutical companies.

If the principal reason behind this is the limited market of consumers, other reasons should not be overlooked. They include the necessity of conducting long-lasting and costly preclinical tests and clinical trials, undergoing a marketing authorization procedure with hardly any guarantee of market success. We may also add to this list of obstacles the lack of infrastructure necessary to conduct research on the development of innovative orphan medicinal products.

The phenomena cited above are the reasons of why products that have never been tested for their safety and therapeutic efficacy for these indications are used in the therapy of rare diseases, leading in turn to the popularization of medicinal products used in an "off-label" (unapproved) manner.

Apart from the obvious medical doubts, the use of off-label medicinal products entails problems related to the responsibility of doctors who use them in a therapy. Prescribing medicinal products should be considered a health care service within the meaning of Article 3(a) of Directive 2011/24/EU of

the European Parliament and of the Council of 9 March 2011 on the application of patients' rights in cross-border healthcare (OJ L88, 4. 04. 2011, p. 45–65).

The doctor's decision to use an off-label medicinal product also involves administrative and financial problems with regard to the possibility of reimbursing a therapy conducted with the use of an off-label medicinal product.

In view of this situation, the need to create legal instruments which will support the development of orphan medicinal products is highly important.

The concept of stimulating the development and thus increasing the availability of orphan medicinal products is based on the introduction of changes to the procedure of their authorization for marketing in the European Union and on the creation of an incentive system for the pharmaceutical sector.

The normative activity of the European Union in the field of orphan medicinal products

The *ratio legis* of the Regulation (EC) No. 141/2000 of the European Parliament and of the Council of 16 December 1999 on orphan medicinal products (OJ L 18, 22. 01. 2000, p. 1–5) is based on the assumption that patients suffering from rare conditions should have the right to the same quality of treatment as other patients, and thus it is necessary to support the research and development and subsequent marketing of appropriate medicines by the pharmaceutical industry. An additional stimulus was the fact that incentives for the development of orphan medicinal products have been successful in the United States of America since 1983, and in Japan since 1993.

The European Parliament and the Council eventually adopted Decision 1295/1999/EC of 29 April 1999 adopting a programme of Community action on rare diseases within the framework for action in the field of public health (1999 to 2003; OJ L 155, 22. 06. 1999). This included legislation aimed at the provision of information, the handling of rare disease clusters within the population, and the support of appropriate patient organizations. In the White Paper "Together for Health: A Strategic Approach for the EU 2008–2013" of 23 October 2007, presenting the EU health strategy, the Commission pointed out rare diseases as one of its priorities for action (SEC(2007) 1374-1376).

The strategy selected by the EU for improving the availability of medicinal products intended for rare diseases is also important. Considering the

principle of competence division between Member States and the European Union (Art. 4(1) in connection with Art. 2(2) of the TFEU), and the related principle of subsidiarity, it was concluded that due to the small ratio, specific character and yet high total number of affected people, the problem of rare diseases needs to be solved at the EU level. This explains why the chosen form was a regulation: it is binding in its entirety and directly applicable in all Member States (Art. 288 of the TFEU).

Designation of a medicinal product as an orphan medicinal product

For the easy and unambiguous identification of medicinal products subject to incentives, an open and clear EU procedure allowing for the designation of potential medicinal products as orphan medicinal products was established.

Article 2(b) of Regulation (EC) No. 141/2000 introduces a definition of an orphan medicinal product, the criteria of which are based on the prevalence of the condition for which the means of diagnosis, prevention or treatment are sought. A medicinal product can be designated as an "orphan drug", in accordance with Article 3 of Regulation (EC) No. 141/2000, if its sponsor can establish a) that it is intended for the diagnosis, prevention or treatment of a life-threatening or chronically debilitating condition affecting not more than five in 10 thousand persons in the EU when the application is made, or that it is intended for the diagnosis, prevention or treatment of a life-threatening, seriously debilitating or serious and chronic condition in the EU and that without incentives it is unlikely that the marketing of the medicinal product in the EU would generate sufficient return to justify the necessary investment, and b) that there exists no satisfactory method of diagnosis, prevention or treatment of the condition in question that has been authorized in the EU or, if such method exists, that the medicinal product will be of significant benefit to those affected by that condition.

The notion of sponsor also requires explanation. Article 2(c) of Regulation (EC) No. 141/2000 provides that a "sponsor" means any legal or natural person, established in the European Union, seeking to obtain or having obtained the designation of a medicinal product as an orphan medicinal product. The scope of entities included in the notion of a "sponsor" is thus fairly broad as it covers entrepreneurs who have their registered offices outside of the EU, whilst it is sufficient for them to run their business on the EU territory in the form of a branch.

Particular attention should be paid to the fact that the legislation specifying the criteria the fulfilment of which allows for designating a medicine as an orphan medicine, contains a significant number of notions which are not explicitly defined but still do not influence the clarity of the provisions. The Commission Regulation (EC) 847/2000 of 27 April 2000 laying down the provisions for the implementation of the criteria for the designation of a medicinal product as an orphan medicinal product and definitions of the concepts "similar medicinal product" and "clinical superiority", indicate which documents are to be submitted by the sponsor applying for the designation of a medicine as an orphan medicinal product; however, the issue of how big the sufficient generated return to justify the necessary investment incurred by the pharmaceutical company should be, remains doubtful (OJ L 103, p. 5–8, Art. 2(2).

The most important role in granting the status of an orphan medicinal product is played by the Committee for Orphan Medicinal Products (hereinafter referred to as "the Committee") set up within the European Medicines Agency, referred to in Article 4 of Regulation (EC) No. 141/2000.

The main task of the Committee is to examine any application for the designation of a medicinal product as an orphan medicinal product, which is submitted to it by a sponsor. Apart from that, the Committee also advises the Commission on the establishment and development of a policy on orphan medicinal products for the European Union and assists the Commission in liaising internationally on matters relating to orphan medicinal products, and in liaising with patient support groups. The Committee also assists the Commission in drawing up detailed guidelines.

At any stage of the development process of a medicinal product (yet before an application for marketing authorization is filled), the sponsor submits to the Agency an application to obtain a designation for an 'orphan medicinal product'. The following detailed data and documents are enclosed to the application: a) name and surname or business name and permanent address of the sponsor, b) active substances of the medicinal product, c) proposed therapeutic indication, and d) justification that the criteria laid down in Article 3(1) are met, along with a description of the developmental stages, including the expected indication.

When preparing its opinion, the Committee uses its best endeavors to reach a consensus. If such consensus cannot be reached, the opinion will be adopted by a majority of two-thirds of votes of the

Committee members within 90 days. If the opinion of the Committee is negative, the Agency shall forthwith inform the sponsor as he has 90 days following the receipt of the opinion to submit detailed grounds for appeal, which the Agency shall then submit to the Committee. The Committee will consider at a subsequent meeting whether its opinion might be revised. The Committee meets monthly, which prevents excessive waiting of the sponsor in the case of an appeal against the initial opinion. The Agency immediately forwards the final opinion of the Committee to the Commission, which adopts the decision within 30 days from the receipt of the opinion.

The decision of entering a medicinal product into the EU Register of orphan medicinal products is made by the European Commission. Each year, the sponsor must submit to the Agency a report on the state of development of the designated medicinal product.

To sum up this subject, it should be strongly emphasised that the very designation of a medicinal product as an "orphan" medicinal product does not determine yet whether the marketing authorization can be obtained or not.

The central procedure and reduction of administrative costs

The basic incentive for the development of orphan drugs is the opening of a central procedure regarding the granting of the marketing authorization for medicinal products considered as "orphan" products, even if they do not fulfil the requirements of Regulation (EC) No. 726/2004. The centralized procedure is optional for orphan medicinal products, which means that the method of marketing a medical product depends on the decisions of a pharmaceutical entrepreneur.

Whereas the essence of the concept of a marketing authorization issued by the European Commission is the validity of such marketing authorization throughout the entire European Union, it should be regarded that for entrepreneurs this means conducting one single procedure, the successful completion of which authorizes them to market the medicinal product in each Member State without the necessity of engaging in particular national procedures and conducting 27 separate administrative procedures (5). A central authorization is regarded as the one that grants in each Member State the same rights and imposes the same obligations as any marketing authorization issued by the authorities of a Member State in a decentralized procedure (Art. 12(2) in connection with Art. 13(1) of Regulation (EC) No. 726/2004).

What is important from the perspective of costs related to the centralized procedure, the European Medicines Agency, which gives its opinion on the *dossier* of the orphan drug in this procedure, decreased the costs of the procedure for granting a marketing authorization for orphan medicinal products: the fees regarding the advice for applicants decreased by 80% and other fees by 50%. Apart from that, the Agency annually determines the amount of direct subsidies for usually small companies dealing with the marketing of medicinal products used for the treatment of rare diseases.

The support for industrial property rights

In order to compensate high expenditures incurred by the pharmaceutical industry on the development of orphan medicinal products, the protection rights for these products have been extended.

The sponsor of a medicinal product entered into the EU Register of orphan medicinal products and authorized for marketing in the entire European Union (or based on the authorization issued according to Regulation (EEC) No. 2309/93 or when all Member States issued marketing authorizations in accordance with the procedures of mutual recognition, Art. 19 of the Act of 6 September 2001 on the pharmaceutical law (Journal of Laws 04, No. 53, item 533), according to Article 8 of Regulation No. 141/2000, is granted a 10-year period of market exclusivity for the product. During this period, the relevant authorities are obliged "not to accept another application for a marketing authorization, or issue an authorization, or accept an application to extend an existing marketing authorization, for the same therapeutic indication, in respect of a similar medicinal product". "Similarity" in this case is defined as a similar molecular structure, identical mechanism of action and an equivalent scope of use (6).

Protection granted together with the status of an orphan medicinal product goes much further than the protection resulting from the exclusivity of data, to which the manufacturer of the original medicinal product is entitled according to Article 10 of Directive 2001/83/EC of the pharmaceutical law (7). Referring only to the exclusivity of data, one cannot avoid a situation where another competitive pharmaceutical entrepreneur starts and carries out his own clinical trials and puts on a market a medicine of composition identical to the existing orphan medicinal product. The protection resulting from the status of an orphan medicinal product refers not to the documentation but to specific

substances, and thus makes it impossible to market similar or identical medicines within 10 years.

Apart from that, the relevant authorities issuing a marketing authorization (the Commission or national authorities in case of the procedure of mutual recognition of authorizations), within the period of market exclusivity, cannot allow similar products to be placed on the market, nor can they accept applications in this respect. This is an important provision as the previous practice was that in the period of the 10-year exclusivity the authorities accepted applications and developed them in such a way that directly after the expiry of the exclusivity period, they granted marketing authorizations for similar medicinal products. It means that the effective period of market exclusivity protection related to the status of an orphan drug is thus prolonged by the time necessary for the analysis of applications by the marketing authorities.

However, market exclusivity can be restricted or excluded before the completion of the 10-year period. This applies to cases described in Article 8(2) of Regulation (EC) No. 141/2000. If, at the end of the fifth year of marketing authorization, the criteria laid down in Article 3 are no longer met, the status of an orphan medicinal product may be suspended, effective from the end of the sixth year following the marketing authorization. This applies, for example, to cases where the investor, by marketing the medicine, achieved an economic success; then his market exclusivity is reduced to six years from the date of the marketing authorization.

Apart from the above-mentioned possibility of restricting market exclusivity, Article 8(3) of Regulation (EC) No. 141/2000 provides that authorities regulating the marketing authorization of medicinal products may issue a marketing authorization for a similar orphan drug if the holder of the marketing authorization for the original orphan medicinal product has given a relevant consent to the second applicant, or if the holder of the marketing authorization for the original medicinal product is unable to supply sufficient quantities of the medicinal product, or the second applicant can establish in the application that the second medicinal product, although similar to the orphan medicinal product already authorized, is safer, more effective or otherwise clinically superior to the first one.

The provisions of Regulation (EC) No. 141/2000 do not exclude situations where competing investors obtain at the same time the designation of an orphan medicinal product for the

products that they manufacture (an example may be the fact that an agent called arsentrioxid was registered as an orphan medicinal product by three different companies, cf. http://pharmacos.eudra.org/F2/register/alforphreg.htm.), which *prima facie* may cause a problem with respect to the determination of priority to obtain market exclusivity rights. However, it does not cause any conflicts as the status of an orphan drug and related facilities for the investor are in a sense "launched" after the entrepreneur obtains the marketing authorization. The Regulation thus clearly accepts the rule of "all or nothing" and applies the motto *prior tempore, potior iure*. This means that the first investor who obtained a marketing authorization for his medicinal product may fully use the previously obtained orphan drug status, thus restricting the aspirations of other entrepreneurs, who did not obtain the marketing authorization, for the coming 10 years. It should be emphasized however, that the investor will not benefit if he obtains as the first the marketing authorization for an orphan drug in one Member States only. Only after obtaining the marketing authorization in all EU Member States, may he fully use the instrument of market exclusivity.

Designation of a product as an orphan medicinal product assures special protection, in addition to the patent protection (8), additional protection law (9) and data exclusivity (10).

The specific case of medicinal products used in pediatrics

It is worth noting that approximately 11% of all *orphan drugs*, the status of which is governed by Regulation (EC) No. 141/2000 are intended solely for use in pediatrics (11). Medicinal products used in pediatrics are products authorized for marketing and intended for pediatric use on the basis of clinical trials involving children and adolescents (12). At the EU level, legal aspects of pediatric medicinal products were regulated by Regulation (EC) No. 1901/2006 of 12 December 2006 on medicinal products for pediatric use and amending Regulation (EEC) No. 1768/92, Directive 2001/20/EC, Directive 2001/83/EC, and Regulation (EC) 726/2004 (OJ L 378, 27. 12. 2006, p. 1).

Regulation (EC) No. 1901/2006 extends the period of market exclusivity for orphan medicinal products from 10 to 12 years, if all the stages of clinical trials were performed according to the approved schedule of clinical trials involving a pediatric group (Art. 37 of Regulation (EC) 1901/2006). In the case of *orphan drugs*, the EU

legislation resigned from the option of extending the protection law by six months to prevent the doubling of incentives. It is worth noting that the bonus of 12-year market exclusivity is also used in the situation where trials conducted on a pediatric group will not allow for authorization with pediatric indication. In such a case however, the results of these trials should be included in the information documents of the medicinal product, in particular in the leaflet enclosed to the packaging (13).

The support of research works

The *ratio legis* of the legal shaping of the status of an orphan medicinal product presented above was supported by the European Union and its Member States through trials, the development of and making orphan medicinal products available, in particular, the support of research works conducted in small and medium-sized enterprises, provided for in the framework programmes for technological research and development. Due to the fact that the development of new possibilities of diagnosing and treating rare diseases as well as carrying out of epidemiological tests in this respect requires action covering many countries in order to increase the number of patients undergoing particular trials, rare diseases remain one of the priorities within the Seventh Framework Programme for research and development (14).

CONCLUSIONS

A response to the question of whether EU regulations will contribute to the development and increased availability of orphan medicinal products is related to the readiness of Member States to undertake actions which in practice will allow for meeting the requirements as set out in Regulation (EC) No. 141/2000, on the basis of the principle of loyal cooperation (Art. 4(3) of the Treaty on European Union as amended by the Treaty of Lisbon). Relevant authorities of Member States are responsible for educating doctors specializing in conducting clinical trials that would confirm therapeutic efficacy of medicines used in rare diseases. A particularly important challenge for Member States is the postulated collaboration with respect to the exchange between centres of specialist knowledge, necessary for the determination of an efficient strategy of dealing with rare disease in Europe. In this context, the Council recommends that Member States should work out and approve, as quickly as possible but preferably no later than until the end of 2013, a plan or a strategy aimed at

directing and conducting appropriate actions with regard to rare diseases within the States' health care and social systems, and indicate appropriate specialist centres in their entire territories until the end of 2013, as well as consider their support for the creation of such centres (point 1a) and point 11 of Council Recommendation of 8 June 2009 on an action in the field of rare diseases).

REFERENCES

1. Calliess Ch.: in EUV/EGV Kommentar, Calliess Ch., Ruffert M. Eds., p. 399, C.H. Beck, München 2007.
2. Tambuyzer J.: BioLaw&Business, 4, 8 (2000).
3. Decision 1295/1999/EC of the European Parliament and of the Council of 29 April 1999, adopting a programme of Community action on rare diseases within the framework for action in the field of public health (1999–2003) (OJ L 155, 22. 06. 1999, p. 1). The Decision was revoked by Decision 1786/2002/EC (OJ L 271, 09. 10. 2002, p. 1).
4. Council Recommendation of 8 June 2009 on an action in the field of rare diseases, OJ C 151, p. 7, Motive 5.
5. Miaskowska-Daszkiewicz K.: Regulation of business activity by the European Commission on the example of the Community marketing authorisation for medicinal products (Polish), in Konstytucyjna zasada wolności gospodarczej, Szwajdler W., Nowicki H. Eds., p. 297–321, "Dom Organizatora", Toruń 2009.
6. Hiltl Ch.: PharmaRecht 10, 309 (2001).
7. Krekora M.: Zeszyty Naukowe Uniwersytetu Jagiellońskiego, vol. 83, 2003.
8. Herrmann Ch.: Europäische Zeitschrift für Wirtschaftsrecht 2, 37 (2002).
9. Kondrat M: Przegląd Prawa Handlowego 7, 10 (2004).
10. Gassner U. M.: Gewerblicher Rechtsschutz und Urheberrecht, Internationaler Teil 12, 983 (2004).
11. Heinemann A.-K., Tieben A.: Arzneimittel & Recht, 2, 53 (2007).
12. Miaskowska-Daszkiewicz K.: Wokanda Medyczna 1, 95 (2009).
13. Miaskowska-Daszkiewicz K.: Information as an instrument of patient safety management in pharmaceutical law, in: 8th International Conference on Human Rights: Right to Knowledge and Information in Heterogenic Society, Sitek B., Szczerbowski J. J., Bauknecht A. W., Kaczyńska A. W. Eds., p. 334–349, Cambridge Scholars Publishing, Cambridge 2009.

14. Decision 1982/2006/EC of the European Parliament and of the Council of 18 December 2006 concerning the Seventh Framework Programme of the European Community for research, technological development and demonstration activities (2007–2013) (OJ L 412, 30. 12. 2006).

PRESCRIPTION OF EVIDENCE-BASED MEDICINE DRUGS BY GENERAL PRACTITIONERS TO PATIENTS AFTER MYOCARDIAL INFARCTION: OUTCOMES FROM THE CZECH REPUBLIC

MARTIN DOSEDEL[1]*, TEREZA HENDRYCHOVA[1]*, JOSEF MALY[1], ALES KUBENA[1], SVATOPLUK BYMA[2,3] and JIRI VLCEK[1]

[1] Charles University in Prague, Faculty of Pharmacy in Hradec Kralove, Department of Social and Clinical Pharmacy, Heyrovskeho 1203, 500 05 Hradec Kralove, Czech Republic
[2] Charles University in Prague, Faculty of Medicine in Hradec Kralove, Department of Social Medicine, Division of Practical and Family Medicine, Simkova 870, 500 38, Hradec Kralove, Czech Republic
[3] Society of General Practice of the Czech Medical Association of J.E. Purkyně, U Hranic 16/3221, 100 00 Praha 10, Czech Republic

Abstract: Ischemic heart disease is the most frequent cause of both serious morbidity and mortality of adult population in developed countries. The main aim of the study was to carry out the analysis of general practitioners (GP) prescription of evidence-based therapy in patients after myocardial infarction (MI). Data were retrospectively collected in 2011, by a single application with the help of software that GPs use in their surgeries. All patients of a particular GP who had MI in their history and who were at the time of data collection treated only by GPs (not by the specialists of internal medicine or cardiology) were always included. Four hundred ninety one patients were included in the study. The average age was 70.7 (± 11.6) and 69.2% of the involved patients were men. Seventy nine percent of patients used β-blockers, 80% antiplatelet drugs, 77% statins and 79% used angiotensin-converting enzyme inhibitors or angiotensin receptor blockers (ACEIs/ARBs). Forty four percent of patients used drugs from all four groups. The significant prescription decrease was proved in all four groups in dependence on patients' age (p < 0.05). Although the evidence-based medicine usage in patients after MI in the Czech Republic is comparable to other countries, it is not optimal. More intensive involvement of pharmacists in the care of patients after MI would further improve the situation.

Keywords: myocardial infarction; general practitioners; secondary prevention; evidence-based medicine

Worldwide, coronary artery disease (CAD) continues to represent a major cause of morbidity as 12.8% of all deaths are accounted for it. In Europe, every sixth man and every seventh woman will die of myocardial infarction (MI) (1). In the Czech Republic (CR), the statistical data are as follows: in 2010 the overall mortality of adult population due to cardiovascular disease (CVD) represented 50.2% of all known causes of death. Cardiovascular mortality in women was higher (55.9%) than in men (44.6%) (2). In the same year and country, 23.6% of inhabitants died of CAD. Despite the fact that statistical data from the CR indicate a worse situation compared to those in western European countries, over the last decades a permanent decline in the standardized overall cardiovascular mortality and, in particular, a significant decline in the standardized CAD mortality have been observed. When we focus on central European countries, Germany, Austria, Slovenia and Poland show lower mortality for CAD than the CR. On the other hand, in Slovakia and Romania CAD mortality is more than one third higher (2, 3).

A patient after MI faces a high cardiovascular risk. Unfavorable prognosis of these patients may be changed by a proper secondary prevention which is the most potent when a combination of life style modifications and pharmacotherapy are applied (1, 4, 5). In the CR, the secondary prevention is carried out by GPs who collaborate with cardiologists or internal medicine specialists in patients with unfavorable prognosis and a very high mortality risk.

According to the evidence-based medicine (EBM) long-term pharmacological treatment in patients after MI should include antiplatelet therapy, statin mediated hypolipidemic treatment, β-

* Corresponding author: e-mail: martin.dosedel@faf.cuni.cz; tereza.hendrychova@faf.cuni.cz; terhen@centrum.cz;

blockers and angiotensin-converting enzyme inhibitors (ACEI) or angiotensin receptor blockers (ARBs) for ACEIs intolerance. Treatment with acetylsalicylic acid (ASA) at a daily dose of 75 to 100 mg decreases patient mortality (including recurrence of infarction) by approximately 25%. Clopidogrel (75 mg/day) should function as a substitution, if true ASA allergy is presented. In some cases a dual antiplatelet therapy and an oral anticoagulant are recommended (1, 5).

β-Blockers reduce mortality and recurrence of infarction comparably to ASA (by 20–25%) and should be initiated in all patients (if not contraindicated) after MI regardless of their cardiovascular risk. ACEIs prevent myocardial remodelling and thus participate in prevention of chronic cardiac failure due to coronary emergency. The total reduction of mortality is approximately 20–25%. Current recommendations suggest ACEIs/ARBs to be used in the secondary prevention in all patients without contraindications irrespective of their ejection fraction (1, 6).

Furthermore, statins are recommended in all patients in secondary prevention of MI (if not contraindicated) irrespective of cholesterol concentration because they lower both cardiovascular as well as total mortality (approximately by 30%) (1, 5).

Despite the conclusive evidence of benefit of above mentioned drugs in the secondary prevention of MI, their use in clinical practice is still insufficient (1). That is why it is important to constantly observe and assess clinical practice in order to adopt appropriate measures and further increase the rates of usage of EBM therapy after MI. We could presume that with appropriate treatment, mortality of patients after MI would further decrease (7).

The main aim of the study was to carry out an analysis of GP prescription of evidence-based therapy in patients after MI and to determine the proportion of patients using individual evidence-based drugs and their combinations. In addition, possible differences in prescription of evidence-based drugs and their combinations dependent on gender and age of patients were investigated.

EXPERIMENTAL

A retrospective cross-sectional study was conducted during the year 2011. Eighteen GPs who were at that time also consultants in a professional company (Society of General Practice of Czech Medical Association of J. E. Purkyně) in the area of rational pharmacotherapy and education for other members of this company took part in this study. The Society unites about 4,200 GPs (more than 80% of all GPs in the Czech Republic).

Using the electronic medical records of GPs all patients being positive for MI (International Classification of Diseases, ICD-9: 410.xx; ICD-10: I21, I22) and treated for MI only by GP (not by the specialists of internal medicine or cardiology) at the time of data collection were included in the study.

From each medical record patient gender, age, year of MI, and drug anamnesis were collected. We focused on the prescription of β-blockers, statins, ACEIs or ARBs, antiplatelet agents (EBM drugs

Table 1. Characteristic of the study group.

Patients	Characteristic	Mean ± SD (range)
Total (491)	Age (years)	70.7 ± 11.6 (35–96)
	Years after MI	8.0 ± 6.6 (0–33)
	Total number of prescribed drugs	6.4 ± 3.3 (2–26)
Men (340)	Age (years)	68.8 ± 11.5 (35–96)
	Years after MI	7.9 ± 6.6 (0–33)
	Total number of prescribed drugs	6.2 ± 3.3 (2–26)
Women (151)	Age (years)	75.1 ± 10.7 (43–96)
	Years after MI	8.2 ± 6.4 (0–26)
	Total number of prescribed drugs	6.9 ± 3.4 (2–22)

SD – standard deviation; MI – myocardial infarction (the first episode)

Table 2. Proportions of patients after MI treated with EBM therapy.

Patients	β-Blockers (%)	ACEIs (%)	ARBs (%)	ACEIs or ARBs (%)	Statins (%)	Antiplatelet agents – monotherapy (%)	Antiplatelet agents – dual therapy (%)	Anticoagulants* – only (%)	Combination of antiplatelet** and anticoagulant therapy (%)
Total (491)	79.0	63.3	16.7	79.0	77.2	71.9	7.1	9.8	1.2
Male (340)	79.1	67.7	12.0	79.5	78.3	70.9	8.8	10.2	1.5
Female (151)	78.8	53.6	27.2	77.5	74.2	73,5	3.3	8,6	0.7

MI – myocardial infarction; EBM – evidence-based medicine; ACEI – angiotensin-converting enzyme inhibitor; ARB – angiotensin receptor blocker; * other anticoagulant except for warfarin did not occur in any patient; **acetylsalicylic acid only

after MI) and combinations of all of these drugs. Current medication (at the time when the data were collected) was decisive for us.

Statistical analysis

All statistical analysis of data was carried out in PASW® 18.0 software (version 18.0, IBM Corporation, Armonk, NY, U. S., 2009). A p-value < 0.05 was considered significant. For baseline characteristics, data are presented as percentages for binary variables and as the means ± standard deviations and ranges for metric variables. Actual age of patients and the number of years after MI were compared by means of non-parametric Mann-Whitney test. Dependence of a binary value (typically prescription – non-prescription of a drug from the particular evidence-based group) on factors, covariate or their combination was statistically evaluated by means of Generalized Linear Models (GLM+), variant binary distribution – logistic link function. In the special case of binary independent variable, the odds-ratio result was equivalent to analysis of four-square table. In another special case of continuous metric independent variable (especially age), the numerical results were equivalent to a common logistic regression. Another variant of GLM+ – Poisson Distribution, logarithmic link function, was used for analysis models with the number of evidence-based drugs prescribed as a dependent variable.

RESULTS

All addressed GPs participated in the study and the total cohort of patients after MI comprised 491 patients (i.e., 27.3 patients/GP). The basic characteristic of the study group divided according to gender of patients is shown in Table 1. Men and women differed significantly in the mean age (p < 0.001).

The oldest episode of MI was recorded in the year 1978 and the most actual in 2011.

Drugs from each of four EBM groups were prescribed to 77.2–80.2% of all patients. Proportions of patients treated with EBM therapy according to gender of patients are shown in Table 2. Men and women differed significantly in the prescription rate of ACEIs (ARBs respectively) only (p = 0.002).

Prescription of individual EBM drugs did not differ in any case significantly in dependence on gender (β-blockers p = 0.142; ACEIs/ARBs p = 0.880; statins p = 0.158; antiplatelet agents p = 0.085). Each of all four drug groups was significantly less prescribed to older patients (β-blockers p < 0.001, ACEIs/ARBs p = 0.007, statins p < 0.001; antiplatelet agents p = 0.023). When genders were

analyzed separately, the decrease of prescription probability with the age of patients was significant for men only in ACEIs/ARBs (men p = 0.001; women p = 0.352) and antiplatelet agents (men p = 0.009; women p = 0.864).

Probability of prescription of β-blockers decreased by 4.5% (95% CI = 2.3–6.7), of ACEIs/ARBs by 2.8% (95% CI = 0.7–4.8), of statins by 4.3% (95% CI = 2.3–6.5) and of antiplatelet agents by 2.4% (95% CI = 0.3–4.4) with each year of age.

Furthermore, patients were classified according to the number of EBM drugs prescribed. All four groups of drugs (β-blockers + ACEIs/ARBs + statins + antiplatelet drugs) were given to 44.4% of patients. Numbers of EBM therapies prescribed are shown in Figure 1.

The number of prescribed evidence-based drugs did not significantly differ in dependence of gender. Neither the chance of prescription of all four groups of EBM drugs after MI was different between men and women. However, there was a significant difference according to the age of patients (p = 0.002). Mean number of EBM drugs decreased by 0.7% (95% CI = 0.2–1.1) with each year of age.

DISCUSSION AND CONCLUSION

This study is unique because it assessed the treatment of patients in secondary prevention of MI treated by GPs only (not by specialists in internal medicine or cardiology). Every patient in the Czech Republic is registered with one GP. According to the standard of ischemic heart disease therapy (6),

the secondary prevention in patients after IM is carried out by GPs who collaborate with cardiology specialists or internal medicine specialists in highly risk patients with unfavorable prognosis. One of the reasons for implementation of this precaution is economics because therapy led by GPs is less expensive for health care payer.

The patients' treatment in the study could have been set during the hospitalization in hospital but at the time of data collection was led only by GPs who are therefore fully responsible for treatment.

We found out that the EBM drugs after MI are underused. Approximately every fifth patient does not use β-blocker, ACEI/ARB, statin and it is impossible to predict that this fact was only connected with contraindication of particular drugs. In the case of antiplatelet drugs, the prescription of these drugs after MI is higher. All four recommended groups of drugs were prescribed only to 44.4% of patients. Nevertheless, the results of presented study are comparable to those obtained in other international studies, despite that there are some differences in their design. Tight comparisons between studies are limited by the variation of population selection, measurements of consumption of medications and the year(s) studied. Table 3 shows the approximate comparison of selected parameters from similar studies.

It is important to note that displayed studies derived the data from various national databases, used usually even more sources for better reliability and involved larger numbers of patients than our study did. Further, they observed medication of patients with the diagnosis of MI approximately 3–6
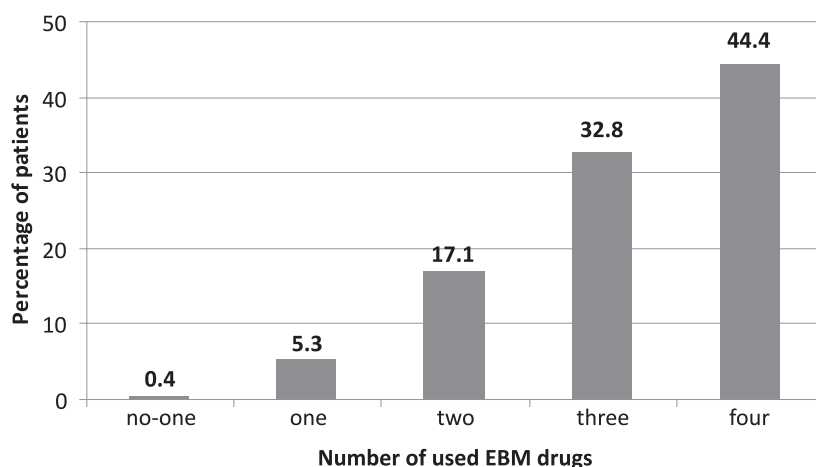

Figure 1. Number of EBM drugs (β-blockers, statins, ACEIs/ARBs, antiplatelet drugs) prescribed after MI (100% = 491 patients). ACEIs – angiotensin-converting enzyme inhibitors, ARBs – angiotensin receptor blockers

months after they were discharged or admitted to the hospital (8–12). The design of our study did not allow us to differentiate patients immediately after their release from hospital from those in long-term secondary prevention of MI. But patients in the long-term secondary prevention prevailed (patients were in average 8.0 ± 6.6 years after MI).

The time frame of other studies is comparable to our work as the evidence for the use of all four drug groups indicated in the secondary prevention of MI was clear at the time when they were conducted. The EBM drug therapy after MI had a definitive breakthrough at the end of the 1990s. Works that observed the trends of prescription of EBM drugs in patients after MI through the years indicated rising prevalence of their use, which is in accordance with the progressive dissemination of the evidence (12, 14).

Nevertheless, it is questionable whether all physicians were aware of this information, as guidelines, usually written by cardiology experts, are applied initially in academic institutions and the education of GPs comes as the final step. This fact could explain higher proportions of patients using recommended drugs, especially statins, antiplatelet agents and combination therapy in French study of Tuppin et al. (8), where higher rates of outpatient cardiologist appointments and hospitalization of patients in university hospitals were found. American study of Lee et al. (11) and Canadian work of Austin et al. (10) similarly indicated that the use of EBM drugs was associated with physician and hospital characteristics and suggested that it therein could be caused by the temporality of the availability of the evidence. As the regional consultants of the Society of General Practice of Czech Medical Association of J. E. Purkyně were approached in our study, we could expect that the results are influenced by greater awareness of evidence-based procedures and willingness to keep them than in other GPs. However, all of them are regularly provided with updated guidelines and other important information. As we do not know any further characteristics (i.e., years of practice) of GPs involved in the study we are not able to yield any conclusion regarding that.

Another reason for higher proportions of patients using recommended drugs in French study of Tuppin et al. (8) could be derived from lower mean age of patients involved (64.8 years). In our study (the mean age of patients was 70.7 ± 11.6 years), we found continuous decline in the prescription of EBM drugs and their combination for older patients, especially in the group of statins and β-

blockers (of 4.3 and 4.5%, respectively, for 1 year of age). For Norwegian study of Reikvam et al. (13) the results for patients over the age of 70 years only are stated in Table 3 and it is likely to be the reason for lower numbers of prescribed EBM drugs after MI in comparison with our work. In the same study (13), the proportions of those drugs prescribed to patients under 70 years were higher (β-blockers 89%; ACEIs 29%; statins 82%). Also other studies confirmed that the age is a negative individual predictive factor of prescription of EBM drugs after MI. Australian work of Vermeer et al. (7) suggested patients over 65 years of age were less likely to receive β-blockers, ACEIs and dual antiplatelet therapy. The study of Schoenenberger et al. (15) yielded similar results for β-blockers and ASA in patients over 60 years and the work of Lee et al. (11) for β-blockers, statins (patients over 65 years) and ACEIs/ARBs (patients over 80 years). In the case of ACEIs/ARBs and antiplatelet drugs, we recorded lower but still significant decrease of their prescription in dependence on the patient age. However, this dependence was only significant in men. Since there were twice more men than women in our study, the overall results could be influenced by this fact. The reason why the chance of prescription of ACEIs/ARBs and antiplatelet drugs decreased only in men could be the aim of further research.

Some authors suggested that the decline of the prescription of EBM drugs with the age of patients could be assigned to the rising number of comorbidities with age (15), which could further prevent the prescription of some drugs because of contraindications or increased risk of adverse events. However, older patients would have greater treatment benefits from EBM drugs, because they are at a higher risk of mortality. For example, data from the PROSPER study (16) concerning use of pravastatin in patients aged 70–82 years or from the CURE study (17) bringing evidence for clopidogrel in patients over 65 years further affirm this claim. Valid data about the use of EBM therapies in older patients (especially over 80 years of age) are lacking, which may further enhance distrust of prescription of preventive drugs.

As we did not observe other diagnoses and possible contraindications or adverse drug events for that a particular EBM therapy was not prescribed or was withdrawn, we are not able to further analyze this problem. However, the importance of possible contraindications should not be overestimated. If theoretical assumptions are kept, then for instance ACEIs should not be indicated in patients with angioedema, oversensitivity to the particular drug or

Table 3. Comparison of selected parameters with chosen international studies.

Place and year of study implementation	Czech (2011)	France (8) (2006)	Austria (9) (2004)	Canada (10) (2003–2005)	USA (11) (2003)	Norway (12) (1999/2000)
Number of patients	491	11671	4105	290767	1135	767
Age [years]	70.7	64.8	68.8	77.0	63.8	> 70
BBs [%]	79.0	82.4	74	78.1	63.9	74
ACEIs/ARBs [%]	79.0	79.5	67	78.4	51.8	38*
Statins [%]	77.2	85.4	67	79.2	62.6	35
Antiplatelet agents [%]	88.5	92.0	–	–	–	70**
BBs+ACEIs/ARBs + statins [%]	51.9	–	41	–	29.9	–
BBs+ACEIs/ARBs + statins + antiplatelet agents [%]	44.4	62.1	–	–	–	–

BBs– β-blockers; ACEIs – angiotensin-converting enzyme inhibitors; ARBs – angiotensin receptor blockers; *ACEIs only; **aspirin/anti-coagulants

pregnancy (total contraindications) (18). The occurrence of these conditions is not, nevertheless, so frequent (19). Conversely, in case of relative contraindications (i.e., hyperkalemia, severe damage to the kidneys) it is not possible to strictly rule out the prescription of ACEI. It depends on the particular case of an individual patient. The similar situation is in statins, too. In the case of β-blockers and antiplatelet agents, there would be a higher impact of possible contraindications on their prescription and, as it was mentioned above, especially these groups are therein less often prescribed to older patients (7, 11, 15). In patients with contraindication of β-blockers (chronic obstructive pulmonary disease), verapamil is a reasonable option for those without heart failure and with caution for those with impaired left ventricular function (1). It was used only by 3.0% of patients in our study so it does not explain another 18% of patients receiving neither β-blocker nor verapamil. It would be noted that some comorbidities may contrary contribute to a higher prescription rate of some drugs (i.e., ACEIs/ARBs in diabetics) (9).

Significant differences in the use of EBM drugs after MI in relation to gender were not found. Conversely, other papers reported such differences in the case of statins that were more likely prescribed to men (7, 11) and even of statins, β-blockers and ACEIs/ARBs together in the same direction (11). From Table 2 it is obvious that women were less often prescribed ACEIs and more often prescribed ARBs than men (p = 0.002). One of the possible explanations can be the fact that cough, as an adverse effect, appears more often in women (20).

The results of our study could be overestimated in dependence on a degree of compliance of patients to the prescribed therapy because we observed only whether a particular drug was prescribed, not if the prescription was filled and the medication really used. This fact probably led to significant differences in the results of Lee et al. (11) and our results as it is stated in Table 3. In the American study, authors obtained the data from the database of pharmacy claims for EBM drugs after MI not the data exactly from prescribed physicians, which would yield higher numbers. For example, Eagle et al. reported that the discontinuation of the evidence-based therapy after 6 months after discharge for acute coronary syndromes ranged between 8–20%. Further analyses of medical and social reasons of non-compliance are necessary and could significantly contribute to the improvement of therapy of patients after MI.

Approximately one fourth of analyzed patients used two or fewer EBM drugs. We can suggest precautions that could contribute to higher rationality of GP prescription. We suppose that among complicated patients, who GP should consult with specialists, should be involved patients after MI if GP hesitates over the prescription of one of the four EMB drugs. Health care payers (health insurance companies) have to play their control role in order to contribute to pharmacotherapy optimization either by targeted analysis of drug consumption or by delegating the control function to pharmacists. Pharmacists can participate in the system both by screening the drug problems in providing consulting service in pharmacies and by developing the cooperation with GPs at drug information centres.

The main limits of our study are the following: the participation of only a specific group of GPs from our country; no information about socio-demographic characteristics of GPs; low number of studied patients; cross-sectional design of the study does not allow us differentiate patients in the long-term secondary prevention of MI from those early after an event; no information about other diagnoses and possible contraindications for not receiving a particular drug and a lack of doses of prescribed evidence-based drugs.

In conclusion, the results of our study show that the use of EBM drugs in patients after MI in the Czech Republic is comparable to other countries although it is suboptimal. In our analysis, we found out a relationship between age and prescription of all of four EBM drugs for secondary prevention of MI. β-Blockers, ACEIs/ARBs, statins and antiplatelet agents were less likely prescribed to older patients. There were not significant differences in the prescription of them in dependence on gender. Despite the fact that the results in the Czech Republic are similar to those abroad, there are still a large percentage of patients who are not treated adequately. It is important to further improve the quality of care of patients in the secondary prevention of MI.

Acknowledgment

REFERENCES

1. Steg G., James S.K., Atar D. et al.: Eur. Heart J. 33, 2569 (2012), DOI:10.1093/eurheartj/ehs215.
2. Deaths 2010. Institute of Health Information and Statistics of the Czech Republic, http://www.uzis.cz/katalog/zdravotnicka-statistika/zemreli (accessed 10. 12. 2012) (in Czech).
3. Ischaemic heart diseases – morbidity and mortality in the Czech Republic in 2003–2010. Institute of Health Information and Statistics of the Czech Republic, www.uzis.cz/system/files/24_12.pdf (accessed 10. 12. 2012) (in Czech).
4. Antman E.M., Anbe D.T., Armstrong P.W. et al.: J. Am. Coll. Cardiol. 44, 671 (2004).
5. Widimský P., Hlinomaz O., Kala P. et al.: Cor Vasa 51, 724 (2009), (in Czech).
6. Hradec J., Býma S.: http://www.svl.cz/Files/nastenka/page_4771/Version1/ICHS-2009.pdf, (accessed 10. 12. 2012) (in Czech).
7. Vermeer N.S., Bajorek B.V.: J. Clin. Pharm. Ther. 33, 591 (2008).
8. Tuppin P., Neumann A., Danchin N. et al.: Arch. Cardiovasc. Dis. 102, 279 (2009).
9. Winkelmayer W.C., Bucsics A.E., Schautzer A. et al.: Eur. J. Epidemiol. 23, 153 (2008).
10. Austin P.C., Tu J.V., Ko D.T. et al.: CMAJ 179, 895 (2008).
11. Lee H.Y., Cooke C.E., Robertson T.A.: J. Manag. Care Pharm. 14, 271 (2008).
12. Margulis A.V., Choundhry N.K., Dormuth C.R.: Pharmacoepidemiol. Drug Saf. 20, 1088 (2011).
13. Reikvam A., Kvan E., Aursnes I.: Cardiovasc. Drugs Ther. 16, 451 (2002).
14. van der Elst M.E., Bouvy M.L., de Blaey C.J., de Boer A: Clin. Ther. 27, 1806 (2005).
15. Schoenenberger A.W., Radovanovic D., Stauffer J.-Ch.: J. Am. Geriatr. Soc. 56, 510 (2008).
16. Shepherd J., Blauw G.J., Murphy M.B.: Lancet 360, 1623 (2002).
17. Alexander K.P., Roe M. T., Chen A.Y.: J. Am. Coll. Cardiol. 46, 1479 (2005).
18. Karen I., Widimský J.: http://www.svl.cz/Files/nastenka/page_4771/Version1/hypertenze.pdf (accessed 10. 12. 2012) (in Czech).
19. Sabroe R.A., Kobza Black A.: Br. J. Dermatol. 136, 153 (1997).
20. Israili Z.H., Hall W.D.: Ann. Intern. Med. 117, 234 (1992).

ANALYSIS OF DIRECT COSTS OF HYPERTENSION TREATMENT AMONG ADOLESCENTS IN POLAND

ANNA PACZKOWSKA[1]*, DOROTA KOLIGAT[1], ELŻBIETA NOWAKOWSKA[1], KAROLINA HOFFMANN[2] and WIESŁAW BRYL[2]

[1] Department of Pharmacoeconomics and Social Pharmacy, Poznań University of Medical Sciences, Dąbrowskiego 79 St., 60-529 Poznań, Poland
Department of Internal Diseases, Metabolic Disorders and Arterial Hypertension, Poznań University of Medical Sciences, Szamarzewskiego 82/84 St., 60-569 Poznań, Poland

Abstract: In adolescents, arterial hypertension (AH) is diagnosed much more frequently than previously thought – it affects 3.2% of the population aged 11–18. In Poland, at present, there are no cost analyses of treatment arterial hypertension among adolescents. The aim of the conducted studies was to analyze direct medical and non-medical costs in the time horizon of one calendar year (2010) of AH treatment in adolescents in Poland. A retrospective study from the societal perspective was based on data from 480 patients medical history cards obtained from the archives of the hospital. From this group, according to the criteria for inclusion in the study, a research group was selected consisting of 36 patients aged 16–18 years, with a diagnosed and treated hypertension. Analysis covered direct medical costs (costs of pharmacotherapy, doctors' visits and laboratory tests, hospitalization) and direct non-medical costs (cost of transport to the outpatient clinic). Average annual cost of hypertension treatment per patient was 89.96 €. The largest part of the structure of total costs related with hypertension treatment in adolescents in Poland were the costs of medical consultation with lab tests and diagnostic examinations – 35.04% and pharmacotherapy costs – 32.95%, with hospital stays rating somewhat lower with 19.12%, and the smallest part were the costs of the patient's transportation to the hypertension outpatient clinic – 12.89%. Early identification of risk factors of such cardiovascular diseases as hypertension as early as in the developmental age, and their subsequent elimination, should be considered a good investment in the reduction of costs associated with hypertension treatment in adulthood.

Keywords: adolescents, arterial hypertension, disease cost analysis

Arterial hypertension is the most important and the most dangerous risk factor of cardiovascular incidents. It is estimated that incidence of AH in children and teenagers in the total population is around 1–3%. In children aged below 10 it is usually secondary. Incidence of primary hypertension increases with age and has become the main cause of arterial hypertension in teenagers. In adolescents, AH is diagnosed much more frequently than previously thought – it affects 3.2% of the population aged 11–18 (1).

The main reasons for increased incidence of AH in adolescents include the changes in the diet (increased consumption of high-calorie foods) and life style (little exercise) taking place over the last few decades. These changes have led to a global obesity epidemics in the younger generation (2). Apart from obesity, the main factors predisposing to development of AH in adolescents include: exces-

sive consumption of salt and comorbid fat and carbohydrate metabolism disorders (3).

AH is not only a major health problem but also a major economic issue both for the health care system and the society as a whole (4, 5). In Poland, at present, there are no cost analyses of undetected, untreated or ineffectively treated hypertension. Due to the major increase in AH incidence in adolescents, there are also no cost analyses of its treatment (6). Only estimation of costs associated with prevention and treatment of AH and its complications throughout the population gives a full representation of the economic burden of AH in Poland.

Analysis of the costs of the disease by estimating the economic burden and establishing the relationship between the individual costs of this disease is an integral part of reasonable functioning of the health care system. Analysis of disease costs allows indication of potential sources of savings in treat-

* Corresponding author: e-mail: divine2204@onet.eu; phone: 48 507 975 635, fax: 48618546894

ment expenditures. It is an argument in making decisions on implementation of preventive and therapeutic programmes and a reference point to estimate the benefits of the treatment applied (7).

The aim of this studies was to analyze direct medical and non-medical costs of AH treatment in adolescents in Poland.

EXPERIMENTAL

The study was conducted at the Chair and Clinic of Internal Diseases, Metabolic Disorders and Hypertension in Poznań. The study was approved by the bioethics committee.

Study group

A retrospective study from the societal perspective was based on data from 480 patients medical history cards obtained from the archives of the hospital. From this group, taking in account the described below criteria for inclusion in the study, there was selected research group consisting of 36 patients (11 women and 25 men) aged 16–18 years, with a diagnosed and treated primary hypertension (according to the International Statistical Classification of Diseases and Related Health Problems – ICD-10).

Inclusion criteria in the study were:
- age of 16-18;
- primary hypertension diagnosed (code I10 according to ICD-10) and treated at the selected outpatient clinic;
- continuation of hypertension treatment in the analyzed time horizon (provided at least two medical visits).

Research time horizon

Analysis covered treatment costs of patients who continued their treatment for a year at the selected health care facility. Time horizon adopted in the study was one calendar year (1. 01. 2010 to 31. 12. 2010).

Analytical technique

The study was based on data from the patients' medical records, doctors' request cards and data from the hospital organization and settlement department.

Analysis covered direct medical costs (costs of pharmacotherapy, doctors' visits and laboratory tests, hospitalization) and direct non-medical costs (cost of transport to the outpatient clinic). Estimated costs presented in euro, according to the table of average rates of the National Bank of Poland (number 012/A/ of 17. 01. 2013, 1 € = 4.1178 PLN).

Pharmacotherapy costs were calculated in relation to patients whose drug therapies were implemented, on the basis of wholesale drug prices set for quarters 1 to 4 in the study calendar year. Total costs of pharmacotherapy, other than expenses for antihypertensive drugs, in line with the guidelines of the Polish Hypertension Association (8) covered also expenses for hypolipidemic drugs, anti-platelet agents and potassium-containing preparations.

Costs of doctors' visits, lab tests and hospital stays were based on prices for medical services set by the National Health Fund (NFZ) in a contract with the selected health care facility. In the case of contracts with the NFZ, the costs of lab and diagnostic tests were included in the cost of medical consultation. In 2010, in the selected health care facility, the cost of medical consultation with the ordered lab/diagnostic tests based on a contract with the National Health Fund was valued at 9.96 €. The value of hospital stays based on the system of homogeneous patient groups on the basis of a contract with the National Health Fund amounted to 123.86 € per patient. The above-mentioned values were constant regardless of the number of tests ordered. The costs of hospital stays were calculated in relation to patients who required hospitalization for diagnosis and treatment of hypertension.

Costs of the patient's transport to the outpatient clinic were evaluated on the basis of single fare price list for the given calendar year agreed by the City Transportation Board in Poznań (MPK) and single fare price list agreed by Poznań bus company – PKS Poznań.

In the study group, none of the patients was occupationally active because of their age, and thus they did not generate any indirect costs related to productivity lost due to AH.

Analysis of costs of hypertension treatment did not take into account the cost of non-pharmacological treatment as it is not possible to estimate them reliably.

RESULTS

Study characteristics

Baseline characteristics of the participants are given in Table 1. The study group comprised 36 patients (11 women and 25 men) aged 17.2 ± 0.8 years. All patients included in the study were still studying (were not occupationally active) and thus did not generate any indirect costs related to productivity lost due to AH. Average duration of AH was 1.7 ± 0.7 years. Average value of systolic blood pressure for total study population over the analyzed

time horizon was 138 ± 11 mmHg and diastolic blood pressure – 81 ± 10 mmHg.

Analysis of antihypertensive therapy

In the analyzed study group, antihypertensive therapy was chosen by the managing physician. Of the entire study group, 44.4% of the subjects were treated solely non-pharmacologically. Pharmacological treatment was implemented for 55.6% of the subjects, of which 60% had monotherapy and for 40% combined therapy was applied. Supplementary therapy, consisting in the use of drugs containing potassium to maintain correct electrolyte balance, was implemented only for one person receiving combined therapy (2.7% of all subjects). In this case, the total cost of supplementary therapy was 21.3 €/year.

In the group treated pharmacologically, the most commonly used antihypertensive drugs were: β-adrenolytics (45% of subjects), angiotensin convertase inhibitors (35% of subjects), calcium antagonists (35% of subjects), AT_1 receptor antagonists (10% of subjects), diuretics (10% of subjects) and α-adrenolytics (5% of subjects).

Cost analysis

Total cost of AH pharmacotherapy for adolescents over the study time horizon amounted in total to 1067.09 €. Average annual cost of AH pharmacotherapy per patient was 53.35 €.

The largest part of the structure of total costs related with AH pharmacotherapy were the costs of antihypertensive drugs – 98% (1045.82 €, 52.28 €/patient per year). Potassium-containing agents accounted 2% (21.27 €, 1.07 €/patient per year) of total cost related with AH pharmacotherapy.

Among the costs associated with the use of antihypertensive drugs, the largest part of the total costs structure were the costs of use of the following group of antihypertensive drugs: Angiotensin II receptor antagonists – 24% (254.04 €, 127.03 € per patient), β-blockers – 21% (216.67 €, 24.06 € per patient), calcium channel blockers – 21% (221.93 €, 31.69 € per patient) and angiotensin-converting enzyme – 17% (182.18 €, 26.03 € per patient), combined drugs (combination of two different active substances in one tablet) – 12% (119.84 €, 119.84 € per patient), diuretics – 4% (45.02 €, 22.5 € per patient) and α-blockers – 1% (6.12 €, 6.12 € per patient).

Table 1. General characteristics of adolescents with hypertension (n = 36).

Numbers	Total	36
	Women (%)	11 (30.5%)
	Men (%)	25 (69.4%)
Age	General ($M^1 \pm SD^2$)	17.2 ± 0.8
	Women (M ± SD)	17.4 ± 0.8
	Men (M ± SD)	17.1 ± 0.8
Education	Primary (%)	36 (100%)
Source of income	Supported by parents (%)	36 (100%)
Place of residence	Poznań City (%)	15 (41.6%)
	Towns up to 50 km away from Poznań (%)	12 (33.3%)
	Towns away from the city of Poznań over 50 km (%)	9 (25.1%)
Duration of hypertension (years)	(M ± SD)	1.7 ± 0.7
Systolic blood pressure (mmHg)	(M ± SD)	138 ± 11
Diastolic blood pressure (mmHg)	(M ± SD)	81 ± 10
Controlled blood pressure (< 95 percentile) (%)	16	(44%)

[1] M = Average, [2] SD = Standard deviation

Over the study time horizon in the entire study group with diagnosed AH treated at a selected outpatient clinic, 114 medical consultations have taken place, on average 3.2 ± 0.7 visits/patient.

Tables 2 and 3 show laboratory and diagnostic tests ordered in hypertension treatment in adolescents. During medical consultations, 16 types of laboratory tests were ordered, of which the largest part were measurements of the levels of: fraction of total cholesterol (69% of patients), LDL (69% of patients), HDL (69% of patients), triglycerides (69% of patients), creatinine (50% of patients) and thyroid-stimulating hormone (44% of patients). Furthermore, 3 types of diagnostic tests were ordered, including Holter pressure (22% of patients), Holter electrocardiogram (5% of patients), electrocardiogram (3% of patients). In the study horizon, none of the patients had laboratory or diagnostic tests ordered more than once.

Total costs of doctor's visits and laboratory/diagnostic tests were estimated at 1135.4 €. Average total cost of medical consultations and test per 1 patient was: 31.5 €.

Of the entire study group, 5 patients required hospital treatment to diagnose secondary forms of AH. Average hospital stay time for these 5 patients was 3.4 ± 0.5 days. Total cost of hospital stays amounted to 619.3 € and average cost of hospital stay per patient was 123.86 €.

Direct non-medical costs comprising the cost of travel to the outpatient clinic from the city of Poznań and beyond its limits amounted in total to 417.35 €, with 11.58 € per patient per year.

Table 2. Laboratory tests ordered in hypertension treatment in adolescents (n = 36).

Type of tests	Percentage of patients with tests ordered n [%]
Morphology	22
Biernacki reaction	14
C-reactive protein	14
Urinalysis	11
Uric acid	19
Urea	19
Electrolytes	25
Creatinine	50
Total cholesterol	69
Low density lipoproteins	69
High density lipoproteins	69
Triglycerides	69
Fasting glucose	25
Glutamic oxoloacetic transaminase	36
Glutamic pyruvic transferase	36
Thyroid-stimulating hormone	44

Table 3. Diagnostic tests ordered in hypertension treatment in adolescents (n = 36).

Type of tests	Percentage of patients with tests ordered n [%]
Electrocardiogram	3
Holter pressure	22
Holter electrocardiogram	5

Table 4. Summary of the total cost of hypertension treatment of among adolescents (n = 36).

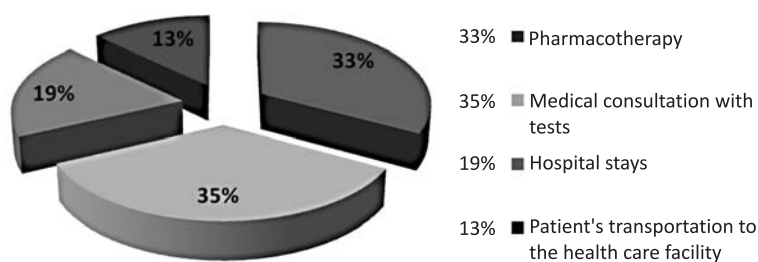| Type of costs	Total costs [€]	Average cost per patient ± SD* [€]
Direct medical costs		
Pharmacotherapy	1067.09	53.35 ± 35.43
Medical consultation with laboratory/diagnostic tests	1135.2	31.5 ± 8.71
Hospital stays	619.3	123.86 ± 0
Indirect medical costs		
Patient's transportation to the health care facility	417.35	11.58 ± 9.25
Total	3238.94	89.96 ± 60.13

*- Standard deviation

Figure 1. Structure of total costs of hypertension treatment in adolescents

Total cost of AH treatment in the adolescent group of 36 over the study time horizon amounted in total to 3238.9 €. Average total cost of hypertension treatment per patient was 89.96 € (Table 4).

According to the aim of conducted studies, structure of total costs of AH treatment in adolescents in Poland has been analyzed. The largest part of the structure of total costs of AH treatment in adolescents in Poland were the costs of medical consultation with tests – 35.04% and pharmacotherapy costs – 32.95%, with hospital stays rating somewhat lower with 19.12%, and the smallest part were the costs of the patient's transportation to the health care facility – 12.89% (Fig. 1).

DISCUSSION AND CONCLUSION

Early prevention aimed at improved detectability of AH by conducting screening measurements of blood pressure and preventing development of the disease by elimination of environmental factors predisposing to development of AH are an important aspect in the context of issues associated with AH in children and adolescents (9). In the United States, it was estimated that the cost associated with screening assays for increase blood pressure values in adolescents aged 12–19 as a part of a two-year programme (in the years 2001–2003) of AH prevention amounted to 107 $ per one subject. This cost included purchase of the necessary medical equipment to measure blood pressure values and fees for the medical staff involved in the program (10).

The knowledge of the economic burden and relationship between the individual components of costs of a disease is an integral part of reasonable management of limited resources of the health care system. Analysis of disease costs allows indication of potential sources of savings in treatment expenditures (11).

Conducted research has shown that the structure of AH treatment costs in adolescents is dominated by direct medical costs (87% of total costs). Average total cost of AH treatment per patient was 89.96 €.

Considering the fact that no papers on similar subjects were found in medical databases, these

results of the evaluation of costs associated with AH treatment in adolescents are the first such data in Poland and worldwide and an important point of reference for further research in this area.

The main reason for the lack of scientific reports on the analysis of costs of AH in adolescents is the strategy of therapeutic procedure. A vast majority of adolescents suffer from AH with the key indirect phenotype being obesity or overweight and secondary metabolic disorders, and thus non-pharmacological treatment is the mainstay of hypertension treatment (12). Non-pharmacological treatment, consisting in the change of lifestyle (increased amount of exercise or appropriate diet) is extremely difficult to estimate and express in monetary values.

Numerous clinical studies have shown that non-pharmacological treatment in antihypertensive therapy yields measurable health and economic effects. It was found that in children and adolescents with AH reduction of the amount of visceral fat and increase of the muscle weight promotes regression of the organ damage by reducing the left ventricular mass and the thickness of the carotid intima media thickness (ITM) (13).

Pharmacological treatment in adolescents with hypertension should be implemented in the case of secondary hypertension, grade II AH and/or the presence of organ damage or if non-pharmacological treatment fails to yield any effect over 3–6 months in adolescents with grade I AH with no organ damage (12).

According to many hypertension specialists, in view of the problem related with the increased incidence of AH in adolescents, it should be a priority to implement effective prevention programme in schools and at primary health care pediatric surgeries to detect hypertension, and, if necessary, strive to normalize blood pressure values to reverse organ damages and prevent cardiovascular incidents in adulthood (14). Such a strategy was adopted for the young population also by the World Health Organization (15).

It should be clearly emphasised that total costs associated with AH treatment comprise expenses on primary prevention, secondary prevention and prevention of complications. Costs incurred at individual stages depend on measures taken and are interrelated. Expenditures for effective prevention of hypertension result in reduced costs of AH treatment, which also minimizes the costs of possible cardiovascular incidents (16). Early identification of risk factors of such cardiovascular diseases as AH as early as in the developmental age, and their subse-

quent elimination, should be considered a good investment in the reduction of costs associated with AH treatment in adulthood (14). In the Framingham Heart Study it was proved that for patients who underwent a long-term antihypertensive therapy the risk of death due to cardiovascular incidents was 13% lower than in patients not treated or treated only occasionally (17).

Results of many pharmacoeconomic analyses confirm that cost-effectiveness of AH treatment depends on many factors, such as: age, sex, baseline blood pressure values and degree of compliance with doctor's recommendations (18, 19).

Evaluation of benefits of antihypertensive therapy based on the risk of cardiovascular events shows that the cost-effectiveness ratio (quality adjusted cost of one life year – QALY) of AH decreases with age as the risk of cardiovascular incidents increases with age (18).

Nevertheless, evaluation of cost-effectiveness of antihypertensive therapy in young people based on the risk of cardiovascular incidents raises many controversies. Therefore, the experts think that evaluation of effects of AH treatment in individual age groups should be based on different criteria. For young people, outcomes of antihypertensive therapy should be defined by evaluating its effect on indirect indicators of the risk of cardiovascular incidents such as hypotensive effect, organ damage regression and normalization of metabolic disorders (1). According to Zanchetti, the cost-effectiveness ratio, where clinical efficacy evaluation is based on long-term observation studies, increases with age, which suggests that early commencement of antihypertensive therapy even brings savings in the longer term (20).

As shown in the present study, the largest part of the structure of total costs related with hypertension treatment in adolescents in Poland were the costs of medical consultation with tests and pharmacotherapy costs. Early identification of risk factors of such cardiovascular diseases as hypertension as early as in the developmental age, and their subsequent elimination, should be considered a good investment in the reduction of costs associated with hypertension treatment in adulthood.

No conflicts of interest were reported.

REFERENCES

1. Litwin M.: Primary hypertension among children and adolescents. Więcek A., Januszewicz A., Szczepańska- Sadowska E., Prejbisz A.

Eds., Hipertensilogy. The pathogenesis, diagnosis and treatment of hypertension (Polish). p. 377, Medycyna praktyczna, Kraków 2011.

2. Fichna P., Skowrońska B.: Family Medicine and Primary Care Review 10, 269 (2008).

3. Pac-Kożuchowska E., Majewski M., Szajner-Milart I., Chrząstek-Spruch H.: Przegląd Pediatryczny 31, 278 (2001).

4. American Heart Association. Heart and stroke facts: 1994 statistical suplement. American Heart Association, Dallas 1994.

5. Hermanowski T., Jaworski R., Czech M., Pachocki R.: Nadciśnienie tętnicze 5, 83 (2001).

6. Wilimski R., Niewada M.: Nadciśnienie tętnicze 10, 551 (2006).

7. Orlewska E.: Principles of pharmacoeconomics (Polish). p. 47, Unimed, Warszawa 1999.

8. Widecka K., Grodzicki T., Narkiewicz K., Tykarski A., Dziwura J.: Nadciśnienie tętnicze 15, 55 (2011).

9. The Fourth Report on the Diagnosis, Evaluation, and Treatment of High Blood Pressure in Children and Adolescents. Pediatrics 114, 555 (2004).

10. Brosnan CH., Swint M., Upchurch S., Meininger J., Johnson G., Lee Y., Nguyen T., Eissa M.: Public Health Nurs. 25, 235 (2008).

11. Kwaśniewska M., Drygas W.: Terapia 8, 65 (2001).

12. Litwin M.: Treatment of primary hypertension in adolescents. in Hipertensilogy. The pathogenesis, diagnosis and treatment of hypertension (Polish), Więcek A., Januszewicz A., Szczepańska-Sadowska E., Prejbisz A. Eds., p. 586, Medycyna praktyczna, Kraków 2011.

13. Litwin M., Niemierska A., Sladowska J. et al.: Pediatr. Nephrol. 25, 2489 (2010).

14. Bryl W.: Nadciśnienie tętnicze 10, 273 (2006).

15. Prevention in childhood and youth of adult cardiovascular disease: time for action. Report of a WHO Expert Committee. World Health Organization, Geneva 1990.

16. Chech M.: Pharmacoeconomics in pharmaceutical care (Polish)., p. 37, Farmapress, Warszawa 2008.

17. Sytkowski P.A., D'Agostino R.B., Belanger A.J., Kannel W.B.: Circulation 93, 697 (1996).

18. Mar J., Rodriguez-Artalejo F.: J. Hypertens. 19, 149 (2001).

19. Ambrosioni E., Costa F.V.: J. Hypertens. Suppl. 14, 47 (1996).

20. Zanchetti A.: Am. J. Cardiol. 79, 3 (1997).

SHORT COMMUNICATION

NEW ABIETATRIENE-TYPE DITERPENES LINKED WITH LANOSTENES FROM OLEO-RESIN OF *PINUS ROXBURGHII* SARG.

MOHD. SHUAIB, MOHAMMED ALI* and KAMRAN J. NAQUVI

Phytochemical Research Laboratory, Department of Pharmacognosy and Phytochemistry,
Faculty of Pharmacy, Jamia Hamdard, New Delhi-110062, India

Pinus roxburghii Sarg., syn. *Pinus longifolia* Roxb. (Pinaceae), commonly known as chir pine, is a tall tree with a spreading crown found in the Himalayan from Kashmir to Bhutan, Afghanistan, Pakistan, China, Nepal and in southern Indian hills. It is also planted in the garden for ornamental purpose. The tapping of the stem produces a clear, transparent oleo-resin with the pungent and bitter taste. Distillation of the turpentine oil from the oleo-resin leaves faintly aromatic and transparent rosin (colophony). It is utilized in the manufacturing of fireworks, insecticides and disinfectants and enters into certain lubricating compositions, hair fixing and nail polishing preparations (1). It is used in preparation of ointments and plasters and in many products such as chewing gum, polishes, and varnishes, but is a common cause of contact allergy. The resin is applied to cure boils (2) and administered orally to combat gastric troubles (3). The rosin is useful as pharmaceutical aids in adhesives, printing ink, electric isolation, paper, soldering flux, varnish and matches. In printing ink industry rosin gives adhesiveness, surface smoothness, hardness, antiblocking and other properties. Rosin has a good electric isolation, being used as oil in cables for high voltage electricity. In soldering process, rosin is beneficial to get rid of oxide compounds in the surface of metal, synthetic rubber and chewing gums (4). Native Americans have used pine resin to treat rheumatism because of its anti-inflammatory properties. The resin acts to remove the joint inflammation caused by rheumatism, which helps to restore movement and to alleviate pain. The Costanoan Indians gained these benefits by chewing on the gum-like resin. A tradi-

tional use for pine resin has been as an external treatment for burns and sores. The pine resin has stimulant, diuretic and laxative properties. In China, the resin from a particular pine tree is used to treat abscesses. Resin from the spruce tree was used by colonial Americans as a cold and cough remedy, as well as straight from the tree as a cancer treatment. Physicians in colonial America also recommended tar water, or ground pine resin mixed with water, as a remedy for ulcers, smallpox, and syphilis (5). Different parts of the plant are prescribed to treat cough, colds, influenza, tuberculosis, bronchitis, as antiseptic, diaphoretic, diuretic, rubefacient, stimulant and febrifuge (6, 7). Rosin consists mainly a mixture of diterpenic acids. The principal acid is abietic acid (37.5%) followed by isopimaric (20.9%), neoabietic (15.1%), levopimaric acid (13.5%), pimaric and dihydroabietic acids. In this paper, we report the isolation and structure elucidation of four triterpenoic acids linked with dehydroabietic acid derivatives obtained from the colophony of *Pinus roxburghii* Sarg., collected from Haldwani (Uttarakhand).

EXPERIMENTAL

Melting points were determined on a Perfit melting apparatus (Ambala, Haryana, India) and are uncurrected. UV spectra were measured with a Lambda Bio 20 spectrophotometer (Perkin-Elmer-Rotkreuz, Switzerland) in methanol. Infra red spectra were recorded on Bio-Rad FTIR 5000 (FTS 135, Kawloon, Hong Hong) spectrophotometer using KBr pellets; v_{max} values are given in cm^{-1}. ^{1}H and ^{13}C NMR spectra were screened on advance DRX 400, Bruker

* Corresponding author: email: maliphyto@gmail.com

spectrospin 400 and 100 MHz instrument in 5 mm spinning tubes at 27°C, respectively (Karlesruthe, Germany), using TMS as an internal standard. Mass spectra were scanned by effecting FAB ionization at 70 eV on a JEOL-JMS-DX 303 spectrometer (Japan) equipped with direct inlet probe system. Column chromatography was performed on silica gel (60–120 mesh; Qualigen, Mumbai, India). TLC was run on silica gel G (Qualigen). Spots were visualized by exposing to iodine vapours, UV radiation, and spraying with ceric sulfate solution.

Plant material

The oleo-resin was procured from a Rosin factory, Haldwani, Uttarakhand. The sample was identified on the basis of exomorphic characters, chemical reactions and reviews of literature by Dr. H.B. Singh, Taxonomist, NISCAIR, CSIR, New Delhi. A voucher specimen of the sample (No. N/R/C/2007/08/851/35) was deposited in the RHM Division, NISCAIR, New Delhi-110012.

Extraction and isolation

The air dried oleo-resin (220 g) was coarsely powdered and dissolved in methanol. The concentrated solution was adsorbed on silica gel particles. It was dried in the air and pulverized to get uniform particle size and chromatographed over silica gel (60–120 mesh) column packed in petroleum ether (b.p. 60–80°C). The column (1.6 m × 16 mm × 2 mm) was eluted successively with petroleum ether, mixture of petroleum ether and chloroform (9 : 1, 3 : 1, 1 : 1, and 1 :3, v/v), chloroform and finally the mixture of chloroform and methanol (99 : 1, 97 : 3, 19 : 1, 23 : 2, 9 : 1, 3 : 1, 1 : 1, 1 : 3, v/v). Various fractions were collected separately and matched by TLC to check homogeneity. Similar fractions having the same R_f values were combined and crystallized. The isolated compounds were recrystallized to get pure compounds. The following compounds were isolated.

Dehydroabietic acid (1)

Further elution of the column with petroleum ether-chloroform (3 : 1. v/v) produced light brown amorphous powder of **1**, recrystallized with methanol-acetone (1 : 1, v/v), 0.24 g (0.109% yield); R_f: 0.86 (chloroform-methanol; 3 : 1, v/v); m.p.: 295–297°C; IR ν_{max} (KBr, cm⁻¹): 3432, 3020, 1705, 1599, 1526; ¹H NMR (DMSO-d₆, δ, ppm): 7.63 (1H, m, H-14), 7.11 (1H, m, H-12), 7.06 (1H, d, J = 9.3 Hz, H-11), 2.48 (2H, m, H-7), 2.25 (2H, m, H-1), 2.19 (1H, m, H-15), 2.05 (1H, m, H-5), 1.52 (2H, m, H-2), 1.31 (2H, m, H-3), 1.29 (2H, m, H-6), 1.21 (3H, brs, H-19), 1.04 (3H, brs, Me-20), 0.83 (3H, d, J = 6.1 Hz,

Me-16), 0.81 (3H, d, J = 6.3 Hz, Me-17); positive ion FAB MS m/z (rel. int.): 300 [M]⁺ ($C_{20}H_{28}O_2$) (36.2).

12-Hydroxydehydroabietic acid (2)

Elution of the column with petroleum ether-chloroform (1 : 1, v/v) produced buff amorphous powder of **2**, recrystallized from methanol-acetone (3 : 1, v/v), 82 mg (0.037% yield); R_f: 0.73 (chloroform-methanol; 3 : 1, v/v); m.p.: 310–312°C; IR ν_{max} (KBr, cm⁻¹): 3518, 3455, 1704, 1525, 1424, 1216, 1044, 928; ¹H NMR (CDCl₃, δ, ppm): 7.13 (1H, brs, H-11), 7.04 (1H, brs, H-14), 1.16 (3H, brs, Me-20), 1.03 (3H, brs, Me-19), 0.97 (3H, d, J = 6.9 Hz, Me-17), 0.84 (3H, d, J = 8.4 Hz, Me-16), 2.74-1.26 (12H, m, 5×CH₂, H-5, H-15); ¹³C NMR (CDCl₃, δ, ppm): 16.05 (C-19), 17.25 (C-20), 17.93 (C-6), 20.94 (C-17), 23.47 (C-16), 29.15 (C-2), 34.78 (C-7), 35.85 (C-3), 35.91 (C-15), 36.27 (C-1), 37.35 (C-10), 45.89 (C-4), 50.37 (C-5), 123.36 (C-14), 127.38 (C-11), 131.52 (C-8), 145.45 (C-9), 151.16 (C-13), 165.76 (C-12), 180.03 (C-18); positive ion FAB MS m/z (rel. int.): 316 [M]⁺ ($C_{20}H_{28}O_3$) (24.8), 253 (36.1).

Pinusoic acid A (3)

Elution of the column with petroleum ether-chloroform (1 : 3, v/v) produced light yellow amorphous powder of **3**, recrystallized from acetone, 1.02 g (0.463% yield). R_f: 0.75 (petroleum ether-chloroform; 1 : 3, v/v), m.p.: 100–102°C; UV λ_{max} (MeOH): 219, 266, 301 nm (log ε 3.1, 5.2, 4.7); IR ν_{max} (KBr, cm⁻¹): 3450, 3360, 3019, 2939, 2852, 2360, 1697, 1645, 1386, 1216, 1043, 928; ¹H NMR (CDCl₃, δ, ppm): 7.13 (1H, d, J = 9.0 Hz, H-12'), 7.08 (1H, d, J = 9.0, H-11'), 5.21 (1H, d, J = 4.2 Hz, H-6), 5.03 (1H, dd, J = 5.3, 6.5 Hz, H-22), 4.92 (1H, m, w₁/₂ = 9.6 Hz, H-23), 4.50 (1H, dd, J = 5.1, 9.2 Hz, H-3α), 3.36 (1H, brs, H-19'α), 3.32 (1H, brs, H-19'β), 1.27 (3H, d, J = 6.0 Hz, Me-27), 1.16 (3H, brs, Me-28), 1.15 (3H, brs, Me-20'), 1.13 (3H, brs, Me-30), 1.03 (3H, brs, Me-19), 1.01 (3H, brs, Me-29), 0.95 (3H, d, J = 6.9 Hz, Me-21), 0.93 (3H, d, J = 6.9 Hz, Me-17'), 0.84 (3H, d, J = 6.6 Hz, Me-16'), 0.76 (3H, brs, Me-18'), 2.74-1.34 (32 H, m, 13×CH₂, 6×CH); ¹³C NMR (CDCl₃, δ, ppm): Table 1; positive ion FAB MS m/z (rel. int.): 770 [M]⁺ ($C_{50}H_{74}O_6$) (1.6), 438 (1.1), 332 (25.2), 301 (64.5), 291 (18.1), 289 (20.5), 287 (21.3), 256 (36.2), 215 (23.8), 141 (59.9).

Pinusquinoic acid (4)

Elution of the column with chloroform-methanol (97 : 3, v/v) produced brown solid mass of **4**, recrystallized from methanol, 65 mg (0.0295% yield); R_f: 0.54 (chloroform-methanol 97 : 3, v/v); m.p.: 68–69°C; UV λ_{max} (MeOH): 212, 267, 310 nm

(log ε 3.2, 3.0, 2.1); IR ν$_{max}$ (KBr): 3418, 2921, 2358, 1725, 1710, 1702, 1698, 1599, 1460, 1331, 1219 cm^{-1}; ^{1}H NMR (DMSO-d$_6$, δ, ppm): 9.22 (1H, brs, H-28), 9.02 (1H, brs, H-30), 6.71 (1H, brs, H-12), 5.75 (1H, d, J = 5.8 Hz, H-7), 5.71 (1H, d, J = 5.8 Hz, H-6), 5.03 (1H, m, $w_{1/2}$ = 9.2 Hz, H-22), 4.93 (1H, m, $w_{1/2}$ = 8.5 Hz, H-23), 4.69 (2H, brs, H$_2$-27), 4.39 (1H, dd, J = 5.5, 9.0 Hz, H-3α), 3.28 (1H, brs, H$_2$-19' α), 3.22 (1H, brs, H$_2$-19' β), 1.13 (3H, d, J = 5.9 Hz, Me-16'), 1.08 (3H, d, J = 6.0 Hz, Me-17'), 1.02 (3H, brs, Me-19), 0.97 (3H, brs, Me-20'), 0.91 (3H, d, J = 7.5 Hz, Me-21), 0.86 (3H, brs, Me-29), 0.63 (3H, brs, Me-18), 2.79–1.40 (27 H, m, 11×CH$_2$, 5×CH); ^{13}C NMR (CDCl$_3$, δ, ppm): Table 1; positive ion FAB-MS m/z (rel. int.): 832 [M]$^+$ (C$_{50}$H$_{72}$O$_{10}$) (2.1), 462 (19.6), 362 (23.4), 360 (18.3), 331 (8.9), 317 (29.5), 315 (36.3), 289 (51.8), 272 (32.0), 241 (28.2), 226 (22.1), 221 (19.8), 197 (41.5), 185 (20.2), 183 (24.8), 169 (31.6), 156 (43.0), 141 (35.7), 121 (73.2), 107 (75.2).

Pinusoic acid B (5)

Elution of the column with chloroform-methanol (9 : 1, v/v) produced brown solid mass of **5**, recrystallized from methanol, 72 mg (0.0327% yield); R$_f$: 0.74 (chloroform-methanol; 9 : 1, v/v); m.p.: 65–66°C; UV λ$_{max}$ (MeOH): 217, 266, 301 nm (log ε 3.1, 4.7, 4.1); IR ν$_{max}$ (KBr, cm^{-1}): 3405, 2939, 2850, 2361, 1710, 1700, 1650, 1449, 1385, 1216, 1041; ^{1}H NMR (DMSO-d$_6$, δ, ppm): 7.11 (1H, d, J = 3.0 Hz, H-14'), 7.00 (1H, dd, J = 3.0, 9.5 Hz, H-12'), 6.89 (1H, d, J = 9.5 Hz, H-10), 5.31 (1H, m, H-6), 5.23 (1H, m, $w_{1/2}$ = 9.3 Hz, H-22), 5.01 (1H, m, $w_{1/2}$ = 8.7 Hz, H-23), 4.13 (1H, dd, J = 5.5, 9.0 Hz, H-3α), 3.53 (1H, brs, H$_2$-19'α), 3.49 (1H, brs, H$_2$-19'β), 1.18 (3H, brs, Me-20'), 1.12 (3H, brs, Me-30), 1.06 (3H, brs, Me-29), 1.04 (3H, brs, Me-19), 1.01 (3H, brs, Me-28), 0.98 (3H, d, J = 6.3 Hz, Me-17'), 0.95 (3H, d, J = 6.3 Hz, Me-21), 0.82 (3H, d, J = 6.2 Hz, Me-16'), 0.80 (3H, d, J = 6.1 Hz, Me-27), 0.72 (3H, brs, Me-18), 2.73–1.45 (31H, m, 12×CH$_2$, 7×CH); ^{13}C NMR (DMSO-d$_6$, δ, ppm): Table 1; positive ion FAB MS m/z (rel. int.): 768 [M]$^+$ (C$_{50}$H$_{72}$O$_6$) (1.3), 439 (6.1), 410 (19.2), 394 (18.3), 330 (21.5), 299 (58.3), 298 (21.3), 287 (17.3), 272 (21.2), 141 (61.9).

Pinusoic acid C (6)

Elution of the column with chloroform-methanol (3 : 1, v/v) produced brown crystalline powder of **6**, recrystallized from methanol 100%, 55 mg (0.025% yield); R$_f$: 0.83 (chloroform-methanol; 3 : 1, v/v); m.p.: 80–81°C; UV λ$_{max}$ (MeOH): 227, 269, 303 nm (log ε 3.1, 4.9, 4.2); IR ν$_{max}$ (KBr, cm^{-1}): 3409, 3380, 3016, 2941, 2837, 1699, 1645, 1446, 1386, 1216, 1044; ^{1}H NMR (DMSO-d$_6$, δ, ppm):

7.39 (1H, brs, H-11'), 6.83 (3H, brs, H-14'), 5.33 (1H, d, J = 4.5 Hz, H-6), 5.09 (1H, m, $w_{1/2}$ = 9.5 Hz, H-22), 4.90 (1H, m, $w_{1/2}$ = 8.3 Hz, H-23), 4.43 (1H, dd, J = 5.1, 9.2 Hz, H-6), 3.40 (2H, brs, H$_2$-19'), 1.26 (3H, d, J = 6.3 Hz, Me-27), 1.16 (3H, brs, Me-30), 1.14 (3H, brs, Me-20'), 1.05 (3H, brs, Me-28), 1.03 (3H, brs, Me-29), 1.01 (3H, brs, Me-19), 0.93 (3H, d, J = 6.1 Hz, Me-21), 0.91 (3H, d, J = 6.4 Hz, Me-17'), 0.85 (3H, d, J = 6.5 Hz, Me-16'), 0.72 (3H, brs, Me-18), 2.48–1.32 (33H, m, 13×CH$_2$, 7×CH); ^{13}C NMR (DMSO-d$_6$, δ, ppm): Table 1; positive ion FAB MS m/z (rel. int.): 770 [M]$^+$ (C$_{50}$H$_{74}$O$_6$) (2.2), 438 (11.6), 334 (38.2), 317 (65.1), 303 (66.3), 297 (31.6), 291 (22.8), 289 (27.5), 141 (53.5), 134 (80.6), 109 (82.1), 95 (100).

RESULTS AND DISCUSSION

Compound **1** and **2** are is the known phytoconstituents identified as dehydroabietic acid and 12-hydroxydehydroabietic acid, respectively (8–11).

Compound **3**, designated as pinusoic acid A, was obtained as a light yellow amorphous powder from petroleum ether-chloroform (1 : 3, v/v) eluants. It produced effervescences with sodium bicarbonate solution and green color with ferric chloride solution. Its IR spectrum displayed characteristic absorption bands for hydroxyl group (3450 cm^{-1}), carboxylic group (3360, 1697 cm^{-1}) and unsaturation (1645 cm^{-1}). On the basis of ^{13}C NMR and positive FAB mass spectra, it displayed a molecular ion peak at m/z 770 consistent with the molecular formula of a triterpene linked with diterpene, C$_{50}$H$_{74}$O$_6$. The important ion peaks arose at m/z 438 [C$_{30}$H$_{46}$O$_2$]$^+$ and 332 [C$_{20}$H$_{28}$O$_4$]$^+$ due to the cleavage of triterpenic linkage attached to diterpenic moiety. The subsequent ion fragments of diterpenic acid moiety arising at m/z 287 [332-COOH]$^+$, 301 [332-CH$_2$OH]$^+$, 256 [301-COOH]$^+$, 289 [332-C$_3$H$_7$]$^+$ suggested the presence of carboxylic, oxygenated methylene and hydroxy groups in it. The fragments of the triterpenic moiety generating ions at m/z 141 [C$_8$H$_{13}$O$_2$; side chain, SC]$^+$ and 291 [432-SC]$^+$ supported the presence of a monounsaturated C$_8$-side chain with one carboxylic group located in a tetracyclic triterpenic moiety with one vinylic linkage. The ^{1}H NMR spectrum of **3** exhibited two one-proton doublets at δ 7.08 (J = 9.0 Hz) and 7.13 (J = 9.0 Hz) ppm assigned correspondingly to *ortho*-coupled H-11' and H-12' aromatic protons. Two one-proton broad signals at δ 3.36 and 3.32 ppm were ascribed to oxygenated H$_2$-19' methylene protons. Two doublets at δ 0.84 (J = 6.6 Hz) and 0.93 (J = 6.9 Hz) ppm and a broad singlet at δ 1.15 ppm, three-protons each, were attributed to secondary Me-

16', Me-17' and tertiary Me-20' methyl protons of the diterpene unit, respectively. A doublet at δ 5.21 (*J* = 4.2 Hz) ppm, a double doublet at δ 5.03 (*J* = 5.3 Hz, 6.5 Hz) ppm and a multiplet at δ 4.92 ($w_{1/2}$ = 9.6 Hz) ppm, were attributed correspondingly to *cis*-vinylic H-6, H-22 and H-23 protons of the triterpenic unit. A double-doublet at δ 4.50 (*J* = 5.1, 9.2 Hz) ppm was ascribed to α-oriented oxygenated methine H-3 proton. Five broad singlets at δ 0.76, 1.03, 1.16, 1.01 and 1.13 ppm were ascribed to tertiary C-18, C-19, C-28, C-29 and C-30 methyl protons, respectively, all attached to saturated carbons. Two three-proton doublets at δ 0.95 (*J* = 6.9 Hz) and 1.27 (*J* = 6.0 Hz) ppm were attributed to secondary C-21 and C-27 methyl protons, respectively. The ^{13}C NMR spectrum of **3** exhibited signals for carboxylic carbons at δ 178.85 (C-26) and 178.79 C-18') ppm; aromatic carbons between δ 123.66–165.76 ppm, vinylic carbons at δ 145.45 (C-5), 122.14 (C-6), 127.38 (C-22) and 123.36 (C-23) ppm, carbinol carbon at δ 70.03 ppm (C-3) and oxygenated methylene carbon at δ 65.21 ppm (C-19'). The shifting of oxygenated H-3 methine proton in the downfield region at δ 4.50 ppm and oxygenated C-19' methylene carbon at δ 65.21 ppm suggested linkage of triterpenoid with C-19' methylene carbon. The ^{1}H and ^{13}C NMR spectral data of **3** were compared with the values of the reported lanostene type triterpenoids (12–15). The spectral data of the abietatriene unit were compared with the reported values of the similar compounds (16–18). The ^{1}H-^{1}H COSY spectrum of **3** showed correlation of H-3 with H-2, Me-28 and H-19; H-6 with H-7; H-22 with H-20, Me-21 and H-23; H-11 with H-12 and Me 20; and H-14 with H-7 and H-12. The HMBC spectrum of **3** displayed interactions of H-2 and H-19 with C-3; H-6, Me-19 and Me 28 with C-5; H-20, Me 21 and H-23 with C-22; Me-27 with C-26; H-19 with C-18; and H-11, H-12 H-14, H-15, Me-16 and Me-17 with C-13. On the basis of above discussion the structure of **3** was elucidated as lanost-5,22-diene-26-oic acid-3β-olyl-(3→19')-dehydroabietic acid (Fig. 1). This is a new dimer form of lanostenoic acid linked with dehydroabietic acid.

Compound **4,** designated as quinoroxburghianoic acid, was obtained as a brown solid mass from chloroform-methanol (97 : 3, v/v) eluants. It produced effervescences with sodium bicarbonate solution. Its IR spectrum displayed absorption bands for aldehydic group (1702 cm⁻¹), carboxylic function (3418, 1698 cm⁻¹) and oxo groups (1725, 1710 cm⁻¹). On the basis of mass and ^{13}C NMR spectra, its molecular weight was established at m/z 832 consistent with the molecular formula of a triterpene linked with abietaquinone, $C_{50}H_{72}O_{10}$. The important frag-

ment ion peaks arose due to the cleavage of ether linkage at m/z 360 $[C_{20}H_{24}O_6]^+$ and 462 $[C_{30}H_{38}O_4]^+$. The subsequent fragment ions of the diterpenic unit arising at m/z 315 [360-COOH]⁺, 272 [315-C_3H_7]⁺, 241 [272-CH_2OH]⁺ and 317 [360-C_3H_7]⁺ indicated the presence of an oxygenated methylene, isopropyl chain and carboxylic group in the diterpenic moiety of **4**. The ion fragments of the triterpenic moiety generated at m/z 139 [$C_8H_{11}O_2$· side chain, SC]⁺, 323 [462-SC]⁺, 433 [462-CHO]⁺, 404 [433-CHO]⁺ and 447 [462-Me]⁺ indicated the presence of two aldehydic groups and a C_8 side chain with a carboxylic group and two double bonds. The ^{1}H NMR spectrum of **4** exhibited a downfield one-proton broad signal at δ 6.71 ppm assigned to H-12' quinone proton. Two one-proton broad signals at δ 3.28 and 3.22 ppm were ascribed to oxygenated H_2-19' methylene protons of the diterpenic unit. Two doublets at δ 1.13 (*J* = 5.9 Hz) and 1.08 (*J* = 6.0 Hz) ppm and one broad singlet at δ 0.97 ppm, three-protons each, were attributed to secondary Me-16', Me-17' and tertiary Me-20' methyl protons, respectively. Two one-proton broad signals appearing in the downfield region at δ 9.22 and 9.01 ppm were due to aldehydic H-28 and H-30 protons, respectively. Two one-proton doublets at δ 5.71 (*J* = 5.8 Hz) and 5.75 (*J* = 5.8 Hz) ppm and two multiplets at δ 5.23 ($w_{1/2}$ = 9.2 Hz) and 4.93 ($w_{1/2}$ = 8.5 Hz) ppm were ascribed correspondingly to *cis*-oriented vinylic H-6, H-7, H-22 and H-23 protons. A two-proton broad singlet at δ 4.69 ppm was attributed to methylene H-27 protons. A double doublet at δ 4.39 (*J* = 5.5, 9.0 Hz) ppm was accounted to oxygenated methine H-3a proton. Three three-proton broad singlets at δ 0.63, 1.02 and 0.86 ppm were assigned to tertiary C-18, C-19 and C-29 methyl protons, respectively. A three-proton doublet at δ 0.91 (*J* = 6.3 Hz) ppm was due to secondary C-21 methyl protons of triterpene unit. The ^{13}C NMR spectrum of **4** displayed important signals for aldehydic carbons at δ 206.66 (C-28), 202.39 (C-30) ppm, oxo carbons at δ 199.60 (C-11'), 199.12 (C-14') and 194.40 (C-3') ppm, carboxylic carbons at δ 182.82 (C-26) and 181.35 (C-18') ppm, vinylic carbons between δ 151.91–106.48 ppm, oxygenated methine at δ 76.58 ppm (C-3) and oxygenated methylene carbon at δ 65.02 ppm (C-19'). The shifting of C-19' carbon signal in the deshielding region at δ 65.02 ppm supported its linkage to C-3 methine carbon through oxygen. The ^{1}H and ^{13}C NMR spectral data of **4** were compared with the values of the reported lanostene type triterpenoids (12–15) The spectral data of the abietatriene unit were compared with the reported values of the similar compounds (16–18). The ^{1}H-^{1}H COSY spectrum of **4** exhibited
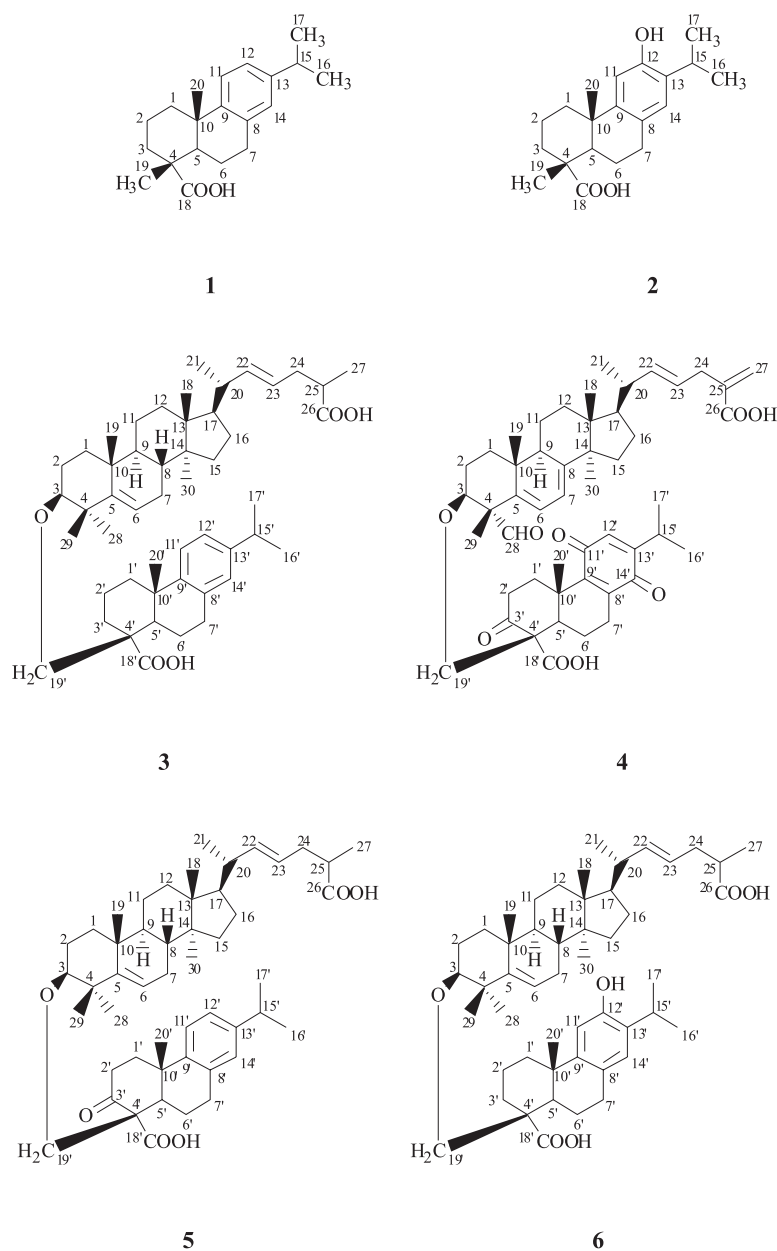
Figure. 1. Structures of compound **1**, **2**, **3**, **4**, **5** and **6**

correlations of H-3 with H-2, Me-28 and H-19; H-7 with H-6 and H-9; H-22 with H-20, Me-21 and H-23; H₂-27 with H₋24; and H-12 with H-15. The HMBC spectrum of **4** displayed interactions of H-2, Me-28 and H-19 with C-3; H-6, H-7 and H-9 with C-8; H-20, Me-21 and H-23 with C-22; H-24 with C-26; and H-7 and H-12 with C-14. On the basis of the spectral data analysis, the structure of **4** has been formulated as lanost-5,7,22,25(27)-tetraen-26-oic acid-28,30-dial-3β-olyl-(3→19')-3-oxoabiet-11',14'-quinone-

18'-oic acid (Fig. 1). This is a new triterpenic linked abietaquinoic acid.

Compound **5**, named pinusoic acid B, was obtained as a brown solid mass from chloroform-methanol (9 : 1, v/v) eluants. It produced effervescences with sodium bicarbonate solution. Its IR spectrum displayed absorption bands for carboxylic group (3405, 1700 cm⁻¹), keto group (1710 cm⁻¹), and unsaturation (1650 cm⁻¹). On the basis of ¹³C NMR and positive FAB mass spectra, it displayed a

Table 1. ¹³C NMR spectral values of **3**, **4**, **5** and **6**.

Position	¹³C NMR **3**	¹³C NMR **4**	¹³C NMR **5**	¹³C NMR **6**
1	36.72	36.84	36.75	36.32
2	26.25	26.47	26.21	26.08
3	70.03	76.58	71.52	70.21
4	42.35	44.52	42.87	42.51
5	145.45	139.99	141.46	145.36
6	122.14	124.69	124.30	121.89
7	31.53	123.49	30.53	31.51
8	45.89	146.48	46.23	45.94
9	45.29	49.37	46.56	46.30
10	38.72	38.68	39.03	38.68
11	23.47	23.26	23.04	23.69
12	29.15	28.62	29.58	31.15
13	43.61	45.79	43.36	44.53
14	50.37	51.33	50.69	50.41
15	31.53	31.12	31.85	30.72
16	32.62	30.17	31.26	31.89
17	51.29	49.58	49.83	51.06
18	13.62	14.30	14.36	13.65
19	17.45	17.68	17.89	17.69
20	41.48	41.84	41.58	40.37
21	20.94	16.04	20.16	20.23
22	127.38	132.18	133.25	128.06
23	123.36	130.39	128.15	123.42
24	45.29	47.06	45.53	44.65
25	39.51	143.80	39.57	39.23
26	178.85	182.82	179.46	179.15
27	16.05	106.48	16.18	16.90
28	25.21	206.66	25.16	25.19
29	23.47	19.38	22.01	23.39
30	16.01	202.39	14.77	17.63
1'	36.41	37.81	36.92	36.26
2'	29.07	34.22	28.07	29.15
3'	31.57	194.40	197.55	36.72
4'	43.52	46.57	45.21	41.30
5'	48.76	50.37	48.82	48.63
6'	16.15	18.14	16.76	16.90
7'	32.71	33.09	32.67	32.67
8'	137.81	134.45	133.67	137.76
9'	144.56	151.91	144.32	145.03
10'	37.83	38.71	37.95	38.05
11'	126.65	199.60	126.67	127.15
12'	123.66	147.78	123.66	164.53
13'	144.18	123.43	145.63	144.32
14'	165.76	199.12	125.68	126.51
15'	33.25	33.62	33.37	33.27
16'	24.55	24.81	24.23	22.89
17'	21.89	17.68	21.66	22.06
18'	178.79	181.35	179.22	178.87
19'	65.21	65.02	65.91	64.93
20'	20.98	20.46	20.94	21.08

molecular ion peak at m/z 768 consistent with the molecular formula of triterpenoid linked with diterpene, $C_{50}H_{72}O_6$. The important ion peaks generating at m/z 439 $[C_{30}H_{47}O_2]^+$ and 330 $[C_{20}H_{26}O_4]^+$ due to the cleavage of triterpenoid linkage with the diterpene indicated that compound **5** consists of triterpenic unit linked with diterpenic acid. The subsequent ion fragments of the diterpenic acid moiety arising at m/z 287 $[330\text{-}C_3H_7]^+$, 272 $[287\text{-}Me]^+$, 284 $[330\text{-}HCOOH]^+$ and 299 $[330\text{-}CH_2OH]^+$ suggested the presence of isopropyl, carboxylic, ketonic and oxygenated methylene groups in the diterpene unit. The ion fragments of triterpenic moiety generating at m/z 141 $[C_8H_{13}O_2$, side chain, SC$]^+$, 298 $[439\text{-}SC]^+$ and 394 $[439\text{-}COOH]^+$ supported the presence of a C_8-mono unsaturated side chain with carboxylic group. The ¹H NMR spectrum of **5** exhibited two downfield doublets at δ 6.89 (J = 9.5 Hz) and 7.11 (J = 3.0 Hz) ppm and a double-doublet at δ 7.00 (J = 3.0, 9.5 Hz) ppm, one proton each, assigned correspondingly to *ortho*-coupled H-11', *meta*-coupled H-14' and *ortho*-, *meta*-coupled H-12' aromatic protons. Two one-proton broad singlets at δ 3.53 and 3.49 ppm were ascribed to oxygenated H_2-19' methylene protons. Two doublets at δ 0.82 (J = 6.2 Hz) and 0.98 (J = 6.3 Hz) ppm and a broad singlet at δ 1.18 ppm were attributed to secondary Me-16', Me-17' and tertiary Me-20' methyl protons of the diterpene unit. Three one-proton multiplets at δ 5.31, 5.23 ($w_{1/2}$ = 9.3 Hz) and 5.01 ($w_{1/2}$ = 8.7 Hz) ppm were ascribed correspondingly to *cis*-oriented vinylic H-6, H-22 and H-23 protons of the triterpenic unit. A double-doublet at δ 4.13 (J = 5.5, 9.0 Hz) ppm was assigned to α-oriented oxygenated methine H-3 proton. The remaining methylene and methine protons resonated between δ 1.45–2.32 ppm. Five broad singlets at δ 0.72, 1.04, 1.01, 1.06, 1.12 ppm and two doublets at δ 0.95 (J = 6.3 Hz) and 0.80 (J = 6.1 Hz) ppm, three-protons each, were ascribed to tertiary C-18, C-19, C-28, C-29, C-30 methyl and secondary C-21 and C-27 methyl protons, respectively, all attached to saturated carbons. The ¹³C NMR spectrum of **5** exhibited signals for ketonic carbon at δ 197.55 ppm (C-3'), carboxylic carbons at δ 179.46 ppm (C-26), 179.22 ppm (C-18'); aromatic and vinylic carbons between δ 123.66–141.46 ppm, oxygenated methine carbon at δ 71.52 ppm (C-3) and oxygenated methylene carbon at δ 65.91 ppm (C-19'), respectively. The shifting of C-19' methylene carbon in the downfield region at δ 65.91 ppm suggested linkage of the triterpenic unit at this carbon. The ¹H and ¹³C NMR spectral data of **5** were compared with the values of the reported lanostene type triterpenoids (12–15).

The spectral data of the abietatriene unit were compared with the reported values of the similar compounds (16–18). The ¹H-¹H COSY spectrum of **5** showed correlations of H-3 with H-2, Me-28 and H-19; H-6 with H-7; H-22 with H-20, Me-21 and H-23; and H-14 with H-7, H-17 and H-15. The HMBC spectrum of **5** exhibited interactions of H-2, Me-28 and H-19 with C-3; H-6, H-7 and Me-28 with C-5; H-20, Me-21 and H-23 with C-22; H-25 and Me-27 with C-26; H-2, H-5 and H-19 with C-3; and H-11, H-12, H-14, Me-17 and Me-16 with C-13. On the basis of above discussion the structure of **5** was formulated as lanost-5,22-dien-26-oic acid-3β-olyl-(3→19')-3-oxodehydroabietic acid (Fig. 1). This is a new lanostenoic acid linked with dehydroabietic acid.

Compound **6,** named pinusoic acid C, was obtained as a brown crystalline powder from chloroform-methanol (3 : 1, v/v) eluants. It produced effervescences with sodium bicarbonate solution and green color with $FeCl_3$ solution. Its IR spectrum exhibited absorption bands characteristic for hydroxyl (3409 cm⁻¹), carboxyl groups (3380, 1699 cm⁻¹) and unsaturation (1645 cm⁻¹). Its positive FAB mass and ¹³C NMR spectra suggested a molecular ion peak at m/z 770 consistent with the molecular formula of a triterpenic unit linked with a diterpene, $C_{50}H_{74}O_6$. The important fragment ion peaks arose at m/z 438 $[C_{30}H_{46}O_2]^+$ and 334 $[C_{20}H_{28}O_4]^+$. The ion fragments of the diterpenic acid moiety produced at m/z 303 $[334\text{-}CH_2OH]^+$, 291 $[334\text{-}C_3H_7]^+$ and 289 $[334\text{-}COOH]^+$ suggested the presence of oxygenated methylene, isopropyl and carboxylic groups in it. The ion fragments of triterpenic unit generating at m/z 141 $[C_8H_{13}O_2$, side chain, SC$]^+$ and 297 $[438\text{-}SC]^+$ indicated the presence of an unsaturated C_8-side chain with carboxylic function in the compound. The ¹H NMR spectrum of **6** displayed two downfield one-proton singlets at δ 7.39 and 6.83 ppm assigned correspondingly to *para*-coupled H-11' and H-14' aromatic protons and supported the existence of the phenolic group at C-12'. A two-proton broad signal at δ 3.40 ppm was attributed to oxygenated H-19' methylene protons. Two doublets at δ 0.85 (J = 6.5 Hz) and 0.91 (J = 6.4 Hz) ppm and one broad singlet at δ 1.14 ppm, each integrating for three protons; were attributed to secondary C-16', C-17' and tertiary C-20' methyl protons, respectively. A one-proton doublet at δ 5.33 (J = 4.5 Hz) ppm and two one-proton multiplets at δ 5.09 ($w_{1/2}$ = 9.5 Hz) and 4.90 ($w_{1/2}$ = 8.3 Hz) ppm were ascribed correspondingly to *cis*-oriented vinylic H-6, H-22 and H-23 protons of triterpenic moiety. A one-proton double-doublet at 4.43 (J = 5.1, 9.2 Hz) ppm was

attributed to α-oriented oxygenated methine H-3 proton. Five three-proton broad singlets at δ 0.72, 1.01, 1.05, 1.03 and 1.16 ppm were ascribed to tertiary C-18, C-19, C-28, C-29 and C-30 methyl protons, respectively. Two three-proton doublets at δ 0.93 (J = 6.1 Hz) and 1.26 (J = 6.3 Hz) ppm were attributed correspondingly to secondary C-21 and C-27 methyl protons of the triterpenic moiety. The ^{13}C NMR spectrum of **6** displayed signals for carboxylic carbons at δ 179.15 (C-26), 178.87 (C-18') ppm, aromatic carbons at δ 127.15–164.53 ppm; vinylic carbons at δ 145.36 (C-5), 121.89 (C-6), 128.06 (C-22), 123.42 (C-23) ppm and carbinol carbon at δ 70.21 ppm (C-3). The shifting of C-19' methylene protons at δ 3.40 ppm in the ^{1}H NMR spectrum and the carbon signal at δ 64.93 ppm in ^{13}C NMR spectrum suggested the linkage of the triterpenic moiety at this carbon. The ^{1}H and ^{13}C NMR spectral data of **6** were compared with the values of the reported lanostene type triterpenoids (12–15). The spectral data of the abietatriene unit were compared with the reported values of the similar compounds (16–18). The ^{1}H-^{1}H COSY spectrum of **6** exhibited correlations of H-3 with H-2, Me-28 and H$_2$-19; H-6 with H-7; H-22 with H-20, Me-21 and H-23; H-14 with H-7; and Me-16 with Me-17. The HMBC spectrum of **6** showed interactions of H-2, Me-28 and H-19 with C-3; H-6, H-7, Me-28 and Me-19 with C-5; H-20, Me-21 and H-23 with C-22; H-19 and H-5 with C-18; and H-11 and H-14 with C-12. On the basis of above discussion, the structure of **6** was characterized as lanost-5,22-dien-26-oic acid-3β-olyl-(3→19')-dehydroabietic acid (Fig. 1). This is a new triterpenic acid linked with dehydroabietic acid.

REFERENCES

1. Anonymous: The Wealth of India, A Dictionary of Indian Raw Materials and Industrial Products, Raw Materials, p. 69. National Institute of Science Communication and Information Resources, CSIR, New Delhi 2003.

2. Rajbhandari K.R.: Ethnobotany of Nepal. Ethnobotanical Society of Nepal, Kathmandu 2001.

3. Manandhar N.P.: Plants and people of Nepal. Timber Press Inc., Portland, Oregon 2002.

4. Wiyono, B., Tachibana, S., Tinambunan, D.: J. Forestry Res., 3, 7 (2006).

5. Langenheim, L.H.: Plant resins: chemistry, evaluation, ecology and ethnobotany, p. 453, Timber Press, Auckland, New Zealand (2003).

6. Chopra R.N., Nayar S.L. Chopra I.C.: Glossary of Indian Medicinal Plant, CSIR, New Delhi 2003.

7. Puri A., Srivastava A.K., Singhal B., Mishra S.K., Srivastava S., Lakshmi V.: Med. Chem. Res., 20, 1589 (2011).

8. Zhu Y., Chen X., Chen Y., Zhong H., Chen Z., Tong Z.: J. Chem. Indust. Eng. 59, 920 (2008).

9. Demirbas A.: Holzforschung, 45, 337 (1991).

10. Wiyono B., Tachibana S., Tinambunan D.: J. Forestry Res. 3, 7 (2006).

11. Ramírez-Macías I., Marín C. Chahboun R., Olmo F., Messouri I., Huertas O., Rosales M.J. et al.: Mem. Inst. Oswaldo Cruz, Rio de Janeiro 107, 370 (2012).

12. Chung I.-M., Ali M., Yang Y.-M., Peebles C.A.M., Chun S.C., Lee S.J., San K.Y., Ahmad A.: Bull. Korean Chem. Soc. 28, 1294 (2007).

13. Chung I.-M, Ali M., Chun S.-C., Lee O.K., Ahmad A.: Asian J. Chem. 19, 1535 (2007).

14. Ansari S.H., Ali M., Naqvi K.J.: Indian Drugs 48, 28 (2011).

15. Ahmad A., Ali M., Tondon S.: Chinese J. Chem. 28, 2474 (2010).

16. Ali M.: Techniques in terpenoids identification, pp. 254–259, Birla Publications, Delhi (2001).

17. Chamy M.C., Piovano M., Garbarino J.A., Miranda C., Gambaro V., Rodriguez M.L., Ruiz-Perez C., Brito L.: Phytochemistry 30, 589 (1991).

18. Georges P., Legault J., Lavoie S., Grenon C., Pichette A.: Molecules 17, 9716 (2012).

Erratum

Instruction for Authors

Scope of the Journal

Acta Poloniae Pharmaceutica - Drug Research publishes papers in all areas of research. Submitted original articles are published in the following sections: Reviews, Analysis, Biopharmacy, Drug Biochemistry, Drug Synthesis, Natural Drugs, Pharmaceutical Technology, Pharmacology, Immunopharmacology, General. Any paper that stimulates progress in drug research is welcomed. Both, Regular Articles as well as Short Communications and Letters to the Editor are accepted.

Preparation of the manuscript

Articles should be written in English, double-spaced. Full name (first, middle initial, last) and address of authors should follow the title written in CAPITAL LETTERS. The abstract should be followed by keywords. We suggest the following structure of paper: 1) introduction, 2) experimental, 3) results, 4) discussion and conclusion.

Instructions for citation of references in the e-journal:

1. In the text, sequential numbers of citations should be in order of appearance (not alphabetically) in parentheses (...) not in brackets [...].
2. In the list of references, for papers the correct order is: number of reference with dot, family name and initial(s) of author(s), colon, proper abbreviation(s) for journal (Pubmed, Web of Science, no dot neither coma after one word journal name), number of volume, number of issue (if necessary) in paranthesis. first page or number of the paper, year of publication (in parentheses), dot. For books: number of reference with dot, family name and initial(s) of author(s), colon, title of chapter and/or book names and initials of editors (if any), edition number, page(s) of corresponding information (if necessary), publisher name, place and year of publication.

EXAMPLES:

1. Gadzikowska M., Grynkiewicz G.: Acta Pol. Pharm. Drug Res. 59, 149 (2002).
2. Gilbert A.M., Stack G.P., Nilakantan R., Kodah J., Tran M. et al.: Bioorg. Med. Chem. Lett. 14, 515 (2004).
3. Roberts S.M.: Molecular Recognition: Chemical and Biochemical Problems, Royal Society of Chemistry, Cambridge 1989.
4. Salem I.I.: Clarithromycin, in Analytical Profiles of Drug Substances And Excipients. Brittain H.G. Ed., pp. 45-85, Academic Press, San Diego 1996.
5. Homan R.W., Rosenberg H.C.: The Treatment of Epilepsy, Principles and Practices. p. 932 , Lea & Febiger, Philadelphia 1993.
6. Balderssarini R.J.: in The Pharmacological Basis of Therapeutics, 8th edn., Goodman L., Gilman A., Rall T.W., Nies A.S., Taylor P. Eds., Vol 1, p. 383, Pergamon Press, Maxwell Macmillan Publishing Corporation, New York 1985.
7. International Conference on Harmonization Guidelines, Validation of analytical procedures, Proceeding of the International Conference on Harmonisation (ICH), Commission of the European Communities, Geneva 1996.
8. http://www.nhlbi.nih.gov/health/health-topics/topics/ms/ (accessed on 03. 10. 2012).

Chemical nomenclature should follow the rules established by the International Union of Pure and Applied Chemistry, the International Union of Biochemistry and Chemical Abstracts Service. Chemical names of drugs are preferred. If generic name is employed, its chemical name or structural formula should be given at point of first citation.

Articles should be written in the Past Tense and Impersonal style. I, we, me, us etc. are to be avoided, except in the Acknowledgment section.

Editor reserves the right to make any necessary corrections to a paper prior to publication.

Tables, illustrations

Each table, figure or scheme should be on a separate page together with the relevant legend and any explanatory notes. Tables ideally should not have more than 70, and certainly not more than 140, characters to the line (counting spaces between columns 4 characters) unless absolutely unavoidable.

Good quality line drawings using black ink on plain A4 paper or A4 tracing paper should be submitted with all lettering etc. included. Good black and white photographs are also acceptable. Captions for illustrations should be collected together and presented on a separate sheet.

All tables and illustrations should be specially referred to in the text.

Short Communications and Letters to the Editor

The same general rules apply like for regular articles, except that an abstract is not required, and the number of figures and/or tables should not be more that two in total.

The Editors reserve the right to publish (upon agreement of Author(s) as a Short Communication a paper originally submitted as a full-length research paper.

Preparation of the electronic manuscript

We encourage the use of Microsoft Word, however we will accept manuscripts prepared with other software. Compact Disc - Recordable are preferred. Write following information on the disk label: name the application software, and the version number used (e.g., Microsoft Word 2007) and specify what type of computer was used (either IBM compatible PC or Apple MacIntosh).